APPLICATIONS OF REHABILITATION ENGINEERING TECHNOLOGIES FOR THE INTERVENTION OF NEURAL AND MOTOR IMPAIRMENT POST STROKE

EDITED BY: Dong Feng Huang and Guanglin Li
PUBLISHED IN: Frontiers in Neurology

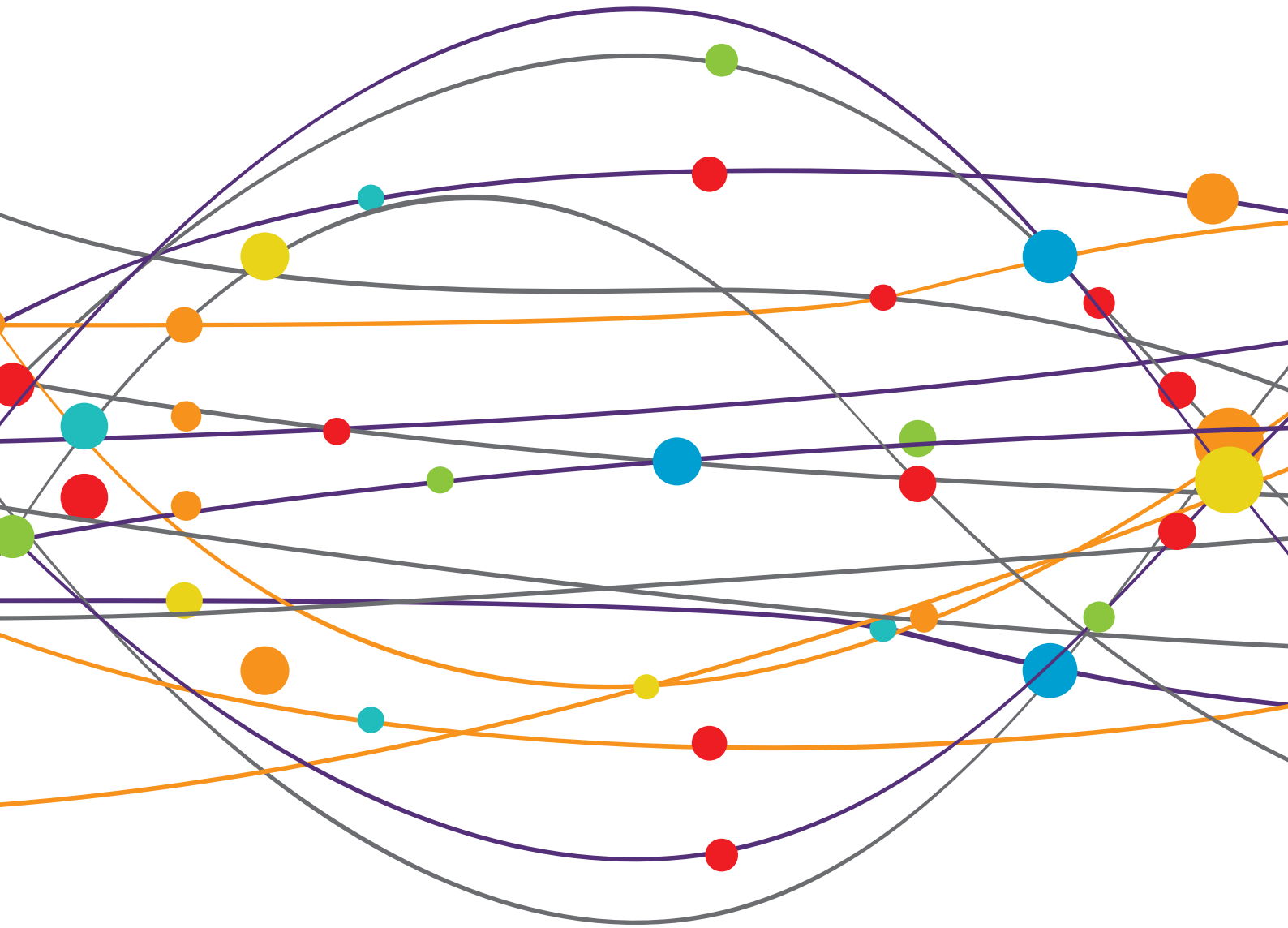

frontiers Research Topics

frontiers

ISSN 1664-8714
ISBN 978-2-88963-301-2
DOI 10.3389/978-2-88963-301-2

About Frontiers

Frontiers is more than just an open-access publisher of scholarly articles: it is a pioneering approach to the world of academia, radically improving the way scholarly research is managed. The grand vision of Frontiers is a world where all people have an equal opportunity to seek, share and generate knowledge. Frontiers provides immediate and permanent online open access to all its publications, but this alone is not enough to realize our grand goals.

Frontiers Journal Series

The Frontiers Journal Series is a multi-tier and interdisciplinary set of open-access, online journals, promising a paradigm shift from the current review, selection and dissemination processes in academic publishing. All Frontiers journals are driven by researchers for researchers; therefore, they constitute a service to the scholarly community. At the same time, the Frontiers Journal Series operates on a revolutionary invention, the tiered publishing system, initially addressing specific communities of scholars, and gradually climbing up to broader public understanding, thus serving the interests of the lay society, too.

Dedication to Quality

Each Frontiers article is a landmark of the highest quality, thanks to genuinely collaborative interactions between authors and review editors, who include some of the world's best academicians. Research must be certified by peers before entering a stream of knowledge that may eventually reach the public - and shape society; therefore, Frontiers only applies the most rigorous and unbiased reviews.
Frontiers revolutionizes research publishing by freely delivering the most outstanding research, evaluated with no bias from both the academic and social point of view. By applying the most advanced information technologies, Frontiers is catapulting scholarly publishing into a new generation.

What are Frontiers Research Topics?

Frontiers Research Topics are very popular trademarks of the Frontiers Journals Series: they are collections of at least ten articles, all centered on a particular subject. With their unique mix of varied contributions from Original Research to Review Articles, Frontiers Research Topics unify the most influential researchers, the latest key findings and historical advances in a hot research area! Find out more on how to host your own Frontiers Research Topic or contribute to one as an author by contacting the Frontiers Editorial Office: researchtopics@frontiersin.org

APPLICATIONS OF REHABILITATION ENGINEERING TECHNOLOGIES FOR THE INTERVENTION OF NEURAL AND MOTOR IMPAIRMENT POST STROKE

Topic Editors:
Dong Feng Huang, Sun Yat-sen University, China
Guanglin Li, Shenzhen Institutes of Advanced Technology (CAS), China

Stroke is the leading cause of disability worldwide. Stroke survivors often have motor impairments which contribute to upper limbs dysfunctions, reduced balance, postural control and reduced mobility and proprioception. These physical symptoms lead to reduced social participation and poor quality of life. Over the past ten years, there had been an enormous focus on the use of virtual reality (VR) and other technologies to improve clinical outcomes for people with stroke. These technologies include large scale bespoke manufactured immersvie virtual reality system, or home based rehabilitation device such as the commercially available device Nitendo Wii and Microsoft XBox. The clinical efficacy of these rehabilitation technologies had been studied extensively but our understanding of the underlying mechanism of recovery induced by these technologies is poor. There are two aspects of "recovery" must be considered. One is the learning compensation strategies where patients acquired "new" skills to improve functional abilities. The other aspect is the neuroplasticity mechanism which leads to cortical map reorganisation. The patient is able to re-use the same body segments in the same way as they did before the stroke. Published studies generally reported improvement in upper limb function, lower limb function, balance and gait. This leads to the uncertainty whether these technologies are effective in promoting "recovery" at neural level or functional level.

With the advance in technology, monitoring techniques such as neural imaging, motion analysis, and EMGs devices have broad applications in the understanding of neural recovery post stroke. Studies that utilize functional outcome measures or observational design may be more effective in identifying functional recovery. A combination of the two designs may be helpful to provide new insights on the recovery mechanism induced by rehabilitation devices.

Citation: Huang, D. F., Li, G., eds. (2019). Applications of Rehabilitation Engineering Technologies for the Intervention of Neural and Motor Impairment Post Stroke. Lausanne: Frontiers Media SA. doi: 10.3389/978-2-88963-301-2

Table of Contents

frontiers in Neurology

ORIGINAL RESEARCH
published: 28 April 2017
doi: 10.3389/fneur.2017.00169

Different Effects of Cold Stimulation on Reflex and Non-Reflex Components of Poststroke Spastic Hypertonia

Sheng Li[1,2], Henry Shin[1,2], Ping Zhou[1,2,3] and Xiaoyan Li[1,2]*

[1] Department of Physical Medicine and Rehabilitation, McGovern Medical School, University of Texas Health Science Center at Houston (UTHealth), Houston, TX, USA, [2] TIRR Memorial Hermann Research Center, TIRR Memorial Hermann Hospital, Houston, TX, USA, [3] Guangdong Work Injury Rehabilitation Center, Guangzhou, China

Objective: To use an established biomechanical approach to quantify reflex and non-reflex responses from spastic–paretic elbow flexors in response to controlled cold and heat stimulation.

Methods: Thirteen spastic–hemiplegic stroke subjects were tested in the experiment. The spastic elbow joint was stretched into extension for 50° at two speeds (5°/s and 100°/s) in a customized apparatus. Thermal stimulation (HEAT at heat pain threshold, COLD at 0°C, or BASELINE at room temperature) was applied to the thenar eminence of the contralateral hand immediately prior to stretching for at least 30 s.

Results: Total torque was greater at 100°/s than at 5°/s. Total torque was significantly increased after COLD, but not HEAT as compared to BASELINE. When normalized to total torque at baseline, HEAT decreased total torque by 6.3%, while COLD increased total torque by 11.0%. There was no significant difference in the reflex torque among three thermal conditions.

Conclusion: The findings demonstrate differentiated effects of cold stimulation on the total resistance from spastic muscles. They provide objective evidence for anecdotal clinical observations of increased muscle spasticity by cold exposure.

Keywords: spasticity, hypertonia, stroke, reflex, cold stimulation, fusimotor

OPEN ACCESS

Edited by:
Dong Feng Huang, Sun Yat-sen University, China

Reviewed by:
Maria Piotrkiewicz, Institute of Biocybernetics and Biomedical Engineering (PAN), Poland
Xiaogang Hu, University of North Carolina at Chapel Hill, USA

****Correspondence:***
Sheng Li
sheng.li@uth.tmc.edu

Specialty section:
This article was submitted to Stroke, a section of the journal Frontiers in Neurology

Received: *30 January 2017*
Accepted: *11 April 2017*
Published: *28 April 2017*

Citation:
Li S, Shin H, Zhou P and Li X (2017) Different Effects of Cold Stimulation on Reflex and Non-Reflex Components of Poststroke Spastic Hypertonia. Front. Neurol. 8:169. doi: 10.3389/fneur.2017.00169

INTRODUCTION

Spasticity is one of a multitude of factors that cause hypertonia. Spasticity is clinically defined as a phenomenon of velocity-dependent increase in resistance to external stretch, i.e., exaggerated stretch reflex (1). Alteration in spasticity can be a sign or reflection of underlying pathology, e.g., increased spasticity can be caused by urinary tract infection. Severity of spasticity could also be affected by many other factors, such as posturing, anxiety, and weather (2). Neurologically stable spinal cord-injured patients may present, or may be perceived to have, different levels of spasticity in the winter time (3) or even with strong air conditioning (4). However, these results are mixed (2). There are also case reports which showed that spasticity was increased by cold weather in stroke patients (5, 6). This pattern of change usually requires adjustment in treatment plan or options, such as increasing dose of botulinum toxin in the winter time.

Cold exposure increases the severity of spasticity in the affected muscles and overall muscle tone of the whole body. This clinical observation of increased tone in response to acute cold challenge is part of common thermal defense responses, including cutaneous vasoconstriction and shivering and non-shivering thermogenesis. The overall increase in muscle tone before the onset of overt shivering is termed "thermal muscle tone" (7). It is related to activation of the fusimotor drive *via* the thermoregulatory reflex during cold exposure (8). In an animal study (8), the efferent fusimotor activity to the rat gastrocnemius muscle was found to increase when the trunk skin was cooled for as short as 30 s by a water-perfused jacket and returned to normal when the skin was rewarmed. The cold-induced fusimotor activation enhanced the afferent discharges of the stretched muscle. However, this activation was blocked by inhibition of neurons in the rostral medullary raphe. In other words, thermal muscle tone is centrally mediated.

Spastic hypertonia consists of reflex-related component, i.e., hyperreflexia and non-reflex-related component (9–12). The hyperreflexia-related spaticity accounts for the commonly observed phenomenon of velocity-dependent increase in resistance. It is indicative of hyperexcitability of spinal stretch reflex circuits as a result of imbalanced descending pathways secondary to disinhibition after stroke (12). On the other hand, a number of peripheral muscular changes can contribute to hypertonia (13, 14). These factors include muscle fiber changes and altered tendon compliance. These peripheral changes may be secondary to paresis. When a paralyzed muscle is maintained in a shortened joint position, for example, a flexed elbow joint position, the muscle is often able to adapt to this situation and becomes shortened. As a result, sarcomeres are lost, muscle fibers become stiffer, and mechanical resistance to stretch increases, i.e., hypertonia (15). Additionally, there is an accumulation of viscous intramuscular substances, such as hyaluronan (16). These changes in the mechanical properties of muscles may gradually lead to increased muscle stiffness (17). These components are not adequately differentiated in common clinical examinations (18) or even in quantitative assessments of muscle stiffness in the laboratory setting (19).

Cold-induced changes in the severity of spasticity are easily perceived by patients and are often assessed with clinical scales, such as modified Ashworth scale (MAS). However, it remains unknown which components of spasticity are influenced by cold exposure. Since cold-induced thermal muscle tone is centrally mediated, its effect on spastic muscles could be quantified by changes in spasticity in the affected muscle in responses to experimentally imposed cold challenge to the contralateral limb. In this way, the peripheral mechanisms in the spastic muscle are not altered by cold stimulation. To achieve this goal, we have developed a thermal-stimulation/biomechanical-quantification approach in this study. In particular, we used a thermal stimulator to provide a brief yet controlled heat/cold stimulation to the contralateral hand in stroke survivors, while an established biomechanical approach was used to quantify the response from the spastic–paretic elbow flexors (20–23). Resistance to slow stretching (e.g., 5°/s) is considered to reflect the passive and non-reflex property of spastic muscles. The difference in resistance between fast (e.g., 100°/s) and slow stretching thus represents the reflex component of spastic muscles. As such, this unique approach allowed us to examine the effects of cold exposure on different components of spasticity.

MATERIALS AND METHODS

Thirteen spastic–paretic hemiplegic stroke subjects (five females, eight males, aged 53–78 years, history of stroke: 68 ± 42 months) participated in the experiment. Subjects were recruited from the TIRR Memorial Hermann outpatient clinic. Inclusion criteria were those who: (1) had spastic hemiplegia secondary to a single ischemic or hemorrhage stroke; (2) had a history of at least 6 months poststroke; (3) had elbow flexor spasticity of the impaired side greater than 0, but less than 3 (rated by MAS) in order to have sufficient range of motion for stretching; (4) were able to understand and follow instructions related to the experiment; and (5) were able to give informed written consent. The exclusion criteria were those who: (1) had a history of multiple strokes or bilateral involvement and (2) had presence of contracture that would limit full elbow range of motion on the impaired side. Spasticity of elbow flexors was MAS of 1+ and 1 in this experiment. The experiment was approved by the UTHealth Committee for the Protection of Human Subjects. All subjects gave written informed consent prior to participation.

For this study, we adopted our recent experimental setup (23, 24). The subjects were seated on a height adjustable chair. The spastic limb was safely secured in a customized apparatus with the shoulder at approximately 45° of abduction and 30° of flexion. The center of the elbow joint and the axis of rotation of the servo motor were perfectly aligned to prevent translation and rotation of the arm. Four vertical plates were used to secure the forearm at the proximal and distal forearm (**Figure 1**). The

FIGURE 1 | Experimental setup.

subjects were instructed to keep the wrist, hand, and fingers relaxed during external stretching. The other arm of the subject rested symmetrically on another table.

External Stretch

A similar stretching protocol was used (23). A ramp-hold stretching at two different speeds (5°/s and 100°/s) was applied. The range of stretching was 50° of elbow extension with reference to the resting joint angle. From the initial elbow joint position, a constant-velocity extension movement was imposed at the elbow until the elbow reached the predetermined end position. The elbow was then held in the end position for 2 s and returned to the initial position at the same velocity. A rest period of about 60 s was allowed between trials to allow adequate recovery and to minimize the influence of stretch history on the response to the subsequent stretch. Subjects were instructed explicitly not to support/facilitate or to oppose the external stretch, i.e., complete relaxation throughout the trials. Two velocities of 5°/s and 100°/s were used with three trials at each velocity.

Thermal Stimulation

There were three thermal conditions: no thermal stimulation (BASELINE, i.e., room temperature), heat stimulation at heat pain threshold (HEAT), and cold stimulation at 0°C (COLD). A 45-s thermal stimulation was delivered to the skin of the contralateral hand *via* a thermode probe (the PATHWAY system, Medoc Ltd., Israel) immediately prior to stretching. As shown in **Figure 1**, a 30 mm × 30 mm advanced thermal stimulator (ATS) probe (thermode) was placed in the marked center of thenar eminence of the contralateral limb. The ATS delivers thermal stimuli at a temperature range of 0–52.5°C with a heating and cooling rate of up to 8°C/s. The thermode rested at room temperature (around 32°C) when not in use. During COLD, the temperature of the thermode decreased at 8°/s till 0°C (it takes about 4 s) and then remained at 0°C till the end of the 45-s trial. During HEAT, the temperature of the thermode increased from the baseline and was maintained at the predetermined heat pain threshold (around 43–45°C). During BASELINE, there was no change in the temperature of the thermode. For all conditions, the previously mentioned computerized external stretching was triggered at the end of the thermal stimulation. Each thermal condition was tested twice at each stretching speed. The interval between two thermal stimulation trials was 2 min. The order of stretching speed and thermal condition was randomized to avoid any bias caused by the stretching order.

Data Analysis

Resistance torque was measured with a torque sensor (Model TRS 500, Transducers Techniques, CA, USA). An angular motion was recorded using encoder (HD FHA-25C-50-US250, Standard Incremental, 2,500 pulses per revolution). All signals were digitized at 1,000 samples/s on a PC with a BNC-2090A data acquisition board (National Instruments, Austin, TX, USA) using custom LabView software (National Instruments). Data were saved for offline analysis using a custom MATLAB (The MathWorks Inc.) program.

Angle and torque signals were analyzed to determine the biomechanical response of the stretch on the spastic elbow flexors (23). For each subject, peak torque was calculated for all speeds between the start and end of arm extension. Total torque was calculated by subtracting the baseline (pre-stretch) torque from the peak value. Reflex torque was defined as the difference in total torque between the fast (100°/s) and the slow (5°/s) stretching. To characterize the pattern of the response, average torque was calculated across all three trials for each speed and each thermal condition.

Statistics

A two-way repeated measures ANOVA was applied to examine the main effects of stretching velocity (SPEED, two levels: 5°/s and 100°/s) and thermal stimulation (THERMAL, three levels: BASELINE, COLD, HEAT) on total torque. To compare changes in total torque from the baseline after thermal stimulation, a two-way ANOVA (SPEED and TEMP, two levels, hot/cold) was used. A One-way ANOVA (THERMAL) was used to investigate the impact of thermal stimulation on reflex torque. $p < 0.05$ was chosen to indicate statistically significant differences.

RESULTS

Total torque was significantly affected by both stretching speed and thermal stimulation (**Figure 2**). According to the two-way ANOVA analyses, there were main effects of SPEED [$F(1,12) = 27.65$, $p < 0.0001$] and THERMAL [$F(2,24) = 3.88$, $p = 0.035$]. No significant interactions were observed. Averaged across different thermal conditions, total torque was significantly greater at 100°/s (5.98 Nm) than at 5°/s (2.82 Nm). Averaged across different speeds, total torque was 4.33 Nm at BASELINE, 4.84 Nm during COLD, and 4.02 Nm during HEAT (**Figure 3A**).

When normalized to the total torque at BASELINE, the percent change in total torque was also speed and temperature-dependent (**Figure 4**). Two-way ANOVA analyses showed main effects of SPEED [$F(1,12) = 0.473$ $p = 0.505$], TEMP [$F(1,12) = 9.078$ $p = 0.011$] and a significant interaction SPEED × TEMP [$F(1, 12) = 6.907$, $p = 0.022$]. Tukey *post hoc* tests further revealed that the percent torque change was significantly greater by COLD (18.1%) than HEAT (−8.7%) at slow speed, but there was no difference in torque change between COLD (4.0%) and HEAT (−3.9%) at fast speed of stretching. Overall, COLD increased total torque by 11.0%, while HEAT decreased total torque by 6.3%.

The reflex torque, obtained visually by subtracting the gray bars from the corresponding black bars on **Figure 3A**, however, did not differ significantly across three thermal conditions [$F(1,12) = 0.661$, $p = 0.551$]. They were 3.29, 3.01, and 3.15 Nm for BASELINE, COLD, and HEAT, respectively (**Figure 3B**).

DISCUSSION

In this experiment, a novel thermal-stimulation/biomechanical-quantification approach was used to quantify spastic hypertonia of elbow flexors in stroke subjects when thermal stimulation was applied to the contralateral hand in three thermal conditions: BASELINE, COLD, and HEAT. There were no changes

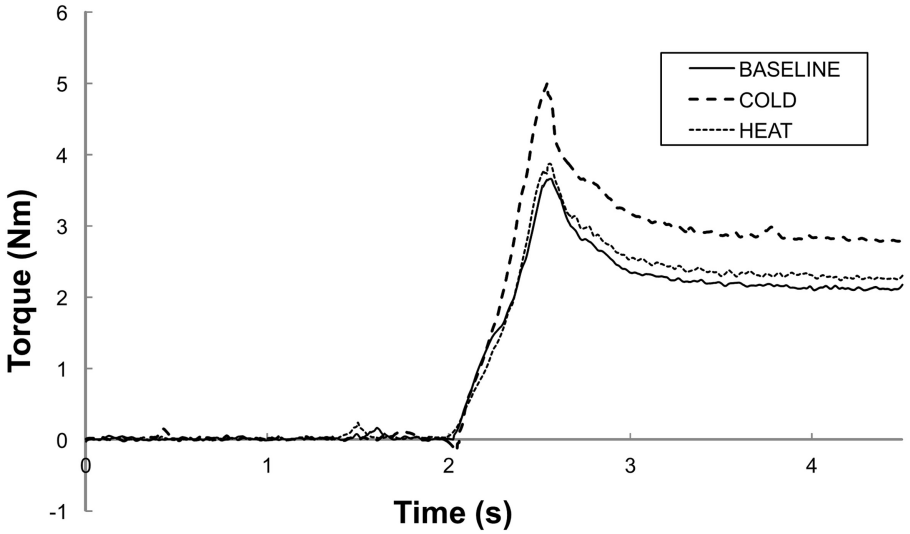

FIGURE 2 | Representative trials of total torque responses at a stretching speed of 100°/s. BASELINE: room temperature, COLD: 0°C cutaneous stimulation to the contralateral thenar eminence; HEAT: thermal stimulation at the heat pain threshold to the contralateral thenar eminence. Note that the peak torque response is greater in COLD as compared to in HEAT and BASELINE. Both HEAT and BASELINE have similar torque peak torque responses.

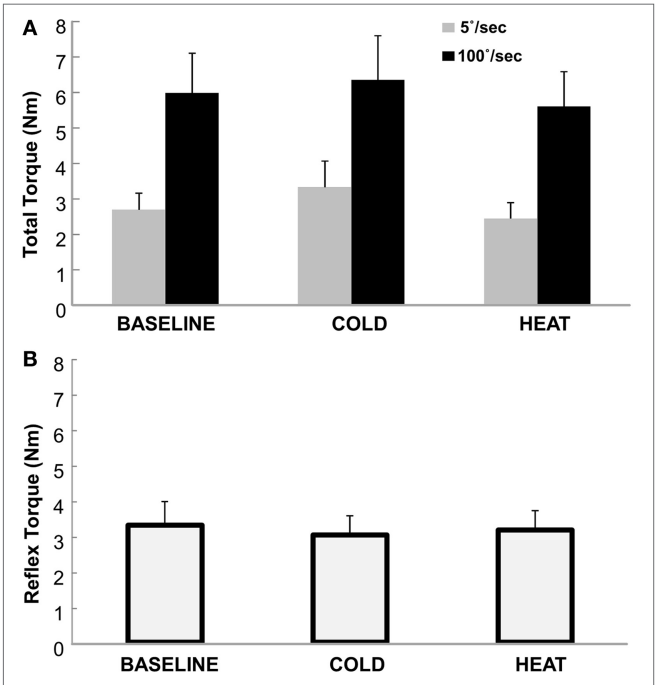

FIGURE 3 | (A) Total Torque at BASELINE, COLD, and HEAT conditions. Gray bars indicate torque responses at slow stretch (passive component) and black bars indicate torque responses at fast stretch (passive + reflex component). A clear difference between speeds is visible, but not necessarily between temperatures. Mean and SEs are shown. **(B)** Reflex torque at BASELINE, COLD, and HEAT conditions. The reflex component of the total torque is the difference between the fast and slow torque responses (Total Torque at 100°/s – at 5°/s). Mean and SE are shown.

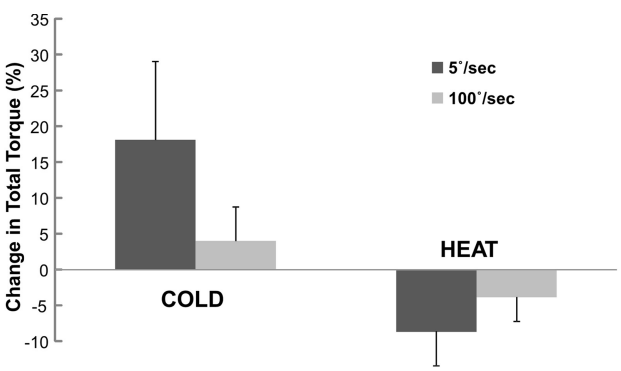

FIGURE 4 | Change in total torque at COLD and HEAT stimulation. Change in total torque refers to percent difference in total torque between COLD/HEAT and BASELINE that is normalized to total torque at BASELINE. Positive change means increase in total torque. Mean and SEs are shown.

in the biomechanical configuration or sensorimotor condition of the spastic limb during subsequent external stretches across different thermal conditions. The thermal-stimulation/biomechanical-quantification approach allows a unique opportunity to individually assess the reflex and non-reflex components of spastic hypertonia. In addition to confirming velocity-dependent increases in total torque, the novel findings included (1) total torque was significantly increased after COLD, but not HEAT as compared to BASELINE and (2) reflex torque did not differ significantly across the three thermal conditions. Our findings of no significant change in reflex torque across thermal conditions and increased total torque after cold stimulation suggest that cold stimulation specifically modulates the non-reflex component without affecting the reflex component in stroke survivors.

This study found that cold stimulation primarily alters non-reflex, passive stiffness of spastic muscles in stroke subjects. It is important to point out that many factors could contribute to non-reflex, passive stiffness, such as viscoelasticity of the muscle

(14, 25), changes in muscle property (26), and accumulation of extracellular deposits (27). Unfortunately, we are not able to differentiate these factors in this study. Our finding was consistent with reports from an earlier study (7). A brief cold exposure specifically increased overall muscle tone, but did not alter fine neuromotor control during force production. The increase in the non-reflex response and the overall muscle tone during cold exposure suggests a central mechanism. This cold-induced increase in overall muscle tone is likely part of cold-defense mechanisms *via* activation of neurons in the rostral medullary raphe (8). In contrast, no effect of cold stimulation on the reflex component suggests that the excitability of reflex pathways is not affected.

The finding of no significant effect of cold stimulation on the reflex component is not trivial. The stretch reflex is a monosynaptic reflex that provides automatic regulation of skeletal muscle. Skeletal muscle contains extrafusal and intrafusal muscle fibers. Extrafusal fibers are innervated by alpha motor neurons, mediating muscle contraction. Intrafusal fibers constitute the muscle spindle. These intrafusal fibers are innervated by gamma motor neurons. The muscle spindle serves as mechanoreceptors for the muscle and provides feedback to the central nervous system. When a muscle is lengthened by passive stretch, both the change in muscle length and its rate are detected by muscle spindles (primarily group Ia and II afferent fibers). Golgi tendon organs also send information on muscle tension through group Ib afferent fibers. The increase in neuronal activity in these fibers in turn increases alpha motor neuron activity in the stretched muscles through the stretch reflex. This causes the extrafusal muscle fibers to contract and thus resist the muscle lengthening or stretching. Meanwhile, Ia afferent fibers also synapse with Ia inhibitory interneurons, producing relaxation of the antagonist muscles ("reciprocal inhibition"). In summary, gamma motor neurons regulate muscle spindles (fusimotor system) and thus the reflex sensitivity.

By subtracting the torque response at 5°/s from that at 100°/s, reflex torque reflects the aggravated reflex response to a fast external stretch. This velocity-dependent reflex torque is likely mediated by velocity-sensitive spindle afferent inputs (Ia and II spindle afferents) (22, 28) and hyperexcitable spinal motor neurons (9, 12, 29). It is viewed as a result of unopposed descending inputs to spinal motor neuron pools from hyperexcitable medial reticulospinal pathways (12, 30). Cold stimulation is known to relate to the activation of the fusimotor drive *via* the thermoregulatory reflex (8). The cold-induced fusimotor activation enhanced the afferent fusimotor discharges. No cold effect on the reflex torque suggests that the cold-induced fusimotor activation does not increase stretch reflex responses in spastic flexors. These findings are in general in consistence with previous findings (31, 32). These studies reported that the reflex amplitude was not disproportionally affected by changes in fusimotor function—by an after-effect of voluntary contraction, cutaneous mechanical stimulation, or electrical nerve stimulation. However, our findings extended previous reports that the fusimotor function could significantly alter the non-reflex component of spastic hypertonia. Further research needs to investigate how the fusimotor activation changes the non-reflex component of passive resistance in spastic muscles.

Limitations of this study include the number of stretch measurements made at each thermal condition. The muscle reflex response is highly variable, but also typically shows a decrease in amplitude with each successive stretch within a short period of time. Only two measurements were made in each thermal condition as to not heavily weigh whichever condition was measured first. This potential bias was also remediated by randomizing the order of the thermal condition. Thermal stimulation was applied only to the contralateral side in this study. The effect of thermal stimulation would be more significant if it was applied on the same side or directly on the target muscles. However, the potential confounding factor is that increased passive stiffness could be induced directly by cold stimulation. In future studies, comparisons of the effects of thermal stimulation to the spastic muscles and on the contralateral side may be able to provide useful information.

CONCLUSION

The findings provide objective evidence for anecdotal clinical observations of increased muscle spasticity due to cold exposure. Increased spastic hypertonia appears to be primarily caused by an alteration in the non-reflex component of spastic hypertonia at a central level.

ETHICS STATEMENT

The experiment was approved by a local Institutional Review Board.

AUTHOR CONTRIBUTIONS

SL, HS, PZ, and XL: study concept and design; analysis and interpretation; critical revision of the manuscript for important intellectual content. HS and XL: acquisition of data. SL: study supervision.

FUNDING

This work was in part supported by NIH/NICHD/NCMRR, 1R21HD087128-01.

REFERENCES

1. Lance JW. Symposium synopsis. In: Feldman RG, Young RR, Koella WP, editors. *Spasticity: Disordered Motor Control*. Chicago: Year Book Medical Publishers (1980). p. 485–94.
2. Phadke CP, Balasubramanian CK, Ismail F, Boulias C. Revisiting physiologic and psychologic triggers that increase spasticity. *Am J Phys Med Rehabil* (2013) 92:357–69. doi:10.1097/PHM.0b013e31827d68a4
3. Shirado O, Shundo M, Kaneda K, Strax TE. Outdoor winter activities of spinal cord-injured patients. With special reference to outdoor mobility. *Am J Phys Med Rehabil* (1995) 74:408–14. doi:10.1097/00002060-199511000-00002
4. Mahoney JS, Engebretson JC, Cook KF, Hart KA, Robinson-Whelen S, Sherwood AM. Spasticity experience domains in persons with spinal cord injury. *Arch Phys Med Rehabil* (2007) 88:287–94. doi:10.1016/j.apmr.2006.12.029

5. Baxter P, Gardner-Medwin D, Green SH, Moss C. Congenital livedo reticularis and recurrent stroke-like episodes. *Dev Med Child Neurol* (1993) 35:917–21. doi:10.1111/j.1469-8749.1993.tb11569.x
6. Mathias G, Cowley R, Morales A, Rogers RC. Congenital livedo reticularis and recurrent strokes in two unrelated young children. *Clin Pediatr (Phila)* (2006) 45:367–72. doi:10.1177/000992280604500411
7. Meigal AY, Oksa J, Gerasimova LI, Hohtola E, Lupandin YV, Rintamaki H. Force control of isometric elbow flexion with visual feedback in cold with and without shivering. *Aviat Space Environ Med* (2003) 74:816–21.
8. Tanaka M, Owens NC, Nagashima K, Kanosue K, McAllen RM. Reflex activation of rat fusimotor neurons by body surface cooling, and its dependence on the medullary raphe. *J Physiol* (2006) 572:569–83. doi:10.1113/jphysiol.2005.102400
9. Katz RT, Rymer WZ. Spastic hypertonia: mechanisms and measurement. *Arch Phys Med Rehabil* (1989) 70:144–55.
10. Gracies JM. Pathophysiology of spastic paresis. II: emergence of muscle overactivity. *Muscle Nerve* (2005) 31:552–71. doi:10.1002/mus.20285
11. Gracies JM. Pathophysiology of spastic paresis. I: paresis and soft tissue changes. *Muscle Nerve* (2005) 31:535–51. doi:10.1002/mus.20284
12. Li S, Francisco G. New insights into the pathophysiology of post-stroke spasticity. *Front Hum Neurosci* (2015) 9:192. doi:10.3389/fnhum.2015.00192
13. Dietz V, Quintern J, Berger W. Electrophysiological studies of gait in spasticity and rigidity. Evidence that altered mechanical properties of muscle contribute to hypertonia. *Brain* (1981) 104:431–49. doi:10.1093/brain/104.3.431
14. Thilmann AF, Fellows SJ, Garms E. The mechanism of spastic muscle hypertonus. Variation in reflex gain over the time course of spasticity. *Brain* (1991) 114: 233–44.
15. Friden J, Lieber RL. Spastic muscle cells are shorter and stiffer than normal cells. *Muscle Nerve* (2003) 27:157–64. doi:10.1002/mus.10247
16. Stecco A, Stecco C, Raghavan P. Peripheral mecahnisms contributing to spasticity and implications for treatment. *Curr Phys Med Rehabil Rep* (2014) 2:121–7. doi:10.1007/s40141-014-0052-3
17. Mirbagheri MM, Tsao CC, Rymer WZ. Changes of elbow kinematics and kinetics during 1 year after stroke. *Muscle Nerve* (2008) 37:387–95. doi:10.1002/mus.20965
18. Vattanasilp W, Ada L, Crosbie J. Contribution of thixotropy, spasticity, and contracture to ankle stiffness after stroke. *J Neurol Neurosurg Psychiatry* (2000) 69:34–9. doi:10.1136/jnnp.69.1.34
19. Malhotra S, Pandyan AD, Day CR, Jones PW, Hermens H. Spasticity, an impairment that is poorly defined and poorly measured. *Clin Rehabil* (2009) 23:651–8. doi:10.1177/0269215508101747
20. Kamper D, Schmit B, Rymer W. Effect of muscle biomechanics on the quantification of spasticity. *Ann Biomed Eng* (2001) 29:1122–34. doi:10.1114/1.1424918
21. Kamper DG, Harvey RL, Suresh S, Rymer WZ. Relative contributions of neural mechanisms versus muscle mechanics in promoting finger extension deficits following stroke. *Muscle Nerve* (2003) 28:309–18. doi:10.1002/mus.10443
22. Li S, Kamper DG, Rymer WZ. Effects of changing wrist positions on finger flexor hypertonia in stroke survivors. *Muscle Nerve* (2006) 33:183–90. doi:10.1002/mus.20453
23. Bhadane MY, Gao F, Francisco GE, Zhou P, Li S. Correlation of resting elbow angle with spasticity in chronic stroke survivors. *Front Neurol* (2015) 6:183. doi:10.3389/fneur.2015.00183
24. Li S, Liu J, Bhadane M, Zhou P, Rymer WZ. Activation deficit correlates with weakness in chronic stroke: evidence from evoked and voluntary EMG recordings. *Clin Neurophysiol* (2014) 125:2413–7. doi:10.1016/j.clinph.2014.03.019
25. Lee HM, Huang YZ, Chen JJJ, Hwang IS. Quantitative analysis of the velocity related pathophysiology of spasticity and rigidity in the elbow flexors. *J Neurol Neurosurg Psychiatry* (2002) 72:621–9. doi:10.1136/jnnp.72.5.621
26. Lieber RL, Friden J. Spasticity causes a fundamental rearrangement of muscle-joint interaction. *Muscle Nerve* (2002) 25:265–70. doi:10.1002/mus.10036.abs
27. Raghavan P, Lu Y, Mirchandani M, Stecco A. Human recombinant hyaluronidase injections for upper limb muscle stiffness in individuals with cerebral injury: a case series. *EBioMedicine* (2016) 9:306–13. doi:10.1016/j.ebiom.2016.05.014
28. Houk JC, Rymer WZ, Crago PE. Dependence of dynamic response of spindle receptors on muscle length and velocity. *J Neurophysiol* (1981) 46:143–66.
29. Chang SH, Francisco GE, Zhou P, Rymer WZ, Li S. Spasticity, weakness, force variability, and sustained spontaneous motor unit discharges of resting spastic-paretic biceps brachii muscles in chronic stroke. *Muscle Nerve* (2013) 48:85–92. doi:10.1002/mus.23699
30. Li S. Spasticity, motor recovery, and neural plasticity after stroke. *Front Neurol* (2017) 8:120. doi:10.3389/fneur.2017.00120
31. Wilson LR, Gandevia SC, Inglis JT, Gracies JM, Burke D. Muscle spindle activity in the affected upper limb after a unilateral stroke. *Brain* (1999) 122:2079–88. doi:10.1093/brain/122.11.2079
32. Wilson LR, Gracies JM, Burke D, Gandevia SC. Evidence for fusimotor drive in stroke patients based on muscle spindle thixotropy. *Neurosci Lett* (1999) 264:109–12. doi:10.1016/S0304-3940(99)00181-0

Conflict of Interest Statement: The authors declare that the research was conducted in the absence of any commercial or financial relationships that could be construed as a potential conflict of interest.

frontiers in Neurology

ORIGINAL RESEARCH
published: 10 May 2017
doi: 10.3389/fneur.2017.00186

The Use of Functional Electrical Stimulation on the Upper Limb and Interscapular Muscles of Patients with Stroke for the Improvement of Reaching Movements: A Feasibility Study

Alicia Cuesta-Gómez[1], Francisco Molina-Rueda[1], Maria Carratala-Tejada[1], Eukene Imatz-Ojanguren[2], Diego Torricelli[3] and Juan Carlos Miangolarra-Page[1,4]*

[1] Motion Analysis, Ergonomics, Biomechanics and Motor Control Laboratory (LAMBECOM), Department of Physical Therapy, Occupational Therapy, Rehabilitation and Physical Medicine, Rey Juan Carlos University, Alcorcón, Spain, [2] Tecnalia, San Sebastián, Spain, [3] Spanish National Research Council (CSIC), Madrid, Spain, [4] Chair of Rehabilitation and Physical Medicine, Fuenlabrada University Hospital, Madrid, Spain

OPEN ACCESS

Edited by:
Dong Feng Huang, Sun Yat-sen University, China

Reviewed by:
Manuel F. Gaviria, Workinbio, France
Margit Alt Murphy, University of Gothenburg, Sweden

***Correspondence:**
Alicia Cuesta-Gómez
alicia.cuesta@urjc.es

Specialty section:
This article was submitted to Stroke, a section of the journal Frontiers in Neurology

Received: *27 January 2017*
Accepted: *18 April 2017*
Published: *10 May 2017*

Citation:
Cuesta-Gómez A, Molina-Rueda F, Carratala-Tejada M, Imatz-Ojanguren E, Torricelli D and Miangolarra-Page JC (2017) The Use of Functional Electrical Stimulation on the Upper Limb and Interscapular Muscles of Patients with Stroke for the Improvement of Reaching Movements: A Feasibility Study. Front. Neurol. 8:186. doi: 10.3389/fneur.2017.00186

Introduction: Reaching movements in stroke patients are characterized by decreased amplitudes at the shoulder and elbow joints and greater displacements of the trunk, compared to healthy subjects. The importance of an appropriate and specific contraction of the interscapular and upper limb (UL) muscles is crucial to achieving proper reaching movements. Functional electrical stimulation (FES) is used to activate the paretic muscles using short-duration electrical pulses.

Objective: To evaluate whether the application of FES in the UL and interscapular muscles of stroke patients with motor impairments of the UL modifies patients' reaching patterns, measured using instrumental movement analysis systems.

Design: A cross-sectional study was carried out.

Setting: The VICON Motion System® was used to conduct motion analysis.

Participants: Twenty-one patients with chronic stroke.

Intervention: The Compex® electric stimulator was used to provide muscle stimulation during two conditions: a placebo condition and a FES condition.

Main outcome measures: We analyzed the joint kinematics (trunk, shoulder, and elbow) from the starting position until the affected hand reached the glass.

Results: Participants receiving FES carried out the movement with less trunk flexion, while shoulder flexion elbow extension was increased, compared to placebo conditions.

Conclusion: The application of FES to the UL and interscapular muscles of stroke patients with motor impairment of the UL has improved reaching movements.

Keywords: electric stimulation therapy, movement disorders, paresis, range of motion, stroke, upper extremity

Abbreviations: ADL, activities of daily living; FES, functional electrical stimulation; LAMBECOM, laboratory of analysis of movement, biomechanics, ergonomics, and motor control; UL, upper limb; ROM, range of movement.

INTRODUCTION

Reaching movements in stroke patients are characterized by decreased amplitudes at the shoulder and elbow joints compared to healthy subjects (1–6). The movement pattern of patients with stroke is highly related to their level of motor function impairment, which becomes modified due to the lack of inter-articular coordination (1). There is a decrease in the range of motion at the elbow joint with a tendency toward flexion, which avoids correct extension of the upper limb (UL), hampering the ability to perform appropriate reaching movements. Excessive shoulder abduction is also observed as a compensatory movement when there is a lack of appropriate shoulder flexion (7).

In the case of the trunk, greater trunk displacements have been observed in patients with stroke, forward displacements, and torsion movements, which are related to deficits in elbow extension, and shoulder flexion and adduction, as compensatory mechanisms that occur during reaching movements or other activity. Patients are able to develop new motor strategies to achieve their goal despite UL deficits (1–7). There is a greater involvement of the trunk and scapula during the execution of reaching movements due to the creation of new movement strategies to compensate for the deficiencies (8).

The scientific literature has shown that stroke patients need to create new movement strategies. This involves the development of pathological synergies to carry out the desired movements. An example of this is the excessive movements of the trunk and scapula to compensate the deficiencies resulting from the pathology (7). Proper activation of the interscapular muscles depends on the position of the trunk. Stroke patients, due to the deficits affecting their trunk and scapular movement patterns, are under unfavorable conditions for being able to perform appropriate and selective activation of these muscles, which has a negative impact on the movement of the UL (9–11).

Regarding the UL muscles involved in reaching movements, a deficit in muscle control and activation has been observed (5, 12, 13). The synergistic contraction of the shoulder flexor and extensor muscles during reach becomes deteriorated due to muscle weakness and; therefore, the resulting movement is deficient (14). Furthermore, spastic muscle patterns may also prevent the correct performance of UL movements (15–18).

Functional electrical stimulation (FES) is a form of treatment that seeks to activate the paretic muscles using short-duration electrical pulses applied *via* surface electrodes through the skin (19). The use of FES and neuroprostheses has spanned almost four decades (20, 21). The use of FES as a neuroprosthesis consists of self-treatment at home by means of a neuroprosthetic neuromuscular stimulation system. The objective of this modality is to assist the performance of an activity of daily living (ADL) (22). Recently, functional and clinical improvements have been reported with the therapeutic application of FES, in which stimulation was used to increase voluntary movement after stroke (22, 23). Therapeutic FES modalities have been used to recruit UL muscles, improving weakness, the dyscoordination of single and multiple joints movements, and spasticity (24).

Most studies employing therapeutic FES for paretic UL rehabilitation are based on stimulation of the shoulder, elbow, and wrist muscles without recruitment of the interscapular muscles (25–28). The importance of an appropriate and specific contraction of the interscapular musculature during UL movement is necessary to adapt the position of the scapulothoracic joint to the degree of movement of the glenohumeral joint. This musculature has a stabilizing function upon the entire glenohumeral complex, which is necessary for a correct reaching movement (29–31). In healthy subjects, the posture of the trunk has been shown to influence changes in scapular movement and interscapular muscle activity during UL elevation (29, 32). The motor control of shoulder movement influences the correct and proper activation and synchronization of these muscles (33).

In this study, we tested the ability of a FES system to assist the UL movement of stroke patients based on the stimulation of interscapular, shoulder, elbow, wrist, and finger muscles. To our knowledge, no empirical study to date directly addresses this question. The authors hypothesized that participants receiving FES to the UL and interscapular muscles would be able to perform the movement with less trunk anteroposterior tilt and major shoulder flexion and elbow extension. The aim of this feasibility study was to evaluate whether the application of FES to the UL and interscapular muscles of stroke patients with UL motor impairment would be able to modify their reaching patterns, measured using instrumental movement analysis systems.

MATERIALS AND METHODS

Subjects

A cross-sectional study was conducted. Recruitment was based on the voluntary participation of patients with stroke and UL motor function impairment. The participants were recruited from rehabilitation facilities and patient associations. Contact with prospective participants was made *via* meetings with their clinicians and informative flyers.

The selection procedure was made by non-probabilistic sampling of consecutive cases of patients who met the inclusion criteria: subjects older than 30 years and younger than 70 years, with a confirmed diagnosis of chronic stroke (more than 6 months of evolution), the ability to manipulate most objects; a modified Ashworth scale score $\leq$2 in the UL muscles, deltoid, triceps brachii, biceps brachii and to the wrist and finger flexor an extensor muscles, the ability to understand instructions and actively cooperate in the tasks indicated by a score $\geq$20 in the Mini-mental Test and suitable family and social support, to assist the patient in the use of the FES device at home. Patients with mixed aphasia, hemineglect, articular rigidities (irreducible contractures and arthrodesis), severe sensitivity alterations that impeded the use of the FES system, and skin conditions that could hamper or render impossible the application of the FES system were excluded. This protocol was approved by the local ethics committee of the Rey Juan Carlos University. Informed consent was obtained from all participants included in this study.

Instrumentation

The Compex® electrical stimulator was used for muscle stimulation. Developed in Zurich, this device is considered one of the

most flexible and versatile FES systems available. It was designed to be used as a medical device for any FES application, either as a neuroprosthesis or as a research tool (34).

The VICON Motion System® (Oxford Metrics, Oxford, UK) was used for the purpose of motion analysis. This system consists of eight 100 Hz infrared capture cameras and a data station where the information is gathered and processed through the VICON Upper Limb 2.0® model (35).

Procedure

The research took place at the Laboratory of Analysis of Movement, Biomechanics, Ergonomics, and Motor Control (LAMBECOM), located in the Department of Physiotherapy, Occupational Therapy, Rehabilitation, and Physical Medicine of the Faculty of Health Sciences of the Rey Juan Carlos University.

In the first place, all patients granted their consent to participate in this study by signing the informed consent. The study protocol consisted primarily of a muscle training program that the patients performed at their own homes for a week. The purpose of these sessions was for the patient to become accustomed to the sensation of electrical stimulation, as well as to the training of the UL muscles, in order to subsequently undergo the evaluation process satisfactorily.

The home training program consisted of two sessions per day, for 7 days, of 30 min of stimulation. In the first session, stimulation was applied to the wrist and finger extensor muscles and to the triceps brachii. In the second session, the anterior deltoid and interscapular muscles were stimulated. The training program was pre-defined and consisted of 2 min at 1 Hz, 200 μs with 7.5 s of stimulation, and 7.5 s of rest; 16 min at 25 Hz, 200 μs and 7.5 s of stimulation, and 7.5 s of rest; and 2 min at 1 Hz, 200 μs and 7.5 s of stimulation, and 7.5 s of rest. The participants were told to indicate all deleterious effects such as skin discomfort, referred pain, paresthesia, and uncomfortable muscle contractions.

Once the training period was carried out, the instrumental evaluation was performed in the LAMBECOM using the Vicon® system. For this purpose, 12 passive reflective markers of 14 mm were placed in specific locations of the affected UL and trunk of the patients according to the Vicon UL model (35). The locations were: the spinous process of the seventh cervical vertebra, the spinous process of the 10th thoracic vertebra, the acromion, the center of the right scapular spine, the sternal manubrium, the xiphoid apophysis, the lateral epicondyle of the humerus, the middle third of the forearm, the radial styloid apophysis, the ulnar styloid apophysis, and the base of the third metacarpal bone.

Four muscle groups were selected for muscle stimulation: the interscapular muscles, the anterior deltoid, the triceps brachii, and the wrist and finger extensor muscles. Adhesive and square shaped Dura-Stick® electrodes were used (5 cm × 5 cm) (**Figure 1**). The placement of these electrodes depended on the muscle area in which the best muscle contraction occurred. The frequency, pulse width, and duration of the FES onset ramp were set at 25 Hz, 200 μs, and 0.5 s, respectively, for the entire session. The current intensity was established according to the optimal amplitude necessary for producing the muscular contraction and the desired movement in each patient, and according to patient tolerance (submaximal contraction). Hence, prior to the evaluation, different trials were performed to choose the most appropriate intensity.

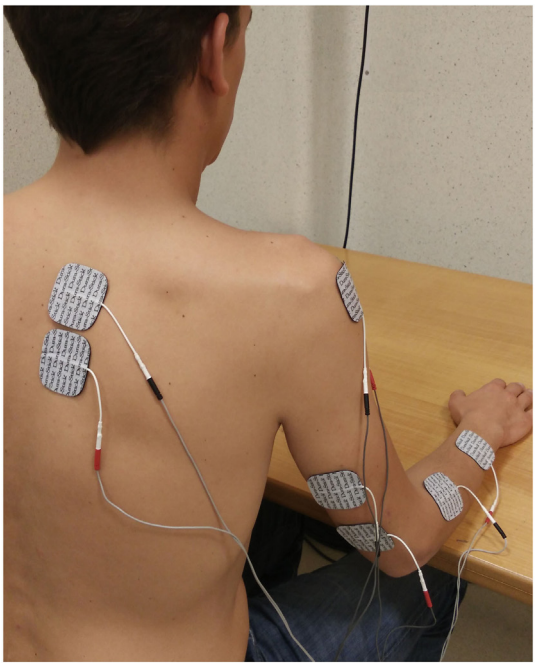

FIGURE 1 | Patient with the functional electrical stimulation device.

The kinematic analysis consisted of the patients performing six repetitions for each condition of the reaching task while being measured with a motion capture platform based on the Vicon Motion (Oxford Metrics, Oxford, UK) optoelectronic system.

The conditions were: condition 1: placebo; and condition 2: FES. In condition 1, the selected muscles were stimulated with electrical impulses, but with an amplitude that did not produce movement. In condition 2, electrical stimuli were applied to the triceps brachii, anterior deltoid, extensor muscles of the wrist, and fingers and interscapular muscles (lower trapezius and rhomboid), to favor the scapular approximation, the stabilization of the scapula with regard to the trunk, the external rotation of the shoulder, and the coaptation of the glenohumeral joint (31, 32).

To perform these trials, the patients were placed in a sitting position on a wooden chair without a backrest. The patient-to-desk distance was 8–10 cm. Patients were asked to put their hands on the desk (palms down) with their shoulder at around 15° flexion, 20° abduction, and with the elbow at around 90° flexion. A hard plastic glass (diameter = 5.5 cm, height = 15 cm) was used as the target. The glass was placed on the desk in line with the patient's sternum and at a distance equal to 75% of the maximum reachable distance with the paretic arm.

Patients were instructed to reach and touch the glass from the starting position using their paretic hand and then they returned to the initial position. All patients practiced the reaching task before motion capture trials. Once this phase was completed, a static calibration recording was performed. Using this recording, we checked that each marker was visible from the scanning

cameras and the analyzed movements were registered. In these, after the verbal instruction "Get ready…go," patients had to lift their arm and reach and touch the glass at a comfortable speed.

For this, each patient performed the reaching task under two different conditions. Each condition was repeated six times in a randomized manner.

The sequence of muscular activation with electrical stimuli was: first the interscapular muscles to get the thorax to extend, followed by the anterior deltoid and the triceps brachii to achieve the reaching movement, and finally, the wrist and fingers extensor muscles to touch the glass.

Outcome Measures

We analyzed the joint kinematics (trunk, shoulder, and elbow) when the affected hand reached the glass from the starting position. The end of the movement was considered as the point when the affected hand touched the glass. The beginning of the movement was when the trunk became straightened or extended because the stimulation with placebo and FES began (**Figure 2**).

We established the beginning of the movement using the Vicon Nexus software v1.8.5®, creating an event immediately when the stimulation begins and the verbal commands ("Get ready…go"). Another event was created at the end of the movement when the affected hand touched the glass and the stimulation ceased. Two raters evaluated these events, and if there were discrepancies between them, a third rater was consulted in order to reach an agreement.

The following kinematic parameters were analyzed: trunk, shoulder, and elbow joint angles at the beginning of the movement; trunk, shoulder, and elbow joint angles at the end of the movement; and trunk, shoulder, and elbow joint range of movement (ROM) during reaching. Range of motion was the difference between the joint angles (degrees) at the beginning and at the end of the reaching movement. Positive values in trunk, shoulder, and elbow joint angles indicated flexion. A negative value or a reduction in the value of the trunk, shoulder, and elbow positions indicated extension.

The Vicon Nexus software v1.8.5® was used to calculate outcome measures based on the biomechanical model of the Vicon Upper limb® model. The output angles for all joints were calculated from the YXZ cardan angles, derived by comparing the relative orientations of the two segments. The trunk angle was measured relative to the laboratory axes. The angle of the shoulder segment was relative to the proximal segment, i.e., the shoulder to the trunk. The angle of the elbow was a relative angle between the upper arm and the forearm (35).

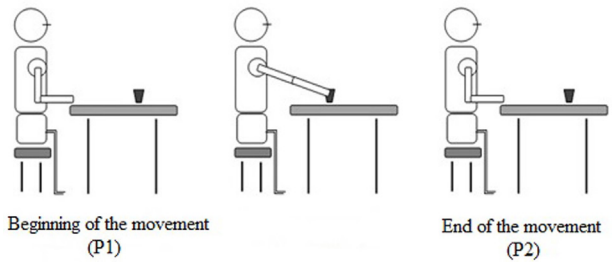

FIGURE 2 | Reaching movement.

Henmi et al. (36) evaluated the validity and reliability of the Vicon Upper Limb® model in healthy subjects. For this, they examined the ranges of movement of the cervical spine, shoulder, elbow, and forearm, using the Vicon Motion System® and a universal goniometer. The authors obtained an excellent Pearson correlation coefficient for shoulder flexion (0.94) and elbow flexion (0.91). In addition, the SD between the repeated measurements was very small: 0.78° for shoulder flexion and 0.89° for elbow flexion.

Statistical Analysis

The statistical analysis was carried out using the SPSS statistical software system (SPSS Inc., Chicago, IL, USA; version 22.0). A normal distribution for the kinematic parameters was found using the Shapiro–Wilk test and Kolmogorov–Smirnov test.

The Student's *t*-test for related samples was used for the analysis of kinematic parameters, comparing the data for the two conditions (FES and placebo). Descriptive statistics were used to summarize data, including calculation of the means and SDs for continuous data. The statistical analysis was performed with a confidence level of 95%, so that significant values were considered at $p < 0.05$.

RESULTS

The sample consisted of a total of 21 male patients with chronic stroke, of the 25 selected at the study onset. Four subjects were excluded because they were unable to attend the evaluation appointments due to logistical problems. The ages of the included participants ranged between 40 and 69 years old (with a mean age of 59.12 ± 10.31 years). The affected UL was analyzed in this study. Concretely, 11 patients presented left UL paresis (52.38%) and 10 has right UL paresis (47.62%). The affected UL was on the dominant side in 14 participants (66.67%) and, on the non-dominant side, in 7 participants (33.33%). The mean time since the stroke episode was 6.18 ± 3.12 years. Regarding the type of stroke, 38.10% (8) were ischemic and 61.90% (13) were hemorrhagic. The mean score of participants on the motor function domain of the UL-FMA was 26.87 out of 66 points (SD 10.6), with 72.25 out of 126 points (SD 20.41) on the total score of the UL-FMA (including the sensory, passive ROM, and pain subscales). The amplitude of the stimulation needed to produce the muscular contraction ranged between 17 and 42 mA, depending on the muscle groups and the stimulation threshold of each participant.

Table 1 summarizes the kinematic parameters studied for the trunk, shoulder, and elbow during the reaching task.

The participants with FES decreased their trunk ROM and showed less trunk flexion in the end of reaching compared to the participants with placebo FES. We did not observe significant differences in the angle of the trunk at the beginning; however, when the stimulation began, the participants with FES also began the reaching movement with less trunk forward flexion (i.e., from a more extended position).

During the reaching movement with FES, the participants increased the shoulder flexion at the end of the movement and the

TABLE 1 | Joint kinematics in the sagittal plane (degrees).

	Placebo functional electrical stimulation (FES)	FES	Within subjects analysis		
			DM	CI 95%	*p*
Trunk P1	6.49 (2.09)	8.06 (2.21)	−1.57	From −3.14 to 0.005	0.054
Trunk P2	15.81 (5.73)	13.44 (5.38)	2.37	From 0.08 to 6.42	0.043*
Trunk ROM	7.31 (5.77)	5.37 (4.49)	−1.93	From −3.44 to −0.43	0.015*
Shoulder P1	15.69 (4.75)	15.71 (4.52)	−0.019	From −1.72 to 1.68	0.981
Shoulder P2	31.75 (16.25)	34.62 (15.31)	−2.86	From −4.43 to −1.30	0.001*
Shoulder ROM	16.05 (14.64)	18.90 (14.93)	−2.84	From −4.93 to −0.76	0.011*
Elbow P1	90.10 (5.51)	91.11 (2.73)	−1.01	From −3.37 to 3.98	0.998
Elbow P2	77.73 (14.71)	72.69 (16.44)	5.03	From 2.17 to 7.90	0.002*
Elbow ROM	−12.37 (11.74)	−17.40 (16.61)	5.03	From 0.42 to 9.64	0.034*

ROM is range of movement (amplitude between the beginning and the end of the movement); a negative elbow range of motion indicates extension. P1 is the beginning of the reaching. P2 is the end of the reaching.

Data are expressed as mean (SD). DM is difference of means. CI 95% is confidence interval.

**p-Value < 0.05 using Student's t-test for related samples.*

ROM compared to the participants who performed the reaching task with placebo FES.

The elbow joint showed significant differences in the final position when the affected hand reached the object. The participants increased their elbow extension using the FES compared to the placebo. In addition, the elbow ROM significantly increased in the FES condition compared to the placebo condition.

The trunk and arm position at the beginning of the movement was similar in both groups. In addition, the SD was low. However, when the stimulation began and the affected hand reached the glass, the SD increased in trunk, shoulder, and elbow P2 and ROM. This is probably because the participants use different patterns to perform the task. For example, some participants in the FES group showed a smaller increase of shoulder flexion and elbow extension because the movement was performed with greater trunk flexion (**Figure 3**).

DISCUSSION

The aim of this feasibility study was to evaluate whether the application of FES to the UL and interscapular muscles (rhomboid and lower trapezius), in stroke patients with motor impairment of the UL, would be able to modify patients' reaching pattern, measured with a motion capture system.

The scientific literature available has shown that FES systems improve subjects' reaching patterns. However, no studies have evaluated the effectiveness of the same using instrumental and objective motion capture systems. These systems help us to discriminate the UL pattern performed by each patient. Therefore, despite the heterogeneity of the sample, the use of the motion capture system has enabled us to examine each movement pattern in order to determine whether FES stimulation was able to modify the subjects' UL pattern. To our knowledge, this is the first study using FES that specifically includes the interscapular muscles within the protocol of stimulated muscles.

Concerning the results obtained for the analyzed variables of the trunk movements in the sagittal plane, we have found significant differences in the trunk ROM and in the end position reached between the conditions. The trunk ROM during reaching was found to be lower in participants who performed the movement with FES, who also displayed a decrease in trunk tilt. This reduction in the ROM and trunk tilt may occur because the participants with FES began the movement with their trunk in a more neutral position. In addition, the interscapular stimulation may improve the trunk posture toward a more extend position. The motion of the scapula is influenced by muscle forces and joint reaction forces, which arise from the thoracic surface as well as the acromioclavicular and glenohumeral joints. Also, the stability of the scapula influences both the trunk and UL motions (37). It is probable that the initial stimulation of interscapular muscles may have helped these patients to achieve this posture. Different authors have shown that trunk flexion complicates the performance of UL tasks. For appropriate UL movements, a correct starting position at the level of the trunk and scapula is necessary (9, 10).

In the case of patients with stroke, the deficits that are typically present in their trunk and scapula movement patterns place them at a disadvantage for achieving an appropriate and selective activation of these muscles and, consequently, this has a detrimental effect on the movement of their UL (9, 10). Notably, a number of authors have reported that the excessive trunk movement of these patients is due to an inappropriate activation of the scapular musculature (8–10), which explains why stimulation at this level should improve the movement pattern with a lesser tendency toward forward trunk bending.

Regarding the application of electrostimulation to the muscles of the UL, the combination of proximal and distal stimulation may potentially restore function to a much larger group of patients compared to previous works that only stimulated hand opening (38, 39). In line with our findings, previous reports have shown that voluntary shoulder movement and reaching effort increases wrist and hand flexion force, requiring additional extension force to open the hand in stroke patients. The correct movement of the UL may reduce the grasp force and may be useful to assist the performance of ADLs in individuals with a hemiparetic arm (40). The importance of the stimulation of the triceps brachii has been demonstrated in previous studies, which have demonstrated that the torques generated by triceps

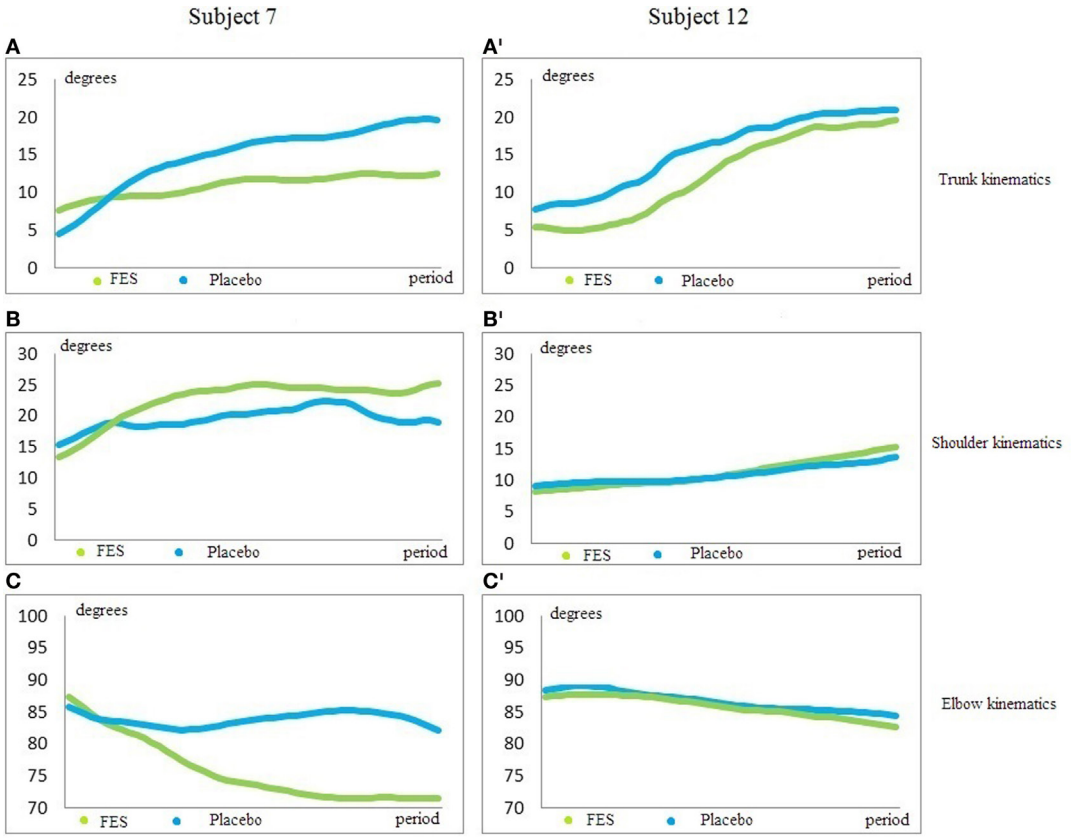

FIGURE 3 | **Trunk, shoulder, and elbow kinematics**. **(A,A')** is trunk kinematics; **(B,B')** is shoulder kinematics; **(C,C')** is elbow kinematics. *X*-axis shows degrees. *Y*-axis is the period between the beginning and the end of the motion. Blue line is the reaching pattern with placebo condition; green line is the reaching pattern with functional electrical stimulation (FES). The subjects begin the movement in a similar position in both conditions. However, the joint positions at the end of the movement are very different in each subject. The participant 7 with FES condition decreased the trunk flexion **(A)**, increased the shoulder flexion **(B)**, and increased the elbow extension **(C)**. The participant 12 with FES condition showed a smaller increase of shoulder flexion **(B')** and elbow extension **(C')** because the movement was performed with greater trunk flexion **(A')**. Both participants performed an improved reaching movement with FES compared to placebo.

stimulation for producing elbow extension may have beneficial effects during dynamic reaching (41).

In stroke subjects, the application of electrostimulation to the muscles of the UL has been found to enhance the reacquisition of motor skills with the affected UL and to increase the degree of shoulder flexion and elbow extension, thus assisting the reaching movement, as measured with motion analysis systems; our results confirm and extend these previous works (42–44) by demonstrating that FES applied to the UL muscles is effective for improving simple single joint movements as well as more complex reach-to-grasp movements performed with the hemiparetic UL. Makowski et al. (42) and Lew et al. (43) studied different reaching movements and ADLs in chronic stroke patients, *via* the application of FES. The results they obtained showed improvements in range distances, hand opening, an increase in forearm muscle activity, and the ability to complete ADLs in which shoulder flexion was required and in which elbow extension was required and which the patients were initially unable to perform. However, the authors of the aforementioned study did not report kinematic values for the different joints, which is why we are unable to discern which joint is able to explain the improvements in movement. Furthermore, the prior study did not stimulate the interscapular muscles and; therefore, we cannot compare our kinematic data. On the other hand, Koesler et al. (44) studied the kinematics of the UL while performing median nerve stimulation to the origin of the brachial biceps in 12 patients with chronic stroke. The results of their study demonstrated improvements in analytical UL movements and in complex movements, such as reach and grip. These data are comparable to our findings although in the case of the former study, there was no electrical stimulation at the muscle level, but rather, stimulation was performed directly upon the nerve. In contrast, after using FES and an exoskeleton for reaching and grasping in 18 patients with stroke, Grimm and Gharabaghi (45) stated that FES alone was insufficient for the correct performance of the selected movements in these patients. They concluded that the use of the relief device was essential to achieve the performance of the reach and grip exercises. Our results differ with the aforementioned study by suggesting that stroke patients are able to perform ROM with FES.

Recent research has shown that the repetitive practice of a motor task combined with positive feedback leads to the reorganization of the motor cortex. Changes in cortical excitability increase even more when motor tasks are performed, which require more skill on the part of the patient (46), thus the active participation in the performance of the task leads to a substantial increase in cortical excitability in comparison with passive or non-functional training (47). Somatosensory input is essential for motor learning, and it has been suggested that an increase in the excitability of corticospinal projections to the muscles of the paretic hand may facilitate functional recovery of dexterity after stroke (48). Corticospinal excitability can be increased by periods of electrical stimulation, transcranial direct current brain stimulation, or a combination of both (49).

In stroke rehabilitation, specific training or repetitive exercise can increase corticospinal excitability and improve function of the paretic hand (50). Therefore, one of the main advantages of FES is the ability of the patient to perform repetitive movements in any environment, which significantly enhances their ability to recover (51). In addition to enhancing function, FES enables people to engage in therapies that require a prescribed level of voluntary ability. Thus, the use of FES during and after therapy is most likely of value in cases of moderate to severe chronic deficiency, where therapeutic interventions to date have been less effective (26). The literature suggests that a small number of individuals with severe impairments are unable to regain motor control in the UL. These individuals with chronic stroke suffer from weakness, spasticity, atrophy, and stiff joints due to the stroke and learned non-use. Our findings suggest that the use of FES may be beneficial for such individuals. We have shown that FES can produce functional arm movement and is able to reduce the pathological pattern of the reaching movement in these patients, such as excessive trunk bending instead of a greater shoulder flexion and elbow extension.

According to the results of this study, the stimulation of interscapular and UL muscles using FES increases the range of motion of the shoulder and elbow compared to placebo conditions. Most studies have used FES stimulation for UL muscles without stimulating the interscapular muscles. These studies reported that the UL ROM also increased. Therefore, further studies are required comparing which type of stimulation is most appropriate: FES for UL muscles alone or a combined stimulation with FES for UL and interscapular muscles. In addition, it is important for future works to include kinematic data of the UL joint in order to compare our results regarding kinematics with other types of FES stimulation. The study demonstrates the suitability of the proposed stimulation with FES, because there were not deleterious events during the application, the performance of the intervention was easy and the systems used for stimulation are accessible. Therefore, it would be possible to carry out this type of intervention in clinical environments.

The present study has several limitations that need to be addressed in the future. Due to the clinical variability inherent to stroke, it was difficult to form a homogeneous experimental group in terms of motor characteristics such as movement patterns. However, despite the heterogeneity of the sample, significant changes in joint kinematics have been observed. Another limitation is that the same patient group was treated under two different conditions. Future studies should include independent groups and add a follow-up to understand the effects of FES stimulation over time. Also, the interscapular muscle stimulation with percutaneous FES was unable to specifically stimulate the rhomboid muscle or lower fibers of trapezius. It is possible that a more specific stimulation of these muscles may improve the trunk position and generate a more physiological reaching movement. In addition, further works should analyze the ROM of trunk movement from the start of the stimulation to the start of the reaching in order to evaluate the influence of the stimulation on the interscapular muscles in trunk posture. Finally, this study did not analyze the wrist and finger kinematics due to the fact that the motion capture systems are shown to be more reliable for shoulder and elbow movements (36).

CONCLUSION

We provide kinematic evidence that the application of FES in the UL and interscapular muscles of stroke patients with motor impairment of the UL has reduced the trunk tilt and increased the shoulder flexion and elbow extension, improving the reaching movement, compared to the placebo stimulation. In addition, the stimulation of interscapular muscles (rhomboid and lower trapezius) may help to improve the trunk position during the UL movements through the scapula. To our knowledge, this is the first study to use a protocol that includes the stimulation of these muscles. The findings of this feasibility study show that FES has no side effects and that the electrical dose described in this manuscript could be taken into account in a large study. Further trials with follow-up, a control group, and larger samples are necessary to compare the effectiveness of this modality of FES.

ETHICS STATEMENT

The study was approved by the Human Ethics Committee of the Rey Juan Carlos University.

AUTHOR CONTRIBUTIONS

All the authors have contributed equally to the research.

ACKNOWLEDGMENTS

This research has been supported by Spanish Ministry of Science project HYPER PROJECT (CONSOLIDER-INGENIO 2010) Hybrid Neuroprosthetic and Neurorobotic Devices for Functional Compensation and Rehabilitation of Motor Disorders. HYPER-CSD2009-00067.

REFERENCES

1. Cirstea MC, Levin MF. Compensatory strategies for reaching in stroke. *Brain* (2000) 123(Pt 5):940–53. doi:10.1093/brain/123.5.940
2. Hingtgen BA, McGuire JR, Wang M, Harris GF. Quantification of reaching during stroke rehabilitation using unique upper extremity kinematic model. *Conf Proc IEEE Eng Med Biol Soc* (2004) 7:4916–9. doi:10.1109/IEMBS.2004.1404359
3. Hingtgen B, McGuire JR, Wang M, Harris GF. An upper extremity kinematic model for evaluation of hemiparetic stroke. *J Biomech* (2006) 39(4):681–8. doi:10.1016/j.jbiomech.2005.01.008
4. Messier S, Bourbonnais D, Desrosiers J, Roy Y. Kinematic analysis of upper limbs and trunk movement during bilateral movement after stroke. *Arch Phys Med Rehabil* (2006) 87(11):1463–70. doi:10.1016/j.apmr.2006.07.273
5. Molina-Rueda F, Rivas-Montero FM, Pérez-de-Heredia-Torres M, Alguacil-Diego IM, Molero Sánchez A, Miangolarra Page JC. Movement analysis of upper extremity hemiparesis in patients with cerebrovascular disease: a pilot study. *Neurologia* (2012) 27(6):343–7. doi:10.1016/j.nrl.2011.12.012
6. Robertson JV, Roby-Brami A. The trunk as a part of the kinematic chain for reaching movements in healthy subjects and hemiparetic patients. *Brain Res* (2011) 25:137–46. doi:10.1016/j.brainres.2011.01.043
7. Roby-Brami A, Jacobs S, Bennis N, Levin MF. Hand orientation for grasping and arm joint rotation patterns in healthy subjects and hemiparetic stroke patients. *Brain Res* (2003) 969(1–2):217–29. doi:10.1016/S0006-8993(03)02334-5
8. Roby-Brami A, Feydy A, Combeaud M, Biryukova EV, Bussel B, Levin MF. Motor compensation and recovery for reaching in stroke patients. *Acta Neurol Scand* (2003) 107:369–81. doi:10.1034/j.1600-0404.2003.00021.x
9. De Baets L, Van Deun S, Desloovere K, Jaspers E. Dynamic scapular movement analysis: is it feasible and reliable in stroke patients during arm elevation? *PLoS One* (2013) 8(11):e79046. doi:10.1371/journal.pone.0079046
10. De Baets L, Van Deun S, Monari D, Jaspers E. Three-dimensional kinematics of the scapula and trunk, and associated scapular muscle timing in individuals with stroke. *Hum Mov Sci* (2016) 48:82–90. doi:10.1016/j.humov.2016.04.009
11. De Baets L, Jaspers E, Janssens L, Van Deun S. Characteristics of neuromuscular control of the scapula after stroke: a first exploration. *Front Hum Neurosci* (2014) 8:933. doi:10.3389/fnhum.2014.00933
12. Levin MF, Selles RW, Verheul MH, Meijer OG. Deficits in the coordination of agonist and antagonist muscles in stroke patients: implications for normal motor control. *Brain Res* (2000) 853(2):352–69. doi:10.1016/S0006-8993(99)02298-2
13. Silva CC, Silva A, Sousa A, Pinheiro AR, Bourlinova C, Silva A, et al. Co-activation of upper limb muscles during reaching in post-stroke subjects: an analysis of the contralesional and ipsilesional limbs. *J Electromyogr Kinesiol* (2014) 24(5):731–8. doi:10.1016/j.jelekin.2014.04.011
14. Kisiel-Sajewicz K, Fang Y, Hrovat K, Yue GH, Siemionow V, Sun CK, et al. Weakening of synergist muscle coupling during reaching movement in stroke patients. *Neurorehabil Neural Repair* (2001) 25(4):359–68. doi:10.1177/1545968310388665
15. Garreta R, Chaler J, Torrequebrada A. Guía de práctica clínica del tratamiento de la espasticidad con toxina botulínica. *Rev Neurol* (2010) 50(11):685–99.
16. Hefter H, Jost WH, Reissig A, Zakine B, Bakheit AM, Wissel J. Classification of posture in poststroke upper limb spasticity: a potential decision tool for botulinum toxin A treatment? *Int J Rehabil Res* (2012) 35:227–33. doi:10.1097/MRR.0b013e328353e3d4
17. Lundstrom E, Terent A, Borg J. Prevalence of disabling spasticity 1 year after first-ever stroke. *Eur J Neurol* (2008) 15:533–9. doi:10.1111/j.1468-1331.2008.02114.x
18. Sommerfeld DK, Eek EU, Svensson AK, Holmqvist LW, von Arbin MH. Spasticity after stroke: its occurrence and association with motor impairments and activity limitations. *Stroke* (2004) 35:134–9. doi:10.1161/01.STR.0000105386.05173.5E
19. Popovic MR, Thrasher TA. Neuroprostheses. In: Wnek GE, Bowlin GL, editors. *Encyclopedia of Biomaterials and Biomedical Engineering*. New York, NY: Marcel Dekker (2004). p. 1056–65.
20. Peckhma PH, Knutson JS. Functional electrical stimulation for neuromuscular applications. *Annu Rev Biomed Eng* (2005) 7:327–60. doi:10.1146/annurev.bioeng.6.040803.140103
21. Gracanin F. Use of electrical stimulation in external control of motor activity and movements of human extremities. Actual situation and problems. *Med Prog Technol* (1977) 4(4):149–56.
22. Ring H, Rosenthal N. Controlled study of neuroprosthetic functional electrical stimulation in sub-acute post-stroke rehabilitation. *J Rehabil Med* (2005) 37:32–6. doi:10.1080/16501970410035387
23. Popovic MB, Popovic DB, Sinkjaer T, Stefanovic A, Schwirtlich L. Restitution of reaching and grasping promoted by functional electrical therapy. *Artif Organs* (2002) 26(3):271–5. doi:10.1046/j.1525-1594.2002.06950.x
24. Daly JJ, Ruff RL. Construction of efficacious gait and upper limb functional interventions based on brain plasticity evidence and model-based measures for stroke patients. *ScientificWorldJournal* (2007) 20(7):2031–45. doi:10.1100/tsw.2007.299
25. Chae J, Bethoux F, Bohine T, Dobos L, Davis T, Friedl A. Neuromuscular stimulation for upper extremity motor and functional recovery in acute hemiplegia. *Stroke* (1998) 29:975–9. doi:10.1161/01.STR.29.5.975
26. Gritsenko V, Prochazka A. A functional electric stimulation-assisted exercise therapy system for hemiplegic hand function. *Arch Phys Med Rehabil* (2004) 85:881–5. doi:10.1016/j.apmr.2003.08.094
27. Meadmore KL, Exell TA, Hallewell E, Hughes AM, Freeman CT, Kutlu M, et al. The application of precisely controlled functional electrical stimulation to the shoulder, elbow and wrist for upper limb stroke rehabilitation: a feasibility study. *J Neuroeng Rehabil* (2014) 30(11):105. doi:10.1186/1743-0003-11-105
28. Peckham PH, Knutson JS. Functional electrical stimulation for neuromuscular applications. *Annu Rev Biomed Eng* (2005) 7:327–60. doi:10.1146/annurev.bioeng.6.040803.140103
29. Nagai K, Tateuchi H, Takashima S, Miyasaka J, Hasegawa S, Arai R, et al. Effects of trunk rotation on scapular kinematics and muscle activity during humeral elevation. *J Electromyogr Kinesiol* (2013) 23:679–87. doi:10.1016/j.jelekin.2013.01.012
30. Phadke V, Ludewig PM. Study of the scapular muscle latency and deactivation time in people with and without shoulder impingement. *J Electromyogr Kinesiol* (2013) 23:469–75. doi:10.1016/j.jelekin.2012.10.004
31. Wickham J, Pizzari T, Stansfeld K, Burnside A, Watson L. Quantifying 'normal' shoulder muscle activity during abduction. *J Electromyogr Kinesiol* (2010) 20:212–22. doi:10.1016/j.jelekin.2009.06.004
32. Yamauchi T, Hasegawa S, Matsumura A, Nakamura M, Ibuki S, Ichihashi N. The effect of trunk rotation during shoulder exercises on the activity of the scapular muscle and scapular kinematics. *J Shoulder Elbow Surg* (2015) 24:955–64. doi:10.1016/j.jse.2014.10.010
33. Ebaugh DD, McClure PW, Karduna AR. Three-dimensional scapulothoracic motion during active and passive arm elevation. *Clin Biomech* (2005) 20:700–9. doi:10.1016/j.clinbiomech.2005.03.008
34. Popovic MR, Keller T. Modular transcutaneous functional electrical stimulation system. *Med Eng Phys* (2005) 27(1):81–92. doi:10.1016/j.medengphy.2004.08.016
35. Vicon Upper Limb Product Guide. Foundation Notes Revision 2.0. *For Use with Plug-in Gait Version 2.0 in Vicon Nexus*. (2010).
36. Henmi S, Yonenobu K, Masatomi T, Oda K. A biomechanical study of activities of daily living using neck and upper limbs with an optical three-dimensional motion analysis system. *Mod Rheumatol* (2006) 16(5):289–93. doi:10.3109/s10165-006-0499-x
37. Seth A, Matias R, Veloso AP, Delp SL. A biomechanical model of the scapulothoracic joint to accurately capture scapular kinematics during shoulder movements. *PLoS One* (2016) 11(1):e0141028. doi:10.1371/journal.pone.0141028
38. Chae J, Hart R. Intramuscular hand neuroprosthesis for chronic stroke survivors. *Neurorehabil Neural Repair* (2003) 17:109–17. doi:10.1177/0888439003017002005
39. Hines AE, Crago PE, Billian C. Hand opening by electrical stimulation in patients with spastic hemiplegia. *IEEE Trans Neural Syst Rehabil Eng* (1995) 3:193–205. doi:10.1109/86.392368
40. Miller LC, Dewald JP. Involuntary paretic wrist/finger flexion forces and EMG increase with shoulder abduction load in individuals with chronic stroke. *Clin Neurophysiol* (2012) 123:1216–25. doi:10.1016/j.clinph.2012.01.009

41. Keller T, Ellis MD, Dewald JP. Overcoming abnormal joint torque patterns in paretic upper extremities using triceps stimulation. *Artif Organs* (2005) 29:229–32. doi:10.1111/j.1525-1594.2005.29041.x
42. Makowski N, Knutson J, Chae J, Crago P. Functional electrical stimulation to augment post stroke reach and hand opening in the presence of voluntary effort: a pilot study. *Neurorehabil Neural Repair* (2014) 28(3):241–9. doi:10.1177/1545968313505913
43. Lew B, Alavi N, Randhawa BK, Menon C. An exploratory investigation on the use of closed-loop electrical stimulation to assist individuals with stroke to perform fine movements with their hemiparetic arm. *Front Bioeng Biotechnol* (2016) 4:20. doi:10.3389/fbioe.2016.00020
44. Koesler IB, Dafotakis M, Ameli M, Fink GR, Nowak DA. Electrical somatosensory stimulation improves movement kinematics of the affected hand following stroke. *J Neurol Neurosurg Psychiatry* (2009) 80(6):614–9. doi:10.1136/jnnp.2008.161117
45. Grimm F, Gharabaghi A. Closed-loop neuroprosthesis for reach-to-grasp assistance: combining adaptive multi-channel neuromuscular stimulation with a multi-joint arm exoskeleton. *Front Neurosci* (2016) 10:284. doi:10.3389/fnins.2016.00284
46. Barsi GI, Popovic DB, Tarkka IM, Sinkjaer T, Grey MJ. Cortical excitability changes following grasping exercise augmented with electrical stimulation. *Exp Brain Res* (2008) 191:57–66. doi:10.1007/s00221-008-1495-5
47. Perez MA, Lungholt BK, Nyborg K, Nielsen JB. Motor skill training induces changes in the excitability of the leg cortical area in healthy humans. *Exp Brain Res* (2004) 159:197–205. doi:10.1007/s00221-004-1947-5
48. Wu CW, Seo HJ, Cohen LG. Influence of electric somatosensory stimulation on paretic hand function in chronic stroke. *Arch Phys Med Rehabil* (2006) 87:351–7. doi:10.1016/j.apmr.2005.11.019
49. Conforto AB, Cohen LG, dos Santos RL, Scaff M, Marie SK. Effects of somatosensory stimulation on motor function in chronic cortico-subcortical strokes. *J Neurol* (2007) 254:333–9. doi:10.1007/s00415-006-0364-z
50. Muellbacher W, Richards C, Ziemann U, Wittenberg G, Weltz D, Boroojerdi B, et al. Improving hand function in chronic stroke. *Arch Neurol* (2002) 59:1278–82. doi:10.1001/archneur.59.8.1278
51. Alon G, Ring H. Gait and hand function enhancement following training with a multi-segment hybrid-orthosis stimulation system in stroke patients. *J Stroke Cerebrovasc Dis* (2003) 12:209–16. doi:10.1016/S1052-3057(03)00076-4

Conflict of Interest Statement: The authors declare that the research was conducted in the absence of any commercial or financial relationships that could be construed as a potential conflict of interest.

frontiers in Neurology

CLINICAL TRIAL
published: 30 October 2017
doi: 10.3389/fneur.2017.00568

Improvement of Upper Extremity Deficit after Constraint-Induced Movement Therapy Combined with and without Preconditioning Stimulation Using Dual-hemisphere Transcranial Direct Current Stimulation and Peripheral Neuromuscular Stimulation in Chronic Stroke Patients: A Pilot Randomized Controlled Trial

Takashi Takebayashi[1,2], Kayoko Takahashi[3], Misa Moriwaki[4], Tomosaburo Sakamoto[5] and Kazuhisa Domen[6]*

[1] Graduate Course of Rehabilitation Science, Hyogo College of Medicine, Nishinomiya, Japan, [2] Department of Occupational Therapy, School of Health Science and Social Welfare, Kibi International University, Takahashi, Japan, [3] Department of Rehabilitation, School of Allied Health Science, Kitasato University, Sagamihara-shi, Japan, [4] Department of Rehabilitation Medicine, Midorigaoka Hospital, Takatsuki, Japan, [5] Department of Rehabilitation, Kansai Rehabilitation Hospital, Toyonaka, Japan, [6] Department of Rehabilitation Medicine, Hyogo College of Medicine, Nishinomiya, Japan

OPEN ACCESS

Edited by:
Guanglin Li,
Shenzhen Institutes of Advanced Technology (CAS), China

Reviewed by:
Vincent Thijs,
Florey Institute of Neuroscience and Mental Health, Australia
Cliff Klein,
Guangdong Province Work Injury Rehabilitation Hospital, China

***Correspondence:**
Takashi Takebayashi
takshi77@kiui.ac.jp

Specialty section:
This article was submitted to Stroke, a section of the journal Frontiers in Neurology

Received: 31 May 2017
Accepted: 11 October 2017
Published: 30 October 2017

Citation:
Takebayashi T, Takahashi K, Moriwaki M, Sakamoto T and Domen K (2017) Improvement of Upper Extremity Deficit after Constraint-Induced Movement Therapy Combined with and without Preconditioning Stimulation Using Dual-hemisphere Transcranial Direct Current Stimulation and Peripheral Neuromuscular Stimulation in Chronic Stroke Patients: A Pilot Randomized Controlled Trial. Front. Neurol. 8:568. doi: 10.3389/fneur.2017.00568

In this study, we investigated the effects of dual-hemisphere transcranial direct current stimulation (dual-tDCS) of both the affected (anodal tDCS) and non-affected (cathodal tDCS) primary motor cortex, combined with peripheral neuromuscular electrical stimulation (PNMES), on the effectiveness of constraint-induced movement therapy (CIMT) as a neurorehabilitation intervention in chronic stroke. We conducted a randomized controlled trial of feasibility, with a single blind assessor, with patients recruited from three outpatient clinics. Twenty chronic stroke patients were randomly allocated to the control group, receiving conventional CIMT, or the intervention group receiving dual-tDCS combined with PNMES before CIMT. Patients in the treatment group first underwent a 20-min period of dual-tDCS, followed immediately by PNMES, and subsequent CIMT for 2 h. Patients in the control group only received CIMT (with no pretreatment stimulation). All patients underwent two CIMT sessions, one in the morning and one in the afternoon, each lasting 2 h, for a total of 4 h of CIMT per day. Upper extremity function was assessed using the Fugl-Meyer Assessment (primary outcome), as well as the amount of use (AOU) and quality of movement (QOM) scores, obtained *via* the Motor Activity Log (secondary outcome). Nineteen patients completed the study, with one patient withdrawing after allocation. Compared to the control group, the treatment improvement in

upper extremity function and AOU was significantly greater in the treatment than control group (change in upper extremity score, 9.20 ± 4.64 versus 4.56 ± 2.60, respectively, $P < 0.01$, $\eta^2 = 0.43$; change in AOU score, 1.10 ± 0.65 versus 0.62 ± 0.85, respectively, $P = 0.02$, $\eta^2 = 0.52$). There was no significant effect of the intervention on the QOM between the intervention and control groups (change in QOM score, 1.00 ± 0.62 versus 0.71 ± 0.72, respectively, $P = 0.07$, $\eta^2 = 0.43$; treatment versus control). Our findings suggest a novel pretreatment stimulation strategy based on dual-tDCS and PNMES may enhance the therapeutic benefit of CIMT.

Keywords: constraint-induced movement therapy, upper extremity, transcranial direct current stimulation, neuromuscular stimulation, stroke, rehabilitation

INTRODUCTION

Approximately 15–30% of stroke survivors experience long-lasting upper extremity hemiparesis (1), with poststroke motor deficits of the upper extremity being a serious clinical concern. Therefore, treatments for upper extremity motor deficits are a critical component of stroke rehabilitation. In the 1980s, Taub et al. developed constraint-induced movement therapy (CIMT) as an intensive treatment for upper extremity motor deficit in chronic stroke patients (2). CIMT consists of task-oriented training for the affected upper extremity and a "transfer package" representing a behavioral method for enhancing adherence to treatment. Many previous studies have confirmed the effectiveness of CIMT for improving upper extremity function in chronic stroke patients (2–4). CIMT has been recommended by several guidelines for the improvement of the affected upper extremity function in chronic stroke patients (5, 6). In addition, several researchers have suggested that CIMT promotes plastic changes in the cortex, both contralateral and ipsilateral to the stroke lesion, in animal models of stroke and human stroke patients (7–9). The plasticity of the primary motor cortex is particularly important for the improvement in upper extremity motor function.

On the other hand, non-invasive brain stimulation has recently been shown to promote plastic changes when combined with standard physical or occupational therapy. Particularly, transcranial direct current stimulation (tDCS) has been used for priming cortical excitability during motor and behavioral training. The therapeutic mechanisms underlying improvement with tDCS involves effects on the activity of the Na^+/Ca^{++} channel and *N*-methyl-D-aspartate receptor (10, 11), and promoting motor cortex plasticity, in a dose dependent, *via* activation effects on brain-derived neurotrophic factor and tropomyosin receptor kinase B (12). Cortex stimulation *via* tDCS is achieved using fine direct current from two electrodes placed on the scalp, which enhances the long-lasting modulation of cortical excitability through the depolarization or hyperpolarization of cells (13).

Two different tDCS strategies are used, namely anodal and cathodal stimulation, which increase or decrease the excitability level of cells, respectively. In an animal model, anodal tDCS of the affected hemisphere increases the excitability of the affected motor cortex for a few hours poststimulation (14). In healthy human subjects and in stroke patients, anodal tDCS of the affected hemisphere, combined with rehabilitation treatment, induced a modulation of cortical excitability of the affected motor cortex and promoted improvement of motor function on the affected side (15, 16). On the contrary, cathodal tDCS of the unaffected hemisphere combined with rehabilitation treatment decreased the excitability of the unaffected motor cortex, downregulating interhemispheric inhibition from the unaffected to the affected hemisphere, and improving motor function on the affected side in stroke patients (17). Recently, several researchers have recommended that both anodal and cathodal tDCS can be applied at the same time to act upon the affected and unaffected motor cortex, respectively (18–20). This tDCS strategy, termed dual-hemisphere tDCS (dual-tDCS), might further downregulate interhemispheric inhibition from the affected to the unaffected hemisphere. In addition, dual-tDCS was found to modulate intracortical and/or interhemispheric processing of primary motor cortex stimuli (21). In fact, Bolognini et al. (22) suggested that, compared to standard CIMT, dual-tDCS combined with CIMT yielded greater improvement in motor function of the affected upper extremity in chronic stroke patients.

While the current body of literature provides evidence that tDCS may promote rehabilitation-induced improvement in the motor function of the affected upper extremity in chronic stroke patients, several weaknesses of tDCS have been described. Uy and Ridding (23) suggested that, while anodal tDCS can increase the excitability of the cortex, the effects lasts <15 min. Nevertheless, these researchers also proposed that peripheral nerve stimulation (PNS) was a good strategy to prolong the effect of tDCS. The mechanism underlying the improvement in motor function with PNS are likely to be influenced by activity of the *N*-methyl-D-aspartate receptors (24–26) and GABAergic interneurons in the sensorimotor cortex. In fact, several researchers have demonstrated the added therapeutic effectiveness of combining tDCS, PNS, or peripheral neuromuscular electrical stimulation (PNMES), with rehabilitation (27–29). However, there are few articles that have shown the effectiveness of tDCS or dual tDCS combined with PNS or PNMES. Therefore, clear evidence of the effectiveness of this combined stimulation has not been established. Additionally, in CIMT's study, the safety and effectiveness of this combined therapy (dual-tDCS combined with PNMES before CIMT) compared to CIMT alone, have yet to be examined.

Therefore, further research based upon the knowledge and experience obtained from previous studies is needed to develop a more efficient treatment strategy in stroke patients with motor

deficit due to hemiparesis. In the present study, we first explored the hypothesis that the combination of dual-tDCS and PNMES, with adjustment of the level of muscle action potential evoked, would promote the effect of behavioral and motor therapy compared to conventional CIMT alone in chronic stroke patients with a paretic upper extremity. Additionally, we also evaluated the safety of the preconditioning treatment before CIMT compared to conventional CIMT alone.

MATERIALS AND METHODS

Study Design

This pilot, multicenter, randomized, controlled study was carried out in accordance with the recommendations of the "Ethical guidelines for medical and health research involving human subject, Ministry of Education, Culture, Sports, Science, and Technology in Japan," with written informed consent from all subjects. All study protocols were approved by the institutional review boards of each participating facility. The study was registered with the University Hospital Medical Information Network Clinical Trial Registry (UMIN000020927), which is a public trial registry.

Subjects

Patients were recruited from outpatient stroke clinics affiliated with three participating facilities. The inclusion criteria were as follows: age, 20–90 years; and with a first stroke in chronic stage (>180 days from stroke onset). The exclusion criteria were as follows: bilateral or brain stem infarct or hemorrhage; voluntary extension of the metacarpophalangeal and interphalangeal joints of three or more fingers ≤10° or voluntary wrist extension ≤20°; severe impairment in balance or walking, indicated by the need for assistance for standing, walking or using the toilet; substantial use of the affected upper extremity before the intervention, indicated by a score of >2.5 points on the amount of use (AOU) scale of the Motor Activity Log (MAL); clear signs of dementia or cognitive disorder, indicated by a score <24 points in the Mini-Mental State Examination; severe aphasia or apraxia, preventing the patient from participating in the activities involved in the study intervention; presence of another uncontrolled medical condition or severe end-stage disease; and severe contraction in the area of the shoulder, elbow, wrist, or fingers.

Sample Size Calculation

Before initiating the trial, we calculated that ten patients with chronic stroke should be enrolled in each group. A previous study suggested that a pilot study sample size should be 10% of sample size of project study (30). The largest CIMT study conducted to date was the EXCITE study (3), which enrolled about 100 patients in each group. Additionally, Hwetzog (31) recommended that pilot studies include 10–40 patients per group to provide an accurate estimation of treatment outcome. Therefore, we estimated 10 patients in each group would be sufficient.

Randomization and Blinding

Participants were randomized into the control group (conventional CIMT) or the treatment group (dual-tDCS and PNMES plus CIMT) by a researcher blinded to group allocation and who was not directly involved in this study. Randomization was performed according to Zelen's method, combined with minimization algorithm to control for the following factors: age (in years), time from stroke onset (in days), and baseline upper extremity score based on Fugl-Meyer Assessment (FMA) (32).

Protocol for This Study

The patients in the treatment group first received dual-tDCS for 20 min, followed immediately by PNMES, and then CIMT for 2 h. Pretreatment stimulation (dual-tDCS and PNMES) was applied both before the morning CIMT session and before the afternoon CIMT session (**Figure 1**). Dual-tDCS was performed using a DC-STIMULATOR PLUS (neuroConn GmbH, Ilmenau, Germany). For dual-tDCS, the anode was placed over the affected primary motor cortex (point C3 or C4 according to the 10–20 system), while the cathode was placed over the unaffected primary motor cortex (point C4 or C3 according to the 10–20 system). The following stimulation protocol was used for tDCS: constant current of 1-mA intensity (15), applied for 20 min (33), followed by PNMES performed using a TORIO stimulation system (Ito Co. Ltd., Tokyo, Japan), with two self-adhesive electrodes placed on the extensor digitorum muscle. Trains of electrical stimulation (20 Hz, on/off duty cycle 150/150μs; pulse duration, 300 μs) were applied at 1 Hz for 10 min. Stimulation intensity was set at a level where each patient reported mild paresthesia, but no pain, and minimal visible muscle contractions were evoked (23). Patients in the control group did not receive any stimulation. Sham stimulation was not used because the PNMES device used in this study did not have a setting permitting sham stimulation.

All patients received 4 h of CIMT (2 h in the morning and 2 h in the afternoon) from Monday to Friday for 2 weeks (10 consecutive weekdays). CIMT was provided by trained occupational therapists, according to a CIMT protocol described in detail elsewhere (34). CIMT is based on three main principles, namely:

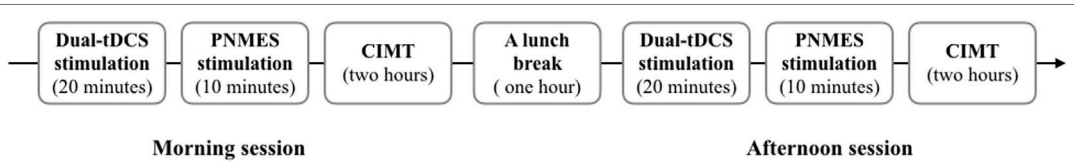

FIGURE 1 | Daily rehabilitation protocol in the treatment group. Dual-tDCS, dual-hemisphere transcranial direct current stimulation; PNMES, peripheral neuromuscular electrical stimulation; CIMT, constraint-induced movement therapy.

repetitive task-oriented training (shaping and task practice); training to facilitate the transfer of functional gains achieved in the clinical setting to the activities of daily living in real life ("transfer-package" training); and restraint of the less affected upper extremity using a mitt.

Functional Assessment

We assessed the motor function of the affected upper extremity and its use in real-world behaviors, before and immediately after CIMT, using the FMA for the upper extremity, primary outcome (32), and MAL [AOU and quality of movement (QOM)], as the secondary outcome, respectively (35). The FMA for the upper extremity consists of 33 items, each scored on a 3-point ordinal scale: 0 point, cannot perform the action; 1 point, can perform the action only partially; and 2 points, can perform the action fully. Thus, the maximum possible upper extremity score was 66 points. The AOU and QOM scores, components of the MAL, indicate how much and how well, respectively, the affected upper extremity is used during 14 activities of daily living. For each activity of daily living, the patient rates the extent of the activity performed and how well it can be performed using the affected upper extremity. MAL scoring uses a 6-point Likert scale, ranging from 0 (never used) to 5 (used as prior to stroke). The mean AOU score reflects the frequency of the activity, whereas the mean QOM score reflects how well the activity was performed. The maximum value for the AOU and QOM scores is 5 points. The FMA and MAL assessments were performed by blinded and trained occupational therapists who was not directly involved in the treatment or patient allocation to intervention groups.

Statistical Analysis

All data were analyzed using JMP version 13.0 (SAS Institute, Cary, NC, USA). Between-group differences in baseline characteristics were assessed using Fisher's exact test (categorical data) or unpaired t test (ordinal data). Treatment effectiveness between the treatment and control group, which was assessed by analysis of covariance (ANCOVA), which was used to control for the baseline FMA score, and the AOU and QOM score of MAL, respectively. Finally, differences in upper extremity motor function, between baseline and postintervention, were assessed within each group using paired *t*-test. In all statistical comparisons, a $P < 0.05$ was considered statistically significant. The effect size index η^2 (ANCOVA) and Δ (paired *t*-test) were also calculated. Data were presented as the mean (SD).

RESULTS

A total of 28 candidates were screened between November 2014 and March 2017, of whom 20 patients were randomized into the treatment group or the control group (**Figure 2**). One patient

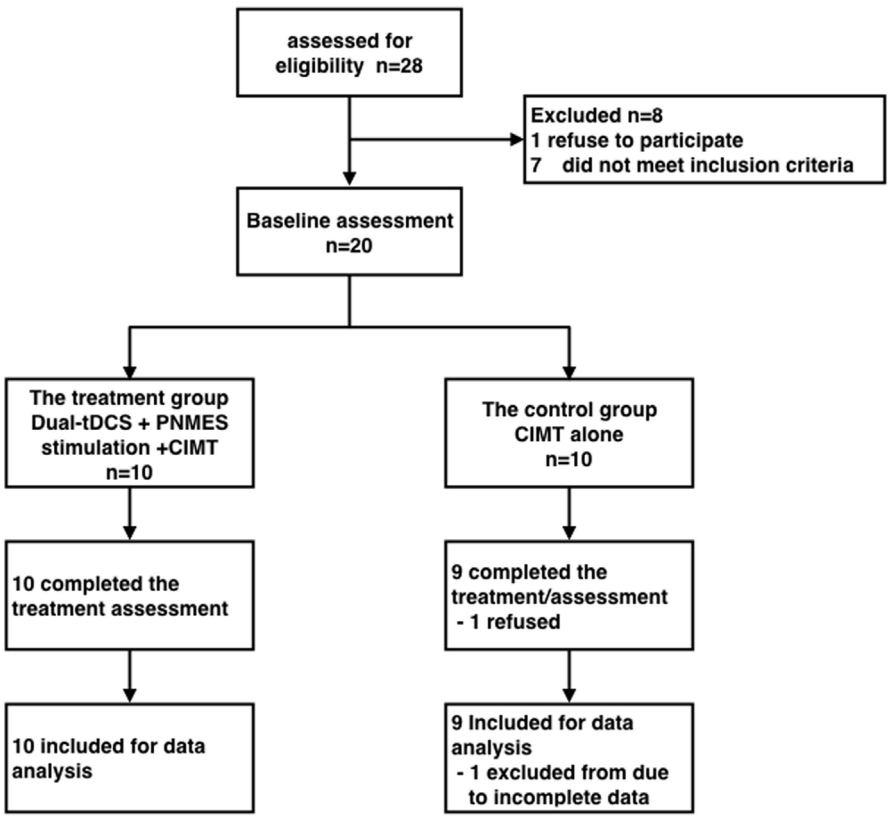

FIGURE 2 | Flow-chart of patient enrollment in the study. Dual-tDCS, dual-hemisphere transcranial direct current stimulation; PNMES, peripheral neuromuscular electrical stimulation; CIMT, constraint-induced movement therapy.

TABLE 1 | Baseline characteristics of the patients enrolled in the study.

Characteristic		Treatment group ($n = 10$)	Control group ($n = 10$)	Difference
				P-value
Age (years)		58.90 (8.28)	59.7 (15.82)	0.89
Gender, male/female		8/2	6/4	0.33
Time from stroke onset (days)		922.30 (693.95)	1,195.7 (1546.48)	0.62
Affected side, right/left		5/5	5/5	1.00
Hand dominance, right/left		10/0	9/1	0.30
Stroke type, hemorrhage/infarction		4/6	2/8	0.33
Site of lesion	Putamen	3	3	
	Prefrontal cortex	2	3	
	Corona radiata	1	1	
	Thalamus	3	2	
	Internal capsule	1	1	
Upper extremity score *via* FMA		43.00 (9.82)	44.00 (8.01)	0.81
AOU score *via* MAL		1.51 (0.78)	1.42 (0.79)	0.80
QOM score *via* MAL		1.55 (0.77)	1.36 (0.71)	0.57

Data shown as average (SD) or number of observations.
AOU, amount of use; FMA, Fugl-Meyer Assessment; MAL, Motor Activity Log; QOM, quality of movement.

allocated to the control group withdrew from the study after allocation. No adverse events were identified in either the treatment or control group. The two groups did not differ significantly in terms of baseline characteristics (**Table 1**).

The ANCOVA identified a greater improvement in the treatment than control group on the FMA upper extremity score [9.20 (4.64) versus 4.56 (2.60) for the treatment versus control, respectively; $P < 0.01$; $\eta^2 = 0.43$] and MAL AOU score [1.10 (0.65) versus 0.62 (0.85), respectively; $P = 0.02$; $\eta^2 = 0.52$]. However, no significant between-group difference in improvement was noted for the QOM scale of MAL [1.00 (0.62) versus 0.71 (0.72) for the treatment versus control, respectively; $P = 0.07$; $\eta^2 = 0.43$] (**Table 2**).

Within the treatment group, all motor performance indicators showed significant improvement from baseline: FMA upper extremity score, 43.00 (9.82) versus 52.20 (8.28), $P < 0.01$, $\Delta = 0.94$, 95% confidence interval (95% CI) 5.89–13.22; AOU score of MAL, 1.51 (0.78) versus 2.61 (0.66), $P < 0.01$, $\Delta = 1.41$, 95% CI = 0.62–1.66; QOM score of MAL, 1.55 (0.77) versus 2.55 (0.65), $P < 0.01$, $\Delta = 1.30$, 95% CI = 0.52–1.53 (all values represent baseline versus posttreatment, respectively).

Similarly, within the control group, all indicators of motor performance improved significantly from baseline, namely: FMA upper extremity score, 45.44 (6.98) versus 50.00 (8.82), $P < 0.01$, $\Delta = 0.65$, 95% CI = 2.91–6.49; AOU score of MAL, 1.40 (0.84) versus 2.02 (0.70), $P = 0.04$, $\Delta = 0.74$, 95% CI = 0.05–1.20; QOM score of MAL, 1.33 (0.74) versus 2.04 (0.68), $P < 0.01$, $\Delta = 0.96$, 95% CI = 0.23–1.21 (all values represent baseline versus posttreatment, respectively).

TABLE 2 | Outcomes of motor performance assessment at baseline and postintervention.

Outcome measure	Treatment group ($n = 10$)	Control group ($n = 9$)	Difference
			P-value[a] (η^2 value)[b]
Upper extremity score *via* FMA			
Baseline	43.00 (9.82)	45.44 (6.98)	
Postintervention	52.20 (8.28)	50.00 (8.82)	
Improvement	9.20 (4.64)	4.56 (2.60)	<0.01 (0.43)
AOU score *via* MAL			
Baseline	1.51 (0.78)	1.40 (0.83)	
Postintervention	2.61 (0.66)	2.02 (0.70)	
Improvement	1.10 (0.65)	0.61 (0.85)	0.02 (0.52)
QOM score *via* MAL			
Baseline	1.55 (0.77)	1.33 (0.74)	
Postintervention	2.55 (0.65)	2.04 (0.68)	
Improvement	1.10 (0.65)	0.71 (0.72)	0.07 (0.43)

AOU, amount of use; FMA, Fugl-Meyer Assessment; MAL, Motor Activity Log; QOM quality of movement.
[a]*Between-group comparisons involved analysis of covariance.*
[b]*Effect size was assessed using the η^2 value.*

DISCUSSION

Our present findings indicate that, compared with patients who undergo behavioral and motor treatment alone, those who undergo behavioral and motor treatment after receiving *dual-tDCS* and PNMES recovered motor function (FMA upper extremity) and real-world (AOU in MAL) to a greater extent than patients who received conventional CIMT alone. Additionally, we confirmed that this combined treatment was as safe as the conventional CIMT alone.

Effectiveness of the Dual-tDCS Combined with PNMES

Several researchers have defined the minimum clinically important difference regarding paretic upper extremity motor recovery in chronic stroke patients as an improvement above 4.25 points in the FMA upper extremity score and above 0.5 points in the AOU score (36, 37). In our study, both groups achieved improvements higher than these thresholds of clinically important difference on the FMA and AOU. Additionally, on the FMA upper extremity scale, the improvement was 4.64 points higher in the treatment than in the control group, and this between-group difference

was also above the threshold for a clinically meaningful change. These findings suggest that behavioral motor treatment, combined with tDCS and PNMES, can provide meaningful improvement in upper limb function chronic stroke patients. On other hand, we found no significant between-group difference between in terms of the QOM score of the MAL. However, η^2 of the effect size of the between-group difference was 0.43. According to Cohen, effect size assessed in terms of η^2 is considered small effect for $\eta^2 < 0.01$, medium effect for $0.01 < \eta^2 < 0.06$, and large effect for $\eta^2 > 0.14$ (38). Therefore, although the *P*-value ($P = 0.07$) did not indicate a significant difference between the groups in terms of the QOM score of MAL, the η^2 value indicated that this difference was indicative of a substantial effect of the combined treatment. This discrepancy might be explained by statistical errors (type II error or false negatives), most likely related to the small sample size and thus insufficient power in the statistical analysis. Additionally, Lang et al. (39) reported that the minimum clinically important difference regarding the improvement in the QOM score of MAL in stroke patients amounts to an increase of 1.00–1.10 points. In our study, the minimum clinically important difference in the QOM score of MAL was noted in treatment group but not in the control group, which supports the conclusion that there is consistently higher improvement in the treatment group even though the between-group difference in QOM score improvement was not statistically significant.

Possibility of the PNMES in Neurorehabilitation Using the tDCS

The novelty of the present study lies in that we used a combination of dual-tDCS and PNMES, rather than only dual-tDCS or PNMES, to prolong the duration of the neural modulation effect. We found a clinically meaningful improvement in the motor function of the affected limb, reflected in the 9.2-point improvement in FMA upper extremity score [from 43.00 (9.82) to 52.20 (8.28)]. A previous study reported that dual-tDCS followed by CIMT achieved only a 6.3-point improvement in FMA upper extremity score (from 25.4 to 31.7 points) (22). This previous study used a similar CIMT treatment protocol as that applied in the present study (4 h per day for 10 consecutive weekdays). Compared to these previous observations, our findings indicated higher improvement in motor function on the affected side, although it should be noted that the degree of severity of deficit at baseline differed substantially between the two studies (patients in the present study were less affected upper extremity function compared to patients of the previous study). Therefore, our result showed that the novelty combination stimulation (dual-tDCS combined with the PNMES) strategy holds promise to improve the affected motor function rather than the dual-tDCS stimulation strategy alone. However, in this study, we could not make a strong claim about effectiveness of our novelty stimulation strategy, because we did not directly compare between the above two different stimulation strategies.

Limitations and Scope for Further Study

The limitations of our study should be noted. First, the sample size of the present study was very small, with 10 patients in the treatment group and 9 patients in control group. We are planning to perform future trials after performing power calculations to estimate the minimum sample size necessary to ascertain the effectiveness of the combined treatment. The results obtained in this pilot study will serve for calculating the expected effect size. Second, we did not include a sham group because the device for PNMES did not have a setting for sham stimulation. Our result might include the placebo effect in which patients in the treatment group received some positive psychological effects because they understood that the PNMES might provide a positive treatment effect. Therefore, the placebo effect acting on the data regarding patients in the treatment group cannot be excluded. Third, in this study, we established the group that received CIMT alone as a control group. However, to investigate the effects of dual-tDCS combined with PNMES, we should establish a group that received CIMT combined with the dual-tDCS. We plan to address this issue in a further study.

Conclusion and Clinical Implications

Despite the above limitations, the present trial clearly suggested that, compared to behavioral and motor rehabilitation alone, non-invasive stimulation with dual-tDCS and PNMES followed by behavioral and motor treatment provides greater effectiveness to enhance the recovery of motor function and real-world use of the affected upper extremity in patients with chronic stroke. Therefore, in chronic stroke patients, the novel pretreatment based on dual-tDCS and PNMES may enhance the therapeutic benefit of CIMT.

ETHICS STATEMENT

This study was carried out in accordance with the recommendations of "Ethical guidelines for medical and health research involving human subject, Ministry of Education, Culture, Sports, Science, and Technology in Japan" with written informed consent from all subjects. All study protocols were approved by the institutional review boards of each participating facility (Hyogo College of Medicine, Kansai Rehabilitation Hospital, and Midorigaoka Hospital).

AUTHOR CONTRIBUTIONS

TT contributed equally in the study design, data collection, data analysis, and writing and reviewing the manuscript. KT, MM, TS, and KD contributed to writing and reviewing the manuscript.

ACKNOWLEDGMENTS

The authors express their profound appreciation to all the therapists at Hyogo College of Medicine, Kansai Rehabilitation Hospital, and Midorigaoka Hospital for their diligence and commitment to excellence during this study.

REFERENCES

1. Rosamond W, Flegal K, Furie K, Go A, Greenlund K, Haase N, et al. Heart disease and stroke statistics–2008 update: a report from the American Heart Association Statistics Committee and Stroke Statistics Subcommittee. *Circulation* (2008) 117:e25–146. doi:10.1161/CIRCULATIONAHA.107.187998
2. Taub E, Miller NE, Novack TA, Cook EW III, Fleming WC, Nepomuceno CS, et al. Technique to improve chronic motor deficit after stroke. *Arch Phys Med Rehabil* (1993) 74:347–54.
3. Wolf SL, Winstein CJ, Miller JP, Taub E, Uswatte G, Morris D, et al. Effect of constraint-induced movement therapy on upper extremity function 3 to 9 months after stroke: the EXCITE randomized clinical trial. *JAMA* (2006) 296:2095–104. doi:10.1001/jama.296.17.2095
4. Taub E, Uswatte G, King DK, Morris D, Cargo JE, ChatterJee A. A placebo-controlled trial of constraint-induced movement therapy for upper extremity after stroke. *Stroke* (2006) 37:1045–9. doi:10.1161/01.STR.0000206463.66461.97
5. Miller EL, Murray L, Richards L, Zorowitz RD, Bakas T, Clark P, et al. Comprehensive overview of nursing and interdisciplinary rehabilitation care of the stroke patient: a scientific statement from the American Heart Association. *Stroke* (2010) 41:2402–48. doi:10.1161/STR.0b013e3181e7512b
6. Winstein CJ, Stein J, Arena R, Bates B, Cherney LR, Cramer SC, et al. Guidelines for adult stroke rehabilitation and recovery: a guideline for healthcare professionals from the American Heart Association/American Stroke Association. *Stroke* (2016) 47:e98–169. doi:10.1161/STR.0000000000000098
7. Nudo RJ, Wise BM, SiFuentes F, Milliken GW. Neural substrates for the effects of rehabilitative training on motor recovery after ischemic infarct. *Science* (1996) 272:1791–4. doi:10.1126/science.272.5269.1791
8. Liepert J, Bauder H, Wolfgang HR, Miltner WH, Taub E, Weiller C. Treatment-induced cortical reorganization after stroke in humans. *Stroke* (2000) 31:1210–6. doi:10.1161/01.STR.31.6.1210
9. Pascual-Leone A, Amedi A, Fregni F, Merabet LB. The plastic human brain cortex. *Annu Rev Neurosci* (2005) 28:377–401. doi:10.1146/annurev.neuro.27.070203.144216
10. Liebetanz D, Nitsche MA, Tergau F, Paulus W. Pharmacological approach to the mechanisms of transcranial DC-stimulation-induced after-effects of human motor cortex excitability. *Brain* (2002) 125:2238–47. doi:10.1093/brain/awf238
11. Nitsche MA, Fricke K, Henschke U, Schlitterlau A, Liebetanz D, Lang M, et al. Pharmacological modulation of cortical excitability shifts induced by transcranial direct current stimulation in humans. *J Physiol* (2003) 553:293–301. doi:10.1113/jphysiol.2003.049916
12. Fritsch B, Reis J, Martinowich K, Schambra HM, Ji Y, Cohen LG, et al. Direct current stimulation promotes BDNF-dependent synaptic plasticity: potential implications for motor learning. *Neuron* (2010) 66:198–204. doi:10.1016/j.neuron.2010.03.035
13. Dimyan MA, Cohen LG. Contribution of transcranial magnetic stimulation to the understanding of functional recovery mechanisms after stroke. *Neurorehabil Neural Repair* (2010) 24:125–35. doi:10.1177/1545968309345270
14. Bindman LJ, Lippold OC, Redfearn JWT. The action of brief polarizing currents on the cerebral cortex of the rat (1) during current flow and (2) in the production of long-lasting after-effects. *J Physiol* (1964) 172:369–82. doi:10.1113/jphysiol.1964.sp007425
15. Nitsche MA, Paulus W. Excitability changes induced in the human motor cortex by weak transcranial direct current stimulation. *J Physiol* (2000) 527:633–9. doi:10.1111/j.1469-7793.2000.t01-1-00633.x
16. Kim DY, Lim JY, Kang EK, You DS, Oh BK, Oh BS, et al. Effect of transcranial direct current stimulation on motor recovery in patients with subacute stroke. *Am J Phys Med Rehabil* (2010) 89:879–86. doi:10.1097/PHM.0b013e3181f70aa7
17. Nair DG, Renga V, Lindenberg R, Zhu L, Schlaug G. Optimizing recovery potential through simultaneous occupational therapy and non-invasive brain-stimulation using tDCS. *Restor Neurol Neurosci* (2011) 29:411–20. doi:10.3233/RNN-2011-0612
18. Fregni F, Pascual-Leone A. Technology insight: noninvasive brain stimulation in neurology-perspectives on the therapeutic potential of rTMS and tDCS. *Nat Clin Pract Neurol* (2007) 3:383–93. doi:10.1038/ncpneuro0530
19. Nowak DA, Grefkes C, Ameli M, Fink GR. Interhemispheric competition after stroke: brain stimulation to enhance recovery of function of the affected hand. *Neurorehabil Neural Repair* (2009) 23:641–56. doi:10.1177/1545968309336661
20. Lindenberg R, Renga V, Zhu LL, Nair D, Schlaug G. Bihemispheric brain stimulation facilitates motor recovery in chronic stroke patients. *Neurology* (2010) 75:2176–84. doi:10.1212/WNL.0b013e318202013a
21. Sehm B, Kipping J, Schäfer A, Villringer A, Ragert P. A comparison between uni- and bilateral tDCS effects on functional connectivity of the human motor cortex. *Front Hum Neurosci* (2013) 7:183. doi:10.3389/fnhum.2013.00183
22. Bolognini N, Vallar F, Casati C, Latif LA, El-Nazer R, Williams J, et al. Neurophysiological and behavioral effects of tDCS combined with constraint-induced movement therapy in poststroke patients. *Neurorehabil Neural Repair* (2011) 25:819–29. doi:10.1177/1545968311411056
23. Uy J, Ridding MC. Increased cortical excitability induced by transcranial DC and peripheral nerve stimulation. *J Neurosci Methods* (2003) 127:193–7. doi:10.1016/S0165-0270(03)00142-0
24. Kaelin-Lang A, Luft AR, Sawaki L, Burstein AH, Sohn YH, Cohen LG. Modulation of human corticomotor excitability by somatosensory input. *J Physiol* (2002) 540:623–33. doi:10.1113/jphysiol.2001.012801
25. Celnik P, Hummel F, Harris-Love M, Wolk R, Cohen LG. Somatosensory stimulation enhances the effects of training functional hand tasks in patients with chronic stroke. *Arch Phys Med Rehabil* (2007) 88:1369–76. doi:10.1016/j.apmr.2007.08.001
26. Ridding MC, Pearce SL, Flavel SC. Modulation of intracortical excitability in human hand motor areas. The effect of cutaneous stimulation and its topographical arrangement. *Exp Brain Res* (2005) 163:335–43. doi:10.1007/s00221-004-2176-7
27. Satow T, Kawase T, Kitamura A, Kajitani Y, Yamaguchi T, Tanabe N, et al. Combination of transcranial direct current stimulation and neuromuscular electrical stimulation improves gait ability in a patient in chronic stage of stroke. *Case Rep Neurol* (2016) 8:39–46. doi:10.1159/000444167
28. Celnik P, Pail NJ, Vandermeeren Y, Dimyan M, Cohen LG. Effects of combined peripheral nerve stimulation and brain polarization on performance of a motor sequence task after chronic stroke. *Stroke* (2009) 40:1764–71. doi:10.1161/STROKEAHA.108.540500
29. Sattler V, Acket B, Raposp N, Albucher JF, Thalamas C, Loubinoux I, et al. Anodal tDCS combined with radial nerve stimulation promotes hand motor recovery in the acute phase after ischemic stroke. *Neurorehabil Neural Repair* (2015) 29:743–54. doi:10.1177/1545968314565465
30. Connelly LM. Pilot studies. *Medsurg Nurs* (2008) 17:411–2.
31. Hwetzog MA. Considerations in determining sample size for pilot studies. *Res Nurs Health* (2008) 31:180–91. doi:10.1002/nur.20247
32. Fugl-Meyer AR, Jääskö L, Leyman I, Olsson S, Steglind S. The post-stroke hemiplegic patient. 1. A method for evaluation of physical performance. *Scand J Rehabil Med* (1975) 7:13–31.
33. Giacobbe V, Krebs HI, Volpe BT, Pascual-Leone A, Rykman A, Zeiarati G, et al. Transcranial direct current stimulation (tDCS) and robotic practice in chronic stroke: the dimension of timing. *NeuroRehabilitation* (2013) 33:49–56. doi:10.3233/NRE-130927
34. Takebayashi T, Amano S, Hanada K, Umeji A, Takahashi K, Marumoto K, et al. A one-year follow-up after modified constraint-induced movement therapy for chronic stroke patients with paretic arm: a prospective case series study. *Top Stroke Rehabil* (2015) 22:18–25. doi:10.1179/1074935714Z.0000000028
35. van der Lee JH, Beckerman H, Knol DL, de Vet HC, Bouter LM. Clinimetric properties of the motor activity log for the assessment of arm use in hemiparetic patients. *Stroke* (2004) 35:1410–4. doi:10.1161/01.STR.0000126900.24964.7e
36. Page SJ, Fulk GD, Boyne P. Clinically important differences for the upper-extremity Fugl-Meyer Scale in people with minimal to moderate impairment due to chronic stroke. *Phys Ther* (2012) 92:791–8. doi:10.2522/ptj.20110009
37. van der Lee JH, Wangenaar RC, Lankhorst GJ, Vogelaar TW, Devillé WL, Bouter LM. Forced use of the upper extremity in chronic stroke patients: results from a single-blind randomized clinical trial. *Stroke* (1999) 30:2369–75. doi:10.1161/01.STR.30.11.2369
38. Cohen J. *Statistical Power Analysis for the Behavioral Science*. 2nd ed. New York, NY: Routledge Academic (2005). p. 51–5.

39. Lang CE, Edwards DF, Birkenmeier RL, Dromerick AW. Estimating minimal clinically important differences of upper-extremity measures early after stroke. *Arch Phys Med Rehabil* (2008) 89:1693–700. doi:10.1016/j.apmr.2008.02.022

Conflict of Interest Statement: The authors declare that the research was conducted in the absence of any commercial or financial relationships that could be construed as a potential conflict of interest.

frontiers in Neurology

ORIGINAL RESEARCH
published: 04 December 2017
doi: 10.3389/fneur.2017.00646

Sliding Mode Tracking Control of a Wire-Driven Upper-Limb Rehabilitation Robot with Nonlinear Disturbance Observer

Jie Niu[1†], Qianqian Yang[1†], Xiaoyun Wang[2] and Rong Song[1]*

[1]*Guangdong Provincial Engineering and Technology Center of Advanced and Portable Medical Devices, School of Engineering, Sun Yat-sen University, Guangzhou, China,* [2]*Injury Rehabilitation Hospital of Guangdong Province, Guangzhou, China*

Robot-aided rehabilitation has become an important technology to restore and reinforce motor functions of patients with extremity impairment, whereas it can be extremely challenging to achieve satisfactory tracking performance due to uncertainties and disturbances during rehabilitation training. In this paper, a wire-driven rehabilitation robot that can work over a three-dimensional space is designed for upper-limb rehabilitation, and sliding mode control with nonlinear disturbance observer is designed for the robot to deal with the problem of unpredictable disturbances during robot-assisted training. Then, simulation and experiments of trajectory tracking are carried out to evaluate the performance of the system, the position errors, and the output forces of the designed control scheme are compared with those of the traditional sliding mode control (SMC) scheme. The results show that the designed control scheme can effectively reduce the tracking errors and chattering of the output forces as compared with the traditional SMC scheme, which indicates that the nonlinear disturbance observer can reduce the effect of unpredictable disturbances. The designed control scheme for the wire-driven rehabilitation robot has potential to assist patients with stroke in performing repetitive rehabilitation training.

Keywords: rehabilitation robot, wire-driven, upper limb, tracking control, sliding mode, nonlinear disturbance observer

OPEN ACCESS

Edited by:
Guanglin Li,
Shenzhen Institutes of Advanced Technology (CAS), China

Reviewed by:
Xu Zhang,
University of Science and Technology of China, China
Ru-Lan Hsieh,
Shin Kong WHS Memorial Hospital, Taiwan

****Correspondence:***
Rong Song
songrong@mail.sysu.edu.cn

†Co-first authors.

Specialty section:
This article was submitted to Stroke, a section of the journal Frontiers in Neurology

Received: *11 July 2017*
Accepted: *16 November 2017*
Published: *04 December 2017*

Citation:
Niu J, Yang Q, Wang X and Song R (2017) Sliding Mode Tracking Control of a Wire-Driven Upper-Limb Rehabilitation Robot with Nonlinear Disturbance Observer. Front. Neurol. 8:646. doi: 10.3389/fneur.2017.00646

INTRODUCTION

Stroke, an acute cerebrovascular disease typically caused by hemorrhage or blockage in brain blood vessels, is a major cause of motor dysfunction or even permanent disability (1). Repetitive training and task-oriented exercises of the paretic extremity are significantly beneficial to the recovery of extremity functions (2–4). However, traditional therapy for the rehabilitation relies heavily on the experience and manual manipulation of physical therapists, which is time-consuming, labor-intensive, and costly. Robot-aided rehabilitation has many advantages such as high efficiency, high precision, and controllability (5–7), which can allow more intensive training (8, 9) and reduce the workload of physical therapists.

Abbreviations: SMC, sliding mode control; SMNDO, sliding mode control with nonlinear disturbance observer.

Mechanical structure is one of the most important factors that can affect the effectiveness of the robot-assisted rehabilitation. In the past two decades, many robotic systems have been designed and applied in rehabilitation training. Conventional rehabilitation robots usually consist of several rigid links. MIT-MANUS has two degrees-of-freedom (DOF) and can guide the upper-limb over a horizontal plane (5). Mirror-image movement enabler is an upper-limb rehabilitation robot that can ensure the hemiparetic arm move to the mirror-image position of the opposite arm in a three-dimensional space (8). Fazekas et al. have designed a robotic system based on two industrial robots for upper-limb rehabilitation to assist three-dimensional movements (10). Though these rehabilitation robots can be used for rehabilitation training, they have many limitations like poor workspace, lack of compliance, and relatively high construction costs. Wire-driven rehabilitation robots not only remedy these shortcomings but have simple structures and are easy to assemble/disassemble. Moreover, since the wire-driven rehabilitation robots have lower moving inertia compared to rehabilitation robots that consist of rigid links, the user can feel less constraint and more comfort when participating in robot-assisted rehabilitation training. In the past few years, some wire-driven robots have been designed for rehabilitation. Jones et al. have designed a wire-actuated rehabilitation robot, which is a three DOF robotic exoskeleton for hand rehabilitation (11). Sophia-3, an end-effector based wire-driven rehabilitation robot, has been designed to assist planar movements (12). Gaponov et al. have designed a portable cable-driven rehabilitation robot, which provides assistance for shoulder, abduction, and elbow flexion (13).

Control scheme is another important factor affects the effectiveness of robot-assisted rehabilitation. When delivering task-oriented rehabilitation training, the control scheme is required to assist the robot in guiding the paretic limb to finish predefined movements or trajectory accurately and compliantly. Linear control techniques such as PID (14, 15) and PD (15, 16) controllers have been designed for rehabilitation robot, but they have degraded performance if nonlinear uncertainties of the system are considered (17). Simple nonlinear control techniques such as robust torque control scheme (14, 15) and impedance control scheme (15, 18) cannot meet the requirement under uncertain dynamics. Many other control schemes have been presented such as fuzzy adaption (19) and adaptive control schemes (17, 18), whereas these control schemes perform well for industrial robots but not for rehabilitation robots due to uncertainties and disturbances in rehabilitation training (20). Sliding mode control (SMC) is a variable structure control method, which has inherent insensitivity and robustness against uncertainties and disturbances. Therefore, it can be relatively suitable for the control of human–robot interaction systems. However, to achieve satisfactory tracking performance, traditional SMC needs high-control authority to eliminate model uncertainties and external disturbances, which in turn is the main cause of chattering (21). Chattering is undesirable since it may degrade tracking performance and even cause damage to actuators (22). A relatively easy and effective approach to address this problem is to employ a nonlinear disturbance observer in the control loop to estimate all the lumped uncertainties and disturbances. By this means, the tracking precision can be improved since uncertainties and disturbances can be estimated and compensated for, while the chattering phenomenon can be reduced since the control scheme may not need high-control authority to resist disturbances. Though nonlinear disturbance observer has been investigated in various fields (23, 24), to the largest of our knowledge, it is rarely utilized in a wire-driven rehabilitation robot.

In this paper, a wire-driven rehabilitation robot is designed to deliver task-oriented training exercises for upper-limb, which can work over a three-dimensional space. First, sliding mode control with nonlinear disturbance observer (SMCNDO) is designed for the wire-driven rehabilitation robot against unpredictable disturbances. Then, simulation of tracking a predefined trajectory is conducted to investigate the performance of the designed control scheme. Moreover, a square-shaped and a circle-shaped trajectory are designed, and the forearm of the subject is controlled by the robot to follow the predefined trajectories. Both simulation and experimental results of the designed SMCNDO are compared with that of a traditional SMC.

MATERIALS AND METHODS

System Description

Mechanical architecture of the designed wire-driven rehabilitation robot is shown in **Figure 1A**, which consists of three actuated wire-driven limbs to perform translational movement in a three-dimensional space. The main software program provides control

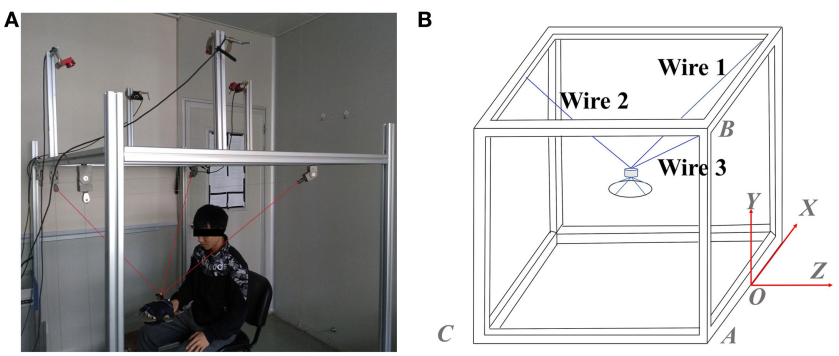

FIGURE 1 | A wire-driven rehabilitation robot. **(A)** Mechanical architecture of the wire-driven rehabilitation robot and **(B)** geometry of the wire-driven rehabilitation robot.

scheme, reference trajectory, and data storage procedures, which is written in VC++. In addition, a personal computer is used to perform real-time processing and real-time communication with I/Os and serves as a user interface that can be used to manage the system. Motion capture system is implemented to ensure relatively accurate measurement. From **Figure 1A**, four cameras are attached on the top of the base frame, and a spherical marker is placed on the top of the end-effector. The position of the marker can be directly obtained by motion capture system, which is used to represent the position of the end-effector and as the feedback in the control loop. Safety is an important factor that needs to be considered. To ensure security and prevent accidents during rehabilitation training, emergency stop switches are designed both in software and hardware. When a patient feels uncomfortable or any accident happens, the power supply for the system can be immediately interrupted by pressing software or hardware emergency stop switch. Moreover, the output force of each actuator is strictly limited when designing software program.

Control Scheme Design

The geometry of the designed wire-driven rehabilitation robot is shown in **Figure 1B**. The origin of the coordinate system is chosen referring to the midpoint of a certain side of the cube-shaped structure, which is shown in **Figure 1B**. The position of the top of each winch pulley can be obtained by measurement. The end-effector is simply treated as a point mass, and its position can be obtained directly by the implementation of the task space coordinates, and it is assumed that the end-effector is lying inside the workspace. Therefore, the length of each wire can be calculated according to the spatial position of the end-effector and the spatial position of related winch pulley:

$$L_i = \sqrt{(x - x_i)^2 + (y - y_i)^2 + (z - z_i)^2} \tag{1}$$

where (x, y, z) represents the position of the end-effector, i varying from 1 to the number of wires, and (x_i, y_i, z_i) represents the position of the associated ith winch pulley.

According to **Table 1**, (x_i, y_i, z_i) can be expressed specifically as follows:

$$\begin{cases} (x_1, y_1, z_1) = (a, b, 0) \\ (x_2, y_2, z_2) = (0, b, -c) \\ (x_3, y_3, z_3) = (-a, b, 0) \end{cases} \tag{2}$$

where a represents the length of $|OA|$, b represents the length of $|AB|$, and c represents the length of $|AC|$. Therefore, from Eqs 1 and 2, the length of the wires can be written exactly as follows:

$$\begin{cases} L_1 = \sqrt{(x-a)^2 + (y-b)^2 + z^2} \\ L_2 = \sqrt{x^2 + (y-b)^2 + (z+c)^2} \\ L_3 = \sqrt{(x+a)^2 + (y-b)^2 + z^2} \end{cases}. \tag{3}$$

Differentiating the length of each wire with respect to time leads to velocity of each wire:

$$\begin{cases} \dot{L}_1 = [\dot{x}(x-a) + \dot{y}(y-b) + \dot{z}z]/L_1 \\ \dot{L}_2 = [\dot{x}x + \dot{y}(y-b) + \dot{z}(z+c)]/L_2 \\ \dot{L}_3 = [\dot{x}(x+a) + \dot{y}(y-b) + \dot{z}z]/L_3 \end{cases}. \tag{4}$$

TABLE 1 | Parameters of the designed wire-driven rehabilitation robot.

Parameter	Symbol	Value
End-effector mass	m	2.5 kg
The length of $\|OA\|$	a	0.81 m
The length of $\|AB\|$	b	1.78 m
The length of $\|AC\|$	c	1.36 m
Gravity acceleration	g	9.8 m/s^2

Moreover, the relation between $\dot{L}_i$ and $\dot{x}$, $\dot{y}$, and $\dot{z}$ can be established based on Jacobian matrix. Jacobian matrix for the designed wire-driven rehabilitation robot can be expressed specifically as follows:

$$\begin{aligned} \boldsymbol{J} &= \begin{bmatrix} \partial L_1/\partial x & \partial L_1/\partial y & \partial L_1/\partial z \\ \partial L_2/\partial x & \partial L_2/\partial y & \partial L_2/\partial z \\ \partial L_3/\partial x & \partial L_3/\partial y & \partial L_3/\partial z \end{bmatrix} \\ &= \begin{bmatrix} (x-a)/L_1 & (y-b)/L_1 & z/L_1 \\ x/L_2 & (y-b)/L_2 & (z+c)/L_2 \\ (x+a)/L_3 & (y-b)/L_3 & z/L_3 \end{bmatrix}. \end{aligned} \tag{5}$$

Moreover, in this study, we assume that the motion is within the workspace and the gravity of the end-effector is able to keep all the wires under tension. Therefore, the relation between externally applied forces and the wire tensile forces can be expressed as follows (25):

$$\begin{bmatrix} u_x & u_y & u_z \end{bmatrix}^{\mathrm{T}} = -\boldsymbol{J}^{\mathrm{T}}\boldsymbol{\tau} \tag{6}$$

where τ denotes the vector of wire-driven forces. In this study, the dynamic equation of the wire-driven rehabilitation robot can be expressed as follows (25):

$$\boldsymbol{M}(\ddot{\boldsymbol{p}})\ddot{\boldsymbol{p}} + \boldsymbol{C}(\boldsymbol{p}, \dot{\boldsymbol{p}})\dot{\boldsymbol{p}} + \boldsymbol{G}(\boldsymbol{p}) = \boldsymbol{u} + \boldsymbol{d} \tag{7}$$

where $\boldsymbol{M}(\ddot{\boldsymbol{p}})$ denotes the inertia matrix, $\boldsymbol{C}(\boldsymbol{p}, \dot{\boldsymbol{p}})$ is the vector of Coriolis and centripetal terms, $\boldsymbol{G(p)}$ is the vector of gravity terms, and $\boldsymbol{d}$ denotes the vector of all the lumped uncertainties (parametric, model, and disturbance). In this study, the designed wire-driven rehabilitation robot is considered to perform only translational movements, low velocities, and accelerations are involved in rehabilitation training, therefore Coriolis forces can be neglected. Hence, Eq. 7 can be simplified as follows:

$$\boldsymbol{M}(\boldsymbol{p})\ddot{\boldsymbol{p}} + \boldsymbol{G}(\boldsymbol{p}) = \boldsymbol{u} + \boldsymbol{d} \tag{8}$$

where

$$\boldsymbol{M} = \begin{bmatrix} m & 0 & 0 \\ 0 & m & 0 \\ 0 & 0 & m \end{bmatrix}, \quad \boldsymbol{G} = \begin{bmatrix} 0 \\ mg \\ 0 \end{bmatrix}, \quad \boldsymbol{d} = \begin{bmatrix} d_x \\ d_y \\ d_z \end{bmatrix}$$

d_x, d_y, and d_z represent the disturbances in X, Y, and Z directions. Therefore, referring to Eqs 6 and 8, wire cable-driven forces in terms of $\boldsymbol{p}$ generalized coordinates can be obtained as:

$$\boldsymbol{\tau} = -(\boldsymbol{J}^{\mathrm{T}})^{-1}(\boldsymbol{M}(\boldsymbol{p})\ddot{\boldsymbol{p}} + \boldsymbol{G}(\boldsymbol{p}) - \boldsymbol{d}). \tag{9}$$

Note that $\boldsymbol{p} = [x\ y\ z]^{\mathrm{T}}$ and $\boldsymbol{p_d} = [x_d\ y_d\ z_d]^{\mathrm{T}}$ represents the actual and the desired position in a three-dimensional space, respectively. For the sake of control scheme design, the vector of sliding surfaces is defined as follows:

$$\boldsymbol{s} = \boldsymbol{\lambda e} + \dot{\boldsymbol{e}} \tag{10}$$

where $\boldsymbol{e} = [x{-}x_d\ x{-}x_d\ x{-}x_d]^{\mathrm{T}}$ is the vector of tracking errors in a three-dimensional space, $\boldsymbol{s} = [s_x\ s_y\ s_z]^{\mathrm{T}}$ and $\boldsymbol{\lambda} = [\lambda_x\ \lambda_y\ \lambda_z]^{\mathrm{T}}$ are positive symmetric diagonal matrices. Taking the derivative of $\boldsymbol{s}$ leads to $\dot{\boldsymbol{s}}$. And $\dot{\boldsymbol{s}}$ is the so-called reaching law, and in this study it can be defined as follows:

$$\dot{\boldsymbol{s}} = -\boldsymbol{ks} - \boldsymbol{\eta}\mathrm{sgn}(\boldsymbol{s}) - \boldsymbol{M}^{-1}\tilde{\boldsymbol{d}} \tag{11}$$

where sgn($\boldsymbol{s}$) is a discontinuous function, it can be given as follows:

$$\mathrm{sgn}(s_i) = \begin{cases} \frac{s_i}{\|s_i\|}, \text{when} & \|s_i\| > 0 \\ 0, \text{ when} & \|s_i\| = 0 \end{cases} \tag{12}$$

and $\mathrm{sgn}(\boldsymbol{s}) = [\mathrm{sgn}(s_x)\ \mathrm{sgn}(s_y)\ \mathrm{sgn}(s_z)]^{\mathrm{T}}$, $\tilde{\boldsymbol{d}}$ denotes the vector of the estimation errors which is given as $\tilde{\boldsymbol{d}} = \boldsymbol{d} - \hat{\boldsymbol{d}}$, $\boldsymbol{k} = \mathrm{diag}(k_x\ k_y\ k_z)$ and $\boldsymbol{\eta} = \mathrm{diag}(\eta_x\ \eta_y\ \eta_z)$ are symmetric diagonal positive matrices need to be designed in practice. In this study, a switching sliding surface is considered by defining control gain as follows:

$$\eta_i = \begin{cases} \eta_1, \text{when} & \|s_i\| \le \beta \\ \eta_2, \text{when} & \|s_i\| > \beta \end{cases}, \quad i = x, y, z. \tag{13}$$

According to Eqs 9–11, through a series of substitutions and transformations, the SMC scheme can be expressed as follows:

$$\boldsymbol{u} = \boldsymbol{M}(\boldsymbol{\lambda}\dot{\boldsymbol{e}} + \ddot{\boldsymbol{p}}_d + \boldsymbol{ks} + \boldsymbol{\eta}\mathrm{sgn}(\boldsymbol{s})) + \boldsymbol{G} - \hat{\boldsymbol{d}}. \tag{14}$$

A nonlinear disturbance observer has been introduced in many studies (26–28). In this study, a nonlinear disturbance observer is designed for the wire-driven robot to estimate and compensate disturbances and uncertainties that exist in the rehabilitation training, which can be defined as follows:

$$\hat{\boldsymbol{d}} = \boldsymbol{q} + \boldsymbol{\gamma M\dot{p}} \tag{15}$$

$$\dot{\boldsymbol{q}} = \boldsymbol{\gamma}(\boldsymbol{G} - \boldsymbol{u} - \hat{\boldsymbol{d}}) \tag{16}$$

where $\boldsymbol{d}$ is estimated as $\hat{\boldsymbol{d}}$, $\boldsymbol{q}$ is an auxiliary vector, $\boldsymbol{\gamma} = \mathrm{diag}(\gamma_x\ \gamma_y\ \gamma_z)$ is a symmetric diagonal positive matrix. In this study, we consider that the disturbances are slow time-varying signal, which means $\dot{\boldsymbol{d}} = \boldsymbol{0}$. According to Eqs 14–16, through a series of translations, we can find that $\dot{\tilde{\boldsymbol{d}}} + \boldsymbol{\gamma}\,\tilde{\boldsymbol{d}} = \boldsymbol{0}$, therefore, it can be noticed that the estimation errors will convergence to 0 exponentially by using the designed nonlinear disturbance observer. Furthermore, to prove the closed-loop stability of the control scheme, the Lyapunov function is chosen as follows:

$$V = \frac{1}{2}\boldsymbol{s}^{\mathrm{T}}\boldsymbol{s} + \frac{1}{2}\tilde{\boldsymbol{d}}^{\mathrm{T}}\tilde{\boldsymbol{d}}. \tag{17}$$

The derivative of V is:

$$\dot{V} = \boldsymbol{s}^{\mathrm{T}}\dot{\boldsymbol{s}} + \tilde{\boldsymbol{d}}^{\mathrm{T}}\dot{\tilde{\boldsymbol{d}}}. \tag{18}$$

Substitute Eq. 11 and $\dot{\tilde{\boldsymbol{d}}} + \boldsymbol{\gamma}\tilde{\boldsymbol{d}} = \boldsymbol{0}$ into the Eq. 18, one can notice that:

$$\dot{V} = -\boldsymbol{s}^{\mathrm{T}}\boldsymbol{k}\dot{\boldsymbol{s}} - \boldsymbol{\eta}\|\boldsymbol{s}\| - \boldsymbol{s}^{\mathrm{T}}\boldsymbol{M}^{-1}\tilde{\boldsymbol{d}} - \tilde{\boldsymbol{d}}^{\mathrm{T}}\gamma\tilde{\boldsymbol{d}}. \tag{19}$$

Therefore, $\dot{V}$ can be rewritten as:

$$\dot{V} = -\boldsymbol{s}^{\mathrm{T}}\boldsymbol{ks} - \tilde{\boldsymbol{d}}^{\mathrm{T}}\boldsymbol{\gamma}\tilde{\boldsymbol{d}} - \sum(\eta_i|s_i| + s_i\tilde{d}_i/m), i = x, y, z. \tag{20}$$

In this study, $|\tilde{d}_i|_{\max}$ represents the maximum value of $|\tilde{d}_i|$, and we assume η_i satisfies $\eta_i \ge |\tilde{d}_i|_{\max}/m$, $i = x,y,z$. Therefore, $\dot{V}$ can be expressed as follows:

$$\dot{V} \le -\boldsymbol{s}^{\mathrm{T}}\boldsymbol{ks} - \tilde{\boldsymbol{d}}^{\mathrm{T}}\boldsymbol{\gamma}\tilde{\boldsymbol{d}}. \tag{21}$$

As mentioned previously that $\boldsymbol{k}$ and $\boldsymbol{\gamma}$ are symmetric diagonal positive matrices, therefore, one can notice that $\dot{V} \le 0$. Therefore, the Lyapunov function is always decreasing, which means the closed-loop system is asymptotically stable. As described previously that sgn($\boldsymbol{s}$) function is a discontinuous function, the control law is discontinuous across the sliding surface, which may cause chattering. Chattering is undesirable since it can cause damage to the actuators being controlled. Chattering reduction can be achieved by using a nonlinear disturbance observer to estimate and compensate disturbances; furthermore, chattering can be reduced by replacing the discontinuous sgn($\boldsymbol{s}$) function with a continuous sat($\boldsymbol{s}$) function. Using sat($\boldsymbol{s}$) function, the discontinuity of the controller is smoothed in a thin boundary layer neighboring the sliding surface. sat($\boldsymbol{s}$) function is defined as follows:

$$\mathrm{sat}(s_i) = \begin{cases} \frac{s_i}{\|s_i\|}, \text{when} & \|s_i\| > \Delta \\ \frac{s_i}{\Delta}, \text{when} & \|s_i\| < \Delta \end{cases}, \quad i = x, y, z \tag{22}$$

where Δ is a small and positive constant. Therefore, control scheme for the wire-driven forces by the SMC scheme with nonlinear disturbance observer can be rewritten as:

$$\boldsymbol{\tau} = -(\boldsymbol{J}^{\mathrm{T}})^{-1}(\boldsymbol{M}(\boldsymbol{\lambda}\dot{\boldsymbol{e}} + \ddot{\boldsymbol{p}}_d + \boldsymbol{ks} + \boldsymbol{\eta}\mathrm{sat}(\boldsymbol{s})) + \boldsymbol{G} - \hat{\boldsymbol{d}}). \tag{23}$$

Simulation and Experimental Setup

To investigate the effectiveness of the presented SMCNDO for the wire-driven rehabilitation robot, first, simulation is carried out in Matlab/Simulink. Both SMCNDO and the traditional SMC are considered in the simulation, and the results of tracking a predefined trajectory *via* SMCNDO are compared with that of the traditional SMC. Parameters for the wire-driven rehabilitation robot are shown in **Table 1**. The reference trajectory is predefined as $\boldsymbol{p}_d(t) = \left[0.1\sin(0.1t) \quad 0.98 \quad 0.1\cos(0.1t) - 0.52\right]^{\mathrm{T}}$. In addition, the vector of the desired velocities and accelerations along the three coordinate directions can be obtained by differentiating $\boldsymbol{p}_d(t)$ once and twice, respectively. The vector of disturbances along three coordinate directions is defined as follows:

$$\boldsymbol{d}(t) = \boldsymbol{d}_1(t) + \boldsymbol{d}_2(t) \tag{24}$$

where $\boldsymbol{d}_1(t) = [5\sin(t)\ 5\sin(t)\ 5\sin(t)]_{\mathrm{T}}$, $\boldsymbol{d}_2(t)$ is a vector of pulse-like disturbances which is defined as follows:

$$\boldsymbol{d}_2(t) = \begin{cases} \begin{bmatrix} -200 & -200 & 200 \end{bmatrix}^{\mathrm{T}}, & \text{if} \quad 0 \le t < 15\text{s} \\ \begin{bmatrix} 200 & 200 & -200 \end{bmatrix}^{\mathrm{T}}, & \text{if} \quad 15\text{s} \le t < 45\text{s} \\ \begin{bmatrix} -200 & -200 & 200 \end{bmatrix}^{\mathrm{T}}, & \text{if} \quad 45\text{s} \le t < 62.8\text{s} \end{cases} . \tag{25}$$

Both the traditional SMC and SMCNDO can be designed according to Eq. 23, and $\hat{\boldsymbol{d}}$ term is considered as 0 for the traditional SMC. A nonlinear disturbance is designed based on Eqs 15 and 16. According to the design procedures, proper control parameters for SMC are given as: $\boldsymbol{\lambda} = \mathrm{diag}(10,10,10)$, $\boldsymbol{k} = \mathrm{diag}(5,5,5)$, $\eta_1 = 0.1$, $\eta_2 = 80$, $\beta = 0.5$, and proper control parameters for SMCNDO are given as: $\boldsymbol{\lambda} = \mathrm{diag}(10,10,10)$, $\boldsymbol{k} = \mathrm{diag}(5,5,5)$, $\boldsymbol{\gamma} = \mathrm{diag}(50,50,50)$, $\eta_1 = 0.1$, $\eta_2 = 80$, $\beta = 0.5$.

Experiments are carried out based on a real-time system to verify the performance of the presented controller for practical applications. It has been approved by the ethics committee of the Injury Rehabilitation Hospital of Guangdong Province. During the experiments, a healthy subject (23 years old, height of 173 cm, and weight of 60 kg) is seated beside the wire-driven rehabilitation robot with his forearm placed on the splint. The subject is instructed to keep relaxed during the experiments. Then, the forearm of the subject is controlled by the robot to follow predefined trajectories, and two different types of trajectories are considered in this section, including a square-shaped and a circle-shaped trajectory. The results of SMCNDO are compared with that of the traditional SMC. The traditional SMC and SMCNDO are designed according to Eq. 23 and $\hat{\boldsymbol{d}}$ is also considered as 0 for the traditional SMC, which is the same as previous simulation. A nonlinear disturbance observer is also designed based on Eqs 15 and 16. According to the design procedures and considering the practical application, proper control parameters for SMC and SMCNDO are given as: $\boldsymbol{\lambda} = \mathrm{diag}(55,55,55)$, $\boldsymbol{k} = \mathrm{diag}(20,20,20)$, $\eta_1 = 2{,}000$, $\eta_2 = 500$, $\beta = 0.1$, and proper control parameters for SMCNDO is chosen as: $\boldsymbol{\lambda} = \mathrm{diag}(55,55,55)$, $\boldsymbol{k} = \mathrm{diag}(20,20,20)$, $\eta_1 = 2{,}000$, $\eta_2 = 500$, $\beta = 0.1$, $\boldsymbol{\gamma} = \mathrm{diag}(3,3,3)$. The square-shaped trajectory which is predefined as the reference trajectory for the experiment is shown in **Figure 2**, and the side length is $0.1\sqrt{2}$ meters. Each experiment of tracking the square-shaped trajectory lasts 60 s. And the circle-shaped reference trajectory with a radius of 0.1 m is predefined as $\boldsymbol{p}_d(t) = \begin{bmatrix} 0.1\sin(0.1t) & 0.98 & 0.1\cos(0.1t) - 0.52 \end{bmatrix}^{\mathrm{T}}$.

The desired velocity and acceleration can be obtained by differentiating the desired position once and twice, respectively, each experiment of tracking the circle-shaped trajectory lasts 62.8 s. The predefined circle-shaped trajectory is visually shown in **Figure 2**. The root mean square errors are calculated to evaluate the tracking accuracy of the two applied control schemes when tracking the two predefined trajectories. The root mean square error between actual position and desired position is used to evaluate the tracking accuracy, which can be expressed as follows:

$$\mathrm{RMSE} = \sqrt{\frac{1}{N}\sum_{i=1}^{N}(\delta_d(i) - \delta(i))^2}, \quad \delta = x, y, z. \tag{26}$$

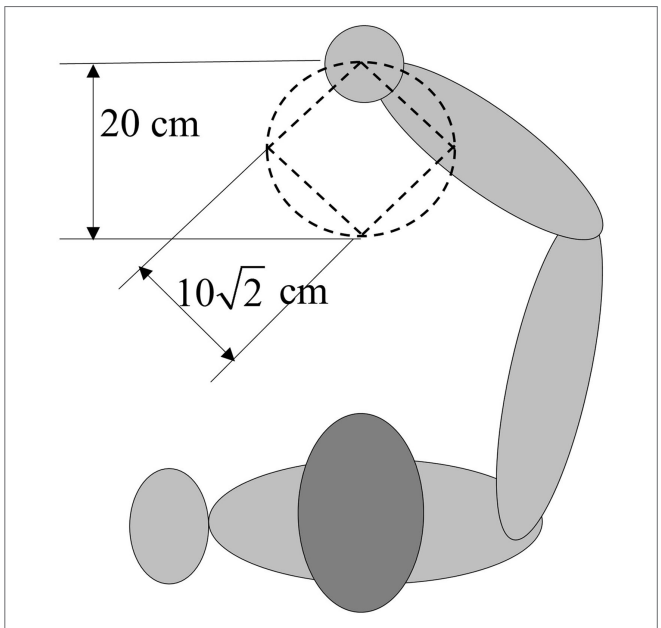

FIGURE 2 | Predefined square-shaped and circle-shaped trajectories in experiments. The side length of square-shaped trajectory is $0.1\sqrt{2}$ m, and the radius of the circle is 0.1 m.

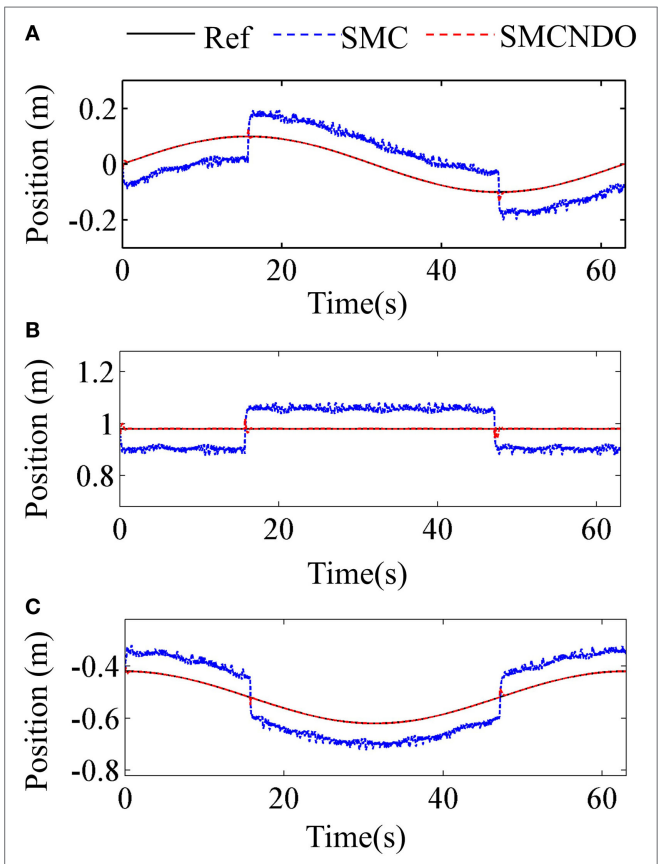

FIGURE 3 | Tracking performance in the three coordinate directions *via* sliding mode control (SMC) and sliding mode control with nonlinear disturbance observer (SMCNDO). **(A)** Tracking performance in *X* direction, **(B)** tracking performance in *Y* direction, and **(C)** tracking performance in *Z* direction.

RESULTS

Tracking performance of the traditional SMC and SMCNDO in simulation are shown in **Figure 3**, and tracking performance along *X*, *Y*, and *Z* directions are shown in **Figures 3A–C**, respectively. In **Figure 3**, tracking performance *via* the traditional SMC and SMCNDO are drawn in blue dashed line and red dashed line, respectively, and the predefined trajectory is drawn in black-solid line. The output forces for the three wires in simulation *via* SMC and SMCNDO are shown in **Figure 4**. **Figures 4A–C** are the output forces *via* SMC for wire 1, wire 2, and wire 3, respectively. **Figures 4D–F** are the output forces *via* SMCNDO for wire 1, wire 2, and wire 3, respectively. From **Figure 4**, we can find that chattering of the output forces *via* SMC is relatively severe, whereas chattering is reduced effectively by implementation of SMCNDO. These simulation results indicate that when control the wire-driven robot follow a predefined trajectory in the presence of unknown disturbances, SMCNDO has better tracking performance and lower chattering compared with the traditional SMC.

The tracking errors of the two applied control schemes in the three coordinate directions when a healthy subject follows the predefined square-shaped trajectory are shown in **Figure 5**, where the tracking errors by implementation of the traditional SMC and SMCNDO are drawn in blue-solid line and red-solid line, respectively, the black-solid line is added as a reference whose value is always 0. From **Figure 5**, it is observed that SMCNDO has obviously smaller tracking errors along all the three directions. In addition, the root mean square errors along the three coordinate directions of tracking the square-shaped trajectory are calculated based on Eq. 26 and are show in **Table 2**. It can be found in **Table 2** that the root mean square errors of SMCNDO are obviously less

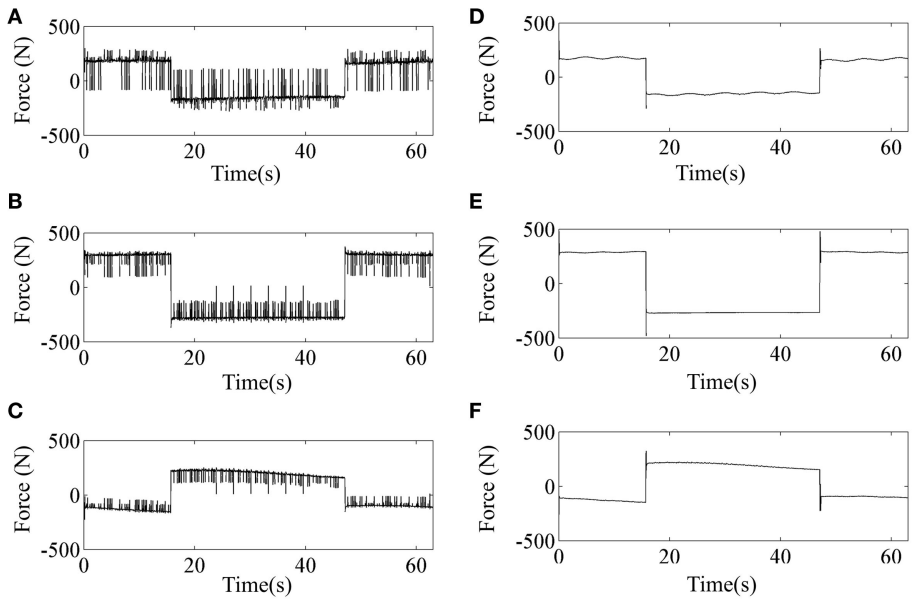

FIGURE 4 | The output forces for the three wires *via* sliding mode control (SMC) and sliding mode control with nonlinear disturbance observer (SMCNDO). **(A)** The output force for wire 1 *via* SMC, **(B)** the output force for wire 2 *via* SMC, **(C)** the output force for wire 3 *via* SMC, **(D)** the output force for wire 1 *via* SMCNDO, **(E)** the output force for wire 2 *via* SMCNDO, and **(F)** the output force for wire 3 *via* SMCNDO.

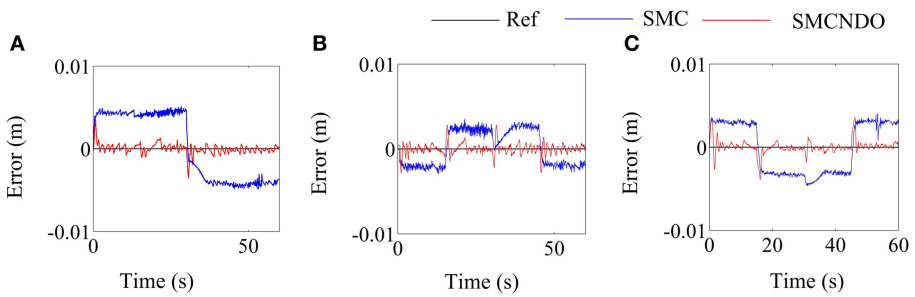

FIGURE 5 | Comparison of tracking errors in the three coordinate directions by implementation of sliding mode control (SMC) and sliding mode control with nonlinear disturbance observer (SMCNDO) when a healthy subject follows a square-shaped trajectory. **(A)** Tracking errors in the *X* direction by implementation of SMC and SMCNDO, **(B)** tracking errors in the *Y* direction by implementation of SMC and SMCNDO, and **(C)** tracking errors in the *Z* direction by implementation of SMC and SMCNDO.

TABLE 2 | Root mean square errors (cm) in the three coordinate directions by implementation of sliding mode control (SMC) and sliding mode control with nonlinear disturbance observer (SMCNDO) when a healthy subject follows a square-shaped and a circle-shaped trajectory.

Type of trajectory	*X position*		*Y position*		*Z position*	
	SMC	**SMCNDO**	**SMC**	**SMCNDO**	**SMC**	**SMCNDO**
Square-shaped	0.301	0.047	0.177	0.061	0.389	0.071
Circle-shaped	0.411	0.075	0.214	0.066	0.313	0.081

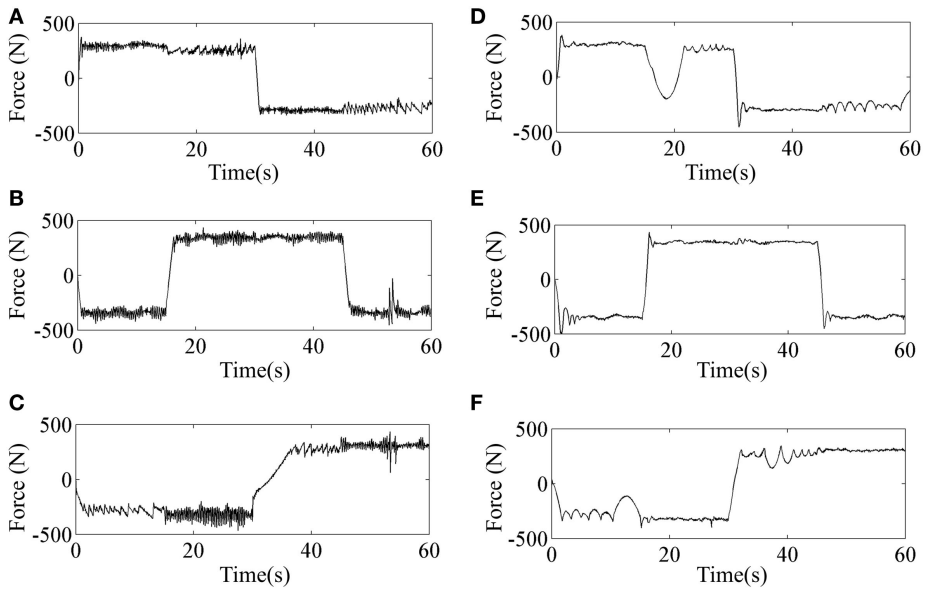

FIGURE 6 | Comparison of output forces for the three wires by implementation of sliding mode control (SMC) and sliding mode control with nonlinear disturbance observer (SMCNDO) when a healthy subject follows a square-shaped trajectory. **(A)** The output force for wire 1 by implementation of SMC, **(B)** the output force for wire 2 by implementation of SMC, **(C)** the output force for wire 3 by implementation of SMC, **(D)** the output force for wire 1 by implementation of SMCNDO, **(E)** the output force for wire 2 by implementation of SMCNDO, and **(F)** the output force for wire 3 by implementation of SMCNDO.

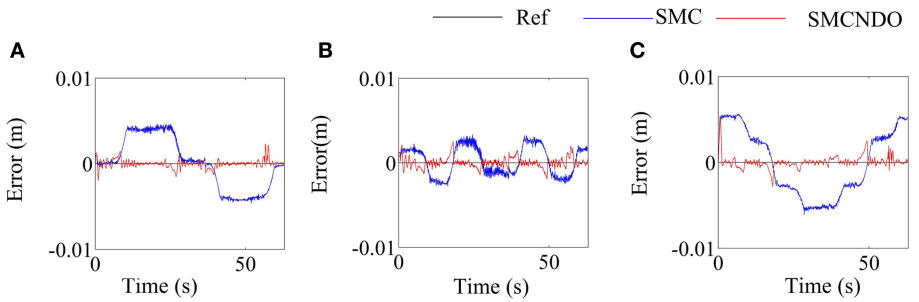

FIGURE 7 | Comparison of tracking errors in the three coordinate directions by implementation of sliding mode control (SMC) and sliding mode control with nonlinear disturbance observer (SMCNDO) when a healthy subject follows a circle-shaped trajectory. **(A)** Tracking errors in the *X* direction by implementation of SMC and SMCNDO, **(B)** tracking errors in the *Y* direction by implementation of SMC and SMCNDO, and **(C)** tracking errors in the *Z* direction by implementation of SMC and SMCNDO.

than the traditional SMC in all the three coordinate directions. The output forces for the three wires when tracking the square-shaped trajectory by implementation of the traditional SMC and SMCNDO are shown in **Figure 6**. **Figures 6A–C** are the results of the output force by implementation of SMC, and **Figures 6B,C** and **7A** are the results of the output forces by implementation of SMCNDO. It can be seen from these plots that the output forces for the three wires by implementation of SMCNDO are much smoother than that of the traditional SMC, which means chattering is effectively reduced by implementation of SMCNDO.

The tracking errors along the three coordinate directions when tracking the predefined circle-shaped trajectory by

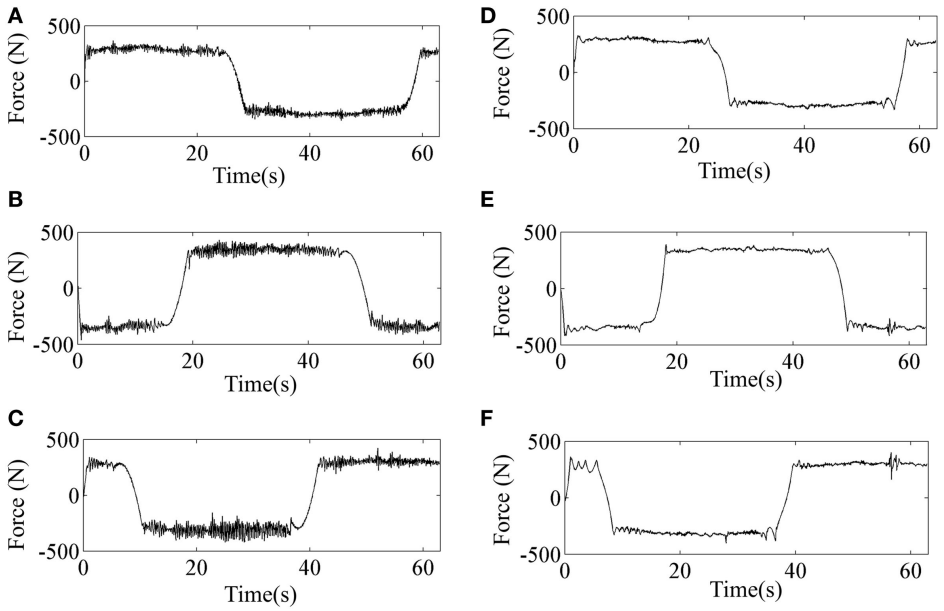

FIGURE 8 | Comparison of the output forces for the three wires by implementation of sliding mode control (SMC) and sliding mode control with nonlinear disturbance observer (SMCNDO) when a healthy subject follows a circle-shaped trajectory. **(A)** The output force for wire 1 by implementation of SMC, **(B)** the output force for wire 2 by implementation of SMC, **(C)** the output force for wire 3 by implementation of SMC, **(D)** the output force for wire 1 by implementation of SMCNDO, **(E)** the output force for wire 2 by implementation of SMCNDO, and **(F)** the output force for wire 3 by implementation of SMCNDO.

implementation of SMC and SMCNDO are shown in **Figure 7**. It can be noticed from **Figure 7** that SMCNDO has better tacking performance in a three-dimensional space as compared with the traditional SMC. The root mean square errors along the three coordinate directions are also calculated in this experiment according to Eq. 26 and are shown in **Table 2**, which also indicates that SMCNDO has less tracking errors in the three coordinate directions as compared with the traditional SMC. The output forces for the three wires when tracking the predefined circle-shaped trajectory by implementation of SMC and SMCNDO are shown in **Figure 8**. **Figures 8A–C** are the results of the output forces by implementation of SMC, and **Figures 8A–C** are the results of the output forces by implementation of SMCNDO. From these plots, it can be observed that chattering is effectively reduced by SMCNDO, as the output forces by implementation of SMCNDO is much smoother than that of the traditional SMC.

DISCUSSION

The designed wire-driven rehabilitation in this paper has three DOF and its architecture makes it possible to assist the subject in performing predefined movements in a three-dimensional space. Coordinate system that applied in the control scheme design procedure is considered in this paper, which can be classified into the wire length coordinate system and the task space coordinate system. In the wire length coordinate system, the length of each wire is measured by scaling the associated motor encoder count; however, due to the unavailable flexibility of wires, using the wire length coordinate system is not reliable when the implementation may require high accuracy. In this paper, this problem can be effectively addressed by using the task space coordinates (25), where the spatial position of the end-effector is measured directly using the motion capture system (OptiTrack, NaturalPoint, USA).

From the results of both simulation and experiments, the traditional SMC has degraded tracking performance and can cause high chattering in all the three coordinate directions, while tracking performance can be obviously improved and chattering can be effectively reduced *via* SMCNDO. The results of experiments are consistent with those of simulation. In literature, many studies have found that the traditional SMC is not able to achieve satisfactory tracking performance and can cause high chattering (29–31). Mohammed et al. have designed SMCNDO for a pneumatic muscle system (28), Deshpande et al. have designed SMCNDO for an active suspension systems (32), the results of these studies show that the tracking performance is obviously improved by SMCNDO as compared with the traditional SMC, which is consistent with the results of our study. By adding the nonlinear disturbance observer to estimate disturbances and feed them back in the control loop, tracking accuracy can be effectively improved. Moreover, since disturbances can be compensated for and high tracking accuracy can be achieved by SMCNDO, the control gain for SMCNDO may be reduced in this study, this could lead to the result of chattering reduction. When delivering robot-assisted rehabilitation training, many unpredictable disturbance scan affect training such as friction caused by actuators (33), human-applied force due to spasticity (34), and uncertainties due to diverse biomechanical variations (20), whereas SMCNDO could effectively reduce the effect of the above-mentioned unpredictable disturbances.

There are a few limitations of this study that should be addressed in the future. The positions of the wires should be well arranged to ensure enough workspace and the safety for upper-limb rehabilitation in clinical application. In this pilot study, we mainly focus on the investigation of the feasibility of the wire-driven rehabilitation robot using SMCNDO, in the future, we will recruit enough patients after stroke to investigate its clinical effectiveness in rehabilitation training.

CONCLUSION

In this paper, a wire-driven rehabilitation robot is designed for upper-limb rehabilitation training, and SMCNDO is designed for this robot. Simulation and experimental results of trajectory tracking show that the wire-driven rehabilitation robot with the designed control scheme has exhibited two superiorities including tracking performance improvement and chattering reduction as compared with the traditional sliding mode control scheme. The wire-driven rehabilitation robot with the designed control scheme may have great potential in robot-aided rehabilitation training.

ETHICS STATEMENT

This study was approved by the ethics committee of the Injury Rehabilitation Hospital of Guangdong Province.

AUTHOR CONTRIBUTIONS

JN and RS conceived and designed the study. JN and QY performed the experiments, wrote the paper, contributed to the work equally, and should be regarded as cofirst authors. RS reviewed and edited the manuscript. XW made a contribution to experiments. All authors had read and approved the manuscript.

FUNDING

This work was supported by the Guangdong Science and Technology Plan Project (Application Technology Research Foundation) [Grant No. 2015B020233006]; Science and Technology Program of Guangzhou [Grant No. 201604020108]; Guangzhou Key Lab of Body Data Science, [Grant No. 201605030011].

REFERENCES

1. Writing Group M, Mozaffarian D, Benjamin EJ, Go AS, Arnett DK, Blaha MJ, et al. Executive summary: heart disease and stroke statistics – 2016 update: a report from the American Heart Association. *Circulation* (2016) 133(4):447–54. doi:10.1161/cir.0000000000000366
2. Michaelsen SM, Dannenbaum R, Levin MF. Task-specific training with trunk restraint on arm recovery in stroke: randomized control trial. *Stroke* (2006) 37(1):186–92. doi:10.1161/01.str.0000196940.20446.c9
3. Luft AR, McCombe-Waller S, Whitall J, Forrester LW, Macko R, Sorkin JD, et al. Repetitive bilateral arm training and motor cortex activation in chronic stroke: a randomized controlled trial. *JAMA* (2004) 292(15):1853–61. doi:10.1001/jama.292.15.1853
4. Wilkins KB, Owen M, Ingo C, Carmona C, Dewald JPA, Yao J. Neural plasticity in moderate to severe chronic stroke following a device-assisted task-specific arm/hand intervention. *Front Neurol* (2017) 8:284. doi:10.3389/fneur.2017.00284
5. Hogan N, Krebs HI, Charnnarong J, Srikrishna P, Sharon A, editors. MIT-MANUS: a workstation for manual therapy and training. I. *Proceedings IEEE International Workshop on Robot and Human Communication*. Tokyo, Japan: IEEE (1992). p. 161–5.
6. Morris DM, Taub E. Constraint-induced therapy approach to restoring function after neurological injury. *Top Stroke Rehabil* (2001) 8(3):16–30. doi:10.1310/bljx-m89n-ptpy-jdkw
7. Frisoli A, Loconsole C, Bartalucci R, Bergamasco M. A new bounded jerk on-line trajectory planning for mimicking human movements in robot-aided neurorehabilitation. *Rob Auton Syst* (2013) 61(4):404–15. doi:10.1016/j.robot.2012.09.003
8. Lum PS, Burgar CG, Shor PC, Majmundar M, Van der Loos M. Robot-assisted movement training compared with conventional therapy techniques for the rehabilitation of upper-limb motor function after stroke. *Arch Phys Med Rehabil* (2002) 83(7):952–9. doi:10.1053/apmr.2001.33101
9. Masiero S, Armani M, Rosati G. Upper-limb robot-assisted therapy in rehabilitation of acute stroke patients: focused review and results of new randomized controlled trial. *J Rehabil Res Dev* (2011) 48(4):355–66. doi:10.1682/JRRD.2010.04.0063
10. Fazekas G, Horvath M, Troznai T, Toth A. Robot-mediated upper limb physiotherapy for patients with spastic hemiparesis: a preliminary study. *J Rehabil Med* (2007) 39(7):580–2. doi:10.2340/16501977-0087
11. Jones CL, Wang F, Morrison R, Sarkar N, Kamper DG. Design and development of the cable actuated finger exoskeleton for hand rehabilitation following stroke. *IEEE/ASME Trans Mechatron* (2014) 19(1):131–40. doi:10.1109/TMECH.2012.2224359
12. Zanotto D, Rosati G, Minto S, Rossi A. Sophia-3: a semiadaptive cable-driven rehabilitation device with a tilting working plane. *IEEE Trans Robot* (2014) 30(4):974–9. doi:10.1109/TRO.2014.2301532
13. Gaponov I, Popov D, Lee SJ, Ryu J-H. Auxilio: a portable cable-driven exosuit for upper extremity assistance. *Int J Control Autom. Syst* (2017) 15(1):73–84. doi:10.1007/s12555-016-0487-7
14. Yu W, Rosen J, editors. A novel linear PID controller for an upper limb exoskeleton. *49th IEEE Conference on Decision and Control (CDC)*. Atlanta (2010).
15. Babaiasl M, Mahdioun SH, Jaryani P, Yazdani M. A review of technological and clinical aspects of robot-aided rehabilitation of upper-extremity after stroke. *Disabil Rehabil Assist Technol* (2016) 11(4):263–80. doi:10.3109/17483107.2014.1002539
16. Nef T, Mihelj M, Riener R. ARMin: a robot for patient-cooperative arm therapy. *Med Biol Eng Comput* (2007) 45(9):887–900. doi:10.1007/s11517-007-0226-6
17. Hill J, Fahimi F. Active disturbance rejection for walking bipedal robots using the acceleration of the upper limbs. *Robotica* (2014) 33(2):264–81. doi:10.1017/S0263574714000332
18. Rahman MH, Rahman MJ, Cristobal OL, Saad M, Kenné JP, Archambault PS. Development of a whole arm wearable robotic exoskeleton for rehabilitation and to assist upper limb movements. *Robotica* (2014) 33(1):19–39. doi:10.1017/S0263574714000034
19. Xianzhi J, Zenghuai W, Chao Z, Liangliang Y. Fuzzy neural network control of the rehabilitation robotic arm driven by pneumatic muscles. *Ind Robot Int J* (2015) 42(1):36–43. doi:10.1108/IR-07-2014-0374
20. Guga J. Cyborg tales: the reinvention of the human in the information age. In: Romportl J, Zackova E, Kelemen J, editors. *Beyond Artificial Intelligence: The Disappearing Human-Machine Divide*. Cham: Springer International Publishing (2015). p. 45–62.
21. Choi S-B, Kim J. A fuzzy-sliding mode controller for robust tracking of robotic manipulators. *Mechatronics* (1997) 7(2):199–216. doi:10.1016/S0957-4158(96)00045-1
22. Young KD, Utkin VI, Ozguner U. A control engineer's guide to sliding mode control. *IEEE Trans Control Syst Technol* (1999) 7(3):328–42. doi:10.1109/87.761053
23. Xu JX, Guo ZQ, Lee TH. Design and implementation of integral sliding-mode control on an underactuated two-wheeled mobile robot. *IEEE Trans Ind Electron* (2014) 61(7):3671–81. doi:10.1109/TIE.2013.2282594
24. Li Z, Su CY, Wang L, Chen Z, Chai T. Nonlinear disturbance observer-based control design for a robotic exoskeleton incorporating fuzzy approximation. *IEEE Trans Ind Electron* (2015) 62(9):5763–75. doi:10.1109/TIE.2015.2447498
25. Zi B, Duan BY, Du JL, Bao H. Dynamic modeling and active control of a cable-suspended parallel robot. *Mechatronics* (2008) 18(1):1–12. doi:10.1016/j.mechatronics.2007.09.004

26. Wen-Hua C, Ballance DJ, Gawthrop PJ, Reilly JO. A nonlinear disturbance observer for robotic manipulators. *IEEE Trans Ind Electron* (2000) 47(4):932–8. doi:10.1109/41.857974
27. Wen-Hua C. Disturbance observer based control for nonlinear systems. *IEEE/ASME Trans Mechatron* (2004) 9(4):706–10. doi:10.1109/TMECH.2004.839034
28. Mohammed S, Huo W, Huang J, Rifaï H, Amirat Y. Nonlinear disturbance observer based sliding mode control of a human-driven knee joint orthosis. *Rob Auton Syst* (2016) 75(Pt A):41–9. doi:10.1016/j.robot.2014.10.013
29. Erbatur K, Çallı B. Fuzzy boundary layer tuning for sliding mode systems as applied to the control of a direct drive robot. *Soft Comput* (2008) 13(11):1099. doi:10.1007/s00500-008-0383-z
30. Wai RJ. Fuzzy sliding-mode control using adaptive tuning technique. *IEEE Trans Ind Electron* (2007) 54(1):586–94. doi:10.1109/TIE.2006.888807
31. Lee H, Utkin VI. Chattering suppression methods in sliding mode control systems. *Annu Rev Control* (2007) 31(2):179–88. doi:10.1016/j.arcontrol.2007.08.001
32. Deshpande VS, Mohan B, Shendge PD, Phadke SB. Disturbance observer based sliding mode control of active suspension systems. *J Sound Vib* (2014) 333(11):2281–96. doi:10.1016/j.jsv.2014.01.023
33. Xie WF. Sliding-mode-observer-based adaptive control for servo actuator with friction. *IEEE Trans Ind Electron* (2007) 54(3):1517–27. doi:10.1109/TIE.2007.894718
34. Mukherjee A, Chakravarty A. Spasticity mechanisms – for the clinician. *Front Neurol* (2010) 1:149. doi:10.3389/fneur.2010.00149

Conflict of Interest Statement: The authors declare that the research was conducted in the absence of any commercial or financial relationships that could be construed as a potential conflict of interest.

frontiers in Neurology

CORRECTION
published: 28 June 2018
doi: 10.3389/fneur.2018.00511

Corrigendum: Sliding Mode Tracking Control of a Wire-Driven Upper-Limb Rehabilitation Robot with Nonlinear Disturbance Observer

Jie Niu[1†], *Qianqian Yang*[1†], *Xiaoyun Wang*[2] *and Rong Song*[1*]

[1] *Guangdong Provincial Engineering and Technology Center of Advanced and Portable Medical Devices, School of Engineering, Sun Yat-sen University, Guangzhou, China,* [2] *Injury Rehabilitation Hospital of Guangdong Province, Guangzhou, China*

Keywords: rehabilitation robot, wire-driven, upper limb, tracking control, sliding mode, nonlinear disturbance observer

OPEN ACCESS

Edited and reviewed by:
Jean-Claude Baron,
University of Cambridge,
United Kingdom

***Correspondence:**
Rong Song
songrong@mail.sysu.edu.cn

†Co-first authors.

Specialty section:
This article was submitted to Stroke, a section of the journal Frontiers in Neurology

Received: *09 April 2018*
Accepted: *11 June 2018*
Published: *28 June 2018*

Citation:
Niu J, Yang Q, Wang X and Song R (2018) Corrigendum: Sliding Mode Tracking Control of a Wire-Driven Upper-Limb Rehabilitation Robot with Nonlinear Disturbance Observer. Front. Neurol. 9:511. doi: 10.3389/fneur.2018.00511

A corrigendum on

Sliding Mode Tracking Control of a Wire-Driven Upper-Limb Rehabilitation Robot with Nonlinear Disturbance Observer
by Niu, J., Yang, Q., Wang, X., and Song, R. (2017). Front. Neurol. 8:646. doi: 10.3389/fneur.2017.00646

In the original article, there was an error. The article partly overlaps with previously published conference proceedings. A correction has been made to add an Acknowledgments section.

ACKNOWLEDGMENTS

This article is partially based on our previous work which is shown in a conference paper (1).

The authors apologize for this error and state that this does not change the scientific conclusions of the article in any way.

REFERENCES

1. Niu J, Yang Q, Chen G, Song R. Nonlinear disturbance observer based sliding mode control of a cable-driven rehabilitation robot. *IEEE Int Conf Rehabil Robot*. (2017) 2017:664–9. doi: 10.1109/icorr.2017.8009324

Conflict of Interest Statement: The authors declare that the research was conducted in the absence of any commercial or financial relationships that could be construed as a potential conflict of interest.

frontiers in Neurology

ORIGINAL RESEARCH
published: 08 December 2017
doi: 10.3389/fneur.2017.00654

Usability of Videogame-Based Dexterity Training in the Early Rehabilitation Phase of Stroke Patients: A Pilot Study

Tim Vanbellingen[1,2†], Suzanne J. Filius[3,4†], Thomas Nyffeler[1,2] and Erwin E. H. van Wegen[5]*

[1] Neurology and Neurorehabilitation Center, Luzerner Kantonsspital, Luzern, Switzerland, [2] Gerontechnology and Rehabilitation Group, University of Bern, Bern, Switzerland, [3] Faculty of Behavioral and Movement Sciences, Amsterdam Movement Sciences, VU University Amsterdam, Amsterdam, Netherlands, [4] Mechanical, Marine and Materials Engineering, Technical University of Delft, Delft, Netherlands, [5] Department of Rehabilitation Medicine, Amsterdam Movement Sciences, Amsterdam Neurosciences, Vrije Universiteit Medical Center, Amsterdam, Netherlands

Background: Approximately 70–80% of stroke survivors have limited activities of daily living, mainly due to dexterous problems. Videogame-based training (VBT) along with virtual reality seems to be beneficial to train upper limb function.

Objective: To evaluate the usability of VBT using the Leap Motion Controller (LMC) to train fine manual dexterity in the early rehabilitation phase of stroke patients as an add-on to conventional therapy. Additionally, this study aimed to estimate the feasibility and potential efficacy of the VBT.

Methods: During 3 months, 64 stroke patients were screened for eligibility, 13 stroke patients were included (4 women and 9 men; age range: 24–91 years; mean time post stroke: 28.2 days).

Intervention: Nine sessions of 30 min VBT, three times per week as an add-on to conventional therapy with stroke inpatients.

Outcome measures: Primary outcome was the usability of the system measured with the System Usability Scale. Secondary outcomes concerning feasibility were the compliance rate calculated from the total time spent on the intervention (TT) compared to planned time, the opinion of participants via open-end questions, and the level of active participation measured with the Pittsburgh Rehabilitation Participation Scale. Regarding the potential efficacy secondary outcomes were: functional dexterity measured with the Nine Hole Peg Test (NHPT), subjective dexterity measured with the Dexterity Questionnaire 24, grip strength measured with the Jamar dynamometer, and motor impairment of the upper limb measured with the Fugl-Meyer Upper Extremity (FM-UE) scale.

Results: Primarily, the usability of the system was good to excellent. The patient's perception of usability remained stable over a mean period of 3 weeks of VBT. Secondly, the compliance rate was good, and the level of active participation varied between good and very good. The opinion of the participants revealed that despite individual differences, the overall impression of the therapy and device was good. Patients showed significant

OPEN ACCESS

Edited by:
Dong Feng Huang, Sun Yat-sen University, China

Reviewed by:
Alessandro Tognetti, University of Pisa, Italy
Katharina Stibrant Sunnerhagen, University of Gothenburg, Sweden

***Correspondence:**
Erwin E. H. van Wegen
e.vanwegen@vumc.nl

†These authors have contributed equally to this work.

Specialty section:
This article was submitted to Stroke, a section of the journal Frontiers in Neurology

Received: *12 September 2017*
Accepted: *21 November 2017*
Published: *08 December 2017*

Citation:
Vanbellingen T, Filius SJ, Nyffeler T and van Wegen EEH (2017) Usability of Videogame-Based Dexterity Training in the Early Rehabilitation Phase of Stroke Patients: A Pilot Study. Front. Neurol. 8:654. doi: 10.3389/fneur.2017.00654

improvements in hand dexterity. No changes were found in motor impairment of the upper limb (FM-UE) during intervention.

Conclusion: VBT using LMC is a usable rehabilitation tool to train dexterity in the early rehabilitation phase of stroke inpatients.

Keywords: stroke, dexterity, videogame-based training, Leap Motion Controller, virtual reality, usability

INTRODUCTION

Stroke is a serious global health-care problem and is one of the greatest causes of acquired adult disability (1). Approximately 70–80% of stroke survivors have limited activities of daily living after discharge home (2). They experience for example difficulties with feeding, dressing, and grooming, mainly due to impaired dexterity (3, 4). Neurorehabilitation plays a major role in the treatment of stroke patients (1), in which improving dexterity is a core element of treatment protocols (5).

Most improvements in upper limb function usually occur within the first month poststroke (6–8). It is suggested that neurorehabilitation can enhance neurological recovery (9, 10) and to elicit neuro-plastic adaptations it is important that exercise programs are intensive, highly repetitive, and task-specific (5, 11–13). Additionally, it is recommended to start interventions early poststroke because of heightened brain plasticity in this period (7, 9).

To further enhance upper limb outcome, research continues to investigate new approaches (14). An upcoming therapeutic method is videogame-based training (VBT) along with virtual reality (VR) (15, 16). Recent meta-analyses claim that there is moderate evidence that VR training may be beneficial for upper limb recovery after stroke (3, 17). VBT has several advantages such as variety in games and variance in artificial environments or stimuli and it can be used in a home-based situation (12, 15). These advantages could improve the motivation to sustain a repetitive intervention. Another important property of VBT is online feedback, which can increase the effectiveness of motor learning-based training by perceiving and correcting movement error (18, 19). Especially in VBT, visual and auditory feedback is important because there is no sensory feedback of real-world object in the hands.

Devices such as Microsoft Kinect™ and Nintendo Wii-Fit could be used in VBT [e.g., (20, 21)]. However, these devices fail to detect fine hand and finger movements (15), which is needed to train dexterity. Several studies report moderate improvements in dexterity using VBT in stroke, but these systems are not commercially available (22–25). A commercially available device called Leap Motion Controller (LMC) is a low-cost, low-complexity optoelectronic system, which can track hand movements (15, 26). The LMC is delivered with software in which several videogames can be uploaded. So far, one explorative small sample feasibility study looked at the use of LMC in four chronic stroke patients and demonstrated good compliance but failed to show significant effects on hand dexterity (15). However, while important, the level of active participation is not sufficient as feasibility measure alone. Active participation can be influenced by several factors such as intrinsic motivation to recover, enthusiasm of the therapist, system usability, and complexity etcetera. Therefore, the present study evaluates the usability of the LMC system with the System Usability Scale (SUS) (27), which is well validated to evaluate new technologies, including software. In addition to system usability, this pilot study aimed to get a comprehensive estimation of the feasibility of the VBT. Consequently, the compliance rate, the level of active participation, and the opinion of the participants were systematically evaluated. Furthermore, we aimed to evaluate the potential efficacy of a specific dexterity LMC training program by evaluating recovery of motor function of the arm, grip strength, and dexterity. We hypothesized that VBT using the LMC, initiated within the early rehabilitation phase (5), would be a usable tool to train manual dexterity in stroke patients as an add-on therapy. Moreover, we expected the compliance rate and level of active participation to be good. Concerning efficacy, we hypothesized that VBT with LMC improves hand dexterity.

MATERIALS AND METHODS

The study was approved by the Ethikkommission Nordwest- und Zentralschweiz of the canton Lucerne. All patients gave written informed consent according to the latest declaration of Helsinki (2013).

Participants

The participants were recruited through medical chart review and regular visits between April and May 2017. Each patient in this study received standard neurorehabilitation care during their hospitalization. Patients were selected according to the following criteria: inclusion criteria were: (1) written informed consent, (2) aged above 18 years, (3) a first-ever stroke in the past 24 h until 3 months, reflecting the early rehabilitation phase (5) (4) experience upper limb impairments due to stroke (Nine Hole Peg Test > 19 s with at least one side) (28), (5) at least able to perform ante-flexion with their upper arm and extent one or more fingers against gravity ($3 \leq$ Medical Research Council scale < 5) (29), and (6) the participants had to be able to understand the instructions and assessments in German. Exclusion criteria were: (1) severe cognitive impairments (Montreal Cognitive

Abbreviations: CVA, cerebrovascular accident; DextQ-24, Dexterity Questionnaire 24; FM-UE, Fugl-Meyer Upper Extremity scale; LMC, Leap Motion Controller; M, mean; MoCa, Montreal Cognitive Assessment; N, number of participants; NHPT, Nine Hole Peg Test; PRPS, the Pittsburgh Rehabilitation Participation Scale; SUS, System Usability Scale; TT, the total time spent on the intervention; PT, planned time; VBT, videogame-based training.

TABLE 1 | Schedule of aimed procedure.

Week 1	Day 1	60 min	T0 + T1	NHPT → Jamar → DextQ-24 → FM-UE → Training → SUS (T1)
	Day 2	30 min	T2	Training
	Day 3	45 min	T3	NHPT → Jamar → DextQ-24 → Training → SUS (T3)
Week 2	Day 1	30 min	T4	Training
	Day 2	30 min	T5	Training
	Day 3	45 min	T6	NHPT → Jamar → DextQ-24 → Training → SUS (T6)
Week 3	Day 1	30 min	T7	Training
	Day 2	30 min	T8	Training
	Day 3	60 min	T9	NHPT → Jamar → DextQ-24 → FM-UE → Training → SUS (T9) → Interview

Interview with open-end questions. The arrows represent the order of actions during the sessions.
T, training session; SUS, Systems Usability Scale; NHPT, Nine Hole Peg Test; DextQ-24, Dexterity Questionnaire 24; FM-UE, Upper Extremity motor section of the Fugl-Meyer Assessment, measures motor impairment of the upper limb.

assessment: MoCa < 14) (30), (2) severe apraxia (Apraxia Screen of TULIA < 9) (31), (3) aphasia (Language screening test < 15) (32), (4) severe self-reported pain, or (5) other severe orthopedic problems of the upper limb impairing participation.

Procedure

The intervention consisted of nine training sessions of 30 min, spread out over a period of 3 weeks, this means three training sessions per week. An intake session was planned with eligible patients. Upon consent, the baseline measures of dexterity, grip strength, and motor impairment of the upper limb were collected. This was, if possible, followed by the first training and evaluation of the usability of the system. The level of active participation and time spent on the intervention were measured during each training session. The second, fourth, fifth, seventh, and eighth session contained only training. In the third, sixth, and ninth session, dexterity and grip strength were measured followed by the training and evaluation of the usability. The reassessment of the motor impairment of the upper limb and evaluation of the open-end questions were at the ninth session. The present study aimed to follow the procedure schedule as shown in **Table 1**.

FIGURE 1 | Research setup. Courtesy of S. Filius.

Intervention

Each training session was performed on a desktop computer at the occupational ward of the neurorehabilitation. The participants (if not in a wheelchair) were sitting on a chair with a rectangular pillow on their lap, so that the elbows could rest on the pillow (see **Figure 1**).

The LMC was placed on a table in front of the participant between the body and the computer screen. During each session, the principal investigator sat next to the participants, providing (if needed) online feedback via verbal, visual, and/or physical instructions.

The LMC incorporates three infrared emitters and two charge-coupled device cameras for capturing the motion of both hands, wrists, and forearms (15, 26). The light of the infrared emitters reflects back from the surfaces of the hands, so no markers are needed (33). Weichert et al. (34) reported that the LMC has an accuracy of 0.2 and 1.2 mm in a static and dynamic setup, respectively.

In February and March 2017, all free access games in the Leap Motion App Store© (https://apps.leapmotion.com/?sign_up=true) were evaluated to determine if the games contained key components of dexterity movements: alternating finger, pincer grasp, fine pointing, and palmar extension/flexion. Five games were selected: Dots Trial, Cut the Rope, Playground, and American Sign Language Digits. Playground contains two games named Blocks and Flower. See **Figure 2** for an impression of the games.

Each therapy session contained about 6 min per game, and the sequence of the five games was randomized by the function "randperm" using MATLAB R2013b (Mathworks, Natick, MA, USA). Each game is played with both hands starting with the non-affected hand.

A HP EliteDesk 800 (Intel Core i5) desktop computer was used, with a 19-inch computer screen with an aspect ratio 4:3 (1,280 × 768).

Outcome Measures

All outcome measurements were collected and/or rated by a single trained assessor (SF) to optimize standardization of outcome measurement.

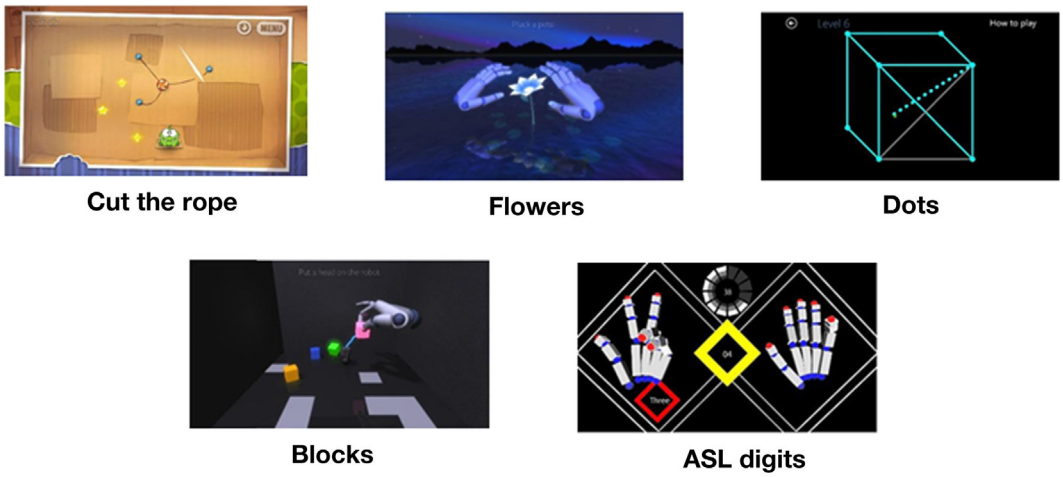

FIGURE 2 | Games. Retrieved from Leap Motion App Store© (https://apps.leapmotion.com/?sign_up=true).

Primary Outcome

The primary outcome measure was self-reported system usability, evaluated by the SUS (27). Two usability aspects are important: that the LMC is able to track the impaired hand and that patients cognitively understand the VBT. The SUS is a generalized usability measure which collects users' subjective perception of interaction with different interfaces (27).

The SUS has ten items with a 5-point scale from 1 (strongly disagree) to 5 (strongly agree), with a range from 0 to 100 (35, 36) and takes into account three usability criteria: effectiveness, efficiency, and satisfaction (36). Brooke stated that the SUS is a robust and reliable evaluation tool with high face validity, but no qualitative values of reliability and validity were found. We used a German translation of the SUS, translated by a native speaker. A system is acceptably usable from a SUS score upwards of 70, with "good products" scoring between high 70s and upper 80s (27). The participants were asked to fill-in the SUS independently.

Secondary Outcomes

Feasibility

Feasibility was comprehensively measured by (1) the compliance rate which was determined by the ratio of the total time spent on intervention (TT) and planned time (PT), (2) the level of active participation, measured with the Pittsburgh Rehabilitation Participation Scale (PRPS) (37), and (3) the subjective opinion of the participants, evaluated by open-end questions in an interview form.

To determine the compliance rate, the time spent on every training session was recorded by the principal investigator. The TT was compared to the PT (4 h 30 min) to evaluate if patients were able and willing to complete the intervention. Patients who were discharged from hospital before end of intervention were excluded from the compliance analysis.

The level of active participation was measured with the PRPS. The PRPS is a six-point scale from 1 "refusal to participate" to 6 "excellent participation" (15) and is a reliable and valid therapist-rated measure of inpatients participation in occupational therapy (intraclass correlation coefficient: ICC = 0.91) and physical therapy (ICC = 0.96) (37).

The open-end questions were about (1) the overall impression of the therapy/LMC device, (2) the duration of the therapy, (3) the potential home-use, (4) possible improvements of the system, (5) overall remarks or commentary, (6) the quality of the instructions of the therapist, and (7) the most favorite and (8) the least favorite game. The answers were given orally and written down by the principal investigator. See Appendix S1 in Supplementary Material for the open-end questions in German.

Efficacy

Since the focus of the training program was dexterity, several standardized outcome measures were performed: (1) dexterity measured with the Nine Hole Peg Test (NHPT), (2) subjective, self-reported dexterity measured with the Dexterity Questionnaire 24 (DextQ-24) (38), (3) grip strength measured with the Jamar dynamometer (39), and (4) the motor impairment of the upper limb measured with the Upper Extremity motor section of the Fugl-Meyer Assessment (FM-UE) (40).

The NHPT is a hand function test, which consists of a plastic peg board (25.0 cm × 12.7 cm × 2.3 cm) with nine holes (2.54 cm between the holes) and nine pegs (3.2 cm long, 0.64 cm wide) (41). Chen et al. found a good test–retest reproducibility of the NHPT (ICC = 0.85 with more-affected side). The participant had to put the nine pegs in the peg board as fast as possible, one at the time with one hand only, and remove them again. The test was performed two times per hand, with the non-affected hand first. The time it takes to fulfill the second trial with the more-affected hand was used for the analysis.

The DextQ-24 is a patient reported outcome measure that evaluates the performance and independence of daily dexterity activities. The DextQ-24 is a valid and reliable (ICC = 0.91; measurement error = 2.9) measurement in patients with Parkinson's disease (38). The DextQ-24 has 24 items with 12

items uni-manual and 12 items bi-manual. The scale goes from 1 "no problems" to 4 "unable to perform the task and needing aid from a third person" (38).

The grip strength is measured with the Jamar baseline® hydraulic hand dynamometer. The Jamar dynamometer is a reliable tool with a high intra-examiner reliability (ICC = 0.97–0.99) and a SEM between 0.98 and 1.69 kg in chronic stroke patients (39). The grip strength is assessed following the recommendations of American Society of Hand Therapists (ASHT) with the shoulder adducted, elbow flexed at 90°, forearm in neutral position, and the second position of the handle is used (42). The participants have to perform the grip strength test three times alternating per hand, and the averaged value of the affected hand is used for analysis.

The use of FM-UE is worldwide recommended for clinical trials of stroke rehabilitation as an evaluation of recovery in the poststroke hemiplegic patient (43). The FM-UE has 34 items which are scored from 0 to 2, with a total range from 0 to 66 points (43).

Statistical Analysis

Descriptive statistics were used to calculate the group mean (*M*), SD, and SEM of clinical and demographic variables.

The distributions of the outcome measures (SUS, PRPS, NHPT, DextQ-24, Jamar, and FM-UE) were examined for normality of distribution to select either the parametric one-way repeated measure ANOVA or the non-parametric Friedman's ANOVA. Wilcoxon Signed Rank Test was used in addition to the non-parametric Friedman's ANOVA. The compliance rate is calculated by: *compliance rate* = TT/PT × 100%. A compliance rate of 80% was defined as good (44). The level of active participation was evaluated by the principal investigator per game. The PRPS scores per training was the average PRPS score of all the games played in that session. The answers of the open-end questions 1, 2, 3, and 6 were grouped in positive, neutral, and negative answers, so that the answers could be organized and analyzed. For the remaining open-end questions, a descriptive summary of the answers is given.

Statistical analyses were performed using the SPSS statistical software system (IBM SPSS Statistics for Windows, Version 22.0. Armonk, NY, USA: IBM Corp.), and a confidence level of 95% was used, so that level of significance was set at $p = 0.05$, two-tailed.

RESULTS

Descriptive Data

During the recruitment period, 64 stroke patients admitted to the neurorehabilitation ward were screened for eligibility. Fifteen patients who were potentially eligible were selected. Two patients did not accept informed consent and were excluded. Thirteen patients started the 3 weeks LMC dexterity training program. Clinical and demographic characteristics are presented in **Table 2**.

Eight of the thirteen patients could complete the whole training program. One participant experienced a new stroke between the seventh and eighth session, and therefore, follow-up measures were excluded from the main analysis. Three other patients were discharged earlier. And finally, one older patient, a 62-year old male, stopped the intervention during the second training session due to lack of motivation. Importantly, there were no severe intervention-related adverse events like severe shoulder pain or severe fatigue.

Overall analyses revealed few missing data in the outcome measures: SUS (3.1%) and DextQ-24 (0.65%). Average imputation was used to correct these gaps. Furthermore, one participant was not able to perform the NHPT with his affected hand and is not included in the NHPT analysis. The other outcome measures had no missing data.

Outcomes

Primary Outcome

The average SUS score of all participants ($N = 13$) was 75.4, SD = 13.8 after the first training session. Patients' perception of usability of the system remained unchanged, $F_{(3, 21)} = 0.09$, $p = 0.96$ over time. The average SUS score of the eight participants who finished the intervention was $M = 78.9$, SD = 11.6 after the first, and $M = 79.1$, SD = 9.7 after the ninth training session (for more details see **Figure 3**).

TABLE 2 | Clinical and demographic characteristics.

Descriptive data	*N* = 13
Gender, male/female, *n*	9/4
Age, years (range)	68.2 ± 17.5 (24–91)
Time post-stroke at inclusion, days (range)	28.2 ± 23.2 (8–88)
Type of stroke, *n*	
Ischemic CVA, A. cerebri media	5
Ischemic CVA, A. cerebri posterior	7
Hemorrhage, CVA	1
Handedness, *n*	
Right/left	11/2
Paretic side, *n*	
Right	8
Left	4
Both	1
Dominant side affected, *n*	7
NHPT, s	50.0 ± 26.9 (17–60)
DextQ-24	41.4 ± 15.8 (27–70)
Fugl Meyer Arm score	57.5 ± 9.3 (42–65)
MoCA	21.7 ± 5.7 (14–30)

All data are presented by the mean ± SD or otherwise stated.
N or n, number of participants; NHPT, Nine Hole Peg Test; DextQ-24, Dexterity Questionnaire-24; MoCA, Montreal Cognitive Assessment; CVA, cerebrovascular accident.

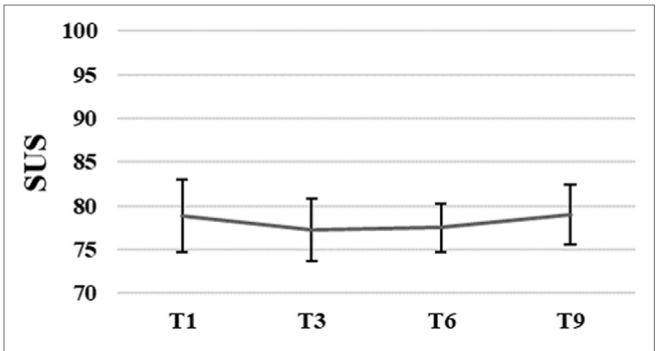

FIGURE 3 | Group means with SEM for the results of the System Usability Scale (SUS) scores measured at different time points.

Secondary Outcomes

Feasibility

The average TT spent on the intervention was, $M = 3$ h 56 min, SD = 1 h 16 min with a range of 42 min to 4 h 45 min. The compliance rate of the participants was 87.4%.

The average level of active participation measured with PRPS varied between good 4.7 and very good 5.4. The PRPS scores slightly increased until sixth training session followed by a small decrease after the seventh training session. However, these changes were not significant, $F_{(1.05, 0.39)} = 2.71$, $p = 0.07$ (for more details, see **Figure 4**).

Efficacy

Nine Hole Peg Test scores decreased significantly during intervention, $\chi^2_{(3)} = 15.34$, $p < 0.00$. The NHPT scores significantly decreased from baseline to third, $Z = -2.03$, $p = 0.04$, from baseline to sixth, $Z = -2.37$, $p = 0.02$, and from baseline to ninth training session, $Z = -2.20$, $p = 0.02$. The NHPT scores also significantly decreased from third to sixth, $Z = -2.4$, $p = 0.02$, and third to ninth training session, $Z = -2.37$, $p = 0.02$. The NHPT decreased 31.5% from baseline ($M = 49.96$ s, SD = 26.85) to ninth training session ($M = 34.21$ s, SD = 7.33).

DextQ-24 scores for subjective experience of dexterity significantly decreased during intervention, $\chi^2_{(3)} = 14.92$, $p < 0.00$. The DextQ-24 scores significantly decreased between baseline to sixth, $Z = -1.28$, $p = 0.01$, baseline to ninth, $Z = -2.54$, $p = 0.01$, and third to ninth training session, $Z = -2.12$, $p = 0.03$. The DextQ-24 scores decreased 16.3% from baseline ($M = 41.4$, SD = 15.8) to ninth training session ($M = 34.6$, SD = 16.0).

Jamar dynamometer scores for grip strength significantly increased during intervention, $F_{(3,21)} = 5.51$, $p = 0.01$. Grip strength (in kilogram) increased 11.3% from baseline ($M = 23.5$ kg, SD = 8.3) to ninth training session ($M = 26.2$ kg, SD = 6.6).

FM-UE scores for motor impairments of the upper limb varied between scores of 42 and 65 at baseline ($M = 57.5$, SD = 9.3), and between 44 and 66 at the ninth training session ($M = 58.5$, SD = 6.7). The FM-UE scores did not significantly change over time ($p > 0.05$) (for more details, see **Figures 5A–C**).

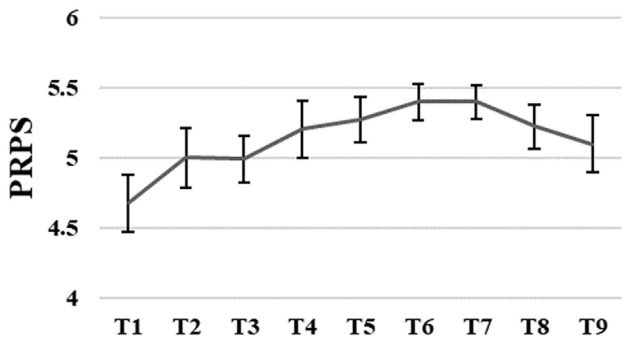

FIGURE 4 | Group means with SEM for the results of the Pittsburgh Rehabilitation Participation Scale (PRPS) scores measured at different time points.

Open End Questions

The first 3 open-end questions revealed that patients had an overall good impression of the therapy and system (7 positive; 1 neutral; 0 negative categorized responses), and that the duration of the therapy (30 min) was fairly good ($N = 2$) to good ($N = 6$). Participants mentioned that the time per session should not be much longer than 30 min, because of loss of concentration and

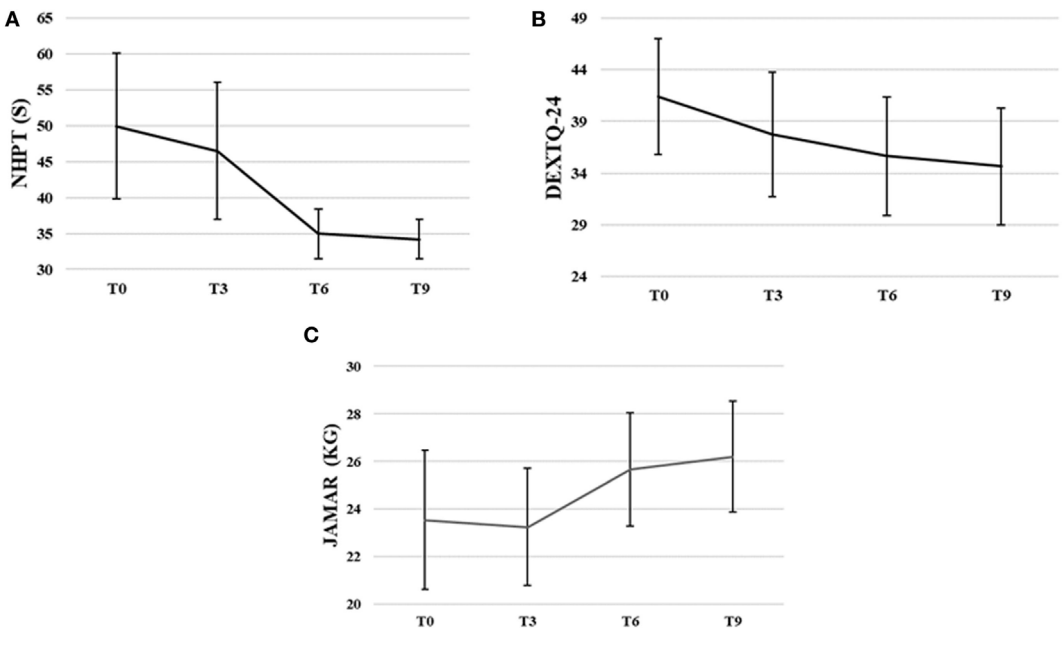

FIGURE 5 | Group means with SEM for the results of **(A)** the Nine Hole Peg Test (NHPT) scores in seconds (s), **(B)** the Dexterity Questionnaire 24 (DextQ-24) scores, and **(C)** the Jamar grip strength in kilograms (kg).

arm-related fatigue. Three participants would consider home-use of the LMC. They stated that it would depend on the price, technical improvements, and the available games. One participant specifically asked to prolong with the VBT and would like to continue at home. The answers on the fourth and fifth question about the possible improvements or overall remarks, revealed that three participants felt that they were either too old for using this kind of technology, were not using a computer at home, or needed help from another person. The majority of participants was enthusiastic about the new experiences with the LMC or had the feeling that they learned from the VBT. Most participants did not have specific practical suggestions to improve the therapy or device, but one participant noticed that it would have been nice to see the personal booked progress in the program of the games. All participants indicated that they benefit from therapist's additional instructions and were satisfied with the support of a therapist.

DISCUSSION

The present study aimed to comprehensively explore the usability and feasibility of a 3-week video game-based dexterity training using the LMC in the early rehabilitation phase of stroke patients. We show for the first time that the LMC is a usable tool, measured by the SUS. In addition, stroke patients demonstrated good compliance to the training protocol and were strongly motivated throughout the 3-week training, underlining high feasibility. In addition, hand strength and dexterity significantly improved, both at the level of function and activities/participation.

The reasons why the LMC is usable are multifold. First, LMC is a small, lightweight, USB powered device which can be plugged-in in every computer. Second, the installation of the integrated software is user friendly. Third, no expert technician is needed since there is no need to attach markers of the device to the hands, making the tool beneficial in its use as compared to other VR upper limb tools such as virtual gloves or exoskeletons (45–47). Fourth, the fact the LMC system is relatively cheap, and easy to purchase it may be easily integrated into the home setting. Interestingly, in contrast to Iosa et al. (15), in our sample, also patients with moderately impaired cognitive abilities were included. They also managed to act well with the LMC further underlining its high usability.

Compliance and Active Participation

Compliance rate was high (87%) and while the only previous LMC study did not report data on compliance rates (15), we consider this high feasibility of VBT with LMC. Active participation level scores were in line with Iosa et al. (15). The slight decrease in PRPS scores after the seventh training session could result from lack of progression in game level difficulty, as all attainable levels were attained after 2 weeks. Such progression in difficulty next to variance and challenge in games is needed to increase the efficacy and compliance. Another reason could be that the LMC is at some point perhaps not sensitive enough anymore to the quality of movement and misses crucial information on upper limb motor recovery (48). For example, the LMC registers the movements as "performed well," while the real-world movements are still not optimal or contain compensation strategies (49). This could affect the level of challenge in the VBT. Nevertheless, the level of active participation remained very good throughout the training program, but it should be kept in mind that the VBT with LMC was performed in the presence of a therapist during hospitalization and therefore possibly attributing to a high participation level of the patients.

Other studies have examined VBT delivered in the home environment of chronic stroke patients (50, 51). Piron et al. used a tele-rehabilitation approach using two computers, a camera, and a magnetic transmitter/receiver to deliver remote upper limb training in chronic stroke patients with favorable results. All participants completed the intervention, but exact compliance rates were not reported (50). Standen et al. implemented upper limb training with a virtual glove with LEDs and an infrared camera, which proved feasible. However, considerable variation was found both in terms of duration of use (1.46–70% of the recommended duration) and the number of days used (10–100%) (51). In our study, we found high compliance rates and good participation, showing that the LMC system, relatively cheap and simple compared to these systems, is feasible already in the early rehabilitation phase in an in-patient setting. However, home-based implementation of the LMC in the early rehabilitation phase needs further study to determine if compliance rate and active participation would also be acceptable.

From the viewpoint of the therapist, we found that participants were not always completely capable to perform the VBT independently. Visual, verbal, and physical instructions were sometimes needed to support participants. Most therapist instructions were related to depth perception in the VR environment. This is indeed already described previously that stroke patients may experience difficulties in perceiving objects in a 3D environment (52). The gameplay instructions were not embedded in the games and personal progress was not recorded in the software. This prompted the need for a therapist to switch between games, record the personal progress, and intervene when there were technical problems with the LMC. Proposed improvements from patient-reported suggestions are in line with these limitations.

Efficacy

Although this pilot study was not designed and powered to evaluate efficacy, we found improvements in the objective and subjective dexterity outcomes (31.5% in NHPT, 16.3% in DextQ-24. resp.). This is in line with previous studies (17, 50, 51). The improvements in dexterity may result from the training being intensive, highly repetitive, and task-specific (5). We also found significant improvements (11.3%) in grip strength. There is no resistance of real-world objects involved in the LMC training so this is somewhat unexpected and may be due to spontaneous neurological recovery in the early rehabilitation phase (1, 7, 49). Iosa et al. (15) also found improvements in grasp force after VBT with LMC. Possibly VBT could improve grip strength through the increased number of repetitions of pinch and grip movements but this needs further investigation.

The neurological recovery of motor function of the upper limb was measured with the FM-UE, for which we did not find

significant changes. The FM-UE is however a general evaluation of pathological synergies in the upper extremity and not a specific dexterity measure and may fail to detect small improvements in fine manual dexterity and grip strength. In addition, the FM-UE may not be sensitive to the quality of the movement (e.g., if a patient was able to completely perform a movement-item at baseline and performed the same movement-item much smoother at ninth session, it was both scored with a 2, "can be performed"). Furthermore, the baseline scores of our participants were already quite high, leaving less room for improvement.

Limitations

The present study was subject to limitations, such as the pre-experimental, this means one group pre-test/post-test, design, small sample size, and the limited duration of the intervention. In addition, although the DextQ-24 was validated in patients with Parkinson's disease (38), it was not formally validated in sub-acute stroke patients.

CONCLUSIONS

The present pilot study is the first to evaluate the usability of the VBT using the LMC to train fine manual dexterity in the early rehabilitation phase of stroke patients as an add-on to conventional therapy. VBT using the commercially available LMC is feasible in the early rehabilitation phase in stroke patients admitted for in-patient rehabilitation. Future studies should investigate the add-on value of home-use of LMC. For home-based training, the software should contain clear build-in instructions for online feedback, options to save and provide feedback on personal progresses and have structured progression and a large variety in challenging games to be successful.

ETHICS STATEMENT

The study was approved by the Ethikkommission Nordwest- und Zentralschweiz of the canton Lucerne. All patients gave informed consent according to the latest declaration of Helsinki (2013).

AUTHOR CONTRIBUTIONS

Study design: TV, SF, and EW; data acquisition: TV and SF; data analysis: TV, SF, and EW; interpretation of data: TV, SF, TN, and EW; drafting and revising: TV, SF, TN, and EW; FINAL approval: TV, SF, TN, and EW.

ACKNOWLEDGMENTS

The work has been financially supported by the Jacques and Gloria Gossweiler Foundation and The European Foundation for Health and Exercise. The authors would like to especially thank the participants who voluntary enrolled in this study. In addition, we are grateful to Judith van Beek, who was involved in the set-up of the exercises.

SUPPLEMENTARY MATERIAL

The Supplementary Material for this article can be found online at http://www.frontiersin.org/article/10.3389/fneur.2017.00654/full#supplementary-material.

REFERENCES

1. Langhorne P, Bernhardt J, Kwakkel G. Stroke rehabilitation. *Lancet* (2011) 377(9778):1693–702. doi:10.1016/S0140-6736(11)60325-5
2. Caimmi M, Carda S, Giovanzana C, Maini ES, Sabatini AM, Smania N, et al. Using kinematic analysis to evaluate constraint-induced movement therapy in chronic stroke patients. *Neurorehabil Neural Repair* (2008) 22(1):31–9. doi:10.1177/1545968307302923
3. Pollock A, Farmer SE, Brady MC, Langhorne P, Mead GE, Mehrholz J, et al. Interventions for improving upper limb function after stroke. *Cochrane Database Syst Rev* (2014) (11):CD010820. doi:10.1002/14651858.CD010820.pub2
4. Ekstrand E, Rylander L, Lexell J, Brogårdh C. Perceived ability to perform daily hand activities after stroke and associated factors: a cross-sectional study. *BMC Neurol* (2016) 16(1):208. doi:10.1186/s12883-016-0733-x
5. Veerbeek JM, van Wegen E, Van Peppen R, Van Der Wees PJ, Hendriks E, Rietberg M, et al. What is the evidence for physical therapy poststroke? A systematic review and meta-analysis. *PLoS One* (2014) 9(2):e87987. doi:10.1371/journal.pone.0087987
6. Duncan PW, Goldstein LB, Matchar D, Divine GW, Feussner J. Measurement of motor recovery after stroke. Outcome assessment and sample size requirements. *Stroke* (1992) 23(8):1084–9. doi:10.1161/01.STR.23.8.1084
7. Buma F, Kwakkel G, Ramsey N. Understanding upper limb recovery after stroke. *Restor Neurol Neurosci* (2013) 31(6):707–22. doi:10.3233/RNN-130332
8. Winters C, van Wegen EE, Daffertshofer A, Kwakkel G. Generalizability of the proportional recovery model for the upper extremity after an ischemic stroke. *Neurorehabil Neural Repair* (2015) 29(7):614–22. doi:10.1177/1545968314562115
9. Murphy TH, Corbett D. Plasticity during stroke recovery: from synapse to behaviour. *Nat Rev Neurosci* (2009) 10(12):861–72. doi:10.1038/nrn2735
10. Zeiler SR, Krakauer JW. The interaction between training and plasticity in the post-stroke brain. *Curr Opin Neurol* (2013) 26(6):609. doi:10.1097/WCO.0000000000000025
11. Birkenmeier RL, Prager EM, Lang CE. Translating animal doses of task-specific training to people with chronic stroke in 1-hour therapy sessions: a proof-of-concept study. *Neurorehabil Neural Repair* (2010) 24(7):620–35. doi:10.1177/1545968310361957
12. Brunner I, Skouen JS, Hofstad H, Aßmuss J, Becker F, Pallesen H, et al. Is upper limb virtual reality training more intensive than conventional training for patients in the subacute phase after stroke? An analysis of treatment intensity and content. *BMC Neurol* (2016) 16(1):219. doi:10.1186/s12883-016-0740-y
13. Fluet GG, Patel J, Qiu Q, Yarossi M, Massood S, Adamovich SV, et al. Motor skill changes and neurophysiologic adaptation to recovery-oriented virtual rehabilitation of hand function in a person with subacute stroke: a case study. *Disabil Rehabil* (2017) 39(15):1524–31. doi:10.1080/09638288.2016.1226421
14. Veerbeek JM, Langbroek-Amersfoort AC, van Wegen EE, Meskers CG, Kwakkel G. Effects of robot-assisted therapy for the upper limb after stroke. *Neurorehabil Neural Repair* (2017) 31(2):107–21. doi:10.1177/1545968316666957
15. Iosa M, Morone G, Fusco A, Castagnoli M, Fusco FR, Pratesi L, et al. Leap motion controlled videogame-based therapy for rehabilitation of elderly patients with subacute stroke: a feasibility pilot study. *Top Stroke Rehabil* (2015) 22(4):306–16. doi:10.1179/1074935714Z.0000000036
16. Orihuela-Espina F, Roldán GF, Sánchez-Villavicencio I, Palafox L, Leder R, Sucar LE, et al. Robot training for hand motor recovery in subacute stroke patients: a randomized controlled trial. *J Hand Ther* (2016) 29(1):51–7. doi:10.1016/j.jht.2016.05.003
17. Laver KE, George S, Thomas S, Deutsch JE, Crotty M. Virtual reality for stroke rehabilitation. *Stroke* (2012) 43(2):e20–1. doi:10.1161/STROKEAHA.111.642439

18. Chiviacowsky S, Wulf G. Feedback after good trials enhances learning. *Res Q Exerc Sport* (2007) 78:40–7. doi:10.1080/02701367.2007.10599402
19. Van Vliet PM, Wulf G. Extrinsic feedback for motor learning after stroke: what is the evidence? *Disabil Rehabil* (2006) 28(13–14):831–40. doi:10.1080/09638280500534937
20. Simonsen D, Popovic MB, Spaich EG, Andersen OK. Design and test of a Microsoft Kinect-based system for delivering adaptive visual feedback to stroke patients during training of upper limb movement. *Med Biol Eng Comput* (2017) 55:1927–35. doi:10.1007/s11517-017-1640-z
21. Yates M, Kelemen A, Sik Lanyi C. Virtual reality gaming in the rehabilitation of the upper extremities post-stroke. *Brain Inj* (2016) 30(7):855–63. doi:10.3109/02699052.2016.1144146
22. Donoso Brown EV, McCoy SW, Fechko AS, Price R, Gilbertson T, Moritz CT. Preliminary investigation of an electromyography-controlled video game as a home program for persons in the chronic phase of stroke recovery. *Arch Phys Med Rehabil* (2014) 95:1461–9. doi:10.1016/j.apmr.2014.02.025
23. Slijper A, Svensson KE, Backlund P, Engström H, Sunnerhagen KS. Computer game-based upper extremity training in the home environment in stroke persons: a single subject design. *J Neuroeng Rehabil* (2014) 11(1):35. doi:10.1186/1743-0003-11-35
24. Hayward KS, Neibling BA, Barker RN. Self-administered, home-based SMART (sensorimotor active rehabilitation training) arm training: a single-case report. *Am J Occup Ther* (2015) 69:1–8. doi:10.5014/ajot.2015.016055
25. Pietrzak E, Cotea C, Pullman S. Using commercial video games for upper limb stroke rehabilitation: is this the way of the future. *Top Stroke Rehabil* (2014) 21:152–62. doi:10.1310/tsr2102-152
26. Smeragliuolo AH, Hill NJ, Disla L, Putrino D. Validation of the leap motion controller using markered motion capture technology. *J Biomech* (2016) 49(9):1742–50. doi:10.1016/j.jbiomech.2016.04.006
27. Bangor A, Kortum PT, Miller JT. An empirical evaluation of the system usability scale. *Int J Hum Comput Interact* (2008) 24(6):574–94. doi:10.1080/10447310802205776
28. Mathiowetz V, Weber K, Kashman N, Volland G. Adult norms for the 9 hole peg test of finger dexterity. *Occup Ther J Res* (1985) 5:24–38.
29. Medical Research Council. *Aids to the Examination of the Peripheral Nervous System*. Memorandum no. 45. London: Her Majesty's Stationery Office (1976).
30. Nasreddine ZS, Phillips NA, Bédirian V, Charbonneau S, Whitehead V, Collin I, et al. The Montreal Cognitive Assessment, MoCA: a brief screening tool for mild cognitive impairment. *J Am Geriatr Soc* (2005) 53(4):695–9. doi:10.1111/j.1532-5415.2005.53221.x
31. Vanbellingen T, Kersten B, Van de Winckel A, Bellion M, Baronti F, Müri R, et al. A new bedside test of gestures in stroke: the apraxia screen of TULIA (AST). *J Neurol Neurosurg Psychiatry* (2011) 82(4):389–92. doi:10.1136/jnnp.2010.213371
32. Koenig-Bruhin M, Vanbellingen T, Schumacher R, Pflugshaupt T, Annoni JM, Müri RM, et al. Screening for language disorders in stroke: German validation of the language screening test (LAST). *Cerebrovasc Dis Extra* (2016) 6(1):27–31. doi:10.1159/000445778
33. Adhikarla VK, Sodnik J, Szolgay P, Jakus G. Exploring direct 3d interaction for full horizontal parallax light field displays using leap motion controller. *Sensors (Basel)* (2015) 15(4):8642–63. doi:10.3390/s150408642
34. Weichert F, Bachmann D, Rudak B, Fisseler D. Analysis of the accuracy and robustness of the leap motion controller. *Sensors (Basel)* (2013) 13(5):6380–93. doi:10.3390/s130506380
35. Brooke J. SUS – a quick and dirty usability scale. *Usability Eval Industry* (1996) 189(194):4–7.
36. Borsci S, Federici S, Lauriola M. On the dimensionality of the System Usability Scale: a test of alternative measurement models. *Cogn Process* (2009) 10(3):193–7. doi:10.1007/s10339-009-0268-9
37. Lenze EJ, Munin MC, Quear T, Dew MA, Rogers JC, Begley AE, et al. The Pittsburgh Rehabilitation Participation Scale: reliability and validity of a clinician-rated measure of participation in acute rehabilitation. *Arch Phys Med Rehabil* (2004) 85(3):380–4. doi:10.1016/j.apmr.2003.06.001
38. Vanbellingen T, Nyffeler T, Nef T, Kwakkel G, Bohlhalter S, Van Wegen EE. Reliability and validity of a new dexterity questionnaire (DextQ-24) in Parkinson's disease. *Parkinsonism Relat Disord* (2016) 33:78–83. doi:10.1016/j.parkreldis.2016.09.015
39. Bertrand AM, Fournier K, Brasey MGW, Kaiser ML, Frischknecht R, Diserens K. Reliability of maximal grip strength measurements and grip strength recovery following a stroke. *J Hand Ther* (2015) 28(4):356–63. doi:10.1016/j.jht.2015.04.004
40. Fugl-Meyer AR, Jääskö L, Leyman I, Olsson S, Steglind S. The post-stroke hemiplegic patient. 1. A method for evaluation of physical performance. *Scand J Rehabil Med* (1975) 7(1):13–31.
41. Chen HM, Chen CC, Hsueh IP, Huang SL, Hsieh CL. Test-retest reproducibility and smallest real difference of 5 hand function tests in patients with stroke. *Neurorehabil Neural Repair* (2009) 23(5):435–40. doi:10.1177/1545968308331146
42. Figueiredo IM, Sampaio RF, Mancini MC, Silva FCM, Souza MAP. Test of grip strength using the Jamar dynamometer. *ACTA FISIATR* (2007) 14(2):104–10.
43. Gladstone DJ, Danells CJ, Black SE. The Fugl-Meyer assessment of motor recovery after stroke: a critical review of its measurement properties. *Neurorehabil Neural Repair* (2002) 16(3):232–40. doi:10.1177/154596802401105171
44. Moore CG, Carter RE, Nietert PJ, Stewart PW. Recommendations for planning pilot studies in clinical and translational research. *Clin Transl Sci* (2011) 4(5):332–7. doi:10.1111/j.1752-8062.2011.00347.x
45. Merians AS, Tunik ES, Adamovich SV. Virtual reality to maximize function for hand and arm rehabilitation: exploration of neural mechanisms. *Stud Health Technol Inform* (2009) 145:109–25. doi:10.3233/978-1-60750-018-6-109
46. Grimm F, Naros G, Gharabaghi A. Closed-loop task difficulty adaptation during virtual reality reach-to-grasp training assisted with an exoskeleton for stroke rehabilitation. *Front Neurosci* (2016) 10:518. doi:10.3389/fnins.2016.00518
47. Levin MF, Weiss PL, Keshner EA. Emergence of virtual reality as a tool for upper limb rehabilitation: incorporation of motor control and motor learning principles. *Phys Ther* (2015) 95(3):415–25. doi:10.2522/ptj.20130579
48. van Kordelaar J, van Wegen E, Kwakkel G. Impact of time on quality of motor control of the paretic upper limb after stroke. *Arch Phys Med Rehabil* (2014) 95(2):338–44. doi:10.1016/j.apmr.2013.10.006
49. Kwakkel G, Lannin NA, Borschmann K, English C, Ali M, Churilov L, et al. Standardized measurement of sensorimotor recovery in stroke trials: consensus-based core recommendations from the stroke recovery and rehabilitation roundtable. *Int J Stroke* (2017) 12(5):451–61. doi:10.1177/1747493017711813
50. Piron L, Turolla A, Agostini M, Zucconi C, Cortese F, Zampolini M, et al. Exercises for paretic upper limbafter stroke: a combined virtual-reality and telemedicine approach. *J Rehabil Med* (2009) 41:1016–20. doi:10.2340/16501977-0459
51. Standen P, Brown D, Battersby S, Walker M, Connell L, Richardson A, et al. A study to evaluate a low cost virtual reality system for home based rehabilitation of the upper limb following stroke. *Int J Disabil Hum Dev* (2011) 10(4):337–41. doi:10.1515/IJDHD.2011.063
52. Lledó LD, Díez JA, Bertomeu-Motos A, Ezquerro S, Badesa FJ, Sabater-Navarro JM, et al. Comparative analysis of 2D and 3D tasks for virtual reality therapies based on robotic-assisted neurorehabilitation for post-stroke patients. *Front Aging Neurosci* (2016) 26(8):205. doi:10.3389/fnagi.2016.00205

Conflict of Interest Statement: The authors declare that the research was conducted in the absence of any commercial or financial relationships that could be construed as a potential conflict of interest.

frontiers in Neurology

CLINICAL TRIAL
published: 14 December 2017
doi: 10.3389/fneur.2017.00679

The Effects of Upper-Limb Training Assisted with an Electromyography-Driven Neuromuscular Electrical Stimulation Robotic Hand on Chronic Stroke

Chingyi Nam, Wei Rong, Waiming Li, Yunong Xie, Xiaoling Hu and Yongping Zheng*

Department of Biomedical Engineering, The Hong Kong Polytechnic University, Hong Kong

Background: Impaired hand dexterity is a major disability of the upper limb after stroke. An electromyography (EMG)-driven neuromuscular electrical stimulation (NMES) robotic hand was designed previously, whereas its rehabilitation effects were not investigated.

Objectives: This study aims to investigate the rehabilitation effectiveness of the EMG-driven NMES-robotic hand-assisted upper-limb training on persons with chronic stroke.

Method: A clinical trial with single-group design was conducted on chronic stroke participants ($n = 15$) who received 20 sessions of EMG-driven NMES-robotic hand-assisted upper-limb training. The training effects were evaluated by pretraining, posttraining, and 3-month follow-up assessments with the clinical scores of the Fugl-Meyer Assessment (FMA), the Action Research Arm Test (ARAT), the Wolf Motor Function Test, the Motor Functional Independence Measure, and the Modified Ashworth Scale (MAS). Improvements in the muscle coordination across the sessions were investigated by EMG parameters, including EMG activation level and Co-contraction Indexes (CIs) of the target muscles in the upper limb.

Results: Significant improvements in the FMA shoulder/elbow and wrist/hand scores ($P < 0.05$), the ARAT ($P < 0.05$), and in the MAS ($P < 0.05$) were observed after the training and sustained 3 months later. The EMG parameters indicated a significant decrease of the muscle activation level in flexor digitorum (FD) and biceps brachii ($P < 0.05$), as well as a significant reduction of CIs in the muscle pairs of FD and triceps brachii and biceps brachii and triceps brachii ($P < 0.05$).

Conclusion: The upper-limb training integrated with the assistance from the EMG-driven NMES-robotic hand is effective for the improvements of the voluntary motor functions and the muscle coordination in the proximal and distal joints. Furthermore, the motor improvement after the training could be maintained till 3 months later.

Trial registration: ClinicalTrials.gov. NCT02117089; date of registration: April 10, 2014.

Keywords: stroke, hand, rehabilitation, robot, neuromuscular electrical stimulation

OPEN ACCESS

Edited by:
Dong Feng Huang,
Sun Yat-sen University, China

Reviewed by:
Hongbo Xie,
Queensland University of Technology, Australia
Xu Zhang,
University of Science and Technology of China, China

****Correspondence:***
Xiaoling Hu
xiaoling.hu@polyu.edu.hk

Specialty section:
This article was submitted to Stroke, a section of the journal Frontiers in Neurology

Received: *18 September 2017*
Accepted: *29 November 2017*
Published: *14 December 2017*

Citation:
Nam C, Rong W, Li W, Xie Y, Hu X and Zheng Y (2017) The Effects of Upper-Limb Training Assisted with an Electromyography-Driven Neuromuscular Electrical Stimulation Robotic Hand on Chronic Stroke. Front. Neurol. 8:679. doi: 10.3389/fneur.2017.00679

INTRODUCTION

Stroke is one of the leading causes of adult disability, and patients with stroke require continuous long-term medical care for reducing physical impairments (1). Only 18% of stroke survivors with severe paralysis achieve complete upper-limb function recovery within the subacute period (i.e., within the first 6 months after stroke onset) (2). Furthermore, approximately 65% of patients with chronic stroke (i.e., 6 months after the onset of a stroke) cannot incorporate their affected hand into their usual activities (3), this limitation markedly affects their independence and ability to perform activities of daily living (ADLs).

According to the traditional viewpoint on neurorehabilitation after stroke, significant motor improvements are usually observed during the subacute period and are associated with a spontaneous recovery in the early period, and motor recovery is expected to be minimal or plateaued during the chronic period (4). However, more recent studies on poststroke rehabilitation have reported that repetitive and high-intensity practice accelerate motor recovery (5, 6) and intensive therapeutic interventions can contribute significantly to reducing motor impairment and improving functional use of the affected arm of patients with chronic stroke (7). Despite these findings, providing high-intensity and repetitive training through traditional "one-to-one" manual-physical therapy is difficult because of resource constraints (8). Rehabilitation robots fill this gap by performing repetitive therapeutic tasks intensively and require minimal supervision by a therapist (9). Various robotic systems have been proposed for hand rehabilitation after stroke, for example, HapticKnob (10) and Haptic Master (11, 12), and their training effects had been investigated. These studies have reported that robot-assisted therapy can facilitate hand function recovery because the robotic system can provide repetitive and intensive training through a consistent and precise manner over a long duration. In addition, the integration of voluntary effort into robotic design for chronic stroke rehabilitation has been recommended (13, 14). Training designs that included this "add-on" feature of voluntary effort from the residual neuromuscular pathways exhibited better motor outcomes and longer sustainability than did passive limb motion training. Electromyography (EMG)-driven strategy is one of the novel and rapidly expanding techniques for maximizing the involvement of voluntary efforts during poststroke training. Many EMG-driven rehabilitation devices have been developed in the past decade (15), and a set of EMG-driven robot-assisted training systems have also been developed for poststroke rehabilitation in our previous studies (14, 16–18). The EMG-driven training systems have exhibited significant motor recovery for patients with chronic stroke, particularly in voluntary motor functions of the upper limb (15, 19).

While the EMG-driven strategy has been widely adopted, the use of robot-assisted therapy remains suboptimal. For example, a robot cannot directly activate the desired muscle groups because the target muscles of patients with stroke usually cooperate with compensatory motions from other muscular activities (20). In contrast to robot systems, neuromuscular electrical stimulation (NMES) can stimulate the required muscles by using electrical currents. NMES generates limb movement by precisely activating the target muscles to restore motor function and evoke sensory feedback to the brain during muscle contraction, thus promoting motor relearning (21). However, using NMES alone also has limitations in activating groups of muscles for dynamic limb movements. Controlling the speed of contraction of individual muscles during limb movements with desired kinematic qualities, such as speed, trajectory, and motion smoothness, is difficult mainly because of delayed evoked muscle contractions during electrical stimulation (22). Consequently, a combination of NMES and robot-assisted therapy has been developed recently for poststroke upper-limb rehabilitation (23–26), and studies have shown that this combination is effective for motor function recovery in patients with chronic stroke. In addition, the combined system can reduce the compensatory muscular activities at the elbow and can improve muscle activation levels related to the wrist in patients with chronic stroke, which was not observed when robot-assisted therapy was used alone (23). A study on the wrist training in patients with chronic stroke by another research group also demonstrated higher rehabilitation effectiveness in the upper-limb motor recovery with the combination therapy than with robot-assisted therapy alone (24).

Nevertheless, previous studies on combinations of NMES and robotic systems have mainly focused on motor recovery of the elbow and wrist joints (23–26). Thus far, only a few studies have reported EMG-driven NMES robot-assisted therapy for hand function recovery although loss of hand function is the primary factor of the upper-limb disability after stroke (27). In our previous work, an EMG-driven NMES exoskeletal hand robot, which could provide fine control of the hand movements and activating the target muscles selectively for fingers extension/flexion, was developed and suggested for hand rehabilitation after stroke (28), where the assistive capacity of the NMES and robot combined system in helping persons with chronic stroke conducting extension/flexion of the fingers were compared with either NMES or robot assistive schemes. NMES and robot combined scheme showed higher motion accuracy and better muscle coordination in the whole upper limb. However, the rehabilitation efficacy and the training effects had not been well investigated by clinical trials previously. In this work, the rehabilitation effectiveness of the EMG-driven NMES-robotic hand assisted upper-limb training on chronic stroke was investigated by a single-group trial. We hypothesized that the participants who received intensive and repetitive upper-limb training with coordinated hand movements assisted by the EMG-driven NMES-robotic hand would demonstrate improvements in hand function and muscular coordination of the fingers. Furthermore, motor gains after the training could contribute to the functional use of the affected hand in ADLs.

METHODOLOGY

EMG-Driven NMES-Robotic Hand

The EMG-driven NMES-robotic hand system used in this study is shown in **Figure 1A**. The system can provide assistance for finger extension and flexion of the paretic limb of patients with stroke.

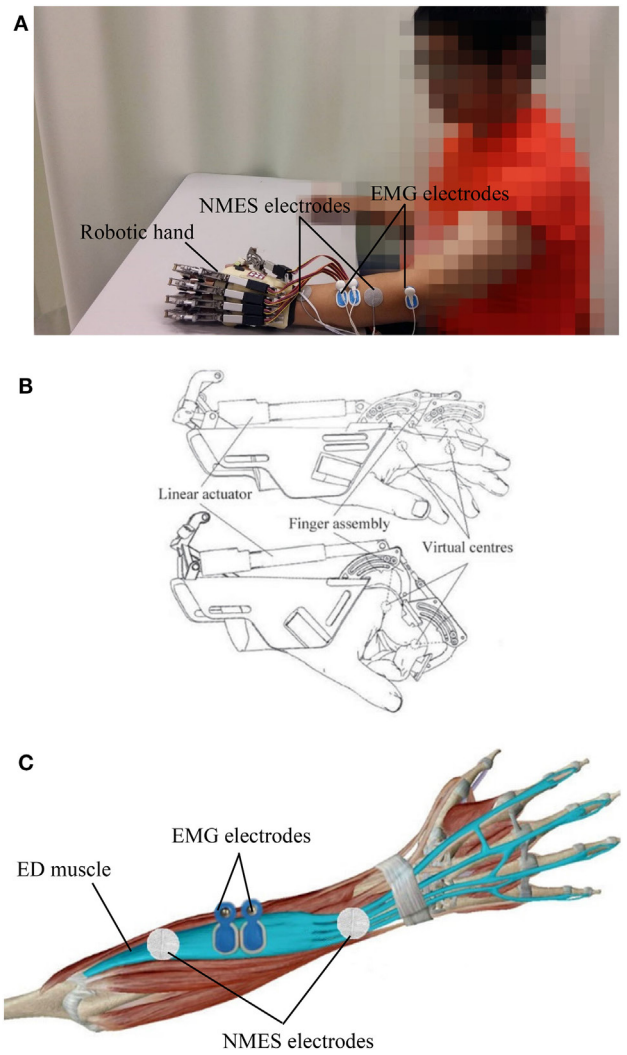

FIGURE 1 | The electromyography (EMG)-driven neuromuscular electrical stimulation (NMES)-robotic hand system: **(A)** the wearable system consisting of a mechanical exoskeleton of the robotic hand, a pair of NMES electrodes attached to the extensor digitorum (ED) muscle, and EMG electrodes on the ED and abductor pollicis brevis muscles; **(B)** illustration of the mechanical structure of the robotic hand; **(C)** the EMG and NMES electrodes' configuration on the ED muscle.

The wearable robotic hand (Firgelli L12, Firgelli Technologies Inc.) provided individual mechanical assistance to the five fingers, and each finger was actuated by a linear actuator (**Figure 1B**) (28, 29). The proximal and distal section of the index, middle, ring, and little fingers were rotated around the virtual centers located at the metacarpophalangeal (MCP) and proximal interphalangeal (PIP). The thumb was rotated around the virtual center of its MCP joint. The finger assembly provided two degrees of freedom for each finger and offered a range of motion (ROM) of 55° and 65° for the MCP and PIP joints, respectively. The angular rotation speeds of the two joints were set as 22°/s and 26°/s at the MCP and PIP joints, respectively, during training.

The NMES electrode pair (30 mm diameter; Axelgaard Corp., Fallbrook, CA, USA), which provided stimulation during finger extension, was attached over the extensor digitorum (ED) muscle. The configuration for the EMG and NMES electrodes on the ED muscle is shown in **Figure 1C**. The outputs of NMES were square pulses with a constant amplitude of 70 V, stimulation frequency of 40 Hz, and a manually adjustable pulse width in the range 0–300 μs. Before the training, the pulse width was set at the minimum intensity, which achieved a fully extended position of the fingers in each patient. No assistance from NMES was provided during finger flexion to avoid the possible increase of finger spasticity after stimulation (30).

The abductor pollicis brevis (APB) and ED muscles were used as voluntary neuromuscular drives to control robot assistance and NMES assistance from the system to facilitate performance of phasic and sequential limb tasks, namely, hand closing and hand opening. The APB was selected as the driving muscle in the hand closing phase, since the EMG signals from the APB of the paretic limb after stroke are less affected by spasticity and are relatively easier to be controlled than the flexor digitorum (FD) muscle for finger movements in chronic stroke (31). EMG-triggered control was used in this study. Three times of the standard deviation (SD) above the EMG baseline in the resting state was set as a threshold level in each motion phase during training. In the "hand closing" phase, as soon as the EMG activation level of the APB muscle reached a preset threshold (3 SD above the baseline), the robotic hand would close with a constant speed (22°/s and 26°/s at the MCP and PIP joints, respectively) and provide mechanical assistance for finger flexion motions. In the "hand opening" phase, once the EMG activation level of the ED muscle reached a preset threshold (3 SD above the baseline), the robotic hand would open with a constant speed (22°/s and 26°/s at the MCP and PIP joints, respectively), and NMES would stimulate the ED muscle during the entire hand opening phase to assist finger extension motions. Once the assistance of the system was initiated, voluntary effort from the patient was not required and the assistance from the NMES and robotic parts would be continuously provided during the entire hand closing and opening phase in the defined ROM.

The EMG signals from the driving muscles captured using EMG electrodes (Blue Sensor N, Ambu Inc. with a contact area of 20 mm × 30 mm) were first amplified 1,000 times (preamplifier: INA 333; Texas Instruments Inc., Dallas, TX, USA), sampled at 1,000 Hz by using a data acquisition card (DAQ, 6218 NI DAQ card; National Instruments Corp.) and filtered by using a band-pass filter in the range 10–500 Hz. After digitization, the EMG signals from the APB and ED muscles were rectified and low-pass filtered (fourth-order, zero-phase forward and reverse Butterworth filter; cutoff frequency, 10 Hz) to obtain an envelope of EMG signals (i.e., the EMG activation level) in the real-time control.

Participants

After obtaining ethical approval from the Human Subjects Ethics Subcommittee of the Hong Kong Polytechnic University, participants in this study were recruited from the local districts through advertisement. A total of 20 patients were screened for the training during the subject recruitment. Fifteen participants with chronic poststroke hemiparesis met the inclusion criteria

and were recruited in this study after obtaining their written consents. Inclusion criteria were as follows: (1) aged from 18 to 78 years (32, 33), (2) at least 6 months after the onset of a singular and unilateral brain lesion due to stroke, (3) both the MCP and PIP joints could be extended to 180° passively, (4) the spasticity during extension at the finger joints and the wrist joint was below 3 as measured by the Modified Ashworth Scale (MAS), ranged from 0 (no increase in the muscle tone) to 4 (affected part rigid) (34), (5) motor impairments in the affected upper limb ranged from severe to moderate as assessed by Fugl-Meyer Assessment (FMA) ($15 < FMA < 45$, with a maximal score of 66 for the upper limb) (35), (6) no visual deficit and able to understand and follow simple instructions as assessed by the Mini-Mental State Examination ($MMSE > 21$) (36), (7) detectable voluntary EMG signals from the driving muscle on the affected side (three times of the SD above the EMG baseline). Subjects were excluded because of the following conditions: (1) did not fulfill the above inclusion criteria, (2) currently pregnant, and (3) had an implanted pacemaker. **Figure 2** shows the CONSORT flowchart of the experimental design.

Training Protocol

All participants received the EMG-driven NMES-robotic hand-assisted upper-limb training, which consisted of 20 training sessions with the intensity of 3–5 sessions/week, within 7 consecutive weeks.

Session-by-Session Pretraining Evaluation Task

An evaluation was conducted at the beginning of each training session. Each participant was first subjected to a maximum voluntary contraction (MVC) test for the following five target muscles: APB, ED, FD, biceps brachii (BIC), and triceps brachii (TRI). EMG electrode pairs with center separation of 2 cm were attached to the skin surface of the muscles of interest according to the configuration specified in Cram's work (37). Then, each participant was instructed to perform a bare hand evaluation task, which was used to monitor the muscle coordination during the recovery, as we did previously in EMG-driven hand robot-assisted upper-limb training of patients with chronic stroke (29). During evaluation, participants were seated at a table to maintain a vertical distance of 30–40 cm between the table surface and the participants' shoulder.

While conducting the MVC test on the ED and FD muscles, participants were seated at a table and the paretic upper limb was placed on the table with elbow joint extended at an angle of 130°, the wrist was held by an experimental operator and positioned around its neutral position, and the finger positions were set by the operator to obtain an angle around 150° at the MCP joints of the index, middle, ring, and little fingers. During the maximum extension of the four fingers, the ED EMG signals were recorded; and during the maximum flexion, the FD EMG signals were captured. For the MVC test on the APB, the operator held the thumb in an extended position (around 30°) and asked the participants to conduct maximum thumb palmar abduction with the same configuration of the wrist and elbow joints as in the ED and FD MVC tests. During the MVC test on the BIC and TRI muscles, the paretic upper limb was positioned with the shoulder abducted at 70° and the elbow flexed at 90°. The MVC test on each target muscle was repeated twice and was maintained for 5 s. A 2-min interval was maintained between two consecutive contractions to prevent muscle fatigue. The maximum EMG amplitude recorded in the two repetitions was selected as the EMG amplitude of MVC for the target muscle.

The bare hand evaluation task, which was conducted after the MVC test, involved lateral and vertical arm reaching-grasping tasks (29). The participants were required to use their paretic limbs to perform the task (without assistance from NMES or the robotic hand) and complete it at their natural speed. In the lateral

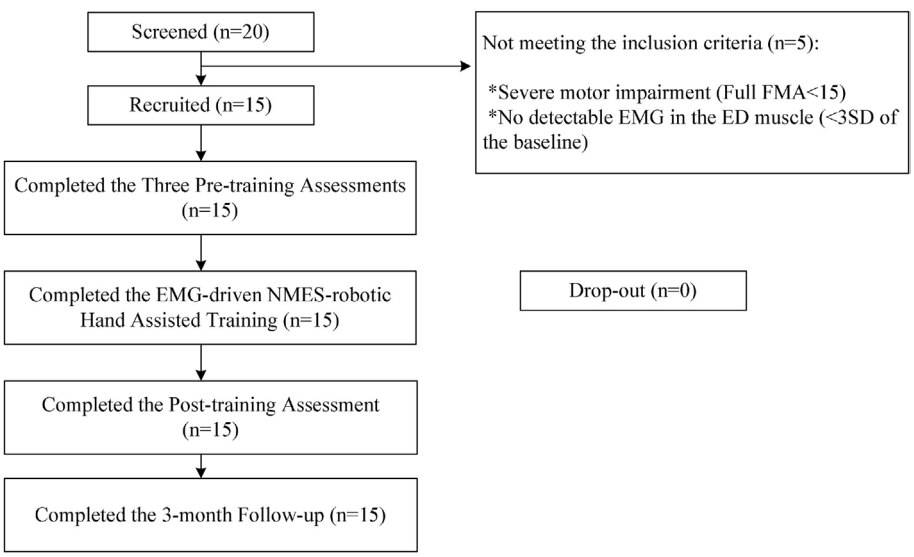

FIGURE 2 | The Consolidated Standards of Reporting Trials flowchart of the experimental design.

task, each participant was instructed to grasp a sponge (thickness 5 cm, weight 30 g) that was placed on one side of a table near the paretic side of the participant, transport the sponge 50 cm horizontally, release it, grasp it again, and return it to the starting point. In the vertical task, each participant was instructed to grasp the sponge on the midline of the lower layer of a shelf, lift it through a vertical distance of 17 cm, place it on the midline of the upper layer of the shelf, grasp it again, and place it back on the starting point. Both lateral and vertical tasks were repeated thrice, with a 2-min interval between two consecutive contractions to prevent muscle fatigue.

The EMG recording was started when the participant began to grasp the sponge (as soon as one finger touched the sponge) to when the participant released the sponge at the starting point (all the fingers left the sponge). The EMG signals from the target muscles (APB, ED, FD, BIC, and TRI) were first amplified 1,000 times, filtered by a band-pass filter in the range 10–500 Hz, and full-wave rectified. The EMG signals were sampled at 1,000 Hz by the data acquisition card and stored in the computer for off-line processing as we did previously (16, 17). In the early sessions of the training, only two participants could release the sponge without using their unaffected hands. A 10-s maximum time limit was set at the end of the attempt of release action for participants who could not release the sponge within 10-s by using their paretic hands. If their paretic hands could not release the sponge within 10-s, the participants could use their unaffected hands to remove the sponge. The EMG signals beyond 10-s were excluded for analysis. At the 20th session of training, five participants could release the sponge without using their unaffected hands.

Training Task Assisted with the EMG-Driven NMES-Robotic Hand

Participants were required to perform lateral and vertical arm reaching–grasping tasks with the EMG-driven NMES-robotic hand on the paretic side with same seating arrangement and movements as the previous evaluation. In each training session, the participants performed 30-min lateral and vertical tasks, respectively, with a 10-min interval between the tasks to prevent muscle fatigue. However, most of the participants ($n = 12$) could not sustain the weight of the paretic limb and the robotic hand without assistance. This was mainly due to weakness of the shoulder and elbow joints. Therefore, during the arm transportation, these participants were allowed to use their unaffected limb to provide self-aware minimal support at the wrist joint of the paretic limb. During the last session of the training, 10 participants could lift the affected limb while wearing the robotic hand.

Evaluation of Training Effects

Clinical Assessments

In this study, the clinical assessments were used for functional evaluation of each participant and are described as follows: the FMA (35) that the full score is 66 for the upper-limb assessment and has been subscaled into shoulder/elbow (42/66) and wrist/hand (24/66) (38), used for poststroke measurement of motor functional impairment in voluntary limb movements; the Action Research Arm Test (ARAT) (39), adopted to evaluate the upper-limb functions with hand tasks included holding/releasing objects with different shapes, sizes and weights; the Wolf Motor Function Test (WMFT) (40), applied to collect the information on the motion speed and functional ability related to different daily tasks; the Motor Functional Independence Measure (FIM) (41), used for evaluation of subject's ADLs; and the MAS (34), adopted to measure the spasticity of the flexors related to the elbow, wrist, and fingers. Before the training, the aforementioned clinical assessments were measured thrice in 2 weeks every 2–3 days to obtain the stability of baseline. The same clinical assessments were also measured immediately after the last training session and 3 months after the training by a training-blinded assessor who was instructed not to communicate regarding the training details with the participants and was not informed about the research purpose and the training protocol of this study.

EMG Parameters

For the cross-sessional monitoring, two EMG parameters were calculated which were (1) the normalized EMG activation level of each target muscle and (2) the normalized EMG Co-contraction Index (CI) between a muscle pairs (16, 17). The EMG activation level of a muscle was calculated as follows:

$$\overline{\mathrm{EMG}} = \frac{1}{T}\int_0^T \mathrm{EMG}_i(t)dt, \tag{1}$$

where $\overline{\mathrm{EMG}}$ referred to the averaged EMG envelope value of muscle *i*. The $\mathrm{EMG}_i(t)$ was the EMG envelope signal after the normalization with respect to the EMG MVC value of the muscle, and T was the length of the signal. **Figure 3** shows the representative EMG signals, and their normalized envelopes captured during a trial of lateral reaching–grasping task. To minimize the variations in the EMG levels of individual participant, the obtained EMG activation level in a session for an individual participant was further normalized using the following equation (Eq. 2), which consider the maximal and minimal EMG activation levels of a participant recorded across the 20 training sessions. The tendency of the EMG activation level (values varying from 0 to 1) of a participant across the 20 training sessions was obtained after this operation.

$$\mathrm{EMG}_N = \frac{\overline{\mathrm{EMG}} - \overline{\mathrm{EMG}}_{\min}}{\overline{\mathrm{EMG}}_{\max} - \overline{\mathrm{EMG}}_{\min}} \tag{2}$$

where $\underline{\mathrm{EMG}}_N$ was the normalized EMG activation level of muscle *i*. The $\underline{\mathrm{EMG}}$ referred to the averaged EMG envelope value of muscle *i*. The $\overline{\mathrm{EMG}}_{\min}$ was the minimum value of the averaged EMG envelope across the 20 training sessions, and the $\overline{\mathrm{EMG}}_{\max}$ was the maximum value of the averaged EMG envelope across the 20 training sessions.

The CI between a pair of muscles were introduced and applied in our previous study and expressed as follows:

$$\mathrm{CI} = \frac{1}{T}\int_0^T A_{ij}(t)dt, \tag{3}$$

where $A_{ij}(t)$ was overlapping activity of EMG linear envelopes for muscles *i* and *j*, and T was the length of the signal. An increase in CI value represents an increased co-contraction phase of a muscle pair (broadened overlapping area), and a

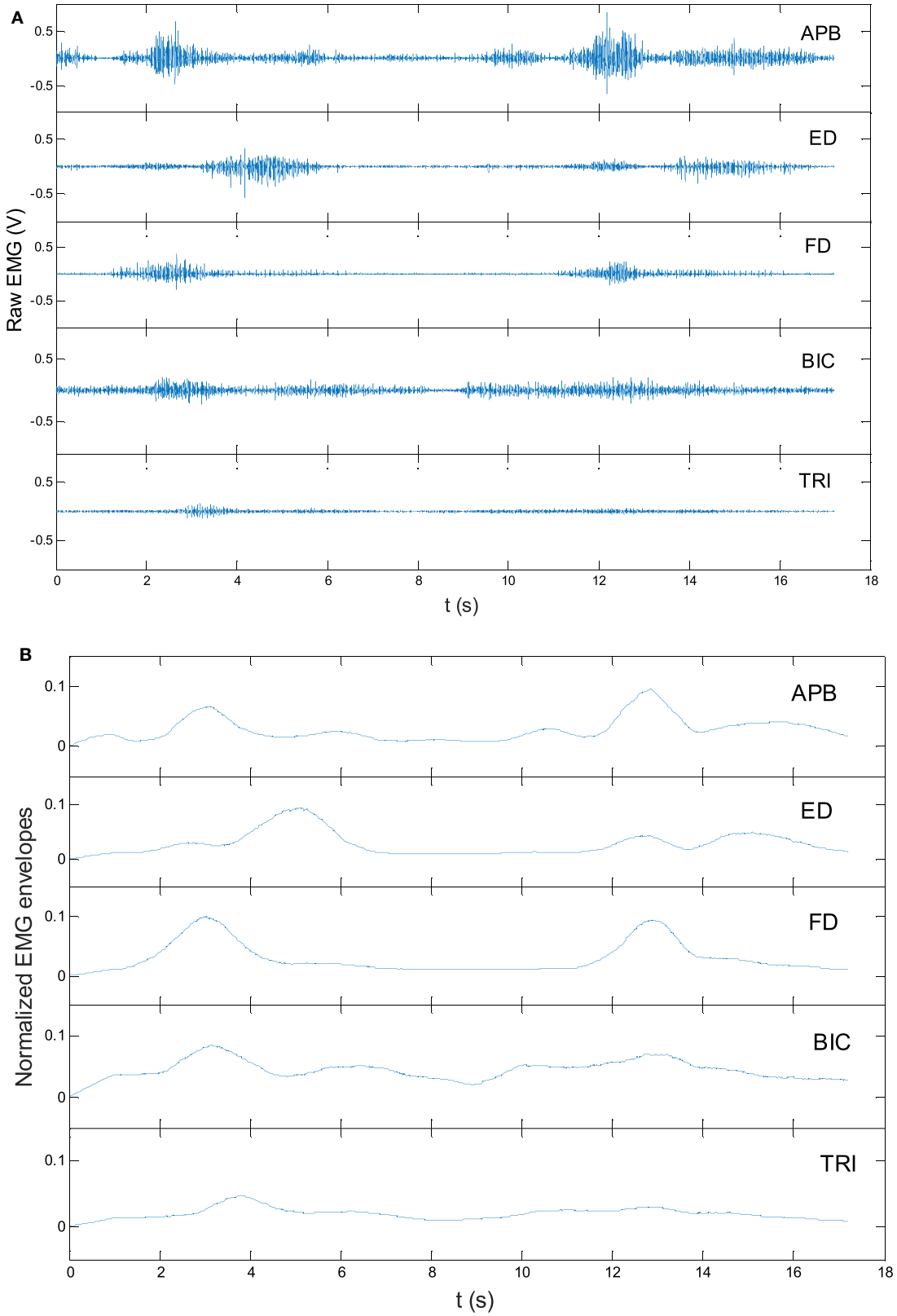

FIGURE 3 | The representative raw electromyography (EMG) trials in a lateral arm reaching–grasping task **(A)** and the EMG envelopes after rectification and normalization **(B)**.

decrease in CI value indicates a decreased co-contraction phase of a muscle pair (lessened overlapping area). The CI value was also further normalized, similar to the EMG activation level, for obtaining the tendency of muscle coordination, which considers the maximal and minimal CI values of a participant recorded across the 20 training sessions and its equation (Eq. 4) was given as follows:

$$CI_N = \frac{CI - CI_{min}}{CI_{max} - CI_{min}}, \quad (4)$$

where CI_N was the normalized CI value between a pair of muscles *i* and *j*. CI_{min} was the minimum value of the averaged overlapping activity of EMG linear envelopes, and CI_{max} was the maximum value of the averaged overlapping activity of EMG linear envelopes across the 20 training sessions. Session-by-session recording of the varying patterns of the two EMG parameters provided information particularly relevant to muscle activation and muscle coordination. Furthermore, it provided quantitative descriptions of the progress of motor function recovery of the affected limb.

Statistical Analysis

The normality tests on the clinical scores and the EMG data by Lilliefors method were performed with a significant level of 0.05 (42). It found that the clinical score and the EMG sample had normal distribution ($P < 0.05$). One-way analysis of variance (ANOVA) with repeated measures (Bonferroni *post hoc* test) were used to evaluate the differences on the clinical assessments across different time points (thrice pretraining assessments, a posttraining assessment, and a 3-month follow-up assessment) and the EMG parameters (i.e., the normalized EMG activation levels and the CIs) across the 20 training sessions. The levels of statistical significance were indicated at 0.05, 0.01, and 0.001 in this study.

RESULTS

All recruited participants ($n = 15$) completed the EMG-driven NMES-robotic hand-assisted upper-limb training. The demographic data of the participants are shown in **Table 1**. **Table 2** lists all clinical scores measured in this study (i.e., the means and 95% confidence intervals of each clinical assessment together with the one-way ANOVA probabilities with the effect sizes (EFs) for the evaluation with respect to the assessment sessions). Significantly difference clinical scores ($P < 0.05$, one-way ANOVA with Bonferroni *post hoc* test) are illustrated in **Figure 4**, which shows the FMA, ARAT and MAS scores evaluated at five time points: thrice pretraining assessments (Pre1, Pre2, and Pre3), posttraining assessments (Post), and 3-month follow-up assessment (3-month FU). **Figures 4A–C** show the variation in FMA scores at thrice pretraining assessments, posttraining assessment, and 3 months follow-up assessment. In **Figure 4A**,

TABLE 1 | Demographic characteristics of the stroke subjects.

Subjects no.	Gender (female/male)	Stroke Types (hemorrhagic/ischemic)	Side of hemiparesis (left/right)	Age (years), mean ± SD	Years after onset of stroke, mean ± SD
15	3/12	7/8	8/7	57.3 ± 8.87	8.26 ± 4.17

TABLE 2 | The means and 95% confidence intervals for each measurement of the clinical assessments, and the probabilities with the estimated effect sizes of the statistical analyses.

Evaluation	Pre 1	Pre 2	Pre 3	Post	3-Month follow-up	One-way ANOVA	
	Mean (95% confidence interval)					*P*-value (partial η^2)	*F*-value
FMA							
Full score	26.5 (21.1–31.9)	28.3 (22.7–33.8)	29.1 (22.7–35.4)	42.4 (36.3–48.5)	44.2 (38.0–50.3)	0.000*** (0.313)	7.96
Wrist/hand	8.0 (5.4–10.6)	9.1 (6.5–11.6)	9.1 (6.4–11.7)	13.9 (11.4–16.4)	14.3 (11.7–16.9)	0.000*** (0.228)	5.18
Shoulder/elbow	18.5 (15.1–21.9)	19.2 (15.7–22.7)	20 (15.9–24.1)	28.5 (24.5–32.5)	29.8 (26.0–33.7)	0.000*** (0.320)	8.23
ARAT	14.2 (8.4–20.0)	14.7 (8.2–20.5)	14.7 (8.8–20.5)	27.1 (20.7–33.4)	26.8 (19.4–34.2)	0.001** (0.226)	5.12
WMFT							
Score	40.5 (29.7–51.2)	40.9 (30.7–51.0)	39.5 (29.5–49.5)	46 (39.2–52.8)	49.3 (42.4–56.2)	0.532 (0.043)	0.79
Time	50.0 (35.8–64.2)	49.6 (35.6–63.6)	50.5 (36.0–64.9)	39.6 (30.0–49.3)	37.7 (28.2–47.2)	0.424 (0.053)	0.98
FIM	65.0 (63.8–66.1)	65.8 (65.3–66.3)	65.6 (64.7–66.5)	66.5 (65.8–67.1)	65.7 (64.7–66.7)	0.177 (0.085)	1.63
MAS							
Elbow	1.7 (1.3–2.1)	1.7 (1.2–2.1)	1.5 (1.0–2.0)	0.8 (0.4–1.2)	0.7 (0.4–1.1)	0.002** (0.214)	4.77
Wrist	1.6 (1.0–2.1)	1.5 (1.0–2.1)	1.5 (0.9–2.0)	0.6 (0.2–1.0)	0.3 (0.0–0.6)	0.000*** (0.224)	5.64
Finger	1.5 (1.0–2.1)	1.4 (0.9–2.0)	1.3 (0.8–1.9)	0.5 (0.1–0.8)	0.4 (0.1–0.7)	0.000*** (0.236)	5.41

Differences with statistical significance (one-way ANOVA with Bonferroni post hoc tests) are marked with "" beside the P values. Significant levels are indicated as follows: * for ≤0.05, ** for ≤0.01, and *** for ≤0.001.*

FMA, Fugl-Meyer Assessment; ARAT, Action Research Arm Test; WMFT, Wolf Motor Function Test; FIM, Functional Independence Measurement; MAS, Modified Ashworth Score; ANOVA, analysis of variance.

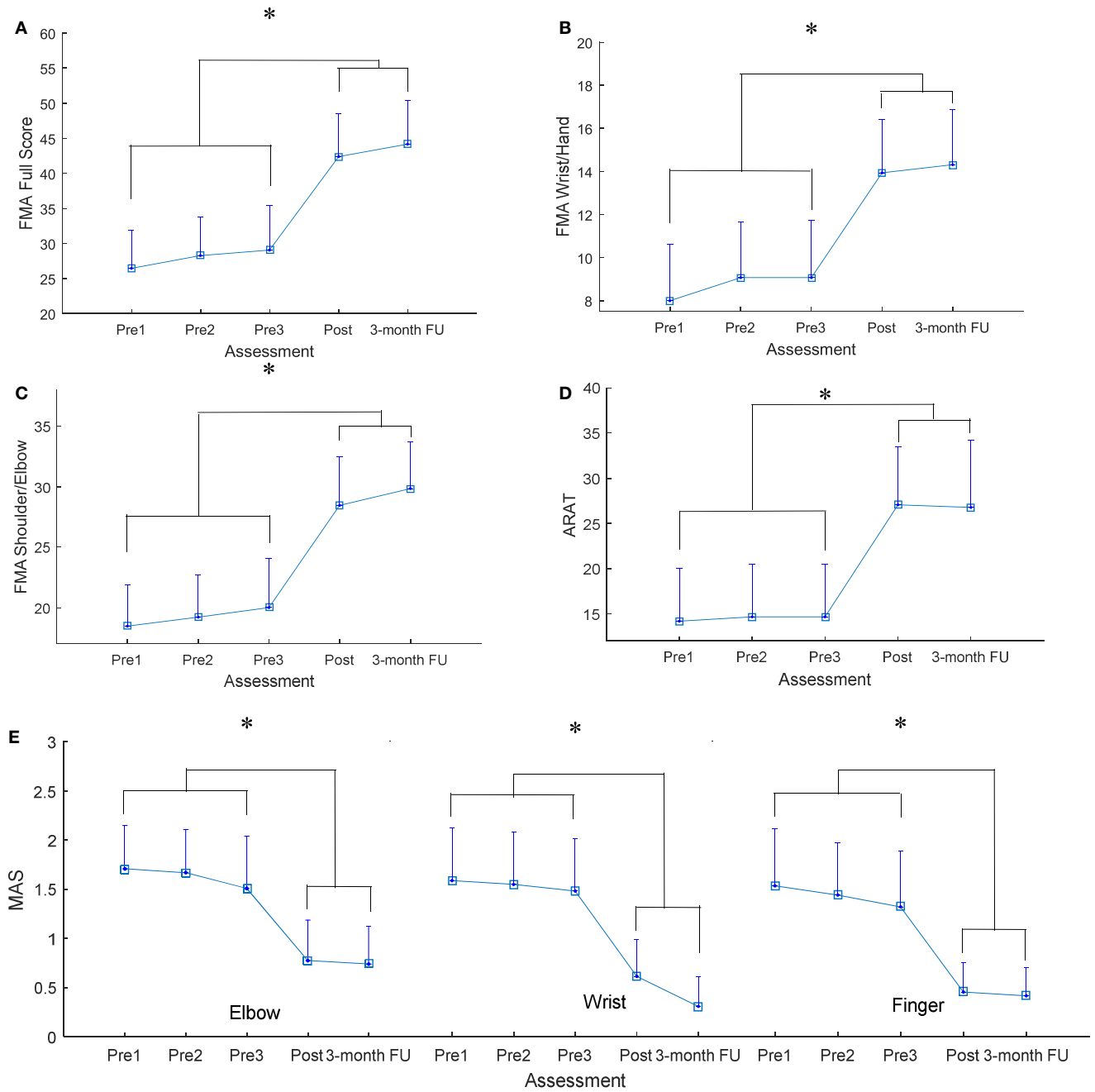

FIGURE 4 | The clinical scores measured before, after, and 3 months later after the training **(A)** Fugl-Meyer Assessment (FMA) full score, **(B)** FMA wrist/hand score, **(C)** FMA shoulder/elbow score, **(D)** Action Research Arm Test (ARAT) score, **(E)** Modified Ashworth Scale (MAS) score at the elbow, the wrist, and the fingers, presented as mean value with two times SE (error bar) in each evaluation session. The significant difference is indicated by "*" ($P < 0.05$, one-way analysis of variance with Bonferroni *post hoc* tests).

the FMA full score significantly increased after the training, and this increase compared with the pretraining values was kept for 3 months ($P < 0.001$, EF = 0.313, $F = 7.96$, one-way ANOVA with Bonferroni *post hoc* test). In **Figure 4B**, a significant increase of the FMA wrist/hand score was detected after the training, and the increments with respect to the pretraining value were maintained 3 months ($P < 0.001$, EF = 0.228, $F = 5.18$, one-way ANOVA with Bonferroni *post hoc* test). A significant increase in the FMA shoulder/elbow score after the training was observed compared with the pretraining values, and the increase was maintained during the assessment at the 3-month follow-up (**Figure 4C**; $P < 0.001$, EF = 0.320, $F = 8.23$, one-way ANOVA with Bonferroni *post hoc* test). The variation in ARAT score at five time points is shown in **Figure 4D**. A significant increase in

the ARAT score after the training was observed, and this increase compared with the pretraining values was maintained for 3 months ($P < 0.01$, EF = 0.226, $F = 5.12$, one-way ANOVA with Bonferroni *post hoc* test). **Figure 4E** shows the variation in MAS scores at the finger, wrist, and elbow at five time points. A significant decrease in the MAS scores was observed in the assessments at different time points. The MAS scores at the elbow significantly declined after training, and these decreases compared with the pretraining values were maintained for 3 months ($P < 0.01$, EF = 0.214, $F = 4.77$, one-way ANOVA with Bonferroni *post hoc* test). Significant decreases were observed in the MAS score at the wrist ($P < 0.001$, EF = 0.224, $F = 5.64$, one-way ANOVA with Bonferroni *post hoc* test) and finger ($P < 0.001$, EF = 0.236, $F = 5.41$, one-way ANOVA with Bonferroni *post hoc* test) after the training, and these deductions with respect to the pretraining values were maintained during the 3-month follow-up.

Figure 5 illustrates the EMG parameters (i.e., the normalized EMG activation level and the normalized CI) that showed statistically significance variations during the evaluation across the 20 training sessions. A significant decrease in EMG activation level was observed in the FD (**Figure 5A**; $P < 0.001$, EF = 0.331, $F = 7.29$, one-way ANOVA with *post hoc* tests) and BIC muscles ($P < 0.001$, EF = 0.207, $F = 3.85$, one-way ANOVA with *post hoc* tests). Regarding the variation patterns of the EMG activation level of the FD muscle, the EMG level showed a rapid decrease of 50% over the first four sessions and was further declined by 19% from the 5th to 20th sessions. Concerning the variation patterns of the EMG activation level of the BIC muscle, the EMG level steadily decreased over the 20 training sessions, with a total decrease of 50%. No descending plateau was reached for the EMG levels of the FD and BIC muscles within the 20 training sessions. **Figure 5B** shows the significant decrease in CI of the FD and TRI muscles ($P < 0.001$, EF = 0.148, $F = 2.56$, one-way ANOVA with *post hoc* tests) and BIC and TRI muscle pair ($P < 0.001$, EF = 0.285, $F = 5.88$, one-way ANOVA with *post hoc* tests) during the evaluation across the 20 sessions of the training. Regarding the variation patterns of CI of the FD and TRI muscles and the BIC and TRI muscle pair, the CIs gradually declined and did not reach a plateau over the 20 training sessions. No significant increases or decreases were observed in the EMG parameters of other target muscles and muscle pairs.

DISCUSSION

In this study, the recruited participants with chronic stroke showed stable baselines without significant variations in all clinical scores before the training. After 20 sessions of the upper-limb training assisted with EMG-driven NMES-robotic hand, motor function improvements associated with the improved clinical scores and cross-session recorded EMG parameters were observed in all the participants, and the improvements after the training could be maintained 3 months later.

Training Effects by Clinical Assessments

Results from the clinical assessments revealed that the voluntary motor functions and muscle coordination of the affected upper limb significantly improved after the training. The significant increase in the FMA (shoulder/elbow and wrist/hand) score after the training indicated an improvement in voluntary motor control at the joints of the entire paretic upper limb, and these motor function improvements were maintained at 3-month follow-up. A significant increase of 6 points in the FMA wrist/hand (max 24) score was observed after the training (mean admission score was 8 points). Compared with a similar study on robot-assisted hand training by using HapticKnob (10), motor improvement exhibited a significant increase of 1 point after the training (mean admission score was 8 points). Because the participants with chronic stroke in both studies practiced hand closing and opening movements through robot-assisted training, the training duration and intensity were also comparable, the additional improvements in hand functions in this study were probably due to the involvement of voluntary efforts from the affected limb and NMES during finger extension. The ARAT score is mainly related to finger movements as well as grasping, gripping, and pinching movements. The significant increase in the ARAT score indicated improvements in the muscle coordination of the fingers for fine precision grasping and joint stability of the fingers. The significant decrease in the MAS score at the elbow implied a release of flexor spasticity (muscle tone) in the elbow joint. The significant decrease in the MAS scores at the flexors of the wrist and fingers indicated that the spasticity of the distal joints was reduced. The muscle tone was graded subjectively by the examiner depending on the amount of the resistance encountered in response to passive movement (34). A higher MAS score reflects poorer control of synergic muscle activity as well as a tendency to stiffen a limb to compensate for poor control (21). Stroke survivors usually exhibit various compensatory motions while using their paretic upper limbs (30). For example, patients with stroke use trunk flexion instead of elbow extension to reach for objects. Similarly, forearm pronation and wrist flexion instead of a neutral forearm position and wrist extension to orient the hand for grasping. The decrease in the MAS scores of the elbow, wrist, and finger joints indicated improved muscle coordination and joint stability of the proximal and distal joints during arm reaching motions as well as during hand grasp and release motions after the training, and these significant improvements were maintained at 3-month follow-up. In our previous study on the EMG-driven robotic hand assisted upper-limb training of patients with chronic stroke (29), the MAS score of the finger joints decreased by a total of 0.5 points after the training with a mean admission score of 1.3 points. However, in this study, a total decrease of 1 point in the MAS score of the finger joints was demonstrated after the training with a mean admission score of 1.5 points. The additional decrease in the spasticity of the finger joints in this study may be due to the NMES assistance for finger extension during training. Further studies should be conducted to assess the effectiveness of training in poststroke rehabilitation of the upper limb assisted with the EMG-driven NMES-robotic hand by comparing the training results with the EMG-driven robotic hand assisted hand training in a randomized controlled trial.

A review on robot-assisted poststroke upper-limb rehabilitation (43) indicated that a significant improvement in the

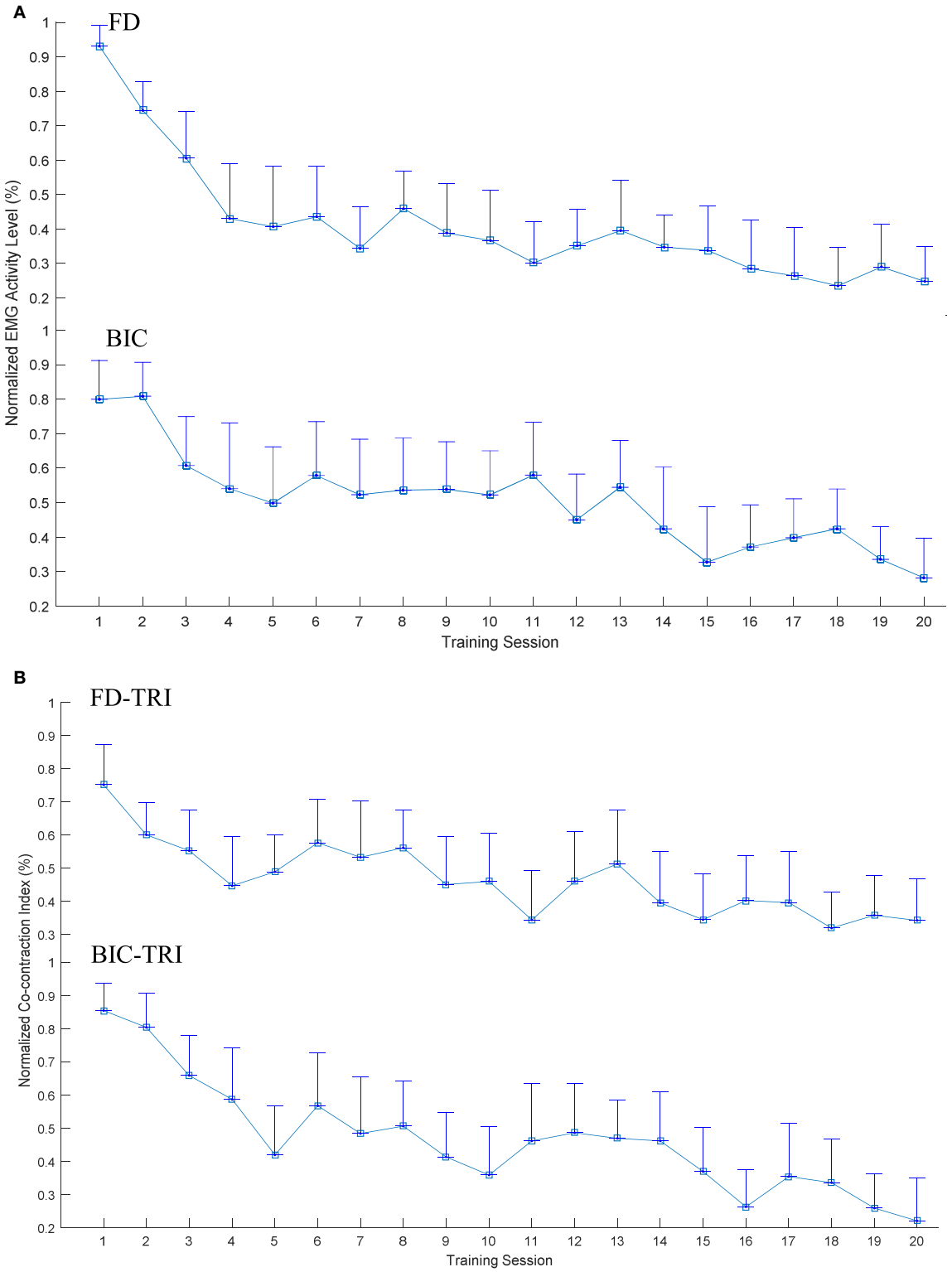

FIGURE 5 | The variation of electromyography (EMG) parameters recorded across the 20 training sessions associated with significant decreases ($P < 0.05$ with one-way analysis of variance with Bonferroni *post hoc* tests): **(A)** the normalized EMG activation levels of the flexor digitorum (FD) and BIC muscles during the bare hand evaluation. **(B)** The changes of the normalized Co-contraction Indexes of the FD and TRI and BIC and TRI muscle pairs with statistical significance during the bare hand evaluation. The values are presented as mean value with two times SE (error bar) in each session.

function of ADLs (i.e., FIM score) must be associated with a significant improvement in the motor function recovery (i.e., FMA score); however, no study has demonstrated significant improvement in ADL functions without motor recovery. Motor function recovery is considered a prerequisite for the ability to perform ADLs. In this study, significant motor function improvements (i.e., FMA and ARAT scores) have been observed, but the improvements in ADLs were not confirmed using the clinical outcome measures (i.e., WMFT and FIM scores). This might suggest that the motor function improvements after the training might not be transferred to the functional use of the upper limb to perform ADLs, which is a common observation in robot-assisted studies on patients with chronic stroke (44). This was probably due to the following features in persons with chronic stroke: (1) learned nonuse that could become a habit, and the limb may not be used in functional activities although the individual can move it (30) and (2) the unaffected limb attempts to execute all motor actions required for daily living (45). Further studies should be conducted on upper-limb rehabilitation of patients with subacute stroke using the assistance of the EMG-driven NMES-robotic hand, which might limit the occurrence of the learned nonuse and increase the functional use of the affected limb in ADLs. In contrast to the WMFT and FIM scores, the FMA, ARAT and MAS scores indicated that significant improvements in arm and hand functions could be maintained 3 months later after the training. This implied that upper-limb training assisted with EMG-driven NMES-robotic hand could provide motor function recovery for the proximal and distal joints of the impaired limb and support the retentive long-term upper-limb rehabilitation for patients with chronic stroke. It was also possible that the participants utilized the affected upper limb more confidently in the daily activities with the improved motor functions after the training, which led to the maintenance of the motor gain 3 months later. However, it did not lead to a significant improvements in the WMFT or FIM.

Training Effects by Cross-Session EMG Monitoring

The cross-sessional EMG monitoring reflected the recovery progress of the muscle coordination during the training program, which also monitored individual muscle activation and coordination patterns among the contracting muscles. The significantly improved muscular coordination of the proximal and distal joints also was achieved through the EMG-driven NMES-robotic hand assisted training, as revealed by both clinical scores and the EMG parameters (i.e., the normalized EMG activation levels and the normalized CIs). The decrease in the EMG activation levels could have two major reasons: (1) the reduced spasticity, which reduced the extra muscle activities (46), and (2) the decreased overactivation of muscles during the initial period of motor learning for a skill-requiring task (47). The significant decrease in the EMG activation levels of the FD and BIC muscle reflected the reduced spasticity of the related joints, which was also manifested as the decreased MAS scores in the elbow, wrist, and finger joints. The significant decrease in the normalized EMG activation levels of the FD and BIC muscle across training sessions also reflected a reduction of excessive muscular activities in the FD and BIC muscle in the bare hand evaluation task during hand opening, hand closing, and arm reaching movements. The reduction of excessive muscle activities suggested improved muscle coordination and voluntary motor controls during arm transportation and hand grasp movements. These improvements also contributed to a significant increase in the FMA (shoulder/elbow and wrist/hand) scores after training. The EMG level of the FD muscle exhibited a rapid decrease of 50% over the first four sessions, and it further declined by 19% from the 5th to 20th sessions in contrast to the relatively gradual decrease of the EMG level of the BIC muscle across 20 training sessions, with a total decrease of 50%. These results demonstrated similar patterns in the motor recovery under EMG-driven NMES robot-assisted upper-limb training as observed in our previous study on the wrist rehabilitation (23). In that work, the EMG activation level of the main flexor in the wrist (flexor carpi radialis) decreased faster in a 20-session EMG-driven NMES robot-assisted wrist training program, in comparison with the training only assisted with the EMG-driven pure robot (without NMES). It suggested that the combined treatment of the robot and NMES could speed up the recovery process (23). In this study, NMES assistance on finger extension may have contributed to the faster release of excessive contraction of the FD muscle, thus further improving muscular coordination of the finger joints. While the results of the EMG levels of the FD muscle showed the acceleration of the recovery process, the EMG levels of the FD and BIC muscles did not reach a plateau within the 20 training sessions. In a review of motor learning studies, the researcher indicated that the learning of a skilled movement is characterized by a plateau of little or no change in performance (48). Therefore, the further improvement in the recovery of the FD and BIC muscles could be obtained by providing additional training sessions.

In addition to the EMG activation levels, the CI revealed the coactivity of a muscle pair and the recovery progress on muscular coordination. Dewald et al. indicated that discoordination among muscles is one of the major factors for motor disability after stroke and highly related to the muscle spasticity and compensatory motions in the affected limb (49). Compensatory movements from proximal joints during motions at distal joints were commonly observed in poststroke survivors, which resulted in excessive co-contractions in muscles related to both the proximal and distal joints (6, 30). In this work, the evolutionary patterns of muscular coactivity within a joint and across joints in the upper limb were investigated by CIs among the related muscles. A decrease in the CI value of a muscle pair indicated a release of the co-contraction between the two muscles, i.e., the two muscles could contract more independently in the desired task. The significantly decreased CI of the FD and TRI muscles indicated the reduction of the coactivity between the elbow joint and finger joints, which suggested the improved isolation of the distal joint movements from the proximal joint. The reduction in cross-joint muscles (i.e., FD and TRI) also indicated reduced compensation movement from

co-contraction on the elbow joint during hand closing and opening motions. The significant decrease in the CI of BIC and TRI muscle pair was observed, and it indicated that the muscle coordination for achieving reaching motions through the elbow flexion and extension was promoted. However, the CI of the FD and TRI muscles and BIC and TRI muscle pair did not reach a plateau within the 20 training sessions. Further decreases in the CI value could be obtained by conducting additional training sessions.

In this work, the motor function improvement was obtained at the elbow, wrist and fingers as reflected by the clinical scores and the EMG parameters. During the training, the assistance from the EMG-driven NMES robot was incorporated in the coordinated tasks related to the arm reaching/withdrawing and hand open/close of the whole upper limb. Multi-joint coordinated upper limb practice simulating daily activities is necessary for stroke survivors to regain meaningful motor functions after training, since the task practiced would be the motor function restored, e.g., task-oriented rehabilitation (50). In the conventional physical rehabilitation on the upper limb, it was hard for a human therapist (or a stroke patient himself/herself in independent practices) to support the arm motions and manage the movements of the distal joints, e.g., finger joints, at the same time. This was one of the reasons that most of stroke survivors experienced reasonable recovery in the proximal joints, whereas little in the distal (51). In this work, the EMG-driven NMES-robot managed the finger motions while the stroke participants practicing the whole upper-limb tasks, which led to the motor improvements at both the proximal and distal joints. It was also noticed that the motor gains measured by FMA for the shoulder/elbow and wrist/hand were both around 20% immediately after the training (8-point increment at the shoulder/elbow with a full mark of 42 and 5-point increment at the wrist/hand with a full mark of 24). Besides the coordinated physical practice of the whole upper limb, another reason associated with the proximal recovery was related to the competitive interaction between the proximal and the distal joints in rehabilitation after stroke (52). Proximal joints (e.g., the shoulder/elbow) could gain more than the distal, e.g., the wrist/fingers, due to the compensatory activities from the proximal joints, which was related to the reduced inhibitory function of the ipsilesional motor cortex. Physical training at a distal joint benefited the motor function at the proximal joints was also observed in our previous robot-assisted wrist rehabilitation even with a fixed position of the elbow joint(14, 23).

LIMITATIONS

It was understood that the combined treatment of NMES and robot could introduce additional muscle fatigue to the target muscle under stimulation, i.e., the ED muscle in this work, in a training program with multiple sessions. Accumulated fatigue in the stimulated muscle might result in an increase in the EMG amplitude of the target muscle across the sessions. Although normalized EMG signals were adopted in this work to minimize the cross-sessional difference in EMG detection, more sensitive EMG representations which are less affected by the muscle fatigue will be explored in our future study. In this work, there was no significant change observed in the ED EMG level, nor in the CIs related to the ED muscle across the training sessions. Randomized controlled trials will be conducted in future studies to compare the rehabilitation effectiveness of the EMG-driven NMES-robotic hand with other device assisted programs (e.g., EMG-driven robotic hand) and with the conventional manual treatment on the upper limb.

CONCLUSION

In this study, the training effects of the poststroke upper-limb training assisted with EMG-driven NMES-robotic hand were investigated through a single-group clinical trial on patients with chronic stroke. The measured outcomes (i.e., clinical scores and EMG parameters) indicated that significant motor function improvements were achieved after the training, which included an increase in the voluntary motor effort on the entire upper limb, improved muscular coordination, and released muscle spasticity in the proximal and distal joints, and the motor improvements could be maintained till 3 months later after the training. Evidence suggests that intensive and repetitive upper-limb training with coordinated hand movements assisted by the voluntary EMG-driven NMES-robotic hand facilitates hand function recovery and improves muscular coordination in the upper limb with long sustainability in patients with chronic stroke.

ETHICS STATEMENT

The study was carried out in accordance with the human ethic guidelines of the Human Subjects Ethics Subcommittee of Hong Kong Polytechnic University.

AUTHOR CONTRIBUTIONS

CN contributed in the NMES-robot hand-assisted training experiment, data collection and analysis, and manuscript drafting. WR and WL contributed in the NMES-robot design and maintenance. YX contributed in the training and data collection. XH conceived of the study and coordinated the whole project, including the trial design, human subject experiments, and manuscript drafting. YZ contributed in the data analysis and manuscript drafting.

FUNDING

The study was supported in part by Innovation and Technology Commission–Hong Kong 10.13039/501100007156 and Hong Kong Polytechnic University 10.13039/501100004377.

REFERENCES

1. Langhorne P, Bernhardt J, Kwakkel G. Stroke rehabilitation. *Lancet* (2011) 377(9778):1693–702. doi:10.1016/S0140-6736(11)60325-5
2. Nakayama H, Jgtgensen H, Raaschou HO, Olsen TS. Recovery of upper extremity function in stroke patients: the Copenhagen Stroke Study. *Arch Phys Med Rehabil* (1994) 74(4):394–8. doi:10.1016/0003-9993(94)90161-9
3. Dobkin BH. Rehabilitation after stroke. *N Engl J Med* (2005) 352(16):1677–84. doi:10.1056/NEJMcp043511
4. Horn SD, DeJong G, Smout RJ, Gassaway J, James R, Conroy B. Stroke rehabilitation patients, practice, and outcomes: is earlier and more aggressive therapy better? *Arch Phys Med Rehabil* (2005) 86(12):101–14. doi:10.1016/j.apmr.2005.09.016
5. Harris JE, Eng JJ. Strength training improves upper-limb function in individuals with stroke. *Stroke* (2010) 41(1):136–40. doi:10.1161/STROKEAHA.109.567438
6. Good DC, Bettermann K, Reichwein RK. Stroke rehabilitation. *CONTINUUM Lifelong Learn Neurol* (2011) 17(3, Neurorehabilitation):545–67. doi:10.1212/01.CON.0000399072.61943.38
7. Hung CS, Hsieh YW, Wu CY, Lin YT, Lin KC, Chen CL. The effects of combination of robot-assisted therapy with task-specific or impairment-oriented training on motor function and quality of life in chronic stroke. *PM R* (2016) 8(8):721–9. doi:10.1016/j.pmrj.2016.01.008
8. Woo J, Chan SY, Sum MW, Wong E, Chui YP. In patient stroke rehabilitation efficiency: influence of organization of service delivery and staff numbers. *BMC Health Serv Res* (2008) 8(1):86. doi:10.1186/1472-6963-1188-1186
9. Norouzi-Gheidari N, Archambault PS, Fung J. Effects of robot-assisted therapy on stroke rehabilitation in upper limbs: systematic review and meta-analysis of the literature. *J Rehabil Res Dev* (2012) 49(4):479–96. doi:10.1682/JRRD.2010.10.0210
10. Lambercy O, Dovat L, Yun H, Wee SK, Kuah CWK, Chua KSG, et al. Effects of a robot-assisted training of grasp and pronation/supination in chronic stroke: a pilot study. *J Neuroeng Rehabil* (2011) 8(1):63. doi:10.1186/1743-0003-1188-1163
11. Amirabdollahian F, Loureiro R, Gradwell E, Collin C, Harwin W, Johnson G. Multivariate analysis of the Fugl-Meyer outcome measures assessing the effectiveness of GENTLE/S robot-mediated stroke therapy. *J Neuroeng Rehabil* (2007) 4:4. doi:10.1186/1743-0003-1184-1184
12. Timmermans AA, Lemmens R, Monfrance M, Geers R, Bakx W, Smeets R, et al. Effects of task-oriented robot training on arm function, activity, and quality of life in chronic stroke patients: a randomized controlled trial. *J Neuroeng Rehabil* (2014) 11(1):45. doi:10.1186/1743-0003-1111-1145
13. Volpe BT, Ferraro M, Lynch D, Christos P, Krol J, Trudell C, et al. Robotics and other devices in the treatment of patients recovering from stroke. *Curr Atheroscler Rep* (2004) 6(4):314–9. doi:10.1007/s11883-004-0064-z
14. Hu XL, Tong KY, Song R, Zheng XJ, Leung WWF. A comparison between electromyography-driven robot and passive motion device on wrist rehabilitation for chronic stroke. *Neurorehabil Neural Repair* (2009) 23(8):837–46. doi:10.1177/1545968309338191
15. Basteris A, Nijenhuis SM, Stienen AH, Buurke JH, Prange GB, Amirabdollahian F. Training modalities in robot-mediated upper limb rehabilitation in stroke: a framework for classification based on a systematic review. *J Neuroeng Rehabil* (2014) 11:1–15. doi:10.1186/1743-0003-11-111
16. Hu XL, Tong KY, Song R, Tsang VS, Leung PO, Li LS. Variation of muscle coactivation patterns in chronic stroke during robot-assisted elbow training. *Arch Phys Med Rehabil* (2007) 88(8):1022–9. doi:10.1016/j.apmr.2007.05.006
17. Hu XL, Tong KY, Song R, Zheng XJ, Lui KH, Leung W, et al. Quantitative evaluation of motor functional recovery process in chronic stroke patients during robot-assisted wrist training. *J Electromyogr Kinesiol* (2009) 19(4):639–50. doi:10.1016/j.jelekin.2008.04.002
18. Hu XL, Tong KY, Li R, Xue JJ, Ho SK, Chen P. The effects of electromechanical wrist robot assistive system with neuromuscular electrical stimulation for stroke rehabilitation. *J Electromyogr Kinesiol* (2012) 22(3):431–9. doi:10.1016/j.jelekin.2011.12.010
19. Prange GB, Jannink MJA, Groothuis-Oudshoorn CGM, Hermens HJ, Ijzerman MJ. Systematic review of the effect of robot-aided therapy on recovery of the hemiparetic arm after stroke. *J Rehabil Res Dev* (2006) 43(2):171–84. doi:10.1682/JRRD.2005.04.0076
20. Levin MF, Kleim JA, Wolf SL. What do motor "recovery" and "compensation" mean in patients following stroke? *Neurorehabil Neural Repair* (2009) 23(4):313–9. doi:10.1177/1545968308328727
21. Chae J, Yang G, Park BK, Labatia I. Muscle weakness and cocontraction in upper limb hemiparesis: relationship to motor impairment and physical disability. *Neurorehabil Neural Repair* (2002) 16(3):241–8. doi:10.1177/154596830201600303
22. Kralj AR, Bajd T. *Functional Electrical Stimulation: Standing and Walking after Spinal Cord Injury*. Boca Raton, FL: CRC Press (1989).
23. Hu XL, Tong RK, Ho NS, Xue JJ, Rong W, Li LS. Wrist rehabilitation assisted by an electromyography-driven neuromuscular electrical stimulation robot after stroke. *Neurorehabil Neural Repair* (2015) 29(8):767–76. doi:10.1177/1545968314565510
24. Lee Y, Lin KC, Cheng H, Wu CY, Hsieh YW, Chen C. Effects of combining robot-assisted therapy with neuromuscular electrical stimulation on motor impairment, motor and daily function, and quality of life in patients with chronic stroke: a double-blinded randomized controlled trial. *J Neuroeng Rehabil* (2015) 12:96. doi:10.1186/s12984-015-0088-3
25. Grimm F, Walter A, Spüler M, Naros G, Rosenstiel W, Gharabaghi A. Hybrid neuroprosthesis for the upper limb: combining brain-controlled neuromuscular stimulation with a multi-joint arm exoskeleton. *Front Neurosci* (2016) 10:367. doi:10.3389/fnins.2016.00367
26. Rong W, Li WM, Pang MK, Hu JY, Wei XJ, Yang BB, et al. A neuromuscular electrical stimulation (NMES) and robot hybrid system for multi-joint coordinated upper limb rehabilitation after stroke. *J Neuroeng Rehabil* (2017) 14(1):34. doi:10.1186/s12984-12017-10245-y
27. Volpe BT, Lynch D, Rykman-Berland A, Ferraro M, Galgano M, Hogan N, et al. Intensive sensorimotor arm training mediated by therapist or robot improves hemiparesis in patients with chronic stroke. *Neurorehabil Neural Repair* (2008) 22(3):305–10. doi:10.1177/1545968307311102
28. Rong W, Tong KY, Hu XL, Ho SK. Effects of electromyography-driven robot-aided hand training with neuromuscular electrical stimulation on hand control performance after chronic stroke. *Disabil Rehabil Assist Technol* (2015) 10(2):149–59. doi:10.3109/17483107.2013.873491
29. Hu X, Tong K, Wei X, Rong W, Susanto E, Ho S. The effects of post-stroke upper-limb training with an electromyography (EMG)-driven hand robot. *J Electromyogr Kinesiol* (2013) 23(5):1065–74. doi:10.1016/j.jelekin.2013.07.007
30. Raghavan P. Upper limb motor impairment after stroke. *Phys Med Rehabil Clin N Am* (2015) 26(4):599–610. doi:10.1016/j.pmr.2015.06.008
31. Towles JD, Kamper DG, Rymer WZ. Lack of hypertonia in thumb muscles after stroke. *J Neurophysiol* (2010) 104(4):2139–46. doi:10.1152/jn.00423.2009
32. Feigin VL, Lawes CM, Bennett DA, Anderson CS. Stroke epidemiology: a review of population-based studies of incidence, prevalence, and case-fatality in the late 20th century. *Lancet Neurol* (2003) 2(1):43–53. doi:10.1016/S1474-4422(03)00266-7
33. Traylor M, Rutten-Jacobs L, Holliday E, Malik R, Sudlow C, Rothwell P, et al. Differences in common genetic predisposition to ischemic stroke by age and sex. *Stroke* (2015) 46(11):3042–7. doi:10.1161/STROKEAHA.115.009816
34. Ashworth B. Preliminary trial of carisoprodol in multiple sclerosis. *Practitioner* (1964) 192:540–2.
35. Fugl-Meyer AR, Jääskö L, Leyman I, Olsson S, Steglind S. The post-stroke hemiplegic patient. 1. a method for evaluation of physical performance. *Scand J Rehabil Med* (1974) 7(1):13–31.
36. Folstein MF, Folstein SE, McHugh PR. "Mini-mental state": a practical method for grading the cognitive state of patients for the clinician. *J Psychiatr Res* (1975) 12(3):189–98. doi:10.1016/0022-3956(75)90026-6
37. Cram JR. *Introduction to Surface Electromyography*. Gaithersburg: Aspen (1998).
38. Krebs HI, Volpe BT. Rehabilitation robotics. *Handb Clin Neurol* (2013) 110:283–94. doi:10.1016/B978-0-444-52901-5.00023-X
39. Carroll D. A quantitative test of upper extremity function. *J Chronic Dis* (1965) 18(5):479–91. doi:10.1016/0021-9681(65)90030-5
40. Wolf SL, Lecraw DE, Barton LA, Jann BB. Forced use of hemiplegic upper extremities to reverse the effect of learned nonuse among chronic stroke

and head-injured patients. *Exp Neurol* (1989) 104(2):125–32. doi:10.1016/S0014-4886(89)80005-6

41. Wallace D, Duncan PW, Lai SM. Comparison of the responsiveness of the Barthel Index and the motor component of the Functional Independence Measure in stroke: the impact of using different methods for measuring responsiveness. *J Clin Epidemiol* (2002) 55(9):922–8.
42. Razali NM, Wah YB. Power comparisons of Shapiro-Wilk, Kolmogorov-Smirnov, Lilliefors and Anderson-Darling tests. *J Stat Model Anal* (2011) 2(1):21–33. Available from: https://www.semanticscholar.org/paper/Power-comparisons-of-Shapiro-Wilk-Kolmogorov-Smirn-Razali-Wah/dcdc0a0be7d65257c4e6a9117f69e246fb227423?tab=abstract
43. Péter O, Fazekas G, Zsiga K, Denes Z. Robot-mediated upper limb physiotherapy: review and recommendations for future clinical trials. *Int J Rehabil Res* (2011) 34(3):196–202. doi:10.1097/MRR.0b013e328346e8ad
44. Mehrholz J, Platz T, Kugler J, Pohl M. Electromechanical and robot-assisted arm training for improving arm function and activities of daily living after stroke. *Cochrane Database Syst Rev* (2008) 4:CD006876. doi:10.1002/14651858.CD006876.pub2
45. Cauraugh J, Light K, Kim S, Thigpen M, Behrman A. Chronic motor dysfunction after stroke recovering wrist and finger extension by electromyography-triggered neuromuscular stimulation. *Stroke* (2000) 31(6):1360–4. doi:10.1161/01.STR.31.6.1360
46. Bakheit A, Maynard VA, Curnow J, Hudson N, Kodapala S. The relation between Ashworth scale scores and the excitability of the α motor neurones in patients with post-stroke muscle spasticity. *J Neurol Neurosurg Psychiatry* (2003) 74(5):646–8. doi:10.1136/jnnp.74.5.646
47. Flament D, Shapiro MB, Kempf T, Corcos DM. Time course and temporal order of changes in movement kinematics during learning of fast and accurate elbow flexions. *Exp Brain Res* (1999) 129(3):441–50. doi:10.1007/s002210050911
48. Georgopoulos AP. On reaching. *Annu Rev Neurosci* (1986) 9(1):147–70. doi:10.1146/annurev.ne.09.030186.001051
49. Dewald JP, Sheshadri V, Dawson ML, Beer RF. Upper-limb discoordination in hemiparetic stroke: implications for neurorehabilitation. *Top Stroke Rehabil* (2001) 8(1):1–12. doi:10.1310/WA7K-NGDF-NHKK-JAGD
50. Timmermans AA, Spooren AI, Kingma H, Seelen HA. Influence of task-oriented training content on skilled arm-hand performance in stroke: a systematic review. *Neurorehabil Neural Repair* (2010) 24(9):858–70. doi:10.1177/1545968310368963
51. Chae J, Kilgore K, Triolo R, Yu D. Neuromuscular stimulation for motor neuroprosthesis in hemiplegia. *Crit Rev Phys Rehabil Med* (2000) 12(1):33–49. doi:10.1615/CritRevPhysRehabilMed.v12.i1.10
52. Takeuchi N, Izumi S. Maladaptive plasticity for motor recovery after stroke: mechanisms and approaches. *Neural Plast* (2012) 2012:359728. doi:10.1155/2012/359728

Conflict of Interest Statement: The authors declare that the research was conducted in the absence of any commercial or financial relationships that could be construed as a potential conflict of interest.

frontiers in Neurology

ORIGINAL RESEARCH
published: 08 February 2018
doi: 10.3389/fneur.2018.00048

The Effect of Visual Stimuli on Stability and Complexity of Postural Control

Haizhen Luo[1†], Xiaoyun Wang[2†], Mengying Fan[1], Lingyun Deng[1], Chuyao Jian[1], Miaoluan Wei[1] and Jie Luo[1]*

[1] Key Laboratory of Sensing Technology and Biomedical Instrument of Guangdong Province, Guangdong Provincial Engineering and Technology Center of Advanced and Portable Medical Devices, School of Engineering, Sun Yat-sen University, Guangzhou, China, [2] Guangdong Work Injury Rehabilitation Center, Guangzhou, China

Visual input could benefit balance control or increase postural sway, and it is far from fully understanding the effect of visual stimuli on postural stability and its underlying mechanism. In this study, the effect of different visual inputs on stability and complexity of postural control was examined by analyzing the mean velocity (MV), SD, and fuzzy approximate entropy (fApEn) of the center of pressure (COP) signal during quiet upright standing. We designed five visual exposure conditions: eyes-closed, eyes-open (EO), and three virtual reality (VR) scenes (VR1–VR3). The VR scenes were a limited field view of an optokinetic drum rotating around yaw (VR1), pitch (VR2), and roll (VR3) axes, respectively. Sixteen healthy subjects were involved in the experiment, and their COP trajectories were assessed from the force plate data. MV, SD, and fApEn of the COP in anterior–posterior (AP), medial–lateral (ML) directions were calculated. Two-way analysis of variance with repeated measures was conducted to test the statistical significance. We found that all the three parameters obtained the lowest values in the EO condition, and highest in the VR3 condition. We also found that the active neuromuscular intervention, indicated by fApEn, in response to changing the visual exposure conditions were more adaptive in AP direction, and the stability, indicated by SD, in ML direction reflected the changes of visual scenes. MV was found to capture both instability and active neuromuscular control dynamics. It seemed that the three parameters provided compensatory information about the postural control in the immersive virtual environment.

Keywords: virtual reality, balance control, entropy, center of pressure, head-mounted display

OPEN ACCESS

Edited by:
Guanglin Li,
Shenzhen Institutes of Advanced Technology (CAS), China

Reviewed by:
Xiaogang Hu,
University of North Carolina at Chapel Hill, United States
Simone Beretta,
Azienda Ospedaliera San Gerardo, Italy

****Correspondence:***
Jie Luo
luoj26@mail.sysu.edu.cn

[†]These authors have contributed equally in this work.

Specialty section:
This article was submitted to Stroke, a section of the journal Frontiers in Neurology

Received: *15 September 2017*
Accepted: *18 January 2018*
Published: *08 February 2018*

Citation:
Luo H, Wang X, Fan M, Deng L, Jian C, Wei M and Luo J (2018) The Effect of Visual Stimuli on Stability and Complexity of Postural Control. Front. Neurol. 9:48. doi: 10.3389/fneur.2018.00048

INTRODUCTION

Virtual reality (VR) has been used to improve balance in patients with stroke (1–3), and the usability and effectiveness have been examined (2–4). However, the mechanisms behind the new intervention and the effect of the virtual environment on balance control have not been fully understood.

The effect of vision information provided by immersive VR has been investigated with the experimental regime of comparing postural sway in the eyes-open (EO), eyes-closed (EC), and VR conditions (5–7). However, there has been no consistent conclusion yet. Horlings et al. showed that best stability was achieved in the EO condition, and a similar body sway was found in the EC and VR condition (5). However, Chiarovano et al. (6) and Robert et al. (7) reported no significant difference between the EO and EC conditions. In addition, it was found that the photo-rendered three-dimensional virtual environment did not increase body sway, but the optokinetic virtual scenes, such as a bundle of random dots moving in the same direction, will alter the postural control. In a word, how the visual stimuli generated by VR influence the postural control need further investigation.

Balance maintenance in the upright stance is a process of changing human body, by coordinating the muscle contractions, to make sure the center of mass (COM) of the body moving around the equilibrium position. The process of postural control has been widely investigated by means of a "motion capture system" (8) or a force plate (8, 9). With the latter apparatus, the center of pressure (COP) can be calculated with the reaction force data. To assess postural control, several parameters have been proposed and can be categorized into static parameters (e.g., position), dynamic parameters (e.g., velocity, root mean square, SD), and non-linear parameters [e.g., sample entropy, fuzzy approximate entropy (fApEn)]. SD of the COP displacement represents the average absolute displacement around the mean position of the COP trajectory (8), which has been employed by numerous researchers (10, 11). Velocity of the COP signal is said to describe the dynamic activity of the balance control by reflecting both the magnitude and frequency of the postural adjustment. Some investigations have shown its high reliability in anterior–posterior (AP) direction (8, 12). fApEn can be used to assess the irregularity of COP motion, and it might be a superior complexity measure in monotonicity and robustness to noise.

The aim of this study was to investigate the effect of visual information provided by VR on dynamic body sway in the upright stance. The virtual environments we used were optokinetic drums, rotating around different axes. 16 healthy subjects were enrolled in the investigation. When they put on the head-mounted display (HMD) device, they could see some black and white stripe-pairs moving in front of them, just like when they were sitting inside a large optokinetic drum. The reason we used the drum scene instead of the dot scene was that stripes were reported more effective in a virtual environment (13). The experiment included five kinds of visual input: EO, EC, and three different VR scenes. The parameters we used were mean velocity (MV), SD, and fApEn of the COP data.

MATERIALS AND METHODS

Participants

Sixteen healthy subjects (11 females, mean age: 22 years, range: 20–24 years) were enrolled by advertisements. All the participants had normal or corrected-to-normal eyesight and reported no history of ocular or neuromuscular disorder or vestibular dysfunction that can alter their balance. They all signed the written informed consent about the purpose and procedures of the study prior to the experiments, and they were free to withdraw from the experiment at any time. Ethical approval in accordance with the Declaration of Helsinki was provided by Guangdong Work Injury Rehabilitation Center.

Apparatus and Stimuli

The experimental devices included: (a) an HMD device (OculusRift Dk2, CA, USA) with a large field of vision (100°) and a high resolution LED screen (960 × 1,080 each eye), to show the VR scenes; (b) a desktop computer, with an Intel i7 CPU and an NVIDIA GTX 970 GPU, to create the VR scenes and drive the HMD device; (c) a multi-component force plate (Kistler type 9260, Kistler AG, Winterthur, Switzerland), placed stably on the ground to, to measure the change of force; (d) a control unit (Type 5233A2) with a built-in 8-channel charge amplifier equipped with filter bridges (cut-off frequency above to 7 kHz); (e) a data acquisition system, whose sampling frequency was set to 1,000 Hz; (f) a portable computer to record and analyze the data of the force plate (**Figure 1A**).

There were five types of visual exposure conditions: EC, eyes open (EO), and three VR conditions. In the VR conditions, an optokinetic drum was generated and rotated around a certain axis. When the participants put on the helmet, they saw some black and white stripe-pairs moving in front of them, just like when they were sitting inside a large drum, whose inner surface was painted with 24 equal-width black-and-white stripe pairs (14, 15). The drum could rotate around three different axes, i.e., yaw (VR1), pitch (VR2), and roll (VR3), with a constant speed (five rounds per minute) (**Figure 1B**). These VR scenes were created with the 3D Unity engine (version 5.3.3, Unity Technologies, CA, USA) and were displayed at a constant rate of 41 frames per second in the HMD.

Experimental Procedures

To provide a comfortable experience to participants, we adjusted the HMD with individual's pupil distance, measured with the built-in configuration utility, before the experiment. The experiment consisted of 10 trials, and one visual exposure condition for a trial. The five conditions were employed in a random order, but the same condition could not be employed in two adjacent trials, and each condition should be repeated twice. The duration of each visual exposure in a trial was 90 s, and there was a 1-min break between each two trials.

During the experiment, participants were required to stand on the force plate. Their feet should be put together, and their arms were required to be at their sides. In the EC condition, the subjects closed their eyes for the whole trial. In the EO trials, they were instructed to look at a fixed point in front of them. In the VR conditions, they put on the HMD device and were required to look straight ahead without attempting to follow the moving scenes. After the subject stood properly, the visual stimulus display and the data recording began synchronously.

Data Analysis

An application was developed in our laboratory using MABLE 2016a (MathWorks, Natick, MA, USA) to perform the data analysis. The length of the raw data of each trial was 90,000. The raw data were digitally filtered with fourth order zero-lag Butterworth low-pass filter, whose cutoff frequency was set to 20 Hz (16). The (AP) displacement and medial-lateral (ML) displacement of the COP were derived from the filtered data (**Figure 2**). We calculated values of MV and SD as follows:

$$SD_{AP} = \sqrt{\frac{1}{N}\sum_{i}^{N}\left|AP_i - \mu_{AP}\right|^2}$$

$$SD_{ML} = \sqrt{\frac{1}{N}\sum_{i}^{N}\left|ML_i - \mu_{ML}\right|^2}$$

where AP_i and ML_i were the COP displacement time series in AP and ML directions, respectively; N was the data length,

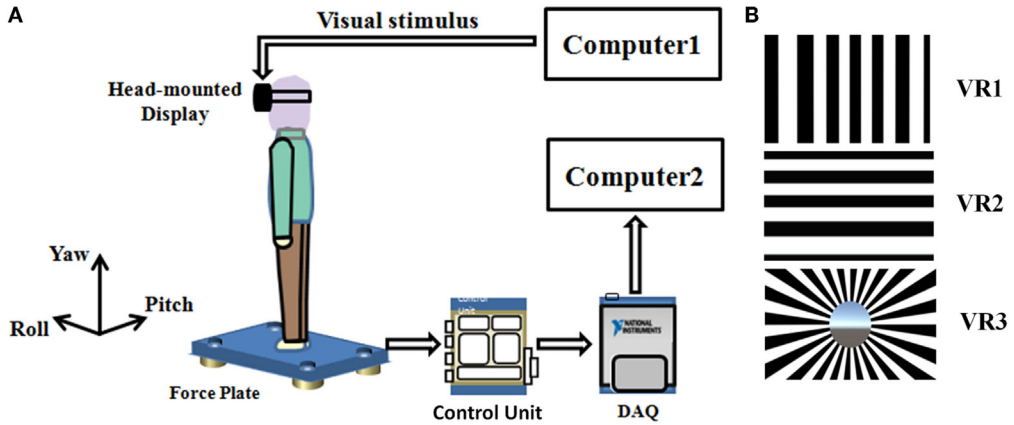

FIGURE 1 | **(A)** Schematic diagram of experimental setup. Scenes generated using computer 1 and transmitted to head-mounted display (HMD). Subjects viewed scenes inside the (HMD) while standing on a force plate. The postural output is then amplified, collected by a multichannel data acquisition system (DAQ), and the data were sent to computer 2 for subsequent analysis. **(B)** Screenshots of the virtual optokinetic drum scenes around three coordinate axes from top to bottom: yaw (VR1), pitch (VR2), and roll (VR3).

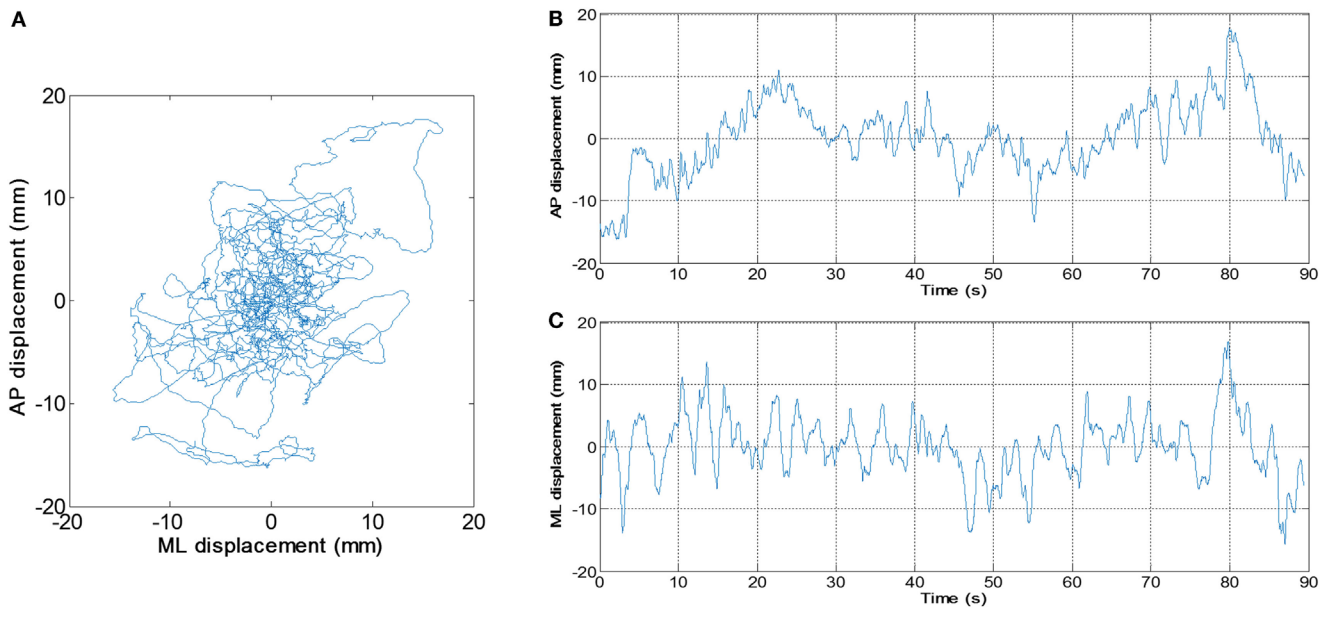

FIGURE 2 | An example of center of pressure (COP) signal. **(A)** Planar COP trajectory. **(B)** Anterior–posterior and **(C)** medial-lateral displacement of COP varies with time, respectively.

i.e., 90,000; μ_{AP} and μ_{ML} were the mean values of AP_i and ML_i, respectively. SD_{AP} and SD_{ML} represented SD of COP signal in AP direction and ML direction, respectively.

We calculated MV of the COP signal in AP and ML directions as follows:

$$MV_{AP} = \frac{1}{N-1}\sum_{i=1}^{N-1}\frac{|AP_{i+1} - AP_i|}{T}$$

$$MV_{ML} = \frac{1}{N-1}\sum_{i=1}^{N-1}\frac{|ML_{i+1} - ML_i|}{T}$$

where T was the sampling interval.

We also calculated fApEn to assess the complexity of the COP signal (17, 18). Higher values of fApEn means lower repeatability of vectors and predictability in the COP time series. As suggested by Lestienne et al. (19), it is necessary for the COP time series to be down-sampled before calculating fApEn, because the effective bandwidth of the COP signal, containing physiological information is 0–10 Hz, and signal oversampling could cause artificial colinearities, hence affect the variability data (20). We down-sampled the filtered COP to 20 Hz. After down-sampling, the length of the filtered COP data was 1,800, and we calculated fApEn in the following steps.

Given an N point time series $\{u(i):1 < i < N\}$, a vector sequence X_i^m could be derived:

$$X_i^m = \{u(i), \ldots, u(i+m-1)\} - \frac{1}{m}\sum_{j=0}^{m-1} u(i+j)$$

And the maximum absolute difference between two different vectors of X_i^m and X_j^m, d_{ij}^m, could be calculated:

$$d_{ij}^m = \max_{k\in(0,m-1)} \left| u(i+k) - \frac{1}{m}\sum_{k=0}^{m-1} u(i+k) - u(j+k) - \frac{1}{m}\sum_{k=0}^{m-1} u(j+k) \right|$$
$$(i, j = 1,2, \ldots, N-m+1;\ i \neq j)$$

$D_{ij}^m(n, r)$ represented the similarity of the two vectors X_i^m and X_j^m, and it could be obtained by the fuzzy membership function:

$$D_{ij}^m(n,r) = \exp\left(-\left(\frac{d_{ij}^m}{r}\right)^n\right)$$

Then, the following function averaged all of D_{ij}^m yielding φ^m:

$$\varphi^m(N,r) = \frac{1}{N-m+1}\sum_{i=1}^{N-m+1} \ln\left(\frac{1}{N-m+1}\sum_{j=1,j\neq i}^{N-m+1} D_{ij}^m\right)$$

Finally, fApEn (m, n, r) was calculated in the following way:

$$\text{fApEn}(m,n,r) = \varphi^m(n,r) - \varphi^{m+1}(n,r)$$

The parameter m was the vector length; n and r determined the similarity boundary (18). In this study, these parameters' values were selected as follows: $m = 2$, $n = 2$, $r = \text{std} \times 0.2$, where std was the SD of the down-sampled COP time series.

Statistical Analysis

The data were tested for statistical significance using 2 × 5 repeated measures analysis of variance (ANOVA) with a Bonferroni *post hoc*. Within-subject factor was visual condition (EO, EC, VR1, VR2, and VR3), and between-subject factor was Direction (AP and ML). All statistical analysis were performed with SPSS (version 19.0.0), and $p = 0.05$ was used as the minimal significance level.

RESULTS

Significant visual condition effect was found in MV, SD, fApEn parameters (**Table 1**). No significant effect was found in direction or direction × visual condition interaction on all three parameters (**Table 1**).

The box-whiskers-plots for MV, SD, as well as fApEn in both AP and ML directions are shown in **Figure 3**. A consistent trend could be observed in all three parameters, i.e., the lowest value was obtained in the EO condition, and the largest was in the VR3 condition. In addition, none of the parameters showed statistical difference when comparing the EC and EO conditions.

In AP direction, values of MV and fApEn in the VR2 and VR3 conditions were significantly higher than that in the EO condition (EO-VR2: $p = 0.04$ for MV, $p = 0.004$ for fApEn; EO-VR3: $p = 0.003$ for MV, $p = 0.004$ for fApEn). fApEn was noticeably larger in the VR1 condition than in the EO condition ($p = 0.008$). There was no statistical significance between each two conditions for SD.

TABLE 1 | Results of two-way analysis of variance (MV, mean velocity; SD, standard deviation; fApEn, fuzzy approximate entropy).

Parameter		*F*	*p*
MV	Visual condition	**18.479**	**<0.001**
	Direction	1.178	0.286
	Direction × visual condition	1.699	0.193
SD	Visual condition	**10.332**	**<0.001**
	Direction	0.305	0.585
	Direction × visual condition	2.379	0.055
fApEn	Visual condition	**9.092**	**0.001**
	Direction	1.768	0.194
	Direction × visual condition	0.993	0.397

Bold font represents significance at p < 0.05 level.

In ML direction, MV in the VR3 condition was significantly larger than that in the EO ($p = 0.01$) and VR2 ($p = 0.04$) conditions. SD in the VR1 condition was remarkably greater than in the EO ($p = 0.03$) and VR2 ($p = 0.018$) conditions. And SD in the VR3 condition was significantly larger than that in the EO ($p = 0.001$) and VR2 ($p = 0.002$) conditions. Therefore, SD discriminated different Visual Conditions better in ML direction than in AP direction. However, fApEn yielded similar results for all visual conditions in ML direction.

DISCUSSION

The main objective of this work was to investigate how the visual feedback and different dynamic visual perturbations in a HMD affected the postural control of healthy young participants during upright stance in both AP and ML directions. In our study, MV and SD of the COP, measured with a force plate, were utilized to assess the dynamic behavior of the balance control, and fApEn was used to measure the complexity of the COP signal.

Trends in the Parameters

Although not every comparison of two visual exposure conditions showed significant difference, the three parameters presented a similar trend: the lowest value was obtained in the EO condition, and the largest value was obtained in the VR3 condition, no matter in which COP direction. Previous studies (6, 19, 21) have found MV and SD of COP were lower in EO condition, compared with EC condition, demonstrating the contribution of visual information to balance maintenance. Our results were in accordance with previous reports. The effect of VR scenes on postural stability could be investigated with inertial sensors, such as gyroscopes (5), and it was found that the postural sway, in terms of shoulder sway angle and its velocity, when viewing simulated 3D-VR scenes was similar to that when standing still with EC but significantly larger than that when standing still with EO. However, two recent studies (6, 7) reported that, in terms of COP parameters, data obtained were similar in the EO and EC

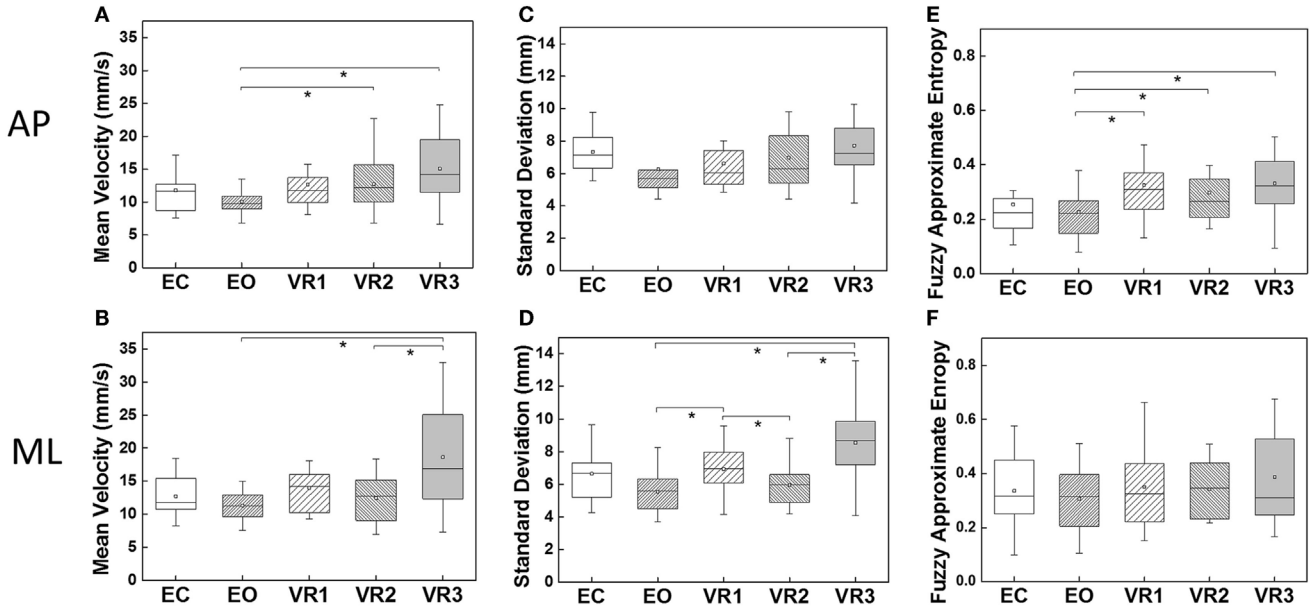

FIGURE 3 | Comparisons of the five visual exposure conditions in terms of the three parameters in anterior–posterior (AP) and medial-lateral (ML) directions; **(A,B)** mean velocity (MV) in AP and ML direction, respectively; **(C,D)** SD in AP and ML direction, respectively; **(E,F)** fuzzy approximate entropy (fApEn) in AP and ML direction, respectively. The mean values of parameters are marked in squares. Asterisks denotes $p < 0.05$.

conditions, and static filmed 3-dimensional virtual environment would not add unstable factor, compared to the EO condition, while simulated optokinetic scenes indeed affected the postural control. In our experiment, besides of amplitude of the COP signal, we also employed velocity and non-linear parameter, i.e., fApEn, to characterize the postural control performance. The three parameters yielded similar results in the EO and EC conditions, and our optokinetic drum scenes affected MV in both directions, SD in ML direction, and fApEn in AP direction. Our results were in agreement with those in the optokinetic dots experiment (6). The EO and EC conditions yielded similar fApEn, which was consistent with previous study, reporting that closing eyes did not produce striking effect on the complexity of postural control system among young people (22).

Meanings of the Parameters

Traditionally, MV and SD of the COP signal were considered as dynamic characteristics of balance control, and fApEn measured the regularity and complexity of the system. In detail, SD was said to characterize the spread of the COP amplitude, indicating postural instability, MV was considered as a more reliable quantity containing both spatial and frequency information of the COP signal (23) and fApEn revealed the coordinated muscle contractions that constrained the COM around the equilibrium position (24). In general, larger COP displacements (larger SD) would be companied with faster COP adjustments (higher MV) for the sake of balance maintenance, and this relationship could also be observed in our experiment. On the other hand, slower COP adjustment (lower MV) was considered to be associated with sensory feedback control (7), and sensory-input was assumed to increase neuromuscular intervention, hence generating a larger fApEn (24). However, this relationship was not observed in our experiment. Instead of considering MV as a parameter reflecting the cause of balance maintenance, such as sensory feedback, we will discuss an alternative interpretation that it was a measure of the performance of body adjustment due to balance control.

We started from the interesting opposing discrimination ability of SD and fApEn: SD was more discriminant in ML direction, and fApEn was more discriminant in AP direction. Since "the COP is the neuromuscular response to the imbalances of the body's COM" (25), the fApEn should reflect the complexity of the neuromuscular response. Our results implied that the balance control in ML direction was more or less in the same pattern since the fApEn means for the five visual exposure conditions were similar, while the system complexity measures in AP direction fell into two levels, one for the EO condition, and the other for the VR condition. It suggested that the active neuromuscular intervention was more diverse and adaptive in AP direction. Opposed to fApEn, SD of COP amplitude was similar in AP direction but different in ML direction in our experiment. It seemed that the similar stable state in AP direction was associated with the multi-level active neuromuscular regulation complexity, while the spread of COP amplitude in ML direction could not be well controlled with similar neuromuscular regulation strategies under different visual exposure. In summary, optokinetic virtual scenes induced a more complex neuromuscular response in AP direction, and affected the stability in ML direction. Since the discrimination ability of MV was similar to fApEn, in AP direction, and SD, in ML direction, we speculated that MV was a measure of movement performance, reflecting both the active neuromuscular response and the instability induced by visual perturbation.

Influences of Visual Scenes

Abundant studies have revealed that visual information contributes to balance maintenance, but visual information could also be a perturbation to balance control. Here, we categorized visual scenes into physical and virtual ones, and static and dynamic ones. The widely used EO condition relates to the static physical scenes, since in most experiment, including ours, the participants were instructed to fix their sights to somewhere in front of them. An example of dynamic physical scene is realized by a "Swinging Room" apparatus (26), which is a large box suspended on four ropes above the floor, and it could swing along the ropes to provide a physical moving scene for a person standing still inside the box. In the experiment of ref (7), a static virtual scene was generated by rendering a photo into a three-dimensional one. The dynamic virtual scenes in the HMD always provide an immersive VR experience. The simplest kind of dynamic virtual scenes is optokinetic simulation (6, 13). In our experiment, we generated an optokinetic drum, which could rotate around different axes.

When standing on a firm platform, the static visual information could not affect the postural control, but the dynamic scenes induced postural sway, no matter whether it is physical or virtual (6, 7, 26). Our results also supported this claim. In addition, our results implied a direction-related influence of the dynamic virtual scenes. In our experiment, in the VR1 condition, the vertical stripes on the optokinetic drum were moving horizontally; in the VR2 condition, the horizontal stripes were moving vertically; in the VR3 condition, the radial stripes were moving in a counterclockwise direction. MV of the VR2 condition was significantly higher than that of the EO condition in AP direction, but not in ML direction, suggesting an induced body sway in AP direction by the VR2 scene. SD of the VR1 condition was significantly larger than that of the EO and VR2 condition in ML direction but not in AP direction, suggesting a modulation of body sway was induced by the VR1 scene. Previous literature also reported that the postural displacement induced by the motion of the visual scene was in the same direction as stimulus (27–29). The velocity of the visual scenes in the literatures ranges from 0.02 and 0.16 (18) to 1/3 Hz (30). Our study showed that this modulation could also be found in a faster moving visual scene (5 rounds/s × 24 pairs/round = 2 pairs/s, i.e., 2 Hz). Since the VR3 scenes contain more complex optic flow information that moving both in horizontal and vertical direction, MV of the VR3 condition was larger than the EO condition in both AP and ML direction. The direction-modulated postural sway in our experiment supported that vision is a source of proprioceptive information for balance control (26), no matter whether it is in physical or virtual environment.

CONCLUSION

We have shown that dynamic virtual environment could induce active neuromuscular regulation and instability. The parameters we have used to characterize balance control were MV, SD, and fApEn of the COP signal, measured with a force plate. We have demonstrated that fApEn revealed active neuromuscular regulation taking place mainly in AP direction, and MV was a measure indicating both active neuromuscular intervention and instability. These COP parameters should benefit quantification of the balance recovery.

Additional Requirements

For additional requirements for specific article types and further information, please refer to Author Guidelines.

ETHICS STATEMENT

All the participants signed the written informed consent about the purpose and procedures of the study prior to the experiments, and they were free to withdraw from the experiment at any time. Ethical approval in accordance with the Declaration of Helsinki was provided by Guangdong Work Injury Rehabilitation Center.

AUTHOR CONTRIBUTIONS

HL conducted most of the experiments, collected and analyzed the data, interpreted the results, and finished the draft manuscript. MW designed the virtual scenes and part of the experiment, and finished part of the draft. JL designed the study, helped to analyze the data, and interpret the results and revised the manuscript. JL and MF participated in the data collection and analysis. LD conducted part of the experiments, recruited the subjects, collected data. XW designed the study, conducted the experiments, and revised the manuscript. CJ participated in the data collection.

ACKNOWLEDGMENTS

The authors would like to thank all the participants and Fengze Sui and Yumou Du for doing part of experiments and collecting data.

FUNDING

This research was supported by the grant from National Nature Science Foundation of China (No. 61403430) and the Guangdong Science and Technology Planning Project (No. 2015B020214003).

REFERENCES

1. Kizony R, Katz N, Weiss PLT. Adapting an immersive virtual reality system for rehabilitation. *J Vis Comput Anim* (2010) 14(5):261–8. doi:10.1002/vis.323
2. Song CG, Kim JY, Kim NG. A new postural balance control system for rehabilitation training based on virtual cycling. *IEEE Trans Inf Technol Biomed* (2004) 8(2):200–7. doi:10.1109/TITB.2004.828887
3. Trombetta M, Bazzanello Henrique PP, Brum MR, Colussi EL, De Marchi ACB, Rieder R. Motion rehab AVE 3D: a VR-based exergame for post-stroke rehabilitation. *Comput Methods Programs Biomed* (2017) 151:15–20. doi:10.1016/j.cmpb.2017.08.008
4. de Rooij IJ, van de Port IG, Meijer JG. Effect of Virtual Reality Training on Balance and Gait Ability in Patients With Stroke: Systematic Review and Meta-Analysis. *Phys Ther* (2016) 96(12):1905–18. doi:10.2522/ptj.20160054
5. Horlings CG, Carpenter MG, Küng UM, Honegger F, Wiederhold B, Allum JH. Influence of virtual reality on postural stability during movements of quiet stance. *Neurosci Lett* (2009) 451(3):227–31. doi:10.1016/j.neulet.2008.12.057

6. Chiarovano E, de Waele C, MacDougall HG, Rogers SJ, Burgess AM, Curthoys IS. Maintaining balance when looking at a virtual reality three-dimensional display of a field of moving dots or at a virtual reality scene. *Front Neurol* (2015) 6:164. doi:10.3389/fneur.2015.00164
7. Robert MT, Ballaz L, Lemay M. The effect of viewing a virtual environment through a head-mounted display on balance. *Gait Posture* (2016) 48:261–6. doi:10.1016/j.gaitpost.2016.06.010
8. Caballero C, Barbado D, Moreno FJ. What COP and kinematic parameters better characterize postural control in standing balance tasks? *J Mot Behav* (2015) 47(6):550. doi:10.1080/00222895.2015.1014545
9. Lin D, Seol H, Nussbaum MA, Madigan ML. Reliability of COP-based postural sway measures and age-related differences. *Gait Posture* (2008) 28(2):337–42. doi:10.1016/j.gaitpost.2008.01.005
10. Berg KO, Maki BE, Williams JI, Holliday PJ, Wood-Dauphinee SL. Clinical and laboratory measures of postural balance in an elderly population. *Arch Phys Med Rehabil* (1992) 73(11):1073–80.
11. Geurts AC, Ribbers GM, Knoop JA, van Limbeek J. Identification of static and dynamic postural instability following traumatic brain injury. *Arch Phys Med Rehabil* (1996) 77(7):639. doi:10.1016/S0003-9993(96)90001-5
12. Lafond D, Corriveau H, Hébert R, Prince F. Intrasession reliability of center of pressure measures of postural steadiness in healthy elderly people. *Arch Phys Med Rehabil* (2004) 85(6):896–901. doi:10.1016/j.apmr.2003.08.089
13. Tossavainen T, Juhola M, Pyykkö I, Aalto H, Toppila E. Development of virtual reality stimuli for force platform posturography. *Int J Med Inform* (2003) 70(2–3):277–83. doi:10.1016/S1386-5056(03)00034-0
14. Bubka A, Bonato F. Optokinetic drum tilt hastens the onset of vection-induced motion sickness. *Aviat Space Environ Med* (2003) 74(4):315–9. doi:10.1007/s10971-010-2180-2
15. Bonato F, Bubka A, Palmisano S. Combined pitch and roll and cybersickness in a virtual environment. *Aviat Space Environ Med* (2009) 80(11):941–5. doi:10.3357/ASEM.2394.2009
16. Caballero Sánchez C, Barbado Murillo D, Davids K, Moreno Hernández FJ. Variations in task constraints shape emergent performance outcomes and complexity levels in balancing. *Exp Brain Res* (2016) 234(6):1611–22. doi:10.1007/s00221-016-4563-2
17. Rigoldi C, Cimolin V, Camerota F, Celletti C, Albertini G, Mainardi L, et al. Measuring regularity of human postural sway using approximate entropy and sample entropy in patients with Ehlers-Danlos syndrome hypermobility type. *Res Dev Disabil* (2013) 34(2):840–6. doi:10.1016/j.ridd.2012.11.007
18. Ao D, Sun R, Tong KY, Song R. Characterization of stroke- and aging-related changes in the complexity of EMG signals during tracking tasks. *Ann Biomed Eng* (2015) 43(4):990–1002. doi:10.1007/s10439-014-1150-1
19. Lestienne F, Soechting J, Berthoz A. Postural readjustments induced by linear motion of visual scenes. *Exp Brain Res* (1977) 28(3–4):363–84.
20. Borg FG, Laxåback G. Entropy of balance – some recent results. *J Neuroeng Rehabil* (2010) 7:38. doi:10.1186/1743-0003-7-38
21. Cabeza-Ruiz R, García-Massó X, Centeno-Prada RA, Beas-Jiménez JD, Colado JC, González LM. Time and frequency analysis of the static balance in young adults with Down syndrome. *Gait Posture* (2011) 33(1):23–8. doi:10.1016/j.gaitpost.2010.09.014
22. Sasaki O, Usami S, Gagey PM, Martinerie J, Le Van Quyen M, Arranz P. Role of visual input in nonlinear postural control system. *Exp Brain Res* (2002) 147(1):1–7. doi:10.1007/s00221-002-1170-1
23. Geurts AC, Nienhuis B, Mulder TW. Intrasubject variability of selected force-platform parameters in the quantification of postural control. *Arch Phys Med Rehabil* (1993) 74(11):1144–50.
24. Tscharner VV, Zandiyeh P, Federolf P. Is sample entropy based entropic half-life and de-trended fluctuation analysis correlated and do they reflect phase regularity of center of pressure measurements? *Biomed Signal Process Control* (2016) 24:103–8. doi:10.1016/j.bspc.2015.09.010
25. Winter DA. *Biomechanics and Motor Control of Human Movement*. 4th ed. New Jersey: John Wiley & Sons, Inc. (2009).
26. Lee DN. Vision – the most efficient source of proprioceptive information for balance control. *Agressologie* (1977) 18:83–94.
27. van Asten WN, Gielen CC, Denier van der Gon JJ. Postural adjustments induced by simulated motion of differently structured environments. *Exp Brain Res* (1988) 73(2):371. doi:10.1007/BF00248230
28. Dichgans J, Brandt T, Held R. The role of vision in gravitational orientation. *Fortschr Zool* (1975) 23(1):255–63.
29. Guerraz M, Thilo KV, Bronstein AM, Gresty MA. Influence of action and expectation on visual control of posture. *Brain Res Cogn Brain Res* (2001) 11(2):259–66. doi:10.1016/S0926-6410(00)00080-X
30. Laurens J, Awai L, Bockisch CJ, Hegemann S, van Hedel HJ, Dietz V, et al. Visual contribution to postural stability: interaction between target fixation or tracking and static or dynamic large-field stimulus. *Gait Posture* (2010) 31(1):37. doi:10.1016/j.gaitpost.2009.08.241

Conflict of Interest Statement: The authors declare that the research was conducted in the absence of any commercial or financial relationships that could be construed as a potential conflict of interest.

frontiers in Neurology

CASE REPORT
published: 23 March 2018
doi: 10.3389/fneur.2018.00187

Estimation of Muscle Force Based on Neural Drive in a Hemispheric Stroke Survivor

*Chenyun Dai, Yang Zheng and Xiaogang Hu**

Joint Department of Biomedical Engineering, University of North Carolina at Chapel Hill and North Carolina State University, Raleigh, NC, United States

Robotic assistant-based therapy holds great promise to improve the functional recovery of stroke survivors. Numerous neural-machine interface techniques have been used to decode the intended movement to control robotic systems for rehabilitation therapies. In this case report, we tested the feasibility of estimating finger extensor muscle forces of a stroke survivor, based on the decoded descending neural drive through population motoneuron discharge timings. Motoneuron discharge events were obtained by decomposing high-density surface electromyogram (sEMG) signals of the finger extensor muscle. The neural drive was extracted from the normalized frequency of the composite discharge of the motoneuron pool. The neural-drive-based estimation was also compared with the classic myoelectric-based estimation. Our results showed that the neural-drive-based approach can better predict the force output, quantified by lower estimation errors and higher correlations with the muscle force, compared with the myoelectric-based estimation. Our findings suggest that the neural-drive-based approach can potentially be used as a more robust interface signal for robotic therapies during the stroke rehabilitation.

Keywords: motor unit decomposition, high-density surface electromyogram, neural drive, stroke, neural control, muscle weakness

OPEN ACCESS

Edited by:
Dong Feng Huang,
Sun Yat-sen University, China

Reviewed by:
Erwin Van Wegen,
VU University Amsterdam, Netherlands
Xu Zhang,
University of Science and Technology of China, China

***Correspondence:**
Xiaogang Hu
xiaogang@unc.edu

Specialty section:
This article was submitted to Stroke, a section of the journal Frontiers in Neurology

Received: *29 November 2017*
Accepted: *12 March 2018*
Published: *23 March 2018*

Citation:
Dai C, Zheng Y and Hu X (2018) Estimation of Muscle Force Based on Neural Drive in a Hemispheric Stroke Survivor. Front. Neurol. 9:187. doi: 10.3389/fneur.2018.00187

INTRODUCTION

Stroke survivors manifest impaired hand functions, especially the finger extension of their affected side. The use of robot-assisted devices (e.g., orthosis) (1–3) has shown great promise as a rehabilitation or assistive tool for stroke survivors. In order to control the robot based on user intention, surface electromyogram (sEMG) signals have been widely used as the neural control signal of the assistive robots or orthoses (4–6). However, since the global electromyogram (EMG) can be regarded as a random process at the macro level, directly using EMG as a control input can mask the actual neural control information (7). Moreover, abnormal muscle activation generated from the affected side can lead to less accurate myoelectric control.

In contrast, motoneuron discharge timings have been introduced as a better neural interface to robotic control (7), because the discharge timings can reflect the input signal to the neuromuscular system, and can be more robust for decoding user intent than the traditional EMG-based approach. The motoneuron discharge timing can be extracted from EMG decomposition, and the descending neural drive to the motor unit (MU) pool then can be estimated based on the firing behaviors of the pool. The neural drive can overcome different inconvenient processes in EMG and motor unit action potential (MUAP) that can interfere myoelectric control, such as the crosstalk of multiple EMG channels (9), cancelation of the waveform of MUAPs (8), and variations of MUAPs generated

by conductive process from muscle fibers to the skin surface or location shift of electrodes. In addition, the neural-drive-based approach could also overcome the variation or abnormal MUAPs due to the tremor and weakness on the affected side of stroke survivors.

Therefore, we quantified the performance of traditional EMG-based approach and the neural-drive-based approach on estimating the forces of individual finger (index, middle, and ring) extension of a stroke survivor. Our case study provided a promising approach that can help improve the utility of rehabilitation/assistive devices for hand functional recovery of stroke survivors.

MATERIALS AND METHODS

Case Report

We reported a case of an 88-year-old woman who suffered a hemispheric ischemic stroke ten years ago. Her Chedoke assessment scale on the hand section was 3 (moderate impairment). Her primary concern regarding her affected hand was muscular weakness in the hand muscles. The maximin force ratios of the finger extension on the affected side relative to the contralateral side were 0.48, 0.45, and 0.6 for index, middle, and ring fingers, respectively. In addition, the subject had difficulty generating forces with her little finger on her affected side. This study was carried out in accordance with the recommendations of the local Institutional Review Board (IRB) with written informed consent from the subject. The subject gave written informed consent in accordance with the Declaration of Helsinki. The protocol was approved by the local IRB. The written informed consent was obtained from the participant for the publication of this case report.

Experimental Setup

The subject sat upright in the experimental chair with the tested forearm comfortably placed on a horizontal table and the elbow supported on a foam pad. Her wrist was secured within two padded boards in a neutral position with respect to the flexion/extension to limit the use of her wrist. The four fingers (index, middle, ring, and little) were comfortably abducted. Each finger was secured to one load cell (Interface, SM-200N) for finger force measurement (with 1 kHz sampling rate). During the experiment, the subject was required to isometrically extend one designated finger (index, middle, or ring) each time. First, maximin voluntary contraction (MVC) of each finger was measured when the subject ramped up contraction force until it reached the maximum level and then maintained for 2 s. The average force value during the 2 s contraction plateau was taken as the MVC. After practice trials, she performed different tracking tasks. The subject was asked to track a targeted force trajectory shown on the screen by adjusting the muscle force of a designated finger. Two target trajectories were tested separately such as sine wave and trapezoid. Two contraction levels (20% or 50% MVC) were tested in each target. For the sine-wave target, the force oscillated either from 10% to 20% or from 25% to 50% at the designated force levels. Two repeated trials were performed for each condition. Additionally, the subject was instructed to only extend one of the designated fingers in each trial, but was allowed to activate other fingers, when she has difficulty isolating other fingers. The order of the finger and the contraction level was randomized during the experiment. A 3 min rest was provided between trials to avoid fatigue. The two sides were tested on two separate sessions separated by a week apart. A total of 24 trials (three fingers × two contraction levels × two tracking tasks × two repetitions) were recorded for each side. The force feedback of the designated finger was displayed via a custom-built program using Matlab (MathWorks, Inc.).

Surface EMG signals were recorded over the extensor digitorum communis muscle (EDC) using an 8 × 16 -channel (**Figure 1D**) high-density (HD) EMG electrode array with an inter-electrode distance of 10 mm (OT Bioelettronica, Torino, Italy). The HD array was attached to the skin surface at the middle of olecranon process and the styloid process with a double-sided sticker. Prior to the array placement, the skin was scrubbed with abrasive alcohol pads and then cleaned with regular alcohol pads. The EMG signals were sampled at 2,048 Hz with a gain of 1,000 and filtered with a cutoff frequency at 10–900 Hz via EMG-USB2 $^{+}$ (OT Bioelettronica, Torino, Italy).

Data Analysis

The neural-drive-based and EMG-based estimates were evaluated using a 500 ms moving window with an overlap of 400 ms between two adjacent windows. Different window

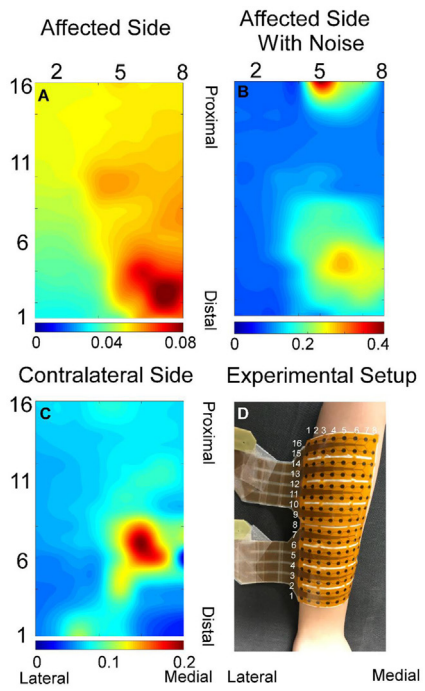

FIGURE 1 | Exemplar root-mean-square map for index finger from both affected **(A)** and contralateral sides **(C)**. **(B)** Root-mean-square map of panel **(A)** with background noise and motion artifact without filtering. **(D)** Experiment electrode placement. All root-mean-square maps were calculated from the trapezoid 50% contraction. All the *X* and *Y* axis labels indicate the row or column number of the electrodes.

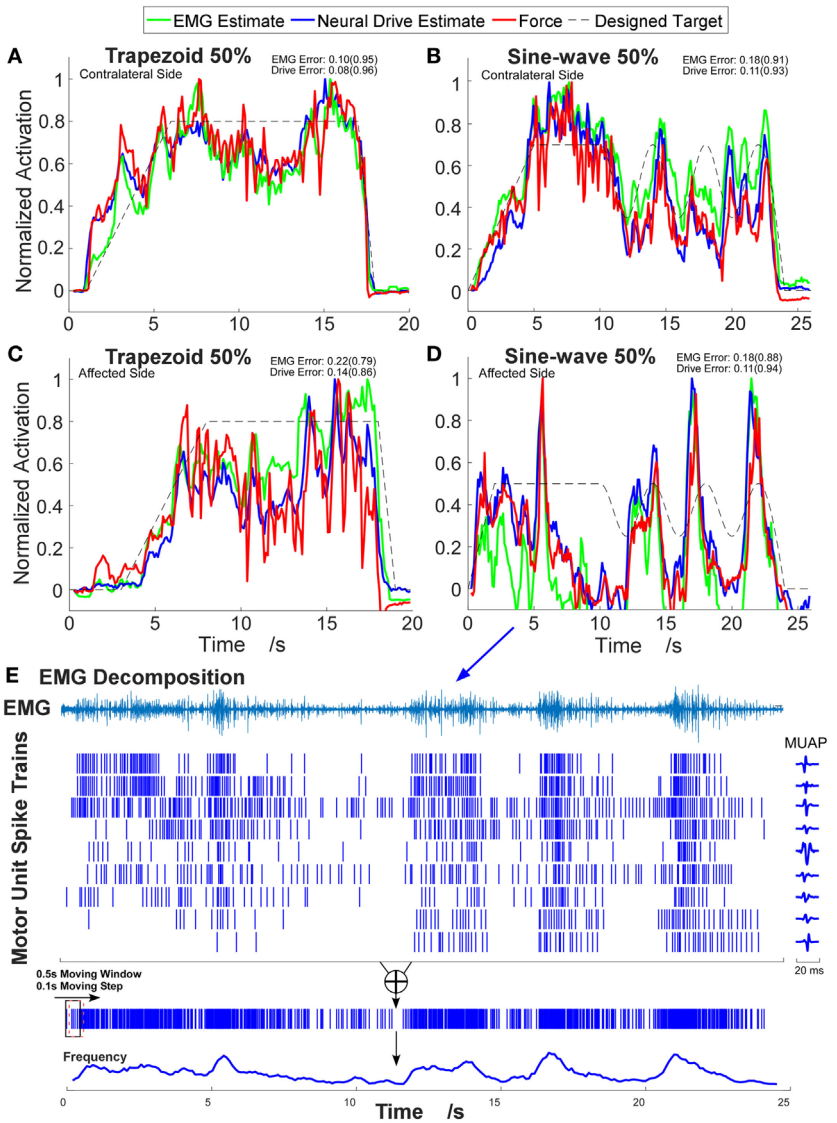

FIGURE 2 | Example time-series plots of four different contraction tasks. **(A,B)** Contralateral side. **(C,D)** Affected side. The corresponding root-mean-square errors (RMSEs) are presented and the correlation coefficients are shown in brackets. **(E)** Illustration of the decomposition results and the neural-drive-based estimation from trial **(D)**. One channel electromyogram (EMG) signal with highest root-mean-square value is shown, and the corresponding waveforms of motor unit action potentials (MUAPs) in that channel are plotted.

parameters tended to influence both estimation approaches in a similar manner. A previous study (10) has demonstrated that the muscle activation of individual finger was localized to particular regions of the muscle. Similar results were further verified in the current study as shown in **Figure 1**. EMG signals in the channels with low amplitude may contain background noise or components from the co-contraction of other fingers. Therefore, only half of the channels with higher signal amplitude were selected for the decomposition and for the root-mean-square calculation of the EMG. Namely, signals from row 1–8, 5–12, and 9–16 were used for index, ring, and middle fingers, respectively.

Electromyogram-Based Estimation

The EMG amplitude has been shown to be the most important and common feature to control external devices. For example, previous studies (11, 12) have indicated that the root-mean-square of EMG exhibited superior performance among the different amplitude-based control features, especially for high-force contractions (≥ 25% MVC). Raw EMG signals were first filtered with a high-pass filter (4th order Butterworth with a cutoff frequency of 50 Hz) to reduce the influence of motion artifacts. A notch filter (2nd order IIR filter at 60 Hz with a bandwidth of 1 Hz) was used to reject the power-line interference. For each sliding window, the root-mean-square of each EMG channel was

calculated and then was averaged across all channels as the force estimation. The average of the root-mean-square of HD EMG signals is defined as [1]:

$$\overline{\mathrm{RMS}} = \frac{1}{M}\sum_{i=1}^{M}\sqrt{\frac{1}{N}\sum_{n=1}^{N}x_i^2(n)},$$

where $x_i(n)$ is the ith channel, n is the index of sample, N is the length of the EMG recording in samples, M is the number of EMG channels, and i is the index of EMG channel.

Neural-Drive-Based Estimation

Raw EMG signals were decomposed into individual MU discharge events using the FastICA method (13) that has been verified as an accurate decomposition algorithm by previous studies (14). All the details of the decomposition algorithm and the parameter selection have been described in Ref. (13, 14). After EMG decomposition, the discharge timings of each individual MU were obtained. The general extension step for EMG decomposition and limitations of the FastICA algorithm (e.g., repeatedly converge to the same MU) usually result in a decomposition output with replicas of the same MU. The replicated MUs were removed for further analysis. Then, the discharge timings of all unique MUs were pooled into a composite spike event train. The composite discharge rate was calculated by dividing the number of events within each window by the window length (500 ms).

The performance of the two approaches was evaluated by the root-mean-square error (RMSE) and the correlation coefficient between the actual force and the estimates. To reduce the interference from the residual muscle activation even when the subject was instructed to relax, the estimation values were subtracted from the baseline values of the initial 2 s of each trial. Due to potential neural-mechanical delay between the neural drive/EMG and the force, the lag cross-correlation coefficient was used to make up the delay before the RMSE and correlation calculations. The lag cross-correlation coefficient was used to find the time delay when the force and the estimate had the highest cross-correlation coefficient. Since the units of EMG (volts), neural drive (Hz) and force (N) are different, the values were all normalized by its maximum value before comparison, leading to a maximum value of 1 (7). The performance differences of the two approaches were compared statistically using paired t-tests.

RESULTS

A total of 48 trials were analyzed. The number of MUs (mean ± SD) obtained from the decomposition was 7.94 ± 3.60 on the affected side and 10.17 ± 3.17 on the contralateral side. **Figure 1** shows the 2-D muscle activation map for index finger from both affected and contralateral sides under the condition of a steady contraction level at 50% MVC. The contralateral side revealed more concentrated and stronger muscle activation, compared with the affected side. The time-series plots of the two force estimation approaches and the corresponding actual forces for the two tracking tasks are shown in **Figure 2**. In general, the neural-drive-based estimate (in blue) showed a better approximation to the actual force (in red), compared with EMG-based estimate (in green). In addition, the overall results of the RMSE and correlation coefficient are summarized in **Table 1**. For most cases, the neural-drive-based approach is better than the EMG-based estimation.

Since four factors (three *fingers* × two *contraction levels* × two *tracking tasks* × two *sides*) were tested, the mean ± SE of the RMSE for each factor was obtained by averaging the values across all the trials among other factors (see **Figure 3**). Overall, the neural-drive-based estimates showed a significant lower error than the EMG-based estimates [paired t-test: $t(47) = 3.473$, $p = 0.001$]. We also observed similar trend for individual factors. Finally, the affected side also showed a larger RMSE than the contralateral side for the EMG-based estimation. Similarly, the neural-drive-based estimates showed a higher correlation with the actual forces than the EMG-based estimates [paired t-test: $t(47) = 3.421$, $p = 0.001$].

DISCUSSION

In this study, we investigated the feasibility of a novel neural drive estimation of the individual finger force of a stroke survivor,

TABLE 1 | Overall results of the root-mean-square error (RMSE) and correlation coefficient.

		Index		Middle		Ring	
		EMG	**Drive**	**EMG**	**Drive**	**EMG**	**Drive**
Sine 20	*C*	*0.15 (0.84)*	*0.22 (0.70)*	0.18 (0.81)	0.14 (0.90)	0.19 (0.86)	0.13 (0.91)
	A	*0.22 (0.70)*	*0.27 (0.67)*	0.23 (0.77)	0.19 (0.85)	0.15 (0.90)	0.10 (0.94)
Sine 50	*C*	0.27 (0.81)	0.21 (0.80)	0.19 (0.80)	0.17 (0.83)	0.16 (0.91)	0.10 (0.92)
	A	0.18 (0.73)	0.10 (0.94)	0.23 (0.76)	0.19 (0.84)	0.25 (0.75)	0.19 (0.85)
Trapezoid 20	*C*	*0.17 (0.91)*	*0.20 (0.89)*	0.22 (0.84)	0.21 (0.88)	0.16 (0.92)	0.16 (0.92)
	A	0.32 (0.32)	0.25 (0.76)	0.14 (0.88)	0.13 (0.89)	0.25 (0.77)	0.15 (0.85)
Trapezoid 50	*C*	*0.10 (0.95)*	*0.16 (0.92)*	*0.12 (0.92)*	*0.13 (0.92)*	0.10 (0.94)	0.10 (0.95)
	A	0.33 (0.28)	0.12 (0.95)	0.25 (0.82)	0.22 (0.86)	0.16 (0.93)	0.12 (0.95)
Mean		0.22 ± 0.08 (0.60 ± 0.36)	0.19 ± 0.06 (0.83 ± 0.11)	0.20 ± 0.05 (0.82 ± 0.06)	0.17 ± 0.04 (0.87 ± 0.03)	0.18 ± 0.05 (0.87 ± 0.07)	0.13 ± 0.03 (0.91 ± 0.04)

The correlation coefficients are written in brackets. C and A represent contralateral and affected sides. Values in italics show the cases that the EMG-based estimation is better than the neural-drive-based estimation.

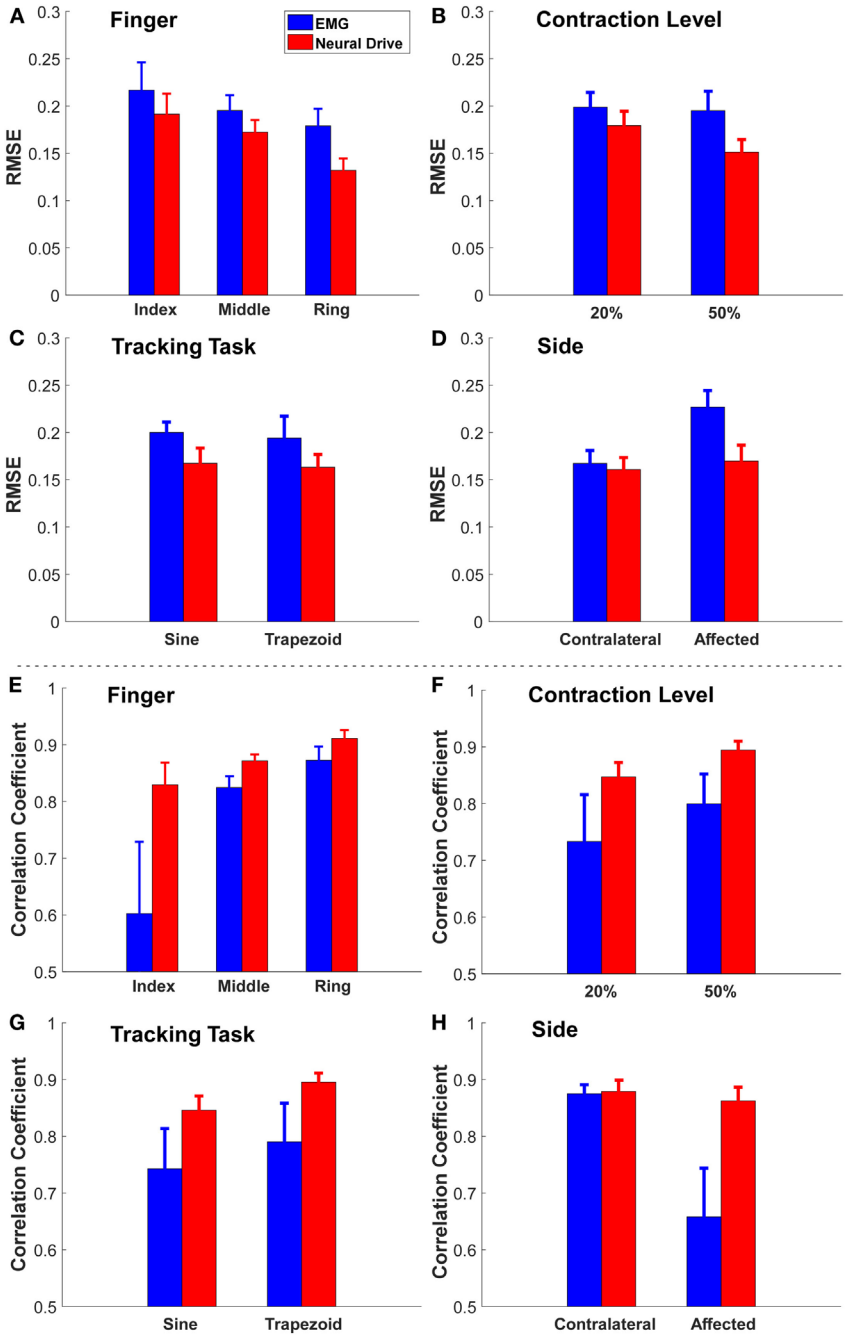

FIGURE 3 | The grand mean ± SE value of RMSE and correlation coefficient of each factor [**(A,E)** finger, **(B,F)** contraction level, **(C,G)** tracking task, and **(D,H)** side]. The error bars represent the SE.

based on motoneuron discharge timings at the population level. The discharge timings of the motoneurons can directly reflect the high-level control from the brain. It provides an alternative control input for the simultaneous and proportional control of individual finger forces. In general, our results show that the neural-drive-based approach was superior to the classic EMG-based approach for a majority of the conditions, especially on the affected side.

Since the EMG signal is regarded as a random Gaussian process at the macro level and the information of high-level neural control can be corrupted in EMG signals. The EMG signal varies due to the variation and cancelation of the waveforms of MUAPs at the macro level. Inevitable, external factors, involving ambient background noise, electrode shift, and changes in electrode-skin contact, can also modify the signal properties. These drawbacks can limit the development of a robust and accurate robotic control

interface for stroke rehabilitation. In contrast, the neural-drive-based approach intuitively has a better translation of the high level neural control, because the population probability/frequency of the discharge at the MU pool level directly encodes the descending input, without the various limitations in the EMG-based approach. Therefore, neural drive estimate reveals an improvement in the estimation accuracy of the muscle force. Previous studies have shown that the neural-drive-based approach can provide accurate estimation of motor output in different populations such as amputees following targeted muscle reinnervation and intact subjects (7). Our results on the stroke subject also showed consistently better performance in the neural-drive based approach. However, we still found some conditions (in *italics* in **Table 1**) showing that the EMG-based estimation is better than the neural-drive-based approach, especially in the index finger. One possibility is that the muscle activation generated from index finger of the stroke survivor is weak. The low signal-to-noise ratio (SNR) can decrease the accuracy of the decomposition (13).

Our preliminary results also showed that different factors (*finger*, *contraction level*, *tracking task*, and *side*) can affect the estimation of both approaches (see **Figure 3**). First (*finger*), the magnitude of sEMG signals from the EDC muscle compartment controlling the index finger was weaker than the other two fingers for this subject. Therefore, the low SNR from the index finger had the highest RMSE. Second (*contraction level*), EMG signals from the 50% contraction level had a higher SNR than the 20% condition, and more MUs can potentially be decomposed, which can lead to a better force estimation. Third (*tracking task*), the sine-wave contraction could induce more variations in the action potential amplitudes, compared with the trapezoid contraction, which could limit the neural-drive-based estimation. Nevertheless, the neural-drive-based estimation still revealed improved performance than the EMG-based estimation. Finally (*side*), the tremor during voluntary contractions on the affected side can cause more errors in EMG-based estimation than the contralateral side. In contrast, the neural-drive-based estimation showed similar performance across the two sides.

Our current study only tested a single stroke survivor. Although the results are promising, further testing involving a large subject cohort with different degrees of impairment is clearly needed. In addition, we did not test larger force levels above 50% MVC, because this particular subject had difficulty generating forces continuously at higher levels. During the experiment, the subject may inevitably perform co-contractions, especially during her ring finger extension. The EMG generated from co-contractions can potentially influence the estimation errors in both approaches. Our study was also limited to an offline analysis. Further studies on real-time decomposition are needed before the neural drive control method can be used for real-time applications. In general, our current work shows that the neural-drive-based estimation performed better than the EMG-based estimation for stroke survivors, especially on the affected side. This case study could provide a promising control input for robotics devices during stroke rehabilitation.

ETHICS STATEMENT

This study was carried out in accordance with the recommendations of the local Institutional Review Board (IRB) with written informed consent from the subject. The subject gave written informed consent in accordance with the Declaration of Helsinki. The protocol was approved by the local IRB. The written informed consent was obtained from the participant for the publication of this case report.

AUTHOR CONTRIBUTIONS

XH and CD conceived, designed, and performed experiments; CD and YZ analyzed data; XH and CD interpreted results; CD prepared figures; XH and CD drafted manuscript; XH, YZ, and CD revised manuscript; and XH, YZ, and CD approved final version of manuscript and agree to be accountable for all aspects of the work.

REFERENCES

1. Kwakkel G, Kollen BJ, Krebs HI. Effects of robot-assisted therapy on upper limb recovery after stroke: a systematic review. *Neurorehabil Neural Repair* (2008) 22:111–21. doi:10.1177/1545968307305457
2. Nordin N, Xie SQ, Wünsche B. Assessment of movement quality in robot-assisted upper limb rehabilitation after stroke: a review. *J Neuroeng Rehabil* (2014) 11:137. doi:10.1186/1743-0003-11-137
3. Chang WH, Kim Y-H. Robot-assisted therapy in stroke rehabilitation. *J Stroke* (2013) 15:174. doi:10.5853/jos.2013.15.3.174
4. Song R, Tong K, Hu X, Zhou W. Myoelectrically controlled wrist robot for stroke rehabilitation. *J Neuroeng Rehabil* (2013) 10:52. doi:10.1186/1743-0003-10-52
5. Stein J, Narendran K, McBean J, Krebs K, Hughes R. Electromyography-controlled exoskeletal upper-limb-powered orthosis for exercise training after stroke. *Am J Phys Med Rehabil* (2007) 86:255–61. doi:10.1097/PHM.0b013e3180383cc5
6. Dipietro L, Ferraro M, Palazzolo JJ, Krebs HI, Volpe BT, Hogan N. Customized interactive robotic treatment for stroke: EMG-triggered therapy. *IEEE Trans Neural Syst Rehabil Eng* (2005) 13:325–34. doi:10.1109/TNSRE.2005.850423
7. Farina D, Vujaklija I, Sartori M, Kapelner T, Negro F, Jiang N, et al. Man/machine interface based on the discharge timings of spinal motor neurons after targeted muscle reinnervation. *Nat Biomed Eng* (2017) 1:25. doi:10.1038/s41551-016-0025
8. Keenan KG, Farina D, Maluf KS, Merletti R, Enoka RM. Influence of amplitude cancellation on the simulated surface electromyogram. *J Appl Physiol* (2005) 98:120–31. doi:10.1152/japplphysiol.00894.2004
9. Solomonow M, Baratta R, Bernardi M, Zhou B, Lu Y, Zhu M, et al. Surface and wire EMG crosstalk in neighbouring muscles. *J Electromyogr Kinesiol* (1994) 4:131–42. doi:10.1016/1050-6411(94)90014-0
10. Hu X, Suresh NL, Xue C, Rymer WZ. Extracting extensor digitorum communis activation patterns using high-density surface electromyography. *Front Physiol* (2015) 6:279. doi:10.3389/fphys.2015.00279
11. Hogan N, Mann RW. Myoelectric signal processing: optimal estimation applied to electromyography-part I: derivation of the optimal myoprocessor. *IEEE Trans Biomed Eng* (1980) 27:382–95. doi:10.1109/TBME.1980.326652
12. Clancy EA, Hogan N. Probability density of the surface electromyogram and its relation to amplitude detectors. *IEEE Trans Biomed Eng* (1999) 46:730–9. doi:10.1109/10.764949
13. Chen M, Zhou P. A novel framework based on FastICA for high density surface EMG decomposition. *IEEE Trans Neural Syst Rehabil Eng* (2016) 24:117–27. doi:10.1109/TNSRE.2015.2412038

14. Negro F, Muceli S, Castronovo AM, Holobar A, Farina D. Multi-channel intramuscular and surface EMG decomposition by convolutive blind source separation. *J Neural Eng* (2016) 13:26027. doi:10.1088/1741-2560/13/2/026027

Conflict of Interest Statement: The authors declare that the research was conducted in the absence of any commercial or financial relationships that could be construed as a potential conflict of interest.

frontiers in Neurology

ORIGINAL RESEARCH
published: 26 March 2018
doi: 10.3389/fneur.2018.00185

The Crucial Changes of Sit-to-Stand Phases in Subacute Stroke Survivors Identified by Movement Decomposition Analysis

Yu Rong Mao†, Xiu Qin Wu†, Jiang Li Zhao, Wai Leung Ambrose Lo, Ling Chen, Ming Hui Ding, Zhi Qin Xu, Rui Hao Bian, Dong Feng Huang and Le Li**

Department of Rehabilitation Medicine, Guangdong Engineering and Technology Research Center for Rehabilitation Medicine and Translation, The First Affiliated Hospital, Sun Yat-sen University, Guangzhou, China

OPEN ACCESS

Edited by:
Valerie Moyra Pomeroy, University of East Anglia, United Kingdom

Reviewed by:
Xu Zhang, University of Science and Technology of China, China
Maurizio Acampa, Azienda Ospedaliera Universitaria Senese, Italy

***Correspondence:**
Dong Feng Huang
huangdf@mail.sysu.edu.cn;
Le Li
lile5@mail.sysu.edu.cn

†These authors have contributed equally to this study.

Specialty section:
This article was submitted to Stroke, a section of the journal Frontiers in Neurology

Received: *08 November 2017*
Accepted: *09 March 2018*
Published: *26 March 2018*

Citation:
Mao YR, Wu XQ, Zhao JL, Lo WLA, Chen L, Ding MH, Xu ZQ, Bian RH, Huang DF and Li L (2018) The Crucial Changes of Sit-to-Stand Phases in Subacute Stroke Survivors Identified by Movement Decomposition Analysis. Front. Neurol. 9:185. doi: 10.3389/fneur.2018.00185

Objective: The aim of this study was to detect the key changes during sit-to-stand (STS) movement cycle in hemiparetic stroke survivors using a five-phase kinematic and kinetic analysis.

Methods: Twenty-five subacute stroke survivors and 17 age-matched healthy adults participated in this study. The kinematic and kinetic parameters during STS cycle were measured using three-dimensional motion analysis system with force plates. The five standard phases of STS cycle were identified by six timing transitional points.

Results: Longer total time as well as larger changes were observed at the initial phase (phase I, 0.76 ± 0.62 VS 0.43 ± 0.09 s; $p = 0.049$) and at the end of hip and knee extension phase (phase IV, 0.93 ± 0.41 VS 0.63 ± 0.14 s; $p = 0.008$) in the stroke group than healthy group. Time to maximal knee joint moment was significantly delayed in the stroke group than in the control group (1.14 ± 1.06 VS 0.60 ± 0.09 s, $p < 0.001$). The maximal hip flexion was lower during the rising phase from seated position on the affected side in the stroke group than in the control group (84.22° ± 11.64°VS 94.11° ± 9.40°; $p = 0.022$). Ground reaction force was lower (4.61 ± 0.73 VS 5.85 ± 0.53 N, $p < 0.001$) in the affected side of the stroke group than in the control group. In addition, knee joint flexion was significantly lower at just-standing phase (T_4) and at end point (T_5) (5.12° ± 5.25° VS 8.21° ± 7.28°, $p = 0.039$; 0.03° ± 5.41° VS 3.07° ± 6.71°, $p = 0.042$) on the affected side than the unaffected side. Crucial decrease of knee joint moment at abrupt transitory (T_2) and the maximal moment was also observed on the affected side in comparison with the unaffected side (0.39 ± 0.29 VS 0.77 ± 0.25 Nm/kg, $p < 0.001$; 0.42 ± 0.38 VS 0.82 ± 0.24 Nm/kg, $p < 0.001$).

Conclusion: The findings of movement decomposition analysis provided useful information to clinical evaluation of STS performance, and may potentially contribute to the design of rehabilitation intervention program for optimum functional recovery of STS after stroke.

Keywords: sit-to-stand, subacute stroke, kinematic, kinetic, rehabilitation

INTRODUCTION

The ability to stand up from a seated position is very important in performing activities of daily living independently. It is also a prerequisite for gait (1, 2). The execution of sit-to-stand (STS) can be affected by several factors, including age, seat height, armrests, feet position, muscle strength, and balance ability (3–6). Stroke survivors suffer from impaired mobility and walking ability (7, 8) and these common symptoms contribute to STS disability that further confines their activities of daily life (9). Stroke survivors are prone to fall during STS because of the reduced ability of standing up from a chair (10). The severity of fear of falling was shown to be correlated with Timed up and Go test (11). Previous study revealed that 37.2% of falls in stroke survivors occurred while changing position from STS (12). The standardized evaluation on effectiveness of intervention to improve STS performance is still insufficient. There is also divergence on the clinical efficacy of standard beside repetitive practice of STS in rehabilitation clinic (9). Thus, the ability of rising from a chair remains difficult to recover after stroke (13). It is necessary to have an improved understanding on STS characteristics during the action implementation to improve training task performance and to decrease the fall rate in hemiparetic stroke survivors (14).

Sit-to-stand movement is the bridge between static position to dynamic body activity from the biomechanical view and defined as a transitional movement to the upright posture (15). The dynamic of STS is usually described using kinematic and kinetic variables. STS is generally assumed as a symmetrical activity of the lower extremity in the sagittal plane in healthy individuals (15–17). Previous researchers demonstrated that the influence of standing up velocity, center of pressure sway, and muscle activation pattern were related to the functional capability (18, 19). Chou and co-workers used a 3D motion analysis system combined with force plate to investigate the relationship between STS and gait parameters. The results indicated that a shorter duration of standing up or less vertical force difference on body weight distribution was associated with better gait performance (20). However, detailed phase analysis in STS is still limited which affects the further understanding of the specific motion deficits in stroke survivors during STS.

Previously, some authors studied the phases of habit development during STS activity from a biomechanical aspect and used it for optimization analysis (16, 21). The kinematic and kinetic data suggested that STS movement cycle could be divided into four or five phases (22–24). Galli and co-workers found prolonged STS in the ascending phase and different vertical forces in people after stroke in comparison with healthy controls (24). However, which specific phases are particularly crucial during the STS motion remains unclear. Previous studies on STS motion reported a wide variety of testing protocols, including difference in seat height, initial joint angle, and foot placement which led to different kinematic and kinetic results and conclusions (16, 21–24). In addition, the kinetic and kinematic characteristics of the timing and transitional points during STS cycle were seldom explored. Quantitative data such as movement duration, joint angle, and moment of timing and phases reference during STS of hemiparetic subjects are scarce, especially in stoke patients at subacute stage. Detailed motion analysis that depends on movement decomposition may identify typical pattern of change during STS after stroke. This would then contribute to the design of subject-specific training program based on the timing point and phase data for stroke survivors to regain the ability to perform STS task.

Therefore, this study aimed to explore the kinematic and kinetic characteristics of STS based on phases and transitional points analysis in bilateral lower limbs of subacute stroke survivors, and to compare the characteristic changes with healthy adults. The results of the current study would contribute to the knowledge of movement characteristics in people after stroke during STS and assist the development or evaluation of rehabilitation intervention of this specific motor task.

MATERIALS AND METHODS

Subjects

Twenty-five subjects (17 male and 8 female, age from 43 to 77 years old) with subacute stroke (from 14 to 85 days after stroke) were recruited for this study. The characteristics of the stroke survivors were summarized in **Table 1**. Patients were selected according to the following inclusion criteria: (1) the occurrence of a first stroke with unilateral hemiparesis lesions confirmed by magnetic resonance imaging or computed tomography; (2) no more than 3 months after stroke; (3) ability to stand up and sit down independently more than six times from a standard chair; (4) abnormal 10-m walk time according to age. Abnormal 10-m walk time was defined as: (i) age <60 = total completion time of over 10 s or slower than 1 m/s, (ii) age 60–69 = over 12.5 s or slower than 0.8 m/s, (iii) age ≥70 = over16.6 s or slower than (0.6 m/s) (25); and (5) adequate mental and auditory capacity to follow oral commands (Mini mental state examination score ≥27).

Seventeen healthy controls matched for age, weight, leg length, and gender participated in this study to provide the reference data for STS movement. All subjects had no history of back pain, joints pain, and no diagnosed lower limbs musculoskeletal disorders within 6 months prior to data collection. This study was approved by the Human Subjects Ethics Sub-committee of the First Affiliated Hospital, Sun Yat-sen University, China (ethic number [2014]0.88). The study was conducted in accordance to the Declaration of Helsinki. All subjects provided informed written consent prior to enrollment.

TABLE 1 | Anthropometric characteristics of the subjects.

	Patients Mean (SD)	Healthy subjects Mean (SD)	*p*-Value
Number of subjects	25	17	
Sex (male:female)	17:8	11:6	1.000
Age (years)	58.24 (10.46)	57.53 (6.63)	0.792
Days of post-injury	43.56 (23.65)	–	
Height (mm)	1,646 (73.43)	1,617 (62.13)	0.178
Body weight (kg)	66.24 (11.1)	64.45 (9.38)	0.858
Leg length (mm)	843.32 (42.21)	829.12 (35.54)	0.337

Instrumentation

Vicon Motion Analysis System (VICON MX13, VICON Peak, Oxford, UK) was used for motion analysis. The locations of passive reflective markers taped to the skin overlying bony landmarks of the pelvis and lower limbs were: (1) the sacrum at the level of the posterior superior iliac spines; (2) anterior superior iliac spines; (3) lower lateral one-third and halfway points on the thighs; (4) lateral epicondyle of knees; (5) lower lateral one-third and halfway points of the shanks; (6) lateral malleolus; (7) the second metatarsal head; (8) the calcaneus at the same height as the second metatarsal head and; and (9) T10. Trajectories of reflective markers were recorded by six wall mounted infrared cameras. Two force plates (OR6-7, AMTI Inc., Watertown, MA, USA) embedded in the floor were used to record ground reaction force (GRF). Kinematic and kinetic data were captured using Vicon Nexus (version 1.7.1) and Plug-in-Gait. The data from VICON cameras were sampled at 100 Hz and the data from force plates were sampled at 1,000 Hz, simultaneously. The data from one frame of cameras parallel with 10 frames of force plate. Temporal, kinematic, and kinetic parameters were processed and analyzed using Polygon (version 3.5.1). A height-adjustable chair without back or armrests was used in the experiment.

Experiment and Tasks

All of the subjects sat on the chair with seat height adjusted to keep the hip and knee joints as closed to 90°as possible. Both feet were placed on the force plates at neutral position and shoulder width apart. Arms were crossed on the chest with head facing forwards at a horizontal direction (**Figure 1**). For a complete movement cycle, subject was asked to stand up, remained stood up for 10 s, and then sat down. This was repeated for 10 cycles. Only the data from STS were analyzed. Subjects had a break of 5 s in between each complete cycle. The subjects were asked to keep their trunks and heads at upright position and to remain stationary as much as possible prior to STS task. They then started to rise from a seated position after the oral cue was heard. The start of STS was defined as the point where trunk flexion first occurred and was marked by the forward movement of T10 marker (22). The endpoint of stable standing was defined as the stoppage of the trunk and lower-limb markers (24). The transitional points of STS action were measured from the data on one force plate and angular movement. The data of the right and left lower limbs were collected by two force plates and markers trajectories. The task was performed at natural speed of the subjects' habit and ability. All subjects were asked to keep both heels in contact with the force plates without moving their feet during STS movement and between cycles. A line marked at 50% of the thigh length was aligned with the anterior border of the seated chair. Kinetic, kinematic, and temporal variables were measured at sagittal plane during STS movement.

Data Analyses and Statistics

The STS analysis was organized into phases that depend on kinematic variables, GRFs and momentum-transfer phase (13), STS movement has consistent pattern that can be divided into five phases and six transitional points based on biomechanical view and kinematic data (22, 24). The six transitional points are as follow: T_0 = the initial point of trunk started to flex; T_1 = the point of maximal hip flexion; T_2 = the point where knee started to extend, which is also called abrupt transitory point; T_3 = the point of maximal ankle dorsiflexion; T_4 = just standing to full extension of hip and knee; T_5 = end of STS (stable standing), also referred to as end point. The five phases of STS obtained from six timing points were defined as: (i) phase I—from T_0 to before the hip left the seat (vector force begin to increase on force plate); (ii) phase II—from hip lifting off seat to T_1; (iii) phase III—from T_2 to T_3; (iv) phase IV, from T_3 to T_4; and (v) phase V—from T_4 to T_5 (**Figure 1**).

Statistics analysis was performed using SPSS version 15.0. Descriptive statistics were computed for demographic characteristics and for all other parameters. Six trials with the smoothest and highest coincidence from the 10 recorded trials were included for data analysis according to reliability and validity of STS repetition (22, 24). The mean of the six STS cycles were computed for each subject. The Fisher's exact test was used to compare the difference of gender ratio between the stroke group and the healthy group. Anthropometric data (age, body height and weight, leg length) for hemiparetic and healthy subjects were analyzed by independent samples *t*-test. Independent *t*-test was also used to assess the between group differences in timing phases and the time in point between stroke and healthy groups. The differences in joint angle, moment, and GRF of each transitional points at sagittal

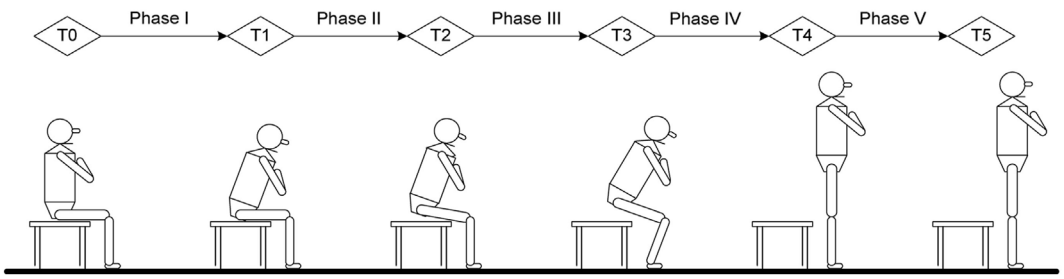

FIGURE 1 | Time point and phase definition in current study: T0, initial point of trunk flexion; T1, point of maximal hip flexion; T2, point of abrupt transitory knee extension; T3, point of maximal ankle dorsiflexion; T4, point of just standing with full extension of hip and knee; T5, end of sit-to-stand (stable standing). Phase I, forward transfer of trunk; Phase II, hip lifting off the chair and maximal hip flexion; Phase III, transitory knee extension point to maximal ankle dorsiflexion; Phase IV, maximal ankle dorsiflexion to point of just standing up in nearly full extension of the knee and hip; Phase V, stable standing.

plane between the three groups (affected, unaffected, and healthy lower limbs) were assessed using one-way ANOVA. Statistical significant level was set as $p < 0.05$ (two tailed).

RESULTS

The stroke and healthy groups had no statistical significant difference in age and anthropometric parameters (**Table 1**).

The total timing of a STS cycle was calculated from T_0 to T_5 and was converted to 100%. Averaged joint angle curves of hip, knee, and ankle during STS movement in the affected, unaffected, and healthy group are shown in **Figure 2**.

Figure 3 shows the timing point from T_1 to T_5 and the five phases in the stroke and healthy groups. All timing transitional points were significantly delayed in the stroke group when compared with the healthy group ($p < 0.05$). Phase I and phase IV were significantly lengthened in the stroke group when compared with the healthy group (0.76 ± 0.62 VS 0.43 ± 0.09 s, $p = 0.049$; 0.93 ± 0.41 VS 0.63 ± 0.14 s, $p = 0.008$, respectively) (**Figure 3A**). The angle at T_1 point of maximal hip flexion was significantly lower in the stroke group (84.22° ± 11.64°) than the healthy group (94.11° ± 9.40°, $p = 0.022$), and maintained more flexion at end point (T_5) of STS. The knee angle of affected limb in full extension point (T_4) (5.12° ± 5.25°) was less flexed than the unaffected limb (8.21° ± 7.28°, $p = 0.039$). There was significantly smaller flexion angle on the affected limb than the unaffected limb at the end point (T_5) of STS cycle for the stroke group (0.03° ± 5.41° VS 3.07° ± 6.71°, $p = 0.042$) (**Figure 3B**).

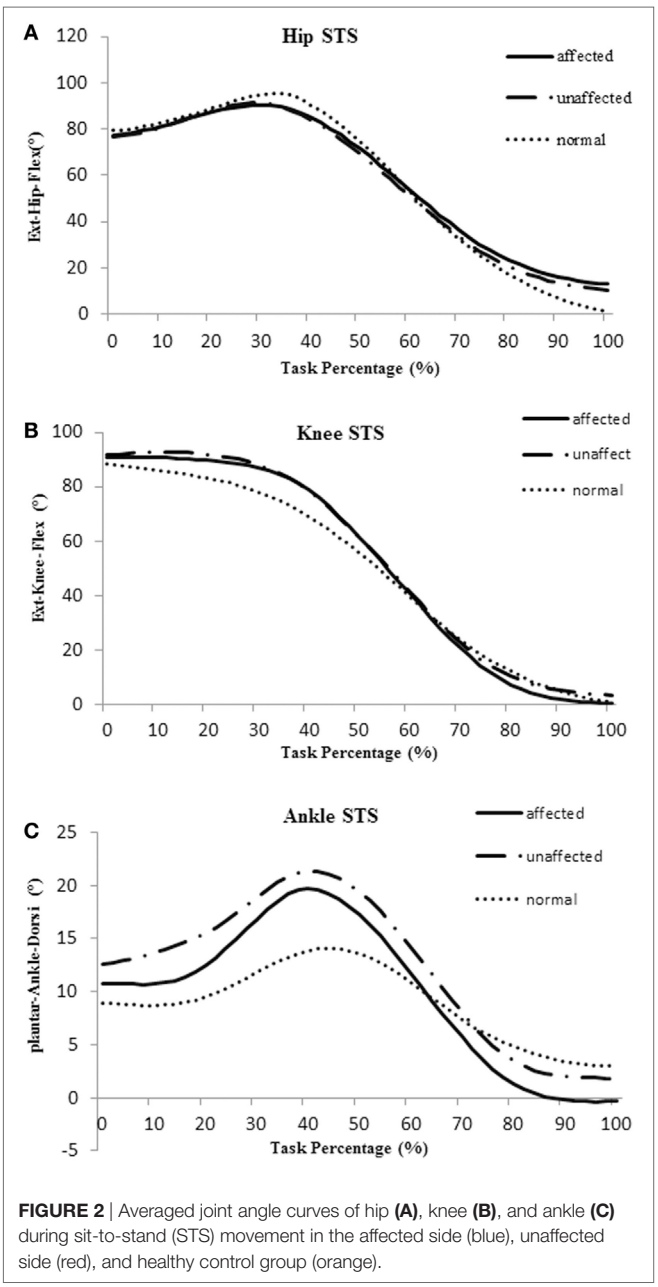

FIGURE 2 | Averaged joint angle curves of hip **(A)**, knee **(B)**, and ankle **(C)** during sit-to-stand (STS) movement in the affected side (blue), unaffected side (red), and healthy control group (orange).

The knee joint moment was significantly lower in the affected limb than unaffected limb at abrupt transitory point (T_2) (0.39 ± 0.29 VS 0.77 ± 0.25 Nm/kg, $p < 0.001$). The unaffected knee moment of the stroke group increased significantly compared with the healthy group at T_2 point (0.77 ± 0.25 VS 0.42 ± 0.22 Nm/kg, $p = 0.006$) (**Figure 4B**). GRF decreased significantly at affected lower limb (4.61 ± 0.73 N) in comparison with the unaffected lower limb (6.69 ± 0.86 N) and healthy lower limb (5.85 ± 0.53 N, $p < 0.001$, respectively).

The maximum knee joint moment was significantly lower on the affected limb than the unaffected limb in the stroke group (0.42 ± 0.38 VS 0.82 ± 0.24 Nm/kg, $p < 0.001$, **Figure 5A**). Time to maximal knee joint moment was significantly delayed in the stroke group when compared with the healthy group (1.14 ± 1.06 VS 0.60 ± 0.09 s, $p < 0.001$). Time to maximal ankle joint moment was significantly delayed in the unaffected limb of the stroke group when compared with the healthy group (1.89 ± 0.72 VS 1.16 ± 0.31 s, $p = 0.027$, **Figure 5B**).

DISCUSSION

This study used 3D motion analysis to explore the phases and transitional points of kinematic and kinetic differences of lower limbs during STS motion in subacute stroke survivors and compared those with age-matched healthy adults.

All of the transitional points were significantly delayed and the total time of STS task was significantly longer in the subacute stroke group when compared with healthy adults (**Figure 3A**). The results of the motion analysis indicated that the increase in total STS time was mostly related to the delay in phase I and phase IV (**Figure 3B**), where the majority of the time was spent on trunk flexion before the hip left the seat, and before hip and knee joints reached full extension. The increased time observed during phase I means that slow velocity of standing up from a seated position derives from the initial stage. Reduced velocity is proportionate to the disability of standing up previously reported in literature (18). Our findings were in line with Galli and co-workers who also found hemiplegic adults had a prolonged initial phase of STS (24). These changes might be related to poor trunk control and weak muscle strength (13, 26, 27). The increased total time of the STS task caused by lower speed indicates rising from a seated position is a challenging activity for subacute stroke survivors. It is recommended to incorporate

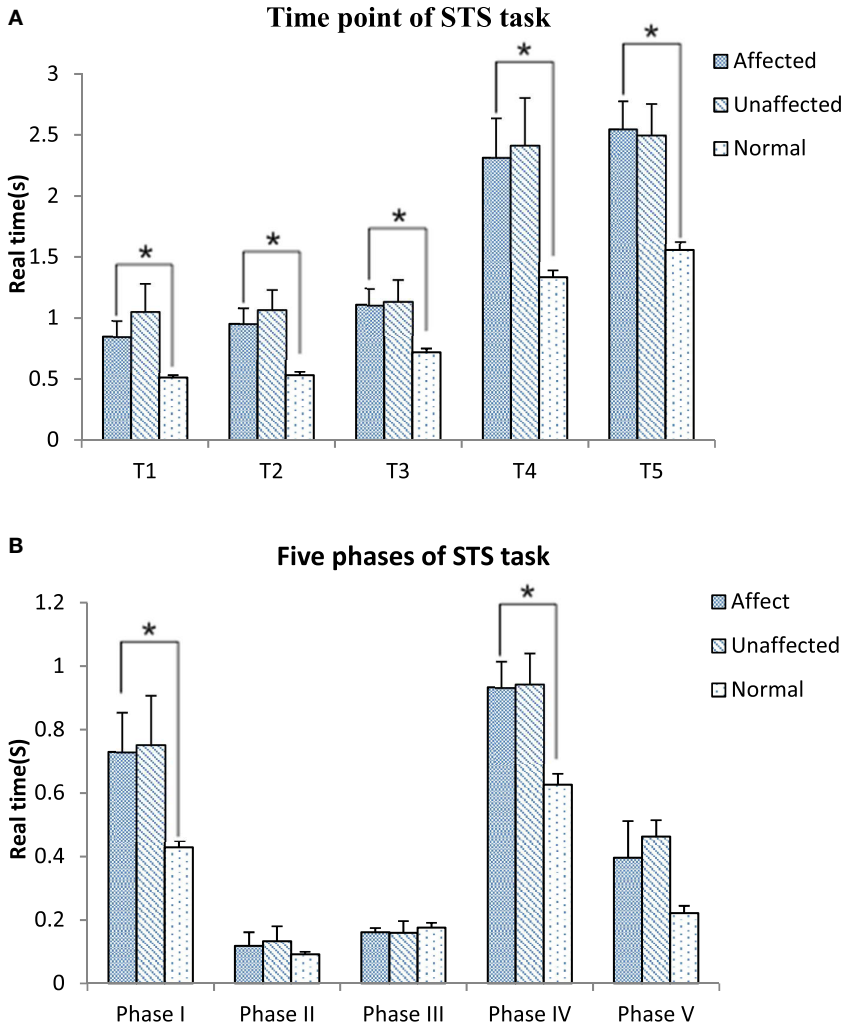

FIGURE 3 | Time point **(A)** and five phases **(B)** comparisons among the affected, unaffected side of stroke and healthy controls during sit-to-stand (STS) task (*$p < 0.05$).

the training of lean forward speed at the early stage of rehabilitation. In addition, the time point of hip lifting off the seat (the beginning of phase II) previously reported was notably earlier than the T_1 point observed in our study. This led to a negative data of phase II in some subacute stroke survivors. This reverse strategy may also influence the stability of posture control (22) that contributes to increase risk of falling (10). Therefore, findings of this study suggest that trunk forward flexion and hip flexion should be particularly trained in people after stroke to enable a higher speed to shorten phase I of STS and keep hip joint fully flexed at T_1.

The body of literature suggested that hip flexion angle contributed to rising from a seated position in healthy subjects (28). The results of this study showed that people with subacute stroke decreased maximal hip flexion angle during T_1 when compared with healthy adults before standing up from a seated position. This indicated the hip left the seat before getting sufficient flexion (**Figures 2A** and **4A**). This partly explained that subacute stroke survivors might encounter difficulty to stand and easy to fall when lifting from a seated position. An interesting finding from our study was that the affected knee joint had close to full extension to maintain stability at upright position (T5) and the unaffected knee joint maintained a slight flexion to maintain postural stability (**Figures 2B** and **4A**). In contrast, hip joint remained slightly flexed at end point (T5). The inability to achieve full hip extension and knee extension in lock position with stroke survivors might be related to the weakness of the gluteus maximus and quadriceps femoris (13) muscles. The higher ankle anterior–posterior swung between dorsiflexion and plantar flexion in the stroke group (**Figure 2C**) might be one of the factors that influenced the balance function of people after stroke (29).

It is important to detect the moment in joint angles when rising from a seated position, which requires larger hip flexion and knee extension than walking or climbing (3). Our results showed that the knee joint moment at the point of abrupt transitory

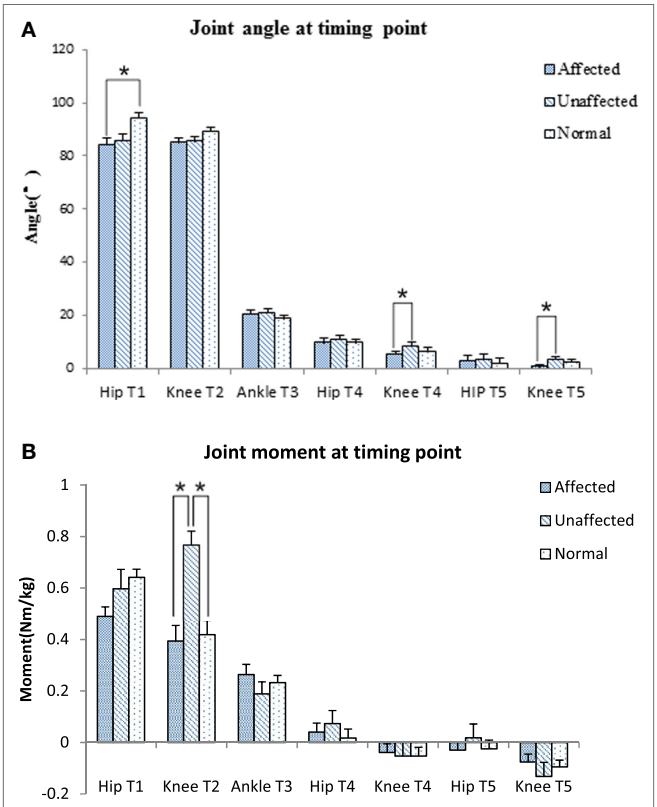

FIGURE 4 | Joint angle **(A)** and joint moment **(B)** at timing point comparison among the affected, unaffected side of stroke, and healthy controls (*$p < 0.05$).

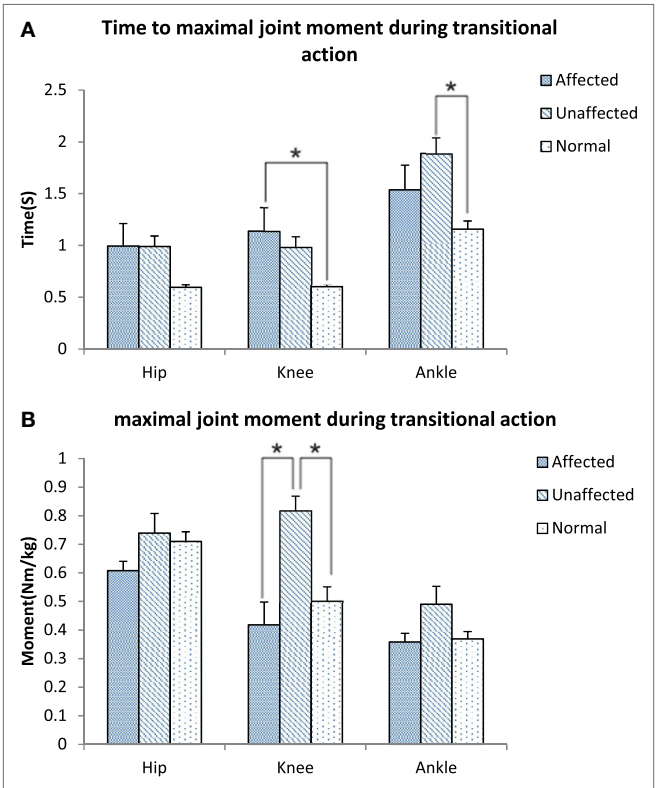

FIGURE 5 | Time to maximal joint moment **(A)** and Maximal joint moment **(B)** during transitional action among the affected, unaffected side of stroke, and healthy controls (*$p < 0.05$).

extension (T2) (**Figure 4B**) and GRF were significantly lower on the affected side when compared with the unaffected side and control subjects. In addition, our study also found the maximal hip flexion moment was synchronous with maximal knee extension moment on the unaffected side of the stroke group and on the healthy group, with the timing point of maximum moment of knee joint occurred after extension began on the affected limb (T2) (**Figure 5B**). These findings revealed that difficulties in rising from seated position might be related to weakness of lower extremity muscle strength and abnormal moment timing point. Subacute stroke subjects depend much more on the unaffected limb while implementing the STS movement, especially when knee extension started (30). Therefore, it might need to increase knee extensors strength in subacute stroke survivors, especially at initial extension position to maintain symmetry of STS movement pattern. Our study showed an unequal GRF between affected and unaffected side, while the total GRF of the stroke group were similar with healthy adults. Impairments in muscles strength, postural control and balance were factors previously shown that contributed to asymmetrical weight-bearing in patients with stroke (20, 31, 32). Subacute stroke survivors put less weight on the affected limb and increased the load of the unaffected limb. Similar results were reported in previous studies (33, 34). All of these findings suggested that balance and weight-bearing training were needed for people with stroke to improve their motor function and posture control to regain ability of STS.

People with stroke have difficulties to rise from a seated position. This ability is not easily recovered due to muscle weakness, impaired motor control, and balance function. In our study, the results would assist the development of a targeted rehabilitation interventions to improve STS ability for people after stroke. The training of trunk leaning forward can begin as early as possible while the person after stroke can sit up, and focus on increasing the velocity and amplitude of trunk and hip joint flexion. The muscles strength of gluteus maximus and quadriceps femoris must be reinforced by exercise, and should be trained at early stage of bed rest. In addition, by means of designing exercises at bed rest stage and exercise that mimic STS motion to increase GRF at affected limb. Therefore, these results may give a cue and guidance to improve STS performance.

This study has several limitations which limits the interpretation and generalizability of the data. First, we only recorded the motion data and GRF during STS. We did not have electromyography recording of the lower limb muscles nor the objective muscle strength data from dynamometer. Further combination of kinematic, electrophysiological signals and muscle strength measurements could increase understanding on the mechanisms of motor control changes during STS following stroke. This would lead to a better understanding of the alteration of movement sequence. Second, we focused on lower limb kinematic and kinetics characteristics and did not consider

movement of the upper body such as the neck and shoulders. This prevented the detailed analysis of whole-body posture comparison and evaluation between healthy control and people after stroke during STS.

CONCLUSION

The total time of STS task was significantly longer in people with subacute stroke when compared with the healthy controls. Knee moment, abnormal timing point, and GRF on the affected side during STS task were reduced. The observed kinematic and kinetic changes in subacute stroke survivors during STS provide suggestions to the clinical intervention of improvement of STS motor performance.

ETHICS STATEMENT

The experiment was approved by the Human Subjects Ethics Subcommittee of the First Affiliated Hospital, Sun Yat-sen University, China (ethic number [2014]88).

AUTHOR CONTRIBUTIONS

YM, XW, and JZ analyzed the data, interpreted the results, and drafted the manuscript. YM, WL, JZ, MD, ZX, LC, and RB conducted the experiment and collected the data. XW contributed to the revision of MS and the answers to the comments from the reviewers and editor. DH and LL designed the study and performed all stages of the study including data collection, analysis, interpretation, and substantial revision of the manuscript. All the authors approved the final version of the manuscript.

FUNDING

This work was funded by National Natural Science Foundation of China (No. 30973165,81372108, 31771016) and in part by 5010 Planning Project of Sun Yat-sen University of China (No.2014001) and Science and Technology Planning Project of Guangdong Province, China (No.2016A020220009, 2015B020233006, 2015B020214003, 2014B090901056), and Guangzhou Research Collaborative Innovation Projects (No. 201604020108).

REFERENCES

1. Guralnik JM, Ferrucci L, Simonsick EM, Salive ME, Wallace RB. Lower-extremity function in persons over the age of 70 years as a predictor of subsequent disability. *N Engl J Med* (1995) 332(9):556–61. doi:10.1056/NEJM199503023320902
2. Nevitt MC, Cummings SR, Kidd S, Black D. Risk factors for recurrent nonsyncopal falls. A prospective study. *JAMA* (1989) 261(18):2663–8. doi:10.1001/jama.261.18.2663
3. Rodosky MW, Andriacchi TP, Andersson GB. The influence of chair height on lower-limb mechanics during rising. *J Orthop Res* (1989) 7(2):266–71. doi:10.1002/jor.1100070215
4. Janssen WG, Bussmann HB, Stam HJ. Determinants of the sit-to-stand movement: a review. *Phys Ther* (2002) 82(9):866–79. doi:10.1093/ptj/82.9.866
5. Ng SS, Kwong PW, Chau MS, Luk IC, Wan SS, Fong SS. Effect of arm position and foot placement on the five times sit-to-stand test completion times of female adults older than 50 years of age. *J Phys Ther Sci* (2015) 27(6):1755–9. doi:10.1589/jpts.27.1755
6. Lord SR, Murray SM, Chapman K, Munro B, Tiedemann A. Sit-to-stand performance depends on sensation, speed, balance, and psychological status in addition to strength in older people. *J Gerontol A Biol Sci Med Sci* (2002) 57(8):M539–43. doi:10.1093/gerona/57.8.M539
7. Olney SJ, Richards C. Hemiparetic gait following stroke. Part I: characteristics. *Gait Posture* (1996) 4(2):136–48. doi:10.1016/0966-6362(96)01063-6
8. Isho T, Usuda S. Association of trunk control with mobility performance and accelerometry-based gait characteristics in hemiparetic patients with subacute stroke. *Gait Posture* (2016) 44:89–93. doi:10.1016/j.gaitpost.2015.11.011
9. Pollock A, Gray C, Culham E, Durward BR, Langhorne P. Interventions for improving sit-to-stand ability following stroke. *Cochrane Database Syst Rev* (2014) 26(5):CD007232. doi:10.1002/14651858.CD007232.pub4
10. Lipsitz LA, Jonsson PV, Kelley MM, Koestner JS. Causes and correlates of recurrent falls in ambulatory frail elderly. *J Gerontol* (1991) 46(4):M114–22. doi:10.1093/geronj/46.4.M114
11. Guan Q, Jin L, Li Y, Han H, Zheng Y, Nie Z. Multifactor analysis for risk factors involved in the fear of falling in patients with chronic stroke from mainland China. *Top Stroke Rehabil* (2015) 22(5):368–73. doi:10.1179/1074935714Z.0000000048
12. Nyberg L, Gustafson Y. Patient falls in stroke rehabilitation. A challenge to rehabilitation strategies. *Stroke* (1995) 26(5):838–42. doi:10.1161/01.STR.26.5.838
13. Boukadida A, Piotte F, Dehail P, Nadeau S. Determinants of sit-to-stand tasks in individuals with hemiparesis post stroke: a review. *Ann Phys Rehabil Med* (2015) 58(3):167–72. doi:10.1016/j.rehab.2015.04.007
14. Britton E, Harris N, Turton A. An exploratory randomized controlled trial of assisted practice for improving sit-to-stand in stroke patients in the hospital setting. *Clin Rehabil* (2008) 22(5):458–68. doi:10.1177/0269215507084644
15. Yoshioka S, Nagano A, Hay DC, Fukashiro S. Biomechanical analysis of the relation between movement time and joint moment development during a sit-to-stand task. *Biomed Eng Online* (2009) 8:27. doi:10.1186/1475-925X-8-27
16. Błażkiewicz M, Wiszomirska I, Wit A. A new method of determination of phases and symmetry in stand-to-sit-to-stand movement. *Int J Occup Med Environ Health* (2014) 27(4):660–71. doi:10.2478/s13382-014-0280-x
17. Schenkman M, Berger RA, Riley PO, Mann RW, Hodge WA. Whole-body movements during rising to standing from sitting. *Phys Ther* (1990) 70(10):638–48,discussion648–51. doi:10.1093/ptj/70.10.638
18. Ada L, Westwood P. A kinematic analysis of recovery of the ability to stand up following stroke. *Aust J Physiother* (1992) 38(2):135–42. doi:10.1016/S0004-9514(14)60558-4
19. Lee MY, Wong MK, Tang FT, Cheng PT, Chiou WK, Lin PS. New quantitative and qualitative measures on functional mobility prediction for stroke patients. *J Med Eng Technol* (1998) 22(1):14–24. doi:10.3109/03091909809009994
20. Chou SW, Wong AM, Leong CP, Hong WS, Tang FT, Lin TH. Postural control during sit-to-stand and gait in stroke patients. *Am J Phys Med Rehabil* (2003) 82(1):42–7. doi:10.1097/00002060-200301000-00007
21. Sadeghi M, Emadi Andani M, Bahrami F, Parnianpour M. Trajectory of human movement during sit to stand: a new modeling approach based on movement decomposition and multi-phase cost function. *Exp Brain Res* (2013) 229(2):221–34. doi:10.1007/s00221-013-3606-1
22. Park ES, Park CI, Lee HJ, Kim DY, Lee DS, Cho SR. The characteristics of sit-to-stand transfer in young children with spastic cerebral palsy based on kinematic and kinetic data. *Gait Posture* (2003) 17(1):43–9. doi:10.1016/S0966-6362(02)00055-3
23. Jeng SF, Schenkman M, Riley PO, Lin SJ. Reliability of a clinical kinematic assessment of the sit-to-stand movement. *Phys Ther* (1990) 70(8):511–20. doi:10.1093/ptj/70.8.511
24. Galli M, Cimolin V, Crivellini M, Campanini I. Quantitative analysis of sit to stand movement: experimental set-up definition and application to healthy and hemiplegic adults. *Gait Posture* (2008) 28(1):80–5. doi:10.1016/j.gaitpost.2007.10.003
25. Wade DT, Wood VA, Heller A, Maggs J, Langton Hewer R. Walking after stroke. Measurement and recovery over the first 3 months. *Scand J Rehabil Med* (1987) 19(1):25–30.

26. Yoshida K, Iwakura H, Inoue F. Motion analysis in the movements of standing up from and sitting down on a chair. A comparison of normal and hemiparetic subjects and the differences of sex and age among the normals. *Scand J Rehabil Med* (1983) 15(3):133–40.
27. Butler PB, Nene AV, Major RE. Biomechanics of transfer from sitting to the standing position in some neuromuscular diseases. *Physiotherapy* (1991) 77(8):521–5. doi:10.1016/S0031-9406(10)61866-4
28. Alqhtani RS, Jones MD, Theobald PS, Williams JM. Correlation of lumbar-hip kinematics between trunk flexion and other functional tasks. *J Manipulative Physiol Ther* (2015) 38(6):442–7. doi:10.1016/j.jmpt.2015.05.001
29. Delahunt E, Monaghan K, Caulfield B. Altered neuromuscular control and ankle joint kinematics during walking in subjects with functional instability of the ankle joint. *Am J Sports Med* (2006) 34(12):1970–6. doi:10.1177/0363546506290989
30. Roy G, Nadeau S, Gravel D, Piotte F, Malouin F, McFadyen BJ. Side difference in the hip and knee joint moments during sit-to-stand and stand-to-sit tasks in individuals with hemiparesis. *Clin Biomech (Bristol, Avon)* (2007) 22(7):795–804. doi:10.1016/j.clinbiomech.2007.03.007
31. Lomaglio MJ, Eng JJ. Muscle strength and weight-bearing symmetry relate to sit-to-stand performance in individuals with stroke. *Gait Posture* (2005) 22(2):126–31. doi:10.1016/j.gaitpost.2004.08.002
32. Malouin F, Richards CL, Doyon J, Desrosiers J, Belleville S. Training mobility tasks after stroke with combined mental and physical practice: a feasibility study. *Neurorehabil Neural Repair* (2004) 18(2):66–75. doi:10.1177/0888439004266304
33. Brunt D, Greenberg B, Wankadia S, Trimble MA, Shechtman O. The effect of foot placement on sit to stand in healthy young subjects and patients with hemiplegia. *Arch Phys Med Rehabil* (2002) 83(7):924–9. doi:10.1053/apmr.2002.3324
34. Engardt M, Olsson E. Body weight-bearing while rising and sitting down in patients with stroke. *Scand J Rehabil Med* (1992) 24(2):67–74.

Conflict of Interest Statement: The authors declare that the research was conducted in the absence of any commercial or financial relationships that could be construed as a potential conflict of interest.

frontiers in Neurology

ORIGINAL RESEARCH
published: 05 October 2018
doi: 10.3389/fneur.2018.00822

Combining Movement-Related Cortical Potentials and Event-Related Desynchronization to Study Movement Preparation and Execution

Hai Li[1†], Gan Huang[2†], Qiang Lin[1,3], Jiang-Li Zhao[1], Wai-Leung Ambrose Lo[1], Yu-Rong Mao[1], Ling Chen[1], Zhi-Guo Zhang[2], Dong-Feng Huang[1] and Le Li[1*]*

[1] Department of Rehabilitation Medicine, Guangdong Engineering Technology Research Center for Rehabilitation Medicine and Clinical Translation, The First Affiliated Hospital, Sun Yat-sen University, Guangzhou, China, [2] Guangdong Provincial Key Laboratory of Biomedical Measurements and Ultrasound Imaging, School of Biomedical Engineering, Health Science Center, Shenzhen University, Shenzhen, China, [3] Department of Rehabilitation Medicine, The Fifth Affiliated Hospital of Guangzhou Medical University, Guangzhou, China

OPEN ACCESS

Edited by:
Guanglin Li,
Shenzhen Institutes of Advanced Technology (CAS), China

Reviewed by:
Bernhard Sehm,
Max-Planck-Institut für Kognitions- und Neurowissenschaften, Germany
Naifu Jiang,
Shenzhen Institutes of Advanced Technology (CAS), China

***Correspondence:**
Dong-Feng Huang
huangdf@mail.sysu.edu.cn
Le Li
lile5@mail.sysu.edu.cn

[†]These authors have contributed equally to this work

Specialty section:
This article was submitted to Stroke, a section of the journal Frontiers in Neurology

Received: 13 February 2018
Accepted: 11 September 2018
Published: 05 October 2018

Citation:
Li H, Huang G, Lin Q, Zhao J-L, Lo W-LA, Mao Y-R, Chen L, Zhang Z-G, Huang D-F and Li L (2018) Combining Movement-Related Cortical Potentials and Event-Related Desynchronization to Study Movement Preparation and Execution. Front. Neurol. 9:822. doi: 10.3389/fneur.2018.00822

This study applied a comprehensive electroencephalography (EEG) analysis for movement-related cortical potentials (MRCPs) and event-related desynchronization (ERD) in order to understand movement-related brain activity changes during movement preparation and execution stage of unilateral wrist extension. Thirty-four healthy subjects completed two event-related potential tests in the same sequence. Unilateral wrist extension was involved in both tests as the movement task. Instruction Response Movement (IRM) was a brisk movement response task with visual "go" signal, while Cued Instruction Response Movement (CIRM) added a visual cue contenting the direction information to create a prolonged motor preparation stage. Recorded EEG data were segmented and averaged to show time domain changes and then transformed into time-frequency mapping to show the time-frequency changes. All components were calculated and compared among C3, Cz, and C4 locations. The motor potential appeared bilaterally in both tests' movement execution stages, and Cz had the largest peak value among the investigated locations ($p < 0.01$). In CIRM, a contingent negative variation (CNV) component presented bilaterally during the movement preparation stage with the largest amplitude at Cz. ERD of the mu rhythm (mu ERD) presented bilateral sensorimotor cortices during movement execution stages in both tests and was the smallest at Cz among the investigated locations. In the movement preparation stage of CIRM, mu ERD presented mainly in the contralateral sensory motor cortex area (C3 and C4 for right and left wrist movements, respectively) and showed significant differences between different locations. EEG changes in the time and time-frequency domains showed different topographical features. Movement execution was controlled bilaterally, while movement preparation was controlled mainly by contralateral sensorimotor cortices. Mu ERD was found to have stronger contra-lateralization features in the movement preparation stage and might be a better indicator for detecting

movement intentions. This information could be helpful and might provide comprehensive information for studying movement disorders (such as those in post-stroke hemiplegic patients) or for facilitating the development of neuro-rehabilitation engineering technology such as brain computer interface.

Keywords: electroencephalography analysis, movement-related cortical potential, event-related desynchronization, contingent negative variation, movement preparation, movement execution

INTRODUCTION

Stroke is one of the most important diseases that threatens human lives and commonly leads to motor impairments in stroke survivors (1). It is essential to understand movement-related brain activity patterns of both healthy people and stroke patients prior to investigating neural recovery mechanisms during stroke rehabilitation processes. Electroencephalograph (EEG)-based electrophysiological technology has been applied in the stroke research area (2–7) in addition to the rehabilitative treatment areas such as motor imagery (MI) and brain computer interface (BCI) (8–13). The aim of this preliminary study was to investigate the different features of movement-related brain activity changes during both motor intentions and motor execution in healthy people, hence facilitating the EEG-based investigational tool in future stroke rehabilitative studies.

Movement-related cortical potentials (MRCPs) and event-related desynchronization/synchronization (ERD/ERS) represent brain activity changes related to movement in the time and time-frequency domains, respectively. Bereitschaftspotential (BP) (14) is the early subcomponent of MRCPs and is believed to be generated by the supplementary motor area (SMA) (15), motor cortex, and cingulate gyrus (14, 16) and represents the motor preparation stage of movement. In addition to BP, a contingent negative variation (CNV) was reported to present in movement preparation stage (17, 18) and reflects motor expectancy and preparation. The late subcomponent, the motor potential (MP), has been proposed to be generated from the underlying motor cortex and partly due to afferents excited by the movement (14). The amplitude of the negativity of MRCPs may relate to the amount of energy required for the movement, while the MRCPs' onset time is interpreted as the length of time taken to plan and prepare the movement (19). Researchers using MRCPs to study motor skill learning found that expert performers showed smaller MRCPs' amplitude and later onset time for the grasped motor skill than beginning learners (19), which indicated that mastery of movement led to reduced energy demand. On the contrary, in cases in which patients with post-stroke hemiparesis performed movements with the paretic limbs, larger MP peak amplitudes were observed, indicating an enhanced energy demand for the lesioned hemisphere (2, 3). ERD refers to the phenomenon of oscillatory components' amplitude decrease resulting from sensory processing or motor behavior (20). Mu ERD is generally regarded as a reliable correlate of increasing cellular excitability in thalamocortical systems during cortical information processing (21) and is observed in motor observation, imagery, preparation, and execution stages. Delayed onset of mu ERD to movement preparation was observed consistently in patients with Parkinson's disease, and patients with somatosensory deficits after stroke showed reduced mu ERD during both movement preparation and actual performance (4, 5). These EEG-based results enhanced the understanding of the mechanisms underlying human movement disorders (14). Since MRCPs and ERD might have different topographical patterns and time course evolution over the movement stages (22), combining these EEG measurements might provide more comprehensive features for understanding movement-related brain functions and detecting movement intentions. Only a few studies have been conducted using the comprehensive EEG analysis method to investigate stroke rehabilitation mechanisms and suggested impairment-specific changes (4). Due to different protocol designs of each study and the small sample size of these studies, more studies combining temporary and oscillatory EEG data to analyze movement-related brain activity changes are necessary for understanding the whole picture of brain motor function.

Motor imagery is a dynamic state of mental rehearsal of movements accompanied by suppression of actual movement (23–25) and might be an alternative treatment for patients with stroke (26). Neuroimaging studies have demonstrated that motor imagery tasks activate brain regions that overlap with brain regions for movement execution (13, 27, 28),and primary motor cortex causes more exchange of causal information among motor areas during a motor execution task than during a motor-imagery task (29). Factors of MI design might affect study outcome, and the first-person perspective kinesthetic-dominant imagery might work better in reorganizing motor-somatosensory networks than other modalities (13). In this study, the ERP protocol created a first-person perspective motor intentions status with inhibition of actual movement, which might help further understanding of MI brain activity changes in electrophysiological aspect.

BCI appears to be a promising technology for helping patients with motor disabilities regain motor control (30, 31). A number of studies have demonstrated the feasibility and possible effects of BCI applied in post-stroke rehabilitation (10, 31–34). However, the technology for detecting motor intention still needs to be refined in order to enhance the accuracy. MRCPs or ERD are indicators commonly chosen to detect the motor intention and results at different accuracy levels (11, 12, 35). Brain activity frequency features seem to yield better accuracy than temporal features in terms of detecting motor intention (35). A study combining MRCPs and ERD/ERS signals for detecting the actual or imagined wrist movement of subjects in different directions reported an average accuracy of 81.5% on the test dataset for two

different directions (36). Because of different protocol designs and small samples size of these studies, a better understanding of the movement-related brain activity in time and frequency domains in motor intention stages might add more evidence for optimizing the BCI indicator solution.

In this study, we investigated brain activity changes in both motor intention and motor execution stages in both time and time-frequency domains. Unilateral wrist movements of both arms were involved in this study to investigate the lateralization phenomenon. Several hypotheses were formed: (1) MRCPs and mu ERD would show different stage-specific topographical patterns; (2) brain activities under both movement intention and execution status would show different features in time and time-frequency domains; and (3) MRCPs and mu ERD would distinctly reflect motor intentions and hence, provide precise information for detecting motor intention.

METHODS

Participants

Thirty-three healthy volunteers (11 males and 23 females) with a mean age of 33.8 (±15.7 SD) years participated in the present study. The subjects were university undergraduate students, postgraduate students, or staff members. The study protocol was approved by the ethics committee of the First Affiliated Hospital of Sun Yat-sen University ([2013]C-068). The inclusion criteria consisted of several parameters: (1) healthy male or female adults; (2) aged 18 years or older; (3) right-handed; (4) interested in this study; and (5) willing to participate in the study as a volunteer, sign the study consent form, and comply with the study protocol. The exclusion criteria consisted of several parameters: (1) individuals with known diseases or conditions that could influence their ability to understand and perform the study tasks. These diseases or conditions included cognitive dysfunction that could affect accurate understanding of study tasks; (2) neural impairments or musculoskeletal disorders affecting upper limb motor function; and (3) other physiological and psychological conditions affecting the ability of accurate understanding and performing the study tasks. All participants were informed of the study protocol, and all questions were explained in detail. Signed informed consent forms were obtained before the study participation. All subjects were self-recognized as right-handed and confirmed by the Edinburgh Handedness Inventory (37) and were ERP study naive.

Experimental Settings and Data Acquisition

All experiments in the present study were conducted at the Laboratory of Brain Functional Informatics of Rehabilitation Medicine Department of the First Affiliated Hospital of Sun Yat-sen University in a shielded room, which provided insulation from electromagnetic signals and background noise distractions. Subjects were sitting in front of a table with both forearms resting on the table. A screen was put on the table to present the ERP paradigms at a 75 cm distance from the subjects on the eye level. A BrainAmp 32-channel amplifier from Brain Products (Munich, Germany) was used to record EEG data. Before the experiment, a 32-channel actiCap (Herrsching, Germany) was mounted onto the subject's head, and the Ag/AgCl electrodes were placed according to the extended international 10–20 system, referenced to the FCz and grounded to AFz (**Figure 1A**). The EEG electrode impedance was kept under 5 kOhm to ensure the quality of EEG recording data, and the sampling rate was 1,000 Hz. Electrooculogram (EOG) was measured by two electrodes, one above the middle point of the right brow to record the EOG vertically and another 2 cm placed aside the outer corner of the right eye in order to record the EOG horizontally.

To measure the movement of wrist extension, EMG electrodes were put on the extensor carpi radialis (ECR) muscles on each side respectively. Before placement of the electrode, the skin was prepared by rubbing slightly with a skin prep gel and cleansing with an alcohol pad in order to reduce the impedance between the electrodes and skin. Bipolar Ag/AgCl round electrodes with a diameter of 2 mm were then put at the middle of proximal half of each forearm, 2 cm apart (**Figure 1B**). The electrodes were connected to the BrainAmp amplifier in order to synchronize EMG data with EEG data. The EMG electrode impedance was kept under 5 kOhm, and the sampling rate was 1,000 Hz.The single amplifier had an input impedance of 10 MOhm, common mode rejection ratio (CMRR) $\geq$90 dB, signal-to-noise ratio $<$ 1 μVpp, and actual gain range of ±16.384 mV. The raw EMG was filtered by a Butterworth filter with low and high pass cut-offs of 1,000 and 0.016 Hz, respectively. The raw EMG was stored in the computer for digital processing offline (38). The EMG add-on component of the Brain Vision Analyzer software was used to analyze EMG data offline.

Software E-prime (Psychology Software Tools, Inc, USA) was used to present the visual directions or cues in the study. Subjects were instructed of ERP experiment tasks orally before the tests and in written words on the screen at the beginning of each test. The paradigm of IRM was to present a solid arrow picture pointing either to the left or the right (regarded as "go" signals in this study), and the subjects were requested to perform left or right wrist extension according to the arrow direction. The paradigm started with a white cross in the middle of a black screen as an attention point, which lasted for 800 ms to 1,000 ms randomly. The visual "go" signal pointing to the left or the right was then presented on the screen for a duration of 3,000 ms. The direction was randomly chosen by E-prime, and the arrow picture was followed by a black screen lasting for 2,000 ms. There were 40 trials for each side movement (8). The movement was performed once for each trial, and the subjects rested the arms on the table after the movement until the next required movement in the next trial.

In CIRM, a visual cue (a hollow arrow) containing the forthcoming "go" direction information was added 1 sec before the "go" signal in each trial. The CIRM paradigm began with a white cross in the middle of a black screen and lasted for 800 to 1,000 ms chosen randomly. A visual cue pointing to the forthcoming "go" direction was presented on the screen and lasted for 1,000 ms. After the cue, the visual "go" signal was presented and lasted for 2,000 ms followed by a black screen lasting for 2,000 ms. There were 40 trials for each direction and a total of 80 trials for CIRM. The subject was required to

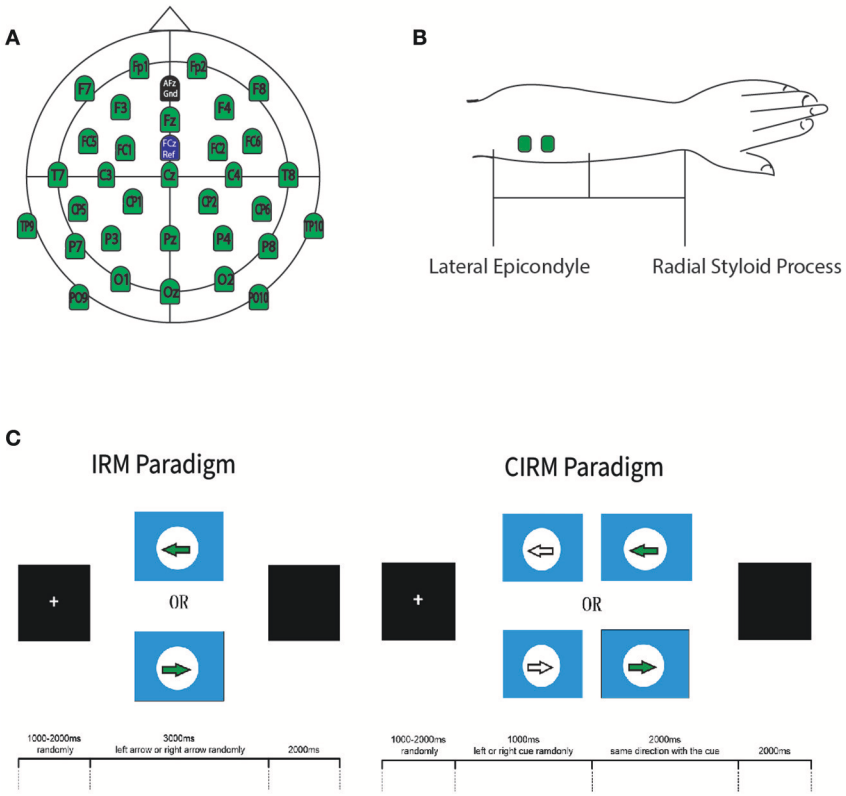

FIGURE 1 | Experimental protocol. **(A)** EEG 32-channel cap used for the recordings. **(B)**. Electrodes location on ECR. **(C)**. E-Prime ERP experiment paradigms.

prepare for the movement when seeing the cue and perform the movement upon the presentation of the "go" signal. The movement was performed once for each trial, and the subjects rested their arms on the table after the movement until the next required movement in the next trial (**Figure 1C**).

Subjects practiced the required movement for 1 to 2 min for each test before the researcher started to record the EEG data. Between the two tests, subjects could take a short break if necessary.

All subjects completed the two tests in the same sequence. EEG, EOG, and EMG data were recorded synchronously by a PC system and analyzed offline later.

Data Processing

All data were analyzed offline using Brain Vision Analyzer 2.1 (Brainproducts, Germany) and Matlab 2014a (The MathWorks Inc., USA). EEG data were re-referenced by the common average of all channels and applied to all channels. Then ICA based Ocular correction was conducted semi-automatically. The Ocular components were classified by the Analyzer and confirmed by the researchers, then removed from the EEG data. A band-filter was applied with a low cutoff at 0.01 Hz (12 decimal/octave), and high cutoff at 50 Hz (12 decimal/octave). Laplacian method was used to remove volume conduction effects which lead to low spatial resolution (39). It has been proved that the Laplacian method, compared with other fixed spatial filter, such as bipolar and common average reference, can effectively improve the Signal-Noise-Ratio of the EEG signal for the ERD/ERS analysis (40). By subtracting the mean activity at surrounding electrodes from the channel of interest, a finite difference method is used to calculate the Laplacian derivations. EEG data were segmented from −1.2 to 3.0 s relative to the GO signal for both test. IRM EEG data were baseline corrected using −1.2 to 0 s as the baseline. While CIRM EEG data were using −1.2 to −1.0 s as the baseline since the visual cue was presented at the time of −1.0 s. Trials of movement sessions of each side were averaged within-subjects, and grand averaged among all subjects later. The peak information of MP and CNV was detected by BrainVision Analyzer and exported

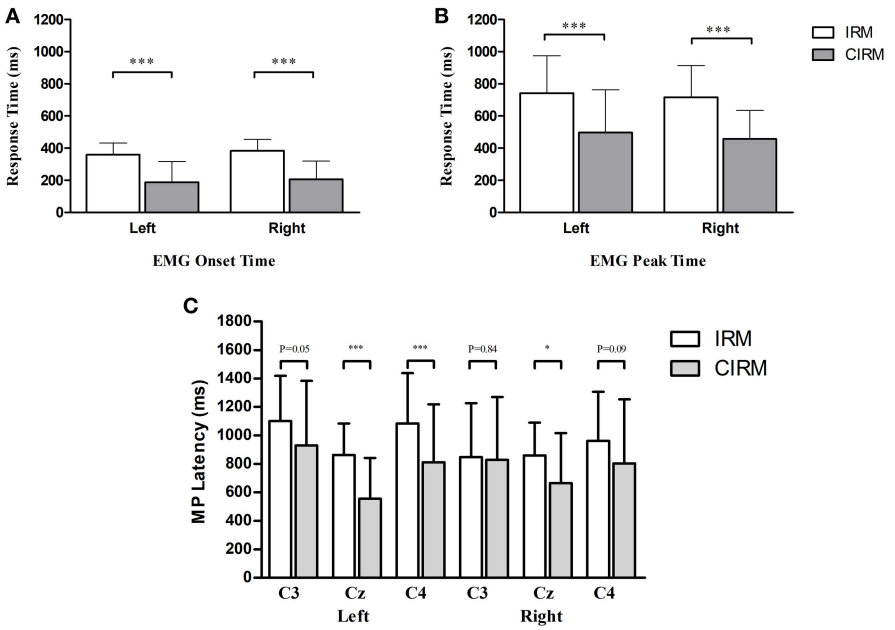

FIGURE 2 | Bar graphs showing averaged EMG onset time **(A)**, EMG peak time **(B)**, and MP latency **(C)** in IRM and CIRM. Error bars represent the SD. Significant differences are indicated by asterisks. **(A)** The average EMG onset time is shorter in CIRM than in IRM. **(B)** The average EMG peak time is shorter in CIRM than in IRM. **(C)** The MP latency was shorter in CIRM than in IRM at Cz during both side movements and at C4 during left wrist movement. $*p < 0.05$, $***p < 0.001$.

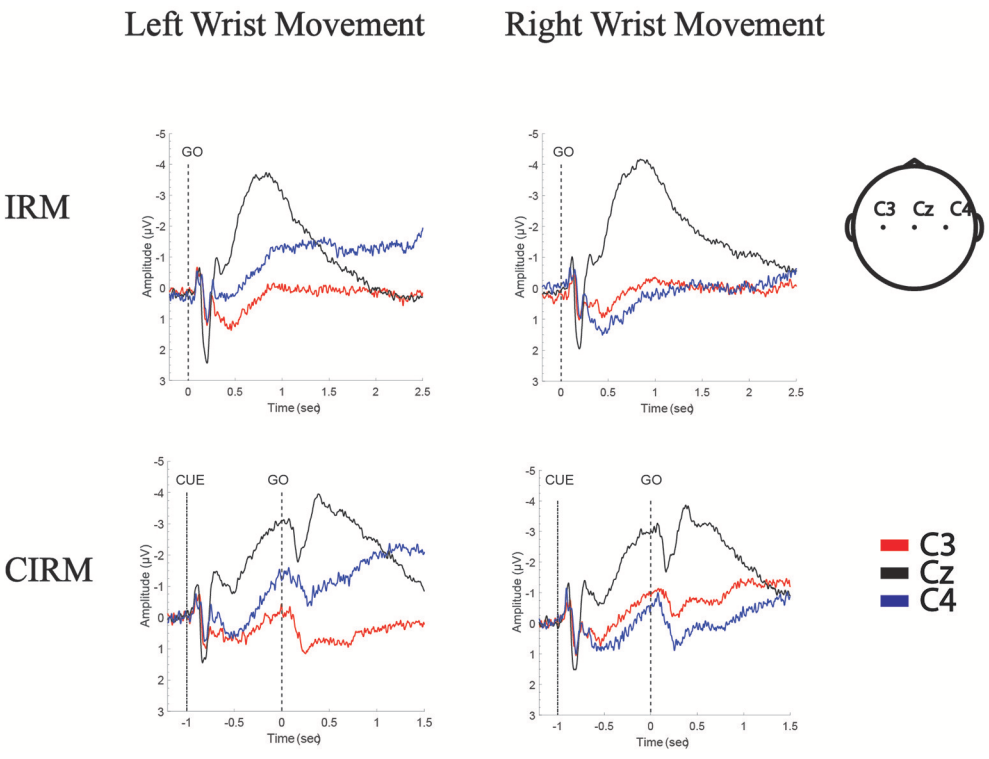

FIGURE 3 | Grand Average of MRCPs of all subjects in IRM and CIRM. MP is presented in movement execution stage of both tests, and CNV is presented in movement preparation stage of CIRM. Negative Upwards.

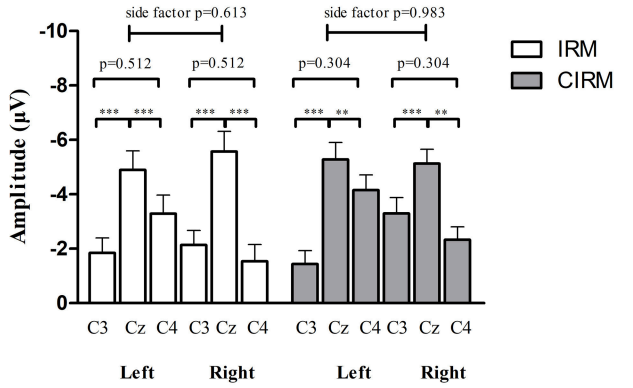

FIGURE 4 | MP amplitude at C3, Cz, and C4 location in IRM and CIRM. There were significant differences between Cz and C3 and between Cz and C4 ($p < 0.01$), but not between C3 and C4 in both tests. Negative upwards. $^{**}p < 0.01$, $^{***}p < 0.001$.

for statistics analysis. Matlab 2014a was used to calculate the time-frequency mapping and mu ERD. The segmented EEG data were transformed with an averaged Continuous Wavelet Transformation (CWT). The 8–12 Hz frequency band data were abstracted from the time-frequency mapping and transformed into mu ERD graph. The EMG activity onset for each trial was determined by crossing the threshold at 4 SD from baseline mean (3) in either direction. EMG peaks were detected by the Brain Vision Analyzer and exported with time and amplitude information.

Statistical Analysis

EMG onset and peak times and EMG peak value were compared between sides by *t*-test and compared between IRM and CIRM by paired sample *t*-test. The MP component in both tests and the CNV component in CIRM were calculated at C3, Cz, and C4 locations. All component information, including latency and each wave's amplitude, were compared among locations and sides by the one-way multivariate analysis of variance (one-way MANOVA). The MP latencies of IRM and CIRM were compared by paired sample *t*-test. The mean values of the time-frequency response were compared among C3, Cz, and C4 locations and among sides and movement stages by one-way MANOVA. To test the contra-lateralization feature of mu ERD and MRCP in motor intention/preparation stage, paired-sample *t*-tests of mu ERD mean values and CNV amplitudes among C3, Cz, and C4 location during unilateral movement preparation stage were performed. All statistical analyses was conducted with software IBM SPSS statistics 21. Statistical significance was set at 0.05 for all tests.

RESULTS

EMG

There were no significant differences found between right and left wrist movements with respect to average EMG onset and peak times and EMG peak value in both tests. There were significant differences of the EMG onset and peak times between IRM and CIRM with both left and right wrist movements ($P < 0.01$). The EMG onset and peak times were shorter in CIRM than in IRM for both right and left wrist movements ($P < 0.01$) (**Figure 2**). There was no significant difference in the EMG peak value between IRM and CIRM.

MRCP and CNV

In the movement execution stage of both tests, the MP appeared bilaterally, with the largest peak at Cz (**Figure 3**). A One-way MANOVA was conducted to assess the differences in MP amplitude among different locations and on arm side movements. The multivariate effect was significant by locations in IRM and CIRM ($F = 15.069$, $p < 0.01$ and $F = 14.248$, $p < 0.01$, respectively). The *post-hoc* tests showed significant differences between Cz and C3 or Cz and C4 ($p < 0.01$) but not between C3 and C4 in both tests (**Figure 4**). The paired-sample *t*-test showed that there were significant differences in MP latencies between IRM and CIRM at Cz during both side movements and at C4 during left wrist movement ($p < 0.01$) (**Figure 2**). However, no significant differences were found in MP amplitude between IRM and CIRM tasks in all three locations.

In CIRM, the visual cue divided the task into prolonged movement preparation and movement execution stages. A CNV wave presented during the movement preparation stage, peaking shortly after the "go" signal followed by the MP (**Figure 3**). One-way MANOVA analysis showed no significant multivariate effects on locations or sides. To test the contra-lateralization feature of CNV, a paired-sample *t*-test of CNV amplitudes between C3 and C4 locations was performed and showed no significant differences.

Time-Frequency Mapping and Mu ERD

The time-frequency mapping and mu ERD calculated from the total average EEG data from all subjects are illustrated in **Figure 5**. The mean values of the time-frequency response in the 8–12 Hz mu rhythm band were compared among by one-way MANOVA. In IRM, there were two factors: (1) locations (C3, Cz, and C4) and (2) movement sides. No significant multivariate effects were found on locations or sides ($F = 1.541$, $p = 0.217$ and $F = 0.116$, $p = 0.864$, respectively). In CIRM, there were three factors: (1) locations; (2) sides; and (3) movement stages (movement preparation and execution). Significant multivariate effects were found with respect to stages ($F = 5.920$, $p = 0.015$) but not for locations ($F = 2.642$, $p = 0.072$) or sides ($F = 0.226$, $p = 0.635$).

To test the contra-lateralization feature of mu ERD, the mean values of the time-frequency response in the 8–12 Hz mu rhythm band were compared among different locations by paired-sample *t*-test. During movement execution stage of both tests, there were no significant differences found between C3 and C4. During the movement execution stage of right wrist extension, there were significant differences found between C3 and Cz or C4 and Cz ($P < 0.05$). During the movement execution stage of left wrist extension, there were significant differences found between C4 and Cz ($P < 0.05$).

In the preparation stage of CIRM, mu ERD showed significant differences between C3 and C4 during both left and right wrist movements ($p = 0.001$ and $p = 0.005$, respectively). There were

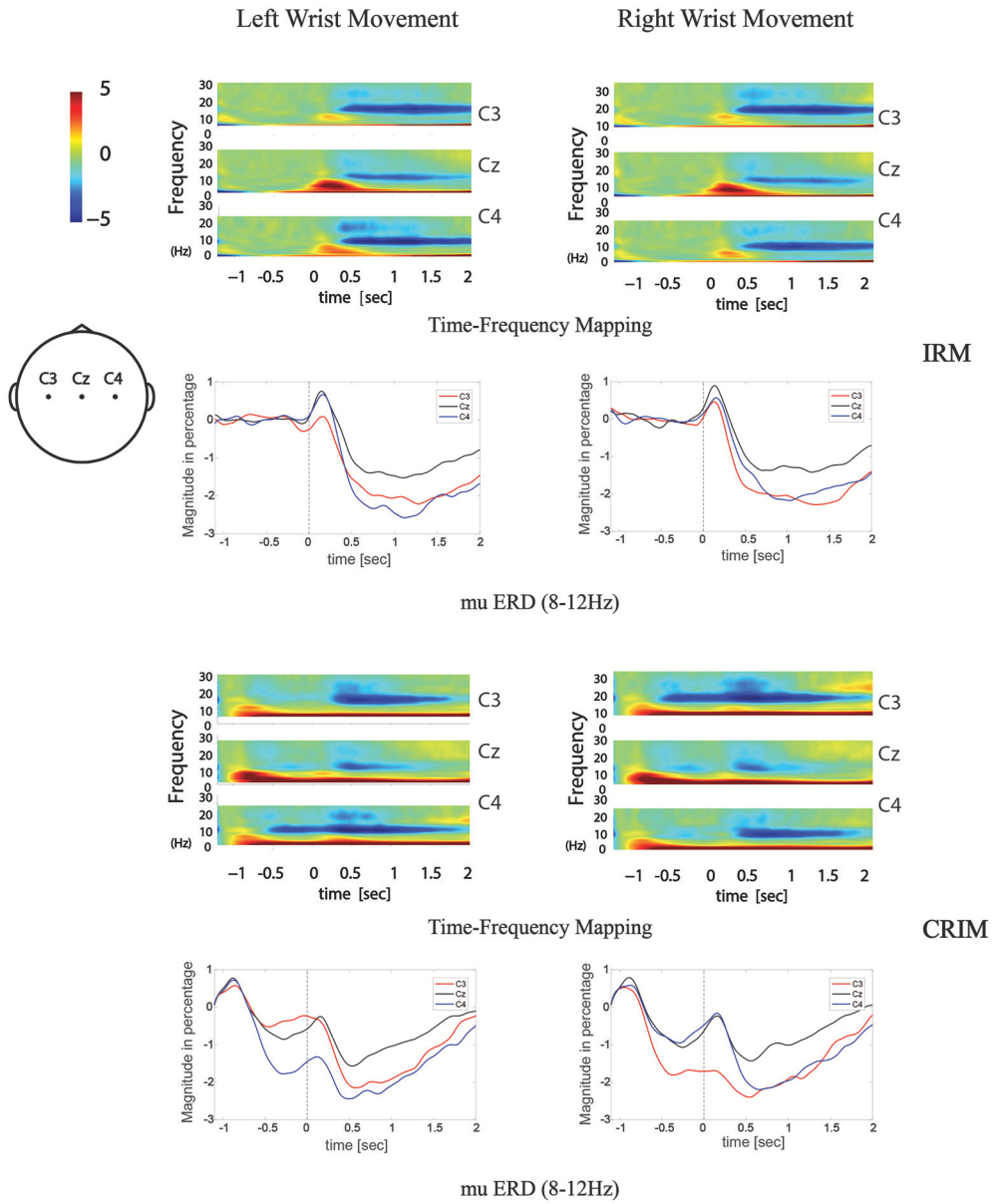

FIGURE 5 | Time-frequency mapping and mu ERD during movement tasks in both tests. Frequency data was transformed from grand average EEG data of all subjects. 8–12 Hz frequency band data was abstracted from the time-frequency mapping and transformed into the mu ERD line graphs.

significant differences found between Cz and the contralateral sensory motor cortex area (C3 for right wrist movement, $p = 0.006$, C4 for left wrist movement, $p = 0.001$). Different from the phenomenon of Cz that showed the largest amplitude of MP and CNV, the mu ERD showed the least amplitude in Cz among the three locations (**Figure 6**).

DISCUSSION

In the present study, we recorded and analyzed brain activity changes in the time and frequency domains during both motor preparation and execution stages. IRM used a motor response paradigm with visual picture instructions, which made a subject perform the required movements in a more impulsive manner compared to self-initiated movements (41). CIRM used a visual cue contenting the forthcoming movement information 1 sec before the "go" signals, which divided the motor task into two clearly separated periods (42). During the 1 sec from the cue to the "go" signal, the brain activity was under a state of motor intention, expectation, and preparation condition.

The EMG onset and peak times were shorter in CIRM rather than in IRM for both side movements, and the MP latency in CIRM was shorter than in IRM. This result confirmed the commonly observed phenomenon that given a cue and extra preparation stage, people respond to the "go" signal faster

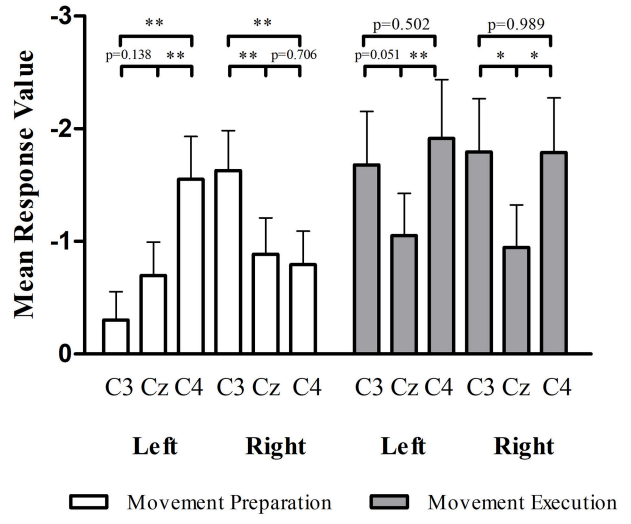

FIGURE 6 | mu ERD at C3, Cz, and C4 in movement preparation and movement execution stage of CIRM. In the movement preparation stage, the contralateral sensory motor cortex (C4 for left wrist movement, C3 for right wrist movement) showed larger mu ERD than other locations ($p < 0.05$). In the movement execution stage, Cz showed the lowest amplitude of mu ERD and no significant differences found between C3 and C4. $^{*}p < 0.05$, $^{**}p < 0.01$

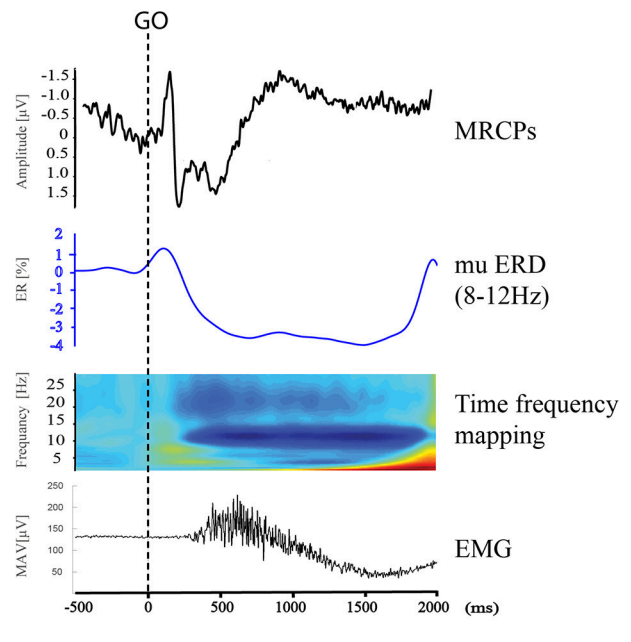

FIGURE 7 | MRCPs, mu ERD, time frequency mapping at C3, and right upper limb EMG during Right Wrist Extension in IRM.

(**Figure 2**). The visual cue containing information relevant to the movement might combine the sensory stimuli responses with sensorimotor area and facilitate movement initiation. The effects of external cues were observed in previous studies and proved to be beneficial for speeding movement of patient with motor deficits (43, 44).

Generally speaking, in the time-voltage change domain, MP reflected the brain activity changes during the movement execution stage (45) while the CNV represented movement intention, expectancy, and preparation in the pre-movement stage (42, 46). In the movement execution stage of both tests in current study, MP amplitude showed no significant differences between C3 and C4, indicating that the movement execution involved the sensorimotor cortex bilaterally. Components of MRCP were proposed to be generated by summed excitatory postsynaptic potentials in apical cortical dendrites (47), which might be an explanation for the largest MP amplitude recorded at Cz. Bilateral excitatory postsynaptic potentials were transferable, and the central area (Cz) gathered the highest sum of potentials. CNV is a complex ERP component related to the cognitive process of stimulus anticipation. Although it was usually investigated with paradigms with cues contenting information differentiate from the "go" signal in previous studies, CNV was observed to be evoked with cues containing similar information to the "go" signal in this study and may mainly contribute to the movement expectancy and motor preparation to the forthcoming movement (42). In the movement preparation stage, CNV also showed a bilateral control phenomenon and the highest peak at Cz.

From the time-frequency mapping and mu ERD data results, we could observe bilateral control phenomenon in the movement execution stage of both tests. However, different from the MRCP findings, the amplitude of frequency changes was lowest at Cz (**Figure 5**). Since mu ERD was regarded as a reflection of brain activation (48) and has a maximum correlation with sensorimotor cortex area (49), we could assume that it has less transferable features than the cortex potentials, hence, it represents brain activity changes more precisely in the topographical view. In the movement intention/preparation stage, the mu ERD appeared mainly contralaterally, indicating that the brain excitability has a contralateral feature in the pre-movement period. Starting from the contralateral Rolandic region and becoming bilaterally symmetrical with the execution of movement, the mu ERD feature presented in this study was consistent with those from previous studies (50).

Combining EEG changes in the time and time-frequency domains during pre- and movement execution stages, we could see that the time courses of MRCP and mu ERD were aligned (**Figure 7**) and consistent with previous studies regarding movement-related brain activity changes (51), while each indicator showed different topographical features. This might suggest different neuronal mechanisms between the generation of the two phenomena (22). MRCPs mainly represent an increase in task-specific responses of the SMA and contralateral M1-S1 and partly reflect the afferents' excitation caused by the movement, while mu ERD reflects changes in the brain activation level such as cortical sensorimotor area involved in movement intention, expectancy, preparation, and execution periods. Taken together, the MRCPs and mu ERD structured a dynamic involvement of human primary, supplementary motor, and sensorimotor cortices for movement planning and

execution (51). The combined EEG analysis method could provide more comprehensive information for the investigation of movement disorders such as the energy demanding and consuming information from MRCPs (52) and the brain activation information from mu ERD (48, 53, 54).

Although the lateralization phenomena differed in MRCP and mu ERD features, it was clear that both contralateral and ipsilateral motor cortices were involved in motor tasks. Neural networks within and between hemispheres are necessary to coordinate motor functions not only for bilateral but also for unilateral movements. The neural network generating the coordination function between hemispheres was proposed to be the cingulate motor area and the cerebellum (55). The ipsilateral hemisphere involved in a motor task might contribute to the modulation, balance, or prohibition of the motor tasks. The present ERD results suggested that this bilateral movement coordination was mostly involved in the motor execution stage (**Figure 5**). The ipsilateral sensorimotor cortex might be an integral part of motor regulation (56). In the movement intention and preparation conditions, the oscillatory brain components showed stronger contralateral dominancy. This feature might have special value in investigational and clinical applications. Specifically, mu ERD could be a more sensitive indicator than MRCPs for BCI technology in order to detect movement intentions (8, 10, 49), especially if the direction information of movements are among study interests (36).

There were some limitations to the present study. The first one was that the initial part of MRCPs was mixed with a Visual Evoked Potential after visual stimuli in both paradigms, and it could not be precisely used to identify the onset of the BP component of the MRCPs. Hence only MP peak information was calculated and analyzed in this study. Another limitation of the study was that only right-handed subjects were recruited in this study. In the previous study, the contralateral preponderance of mu ERD was studied and showed a difference between right-handed and left-handed subjects (50). However, this phenomenon was not studied in this program with only right-handed subjects.

CONCLUSION

This study investigated brain activity changes during movement intention, preparation, and execution stages of wrist extension using the comprehensive EEG analysis method, which combined indicators such as MRCPs, CNV, time-frequency mapping, and mu ERD. EEG changes in the time and time-frequency domains showed different topographical features and might provide comprehensive information for studying movement disorders such as those in post-stroke hemiplegic patients. Additionally, movement execution was controlled bilaterally, while the movement intention was controlled mainly contralaterally by sensorimotor cortices. Mu ERD was found to have stronger contra-lateralization features in the movement intention stage and might be a better indicator for detecting movement intentions in neuro-rehabilitation engineering technology such as BCI.

ETHICS STATEMENT

The study was approved by the Human Subjects Ethics Subcommittee of the First Affiliated Hospital, Sun Yat-sen University, China (ethic number [2013]C-068).

AUTHOR CONTRIBUTIONS

HL and GH analyzed the data and interpreted the results. HL drafted the manuscript. HL, QL, J-LZ, W-LL, Y-RM, and LC conducted the experiment and collected the data, Z-GZ conducted part of the data analysis and interpreted the results. HL and GH contributed to the revision of the Manuscript and the answers to the comments from the reviewers and editor. D-FH and LL designed the study and supervised all stages of the study including data collection, analysis, interpretation, and substantial revision of the manuscript. All the authors approved the final version of the manuscript.

FUNDING

This work was funded by National Natural Science Foundation of China (No. 30973165, 81372108, 61701316) and in part by 5010 Planning Project of Sun Yat-sen University of China (No. 2014001) and Science and Technology Planning Project of Guangdong Province, China (No. 2017B020210011, 2016A020220009, 2015B020233006, 2015B020214003, 2014B090901056), Shenzhen Peacock Plan (NO. KQTD2016053112051497), and Guangzhou Research Collaborative Innovation Projects (No. 201604020108).

ACKNOWLEDGMENTS

The authors would like to thank all the participants for their time and energy dedicated to this study.

REFERENCES

1. Winstein CJ, Stein J, Arena R, Bates B, Cherney LR, Cramer SC, et al. Guidelines for adult stroke rehabilitation and recovery: a guideline for healthcare professionals from the American Heart Association/American Stroke Association. *Stroke* (2016) 47:e98–169. doi: 10.1161/str.0000000000000098
2. Wiese H, Stude P, Sarge R, Nebel K, Diener HC, Keidel M. Reorganization of motor execution rather than preparation in poststroke hemiparesis. *Stroke* (2005) 36:1474–9. doi: 10.1161/01.STR.0000170639.26891.30
3. Yilmaz O, Cho W, Braun C, Birbaumer N, Ramos-Murguialday A. Movement related cortical potentials in severe chronic stroke. *Conf Proc IEEE Eng Med Biol Soc.* (2013) 2013:2216–9. doi: 10.1109/EMBC.2013.6609976
4. Platz T, Kim IH, Pintschovius H, Winter T, Kieselbach A, Villringer K, et al. Multimodal EEG analysis in man suggests impairment-specific changes in movement-related electric brain activity after stroke. *Brain* (2000) 123(Pt 12):2475–90. doi: 10.1093/brain/123.12.2475
5. Stepien M, Conradi J, Waterstraat G, Hohlefeld FU, Curio G, Nikulin VV. Event-related desynchronization of sensorimotor EEG rhythms in

hemiparetic patients with acute stroke. *Neurosci Lett.* (2011) 488:17–21. doi: 10.1016/j.neulet.2010.10.072
6. Dean PJ, Seiss E, Sterr A. Motor planning in chronic upper-limb hemiparesis: evidence from movement-related potentials. *PLoS ONE* (2012) 7:e44558. doi: 10.1371/journal.pone.0044558
7. Jankelowitz SK, Colebatch JG. Movement related potentials in acutely induced weakness and stroke. *Exp Brain Res.* (2005) 161:104–13. doi: 10.1007/s00221-004-2051-6
8. Jochumsen M, Niazi IK, Taylor D, Farina D, Dremstrup K. Detecting and classifying movement-related cortical potentials associated with hand movements in healthy subjects and stroke patients from single-electrode, single-trial EEG. *J Neural Eng.* (2015) 12:056013. doi: 10.1088/1741-2560/12/5/056013
9. Yuan H, He B. Brain-computer interfaces using sensorimotor rhythms: current state and future perspectives. *IEEE Trans Biomed Eng.* (2014) 61:1425–35. doi: 10.1109/TBME.2014.2312397
10. Grosse-Wentrup M, Mattia D, Oweiss K. Using brain-computer interfaces to induce neural plasticity and restore function. *J Neural Eng.* (2011) 8:025004. doi: 10.1088/1741-2560/8/2/025004
11. Niazi IK, Jiang N, Jochumsen M, Nielsen JF, Dremstrup K, Farina D. Detection of movement-related cortical potentials based on subject-independent training. *Med Biol Eng Comput.* (2013) 51:507–12. doi: 10.1007/s11517-012-1018-1
12. Ono T, Tomita Y, Inose M, Ota T, Kimura A, Liu M, et al. Multimodal sensory feedback associated with motor attempts alters BOLD responses to paralyzed hand movement in chronic stroke patients. *Brain Topogr.* (2015) 28:340–51. doi: 10.1007/s10548-014-0382-6
13. Hanakawa T. Organizing motor imageries. *Neurosci Res.* (2016) 104:56–63. doi: 10.1016/j.neures.2015.11.003
14. Colebatch JG. Bereitschaftspotential and movement-related potentials: origin, significance, and application in disorders of human movement. *Mov Disord.* (2007) 22:601–10. doi: 10.1002/mds.21323
15. Yazawa S, Ikeda A, Kunieda T, Ohara S, Mima T, Nagamine T, et al. Human presupplementary motor area is active before voluntary movement: subdural recording of Bereitschaftspotential from medial frontal cortex. *Exp Brain Res.* (2000) 131:165–77. doi: 10.1007/s00221990031
16. Shakeel A, Navid MS, Anwar MN, Mazhar S, Jochumsen M, Niazi IK. A review of techniques for detection of movement intention using movement-related cortical potentials. *Comput Math Methods Med.* (2015) 2015:346217. doi: 10.1155/2015/346217
17. Fromer R, Sturmer B, Sommer W. (Don't) Mind the effort: effects of contextual interference on ERP indicators of motor preparation. *Psychophysiology* (2016) 53:1577–86. doi: 10.1111/psyp.12703
18. Liebrand M, Pein I, Tzvi E, Kramer UM. Temporal dynamics of proactive and reactive motor inhibition. *Front Human Neurosci.* (2017) 11:204. doi: 10.3389/fnhum.2017.00204
19. Wright DJ, Holmes PS, Smith D. Using the movement-related cortical potential to study motor skill learning. *J Motor Behav.* (2011) 43:193–201. doi: 10.1080/00222895.2011.557751
20. Schomer DL, Lopes da Silva FH. *Niedermeyer's Electroencephalography: Basic Principles, Clinical Applications, and Related Fields*. 6th ed. Philadelphia, PA: Wolters Kluwer Health/Lippincott Williams & Wilkins (2011).
21. Middendorf M, McMillan G, Calhoun G, Jones KS. Brain-computer interfaces based on the steady-state visual-evoked response. *IEEE Trans Rehabil Eng.* (2000) 8:211–4. doi: 10.1109/86.847819
22. Shibasaki H, Hallett M. What is the bereitschaftspotential? *Clin Neurophysiol.* (2006) 117:2341–56. doi: 10.1016/j.clinph.2006.04.025
23. Mulder T. Motor imagery and action observation: cognitive tools for rehabilitation. *J Neural Transm.* (2007) 114:1265–78. doi: 10.1007/s00702-007-0763-z
24. Abbruzzese G, Avanzino L, Marchese R, Pelosin E. Action observation and motor imagery: innovative cognitive tools in the rehabilitation of Parkinson's disease. *Parkinson's Dis.* (2015) 2015:124214. doi: 10.1155/2015/124214
25. Lotze M, Cohen LG. Volition and imagery in neurorehabilitation. *Cogn Behav Neurol.* (2006) 19:135–40. doi: 10.1097/01.wnn.0000209875.56060.06
26. Sharma N, Pomeroy VM, Baron JC. Motor imagery: a backdoor to the motor system after stroke? *Stroke* (2006) 37:1941–52. doi: 10.1161/01.STR.0000226902.43357.fc
27. Ehrsson HH, Geyer S, Naito E. Imagery of voluntary movement of fingers, toes, and tongue activates corresponding body-part-specific motor representations. *J Neurophysiol.* (2003) 90:3304–16. doi: 10.1152/jn.01113.2002
28. Hanakawa T, Dimyan MA, Hallett M. Motor planning, imagery, and execution in the distributed motor network: a time-course study with functional MRI. *Cereb Cortex* (2008) 18:2775–88. doi: 10.1093/cercor/bhn036
29. Bajaj S, Butler AJ, Drake D, Dhamala M. Brain effective connectivity during motor-imagery and execution following stroke and rehabilitation. *Neuroimage Clin.* (2015) 8:572–82. doi: 10.1016/j.nicl.2015.06.006
30. Wolpaw JR. Brain-computer interfaces. *Handbook Clin Neurol.* (2013) 110:67–74. doi: 10.1016/B978-0-444-52901-5.00006-X
31. Lazarou I, Nikolopoulos S, Petrantonakis PC, Kompatsiaris I, Tsolaki M. EEG-based brain-computer interfaces for communication and rehabilitation of people with motor impairment: a novel approach of the 21 (st) century. *Front Human Neurosci.* (2018) 12:14. doi: 10.3389/fnhum.2018.00014
32. Pfurtscheller G, Guger C, Muller G, Krausz G, Neuper C. Brain oscillations control hand orthosis in a tetraplegic. *Neurosci Lett.* (2000) 292:211–4. doi: 10.1016/S0304-3940(00)01471-3
33. Kasashima-Shindo Y, Fujiwara T, Ushiba J, Matsushika Y, Kamatani D, Oto M, et al. Brain-computer interface training combined with transcranial direct current stimulation in patients with chronic severe hemiparesis: proof of concept study. *J Rehabil Med.* (2015) 47:318–24. doi: 10.2340/16501977-1925
34. Arvaneh M, Guan C, Ang KK, Ward TE, Chua KSG, Kuah CWK, et al. Facilitating motor imagery-based brain-computer interface for stroke patients using passive movement. *Neural Comput Appl.* (2017) 28:3259–72. doi: 10.1007/s00521-016-2234-7
35. Kamavuako EN, Jochumsen M, Niazi IK, Dremstrup K. Comparison of features for movement prediction from single-trial movement-related cortical potentials in healthy subjects and stroke patients. *Comput Intell Neurosci.* (2015) 2015:858015. doi: 10.1155/2015/858015
36. Lakany H, Conway BA. Understanding intention of movement from electroencephalograms. *Expert Syst.* (2007) 24:295–304. doi: 10.1111/j.1468-0394.2007.00435.x
37. Oldfield RC. The assessment and analysis of handedness: the Edinburgh inventory. *Neuropsychologia* (1971) 9:97–113. doi: 10.1016/0028-3932(71)90067-4
38. Anon. Standards for reporting EMG data. *J Electromyogr Kinesiol.* (2018) 39:1–2. doi: 10.1016/S1050-6411(18)30113-5
39. Winter WR, Nunez PL, Ding J, Srinivasan R. Comparison of the effect of volume conduction on EEG coherence with the effect of field spread on MEG coherence. *Stat Med.* (2007) 26:3946–57. doi: 10.1002/sim.2978
40. Blankertz B, Tomioka R, Lemm S, Kawanabe M, Muller KR. Optimizing spatial filters for robust EEG single-trial analysis. *IEEE Signal Process Mag.* (2008) 25:41–56. doi: 10.1109/MSP.2008.4408441
41. Libet B, Wright EW Jr, Gleason CA. Readiness-potentials preceding unrestricted 'spontaneous' vs. pre-planned voluntary acts. *Electroencephalogr Clin Neurophysiol.* (1982) 54:322–35. doi: 10.1016/0013-4694(82)90181-X
42. Mento G. The passive CNV: carving out the contribution of task-related processes to expectancy. *Front Human Neurosci.* (2013) 7:827. doi: 10.3389/fnhum.2013.00827
43. Praamstra P, Stegeman DF, Cools AR, Horstink MW. Reliance on external cues for movement initiation in Parkinson's disease. Evidence from movement-related potentials. *Brain* (1998) 121 (Pt 1):167–77. doi: 10.1093/brain/121.1.167
44. Amatachaya S, Amatachaya P, Keawsutthi M, Siritaratiwat W. External cues benefit walking ability of ambulatory patients with spinal cord injury. *J Spinal Cord Med.* (2013) 36:638–44. doi: 10.1179/2045772312Y.0000000086
45. Deecke L, Scheid P, Kornhuber HH. Distribution of readiness potential, pre-motion positivity, and motor potential of the human cerebral cortex preceding voluntary finger movements. *Exp Brain Res.* (1969) 7:158–68. doi: 10.1007/bf00235441
46. Walter WG, Cooper R, Aldridge VJ, McCallum WC, Winter AL. Contingent negative variation: an electric sign of sensorimotor association and expectancy in the human brain. *Nature* (1964) 203:380–4. doi: 10.1038/203380a0
47. Birbaumer N, Elbert T, Canavan AG, Rockstroh B. Slow potentials of the cerebral cortex and behavior. *Physiol Rev.* (1990) 70:1–41. doi: 10.1152/physrev.1990.70.1.1

48. Neuper C, Wortz M, Pfurtscheller G. ERD/ERS patterns reflecting sensorimotor activation and deactivation. *Prog. Brain Res.* (2006) 159:211–22. doi: 10.1016/S0079-6123(06)59014-4
49. Yuan H, Doud A, Gururajan A, He B. Cortical imaging of event-related (de)synchronization during online control of brain-computer interface using minimum-norm estimates in frequency domain. *IEEE Trans Neural Syst Rehabil Eng.* (2008) 16:425–31. doi: 10.1109/TNSRE.2008.2003384
50. Stancak A Jr, Pfurtscheller G. The effects of handedness and type of movement on the contralateral preponderance of mu-rhythm desynchronisation. *Electroencephalogr Clin Neurophysiol.* (1996) 99:174–82. doi: 10.1016/0013-4694(96)95701-6
51. Babiloni C, Carducci F, Cincotti F, Rossini PM, Neuper C, Pfurtscheller G, et al. Human movement-related potentials vs desynchronization of EEG alpha rhythm: a high-resolution EEG study. *Neuroimage* (1999) 10:658–65. doi: 10.1006/nimg.1999.0504
52. Lang W, Beisteiner R, Lindinger G, Deecke L. Changes of cortical activity when executing learned motor sequences. *Exp Brain Res.* (1992) 89:435–40. doi: 10.1007/bf00228259
53. Makela JP, Lioumis P, Laaksonen K, Forss N, Tatlisumak T, Kaste M, et al. Cortical excitability measured with nTMS and MEG during stroke recovery. *Neural Plasticity* (2015) 2015:309546. doi: 10.1155/2015/309546
54. Aono K, Miyashita S, Fujiwara Y, Kodama M, Hanayama K, Masakado Y, et al. Relationship between event-related desynchronization and cortical excitability in healthy subjects and stroke patients. *Tokai J Exp Clin Med.* (2013) 38:123–8.
55. Lin Q, Li H, Mao YR, Lo WL, Zhao JL, Chen L, et al. The difference of neural networks between bimanual antiphase and in-phase upper limb movements: a preliminary functional magnetic resonance imaging study. *Behav Neurol.* (2017) 2017:8041962. doi: 10.1155/2017/8041962
56. Ramos-Murguialday A, Birbaumer N. Brain oscillatory signatures of motor tasks. *J Neurophysiol.* (2015) 113:3663–82. doi: 10.1152/jn.00467.2013

Conflict of Interest Statement: The authors declare that the research was conducted in the absence of any commercial or financial relationships that could be construed as a potential conflict of interest.

frontiers in Neurology

ORIGINAL RESEARCH
published: 17 October 2018
doi: 10.3389/fneur.2018.00881

Assessing the Relationship Between Motor Anticipation and Cortical Excitability in Subacute Stroke Patients With Movement-Related Potentials

Ling Chen[1,2], Yurong Mao[1], Minghui Ding[1], Le Li[1], Yan Leng[1], Jiangli Zhao[1], Zhiqin Xu[1], Dong Feng Huang[1,3] and Wai Leung Ambrose Lo[1]**

[1] Department of Rehabilitation Medicine, Guangdong Engineering and Technology Research Center for Rehabilitation Medicine and Translation, The First Affiliated Hospital, Sun Yat-sen University, Guangzhou, China, [2] Department of Acupuncture and Moxibustion, The Secondary Medical College, Guangzhou University of Traditional Chinese Medicine, Guangzhou, China, [3] Xinhua College of Sun Yat-sen University, Guangzhou, China

OPEN ACCESS

Edited by:
Pavel Lindberg,
INSERM U894 Centre de Psychiatrie et Neurosciences, France

Reviewed by:
Jun Yao,
Northwestern University, United States
Henry Ma,
Monash University, Australia
Simon Morand-Beaulieu,
Université de Montréal, Canada

***Correspondence:**
Dong Feng Huang
huangdf@mail.sysu.edu.cn
Wai Leung Ambrose Lo
ambroselo0726@outlook.com

Specialty section:
This article was submitted to Stroke, a section of the journal Frontiers in Neurology

Received: 30 November 2017
Accepted: 28 September 2018
Published: 17 October 2018

Citation:
Chen L, Mao Y, Ding M, Li L, Leng Y, Zhao J, Xu Z, Huang DF and Lo WLA (2018) Assessing the Relationship Between Motor Anticipation and Cortical Excitability in Subacute Stroke Patients With Movement-Related Potentials. Front. Neurol. 9:881. doi: 10.3389/fneur.2018.00881

Background: Stroke survivors may lack the cognitive ability to anticipate the required control for palmar grasp execution. The cortical mechanisms involved in motor anticipation of palmar grasp movement and its association with post-stroke hand function remains unknown.

Aims: To investigate the cognitive anticipation process during a palmar grasp task in subacute stroke survivors and to compare with healthy individuals. The association between cortical excitability and hand function was also explored.

Methods: Twenty-five participants with hemiparesis within 1–6 months after first unilateral stroke were recruited. Twenty-five matched healthy individuals were recruited as control. Contingent negative variation (CNV) was measured using electroencephalography recordings (EEG). Event related potentials were elicited by cue triggered hand movement paradigm. CNV onset time and amplitude between pre-cue and before movement execution were recorded.

Results: The differences in CNV onset time and peak amplitude were statistically significant between the subacute stroke and control groups, with patients showing earlier onset time with increased amplitudes. However, there was no statistically significant difference in CNV onset time and peak amplitude between lesioned and non-lesioned hemisphere in the subacute stroke group. Low to moderate linear associations were observed between cortical excitability and hand function.

Conclusions: The earlier CNV onset time and higher peak amplitude observed in the subacute stroke group suggest increased brain computational demand during palmar grasp task. The lack of difference in CNV amplitude between the lesioned and non-lesioned hemisphere within the subacute stroke group may suggest that the

non-lesioned hemisphere plays a role in the motor anticipatory process. The moderate correlations suggested that hand function may be associated with cortical processing of motor anticipation.

Keywords: stroke, subacute, motor anticipatory, cortical excitability, movement-related potential

INTRODUCTION

Cognitive Process of Movement Anticipation in Stroke Patients

Stroke is among the leading causes of long-term disability worldwide (1). It is one of the most severe issues encountered by the aging population (2). Seventy-five percent of stroke survivors have motor dysfunction that affects body coordination and motor skill (3). Motion prediction is a key component of cognitive function and is a high-level function that affects motor control (4). Motor function recovery is often measured in terms of motor execution, with little consideration given to the high level cognitive processes that feeds into the actual motor response (5). To execute activities of daily living such as reach and grasp, the upper extremity must apply the correct force, move the precise range and accurately coordinate multiple limb segments (6–10). The cognitive ability to anticipate the required movement control is therefore fundamental to hand motor performance. Published literature indicates that stroke patients lack the anticipatory ability of upper limb movement that is associated with palmar grasp (11–13). The lack of ability to anticipate was evidenced in the suboptimal application of force by producing markedly increased grip forces during lifting, holding and moving a hand-held object in patients with acute stroke (14). Patients with chronic stroke demonstrated a slower response to adapt to the perturbing force and exhibited smaller aftereffects when the perturbing force was unexpectedly removed than healthy controls (11).

Contingent Negative Variation

The electrophysiological processes associated with movement anticipation and the relationship between the electrophysiological changes and clinical impairment of hand function in stroke patients remain poorly understood (15). Contingent negative variation (CNV) is one of the electrophysiological substrates of motor anticipation. CNV was first reported by Walter et al. (16) as a slow-going, negative event-related potential (ERP) that reflects the cognitive processing (5). It refers to the sustained negativity that develops after the pre-cue (S1) and before the imperative stimulus (S2) that requires a response. If the interval between S1 and S2 is >2 s, CNV can be distinguished into initial CNV and late CNV (17). The late CNV that occurs before S2 is assumed to be the composition of a readiness potential and stimulus preceding negativity (18). The amplitude of late CNV is also modulated by the amount of advanced information provided by the pre-cue (19–21), which usually shows up as an increase in late CNV. Late CNV tends to increase when people perform intention-based action with advanced information provided by pre-cue (21–23). This is because pre-cue information enables people to have sufficient anticipation for the upcoming action (24). Source analysis suggests that there are multiple sources of the generation of late CNV. These include the cortical and subcortical generators of the (1) anterior cingulate cortex, (2) supplementary motor area, and (3) primary motor area, in particular the inferior parietal cortex (19, 25, 26). CNV is suggested to be an index of anticipation because it reflects the action preparation process (21, 27). Therefore, the CNV amplitude and latency represent cognitive processes of anticipation and movement preparation (28–30). Early literature reported that the time between the onset of brain potential recorded by electroencephalographic (EEG) and movement onset recorded with electromyography (EMG) were indicative of the preparation time for the required action (31). Studies of healthy individuals also indicated that non-dominant hand movement has an earlier onset of cortical potential when compared with the dominant hand movement. Thus, there is evidence to indicate that the longer anticipatory phase reflects the increase in computational demand when executing learned movement (32). In people with chronic stroke, CNV is significantly enhanced at the midline region with markedly slower response time during affected hand preparation (5). The increased amplitude of the midline region CNV correlates with a greater response-priming effect. Enlarged CNV amplitudes during intention-based actions are expected in people with stroke as they need to have increased cognitive preparation for the anticipation process when compared with healthy individuals. Similar findings were also reported in chronic stroke patients who had no residual paretic hand movements (33). Simultaneous recording of EEG and EMG indicated that early onset of cortical potential precede affected rather than unaffected hand movement.

To date, the cognitive process involved in movement anticipation during a palmar grasp task with advance pre-cuing in the subacute stroke population has not been studied using the CNV approach. Understanding the cortical regions that are involved during grasping preparation in the early stages of stroke can provide new insight into the neural plasticity mechanism for grasp motion recovery. The aim of the present study was to investigate the difference in the cognitive anticipation process between the lesioned and non-lesioned hemisphere in subacute stroke survivors and to compare the difference in the anticipation process with healthy individuals. This study hypothesized that subacute stroke patients demonstrated a statistically significant difference in CNV amplitude during intention-based action between the lesioned and non-lesioned side and that this differed significantly from healthy individuals. The study also investigated if the difference in the electrophysiological process was associated with a functional level as measured by the Action Research Arm Test (ARAT).

TABLE 1 | A summary of the demographic data of the included subjects in the stroke group.

	Age	Onset time	NIHSS	ARAT score
Mean	55.2	59.1	5.4	15.2
SD	8.4	24.9	3.0	12.6

METHODS

Participants

Twenty-five participants (thirteen males and 12 females; aged 55.2 ± 8.4 years) with subacute stroke were recruited. Twenty-five age and gender matched healthy individuals (thirteen males and 12 females; aged 53.8 ± 7.9 years) were recruited as controls. The functional level of the participants with subacute stroke was assessed by the ARAT (34), which consists of a total of 19 tests of arm motor function including grasp, hold, pinch and gross motor movement. Each test is allocated an ordinal value of 0, 1, 2, or 3, with higher values indicating better arm motor status. The total ARAT score is the sum of the 19 tests, and the maximum score of the scale is 57 (35). All recruited participants were right hand dominant as assessed by the Edinburgh handedness inventory (36). **Table 1** gives a summary of the demographic data of the sample population.

The inclusion criteria for the subacute stroke cohort were as follows: (1) hemiparesis resulting from a unilateral subcortical lesion of the first occurrence of a stroke; (2) within 1–6 months of stroke occurrence; (3) magnetic resonance imaging (MRI) or computed tomography (CT) confirmed stroke; (4) age between 40 and 80 years old; (5) moderate to severe motor deficit of the affected upper limbs, having at least 10° of finger flexion and extension; (6) be able to sit at least 30 min without assistance; and (7) no severe cognitive impairment (Mini Mental State Examination >21) (37). None of the participants had any prior brain computer interface (BCI) experience. The exclusion criteria were as follows: (1) lacunar infarction; (2) massive cerebral infarction; (3) cerebellum or brainstem lesion; (4) open hand wound or hand deformity; and (5) visual field deficits. All of the healthy individuals had no history of psychiatric/neurological disease or musculoskeletal disorder.

Ethics Considerations

The study was approved by the Ethical Committee of The First Affiliated Hospital of Sun Yat-sen University. Data collection took place in the Department of Rehabilitation Medicine, The First Affiliated Hospital of Sun Yat-sen University. All of the participants were provided with a comprehensive explanation of the experimental protocol. They were given an information sheet about the study and encouraged to ask questions. Written informed consent was obtained from all participants.

Experimental Protocol

Data recording took place in an electrically shielded brain function laboratory. All participants were seated in front of a table. They were asked to place their shoulders at between 0 and 10° flexion, their forearms rested on the table with elbows flexed to 130°, and their wrists were oriented in a neutral position so that opening and closing of the hand occurred in the horizontal plane. Participants were asked to fix their gaze in the middle of the screen straight ahead, avoid eye movement and focus attention on task performance. All participants had one practice session before the ERP recording began.

Experimental Task and Procedure

All the participants first undertook 5 to 10 min of training to familiarize themselves with the entire procedure before the ERP recording began. At the beginning of the experiment, the introduction was displayed on the screen. The instructions given were as follows:

> *"Welcome to this experiment. During the experiment, you will see a fixated white cross appear on the screen to remind you to pay attention to the task. Then, you will see a picture of either a left hand grasp or a right hand grasp displayed on the screen accompanied by a sound to indicate a left or right hand grasp. At this stage, please keep both hands still. The screen will then turn to a grey window. During the grey window, please do a self-paced voluntary palmar grasp according to the previous cue. Throughout the experiment, please refrain from blinking and body movements, particularly during the opening and closing of the hands."*

After understanding the displayed instructions, participants pressed the space bar to start the experiment. Participants first performed a modified audio-visual task that resembled a palmar grasp movement. The fixated white cross appeared on the screen for 500 ms to remind participants to pay attention to the task. Simultaneous visual and auditory imperative cues (S1) were given for 2,000 ms. A picture was displayed on the screen accompanied by a sound to indicate a right or left side palmar grasp. During S1, the participant was required to acquire the visual and auditory cues and judge the palmar grasp task. The screen then turned to a gray reaction window (S2) for 3,000 ms. The participants performed a self-paced voluntary palmar grasp during the S2 window. The experiment consisted of 40 trials for each hand, giving a total of 80 trials. The order of the trials was randomized in each experiment. The inter trial resting interval was marked by a dark screen that was displayed for 2,000 ms. The sequence of events in the trials is illustrated in **Figure 1**. All the participants were asked to avoid blinking and making compensatory/additional movements during the opening and closing of the hand.

EEG Signal Acquisition

The EEG data of each participant was recorded by a 32-channel QuickAmp amplifier and Ag/AgCl scalp electrodes (BrainProducts, Germany). The electrodes were positioned in accordance with the international 10–20 system (FP1, FP2, F3, Fz, F4, FC5, FC3, FC1, FCz, FC2, FC4, FC6, C5, C3, C1, Cz, C2, C4, C6, CP5, CP3, CP1, CPz, CP2, CP4, CP6, P3, POz, P4, POz, O1, O2; reference: FCz, ground: AFz). Data were recorded in DC mode with a sampling rate of

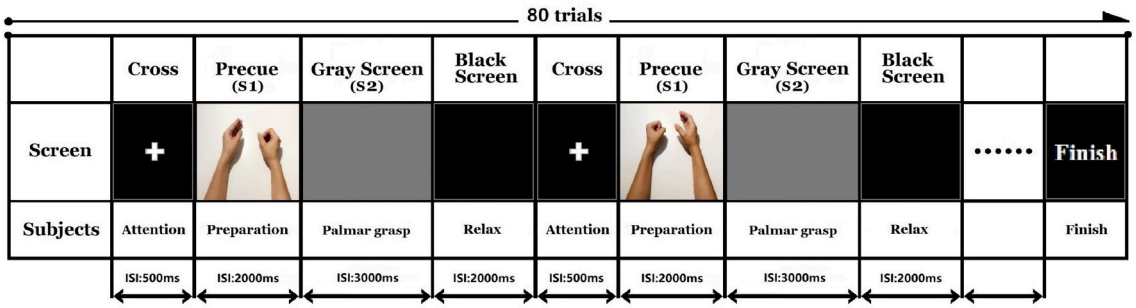

FIGURE 1 | Experimental trial sequence. *Key*: ISI, inter stimulus interval.

1,000 Hz. Electrodes were filled properly with conductive gel to maintain the impedance below 5 kΩ to ensure good quality recording.

For CNV amplitude analysis, topographic mapping was performed using six electrodes of interest. These electrodes were (i) F3 and C3 (left hemisphere), (ii) F4 and C4 (right hemisphere), and (iii) Fz and Cz (midline region). **Figure 2** illustrates the topographic maps of participants when executing left or right hand movement tasks.

EEG Signal Processing

EEG signal analysis was performed using the Brain Vision Analyzer signal processing software 2.0 (BrainProducts, Germany). During the EEG pre-processing, the average potential of the bilateral mastoid was used as a new reference. Eye movement artifacts were removed through the Ocular Correction Independent Component Analysis (ICA) (38). The removal of eye movement artifacts is a standard operating procedure when analyzing EEG signals. The number of trials or the quality of data were not affected. Inspection of the raw data was conducted with a 50 Hz notch filter and a 0.1–30 Hz bandpass filter. The EEG data were segmented into epochs of 500 ms pre to 3,000 ms post-aligned to the cue (S1) to acquire stimulus-locked ERPs, and the baseline was corrected to the first 200 ms of the epochs, which was the 200 ms time window before S1 onset. For each epoch, the late CNV onset time was calculated as the last time the signal crossed the zero line before the rise of the CNV (17) (see **Figure 4**), and the peak amplitude was calculated from 1,000 to 2,000 ms since this time window contained the maximal variation of the CNV potential. CNV onset time and peak amplitude features were extracted.

In this study, the left and right hemispheres of subacute stroke participants were labeled as "lesioned" and "non-lesioned." The left and right sided lateralised scalp sites were flipped in the participants with the right hemispheric lesion, (e.g., C3 and F3 for the right lesions and C4 and F4 for the left lesion) (33) to enable statistical comparisons between the lesioned and non-lesioned hemisphere. Thus, the "left" hemisphere was always the lesioned hemisphere in the subacute stroke group.

Statistical Analysis

All statistical analyses were performed using SPSS Statistic 21. Descriptive statistics were conducted to describe the sample population. CNV onset time and peak amplitudes were analyzed with a mixed model ANOVA analysis that incorporated the within-subjects factors TASK (Left hand movement and Right hand movement) and the LATERALITY (midline, contralateral, and ipsilateral regions). The between-subject factor of GROUP was used to compare the subacute stroke group to the matched healthy control group (stroke vs. control) during right-hand movement (RHM) and left-hand movement (LHM) and to compare the lesioned and non-lesioned hemisphere within the subacute stroke group during RHM and LHM. The Greenhouse-Geisser method were used to adjust the p-value and degrees of freedom when the assumption of sphericity was not met. Separate ANOVAs were calculated for each level of LATERALITY, using the same mixed model ANOVA format. To further investigate the differences between these groups, subsequent independent sample t-tests were performed. The significance level for all statistical analysis was set at 0.05. Bonferroni-adjusted significance tests were performed to correct the p-values of electrodes for multiple comparisons. Thus, the corrected significance level for LATERALITY was $\alpha = 0.05 \div 6 = 0.008$. Spearman's rank correlation analysis was performed to investigate the association between the ARAT and electrophysiological measures. The interpretations of Spearman's rank correlation coefficient were as follow: "slight" (0.0–0.2); "low" (0.2–0.4); "moderate" (0.5–0.7); "high" (0.8–0.9) (39).

RESULTS

Onset Time

The mixed model ANOVA analysis indicated a significant main effect of TASK (RHM, LHM) on the CNV onset time [$F_{(1, 48)} = 2.869$, $p = 0.028$]. CNV onset time for patients with a subacute stroke was earlier than that of the control group both during RHM ($p = 0.015$) and LHM ($p = 0.002$). In addition, the difference was not statistically significant in CNV onset time between RHM ($p = 0.323$) and LHM ($p = 0.202$) within the subacute stroke group. **Figure 3** illustrates the onset time for patients compared with controls.

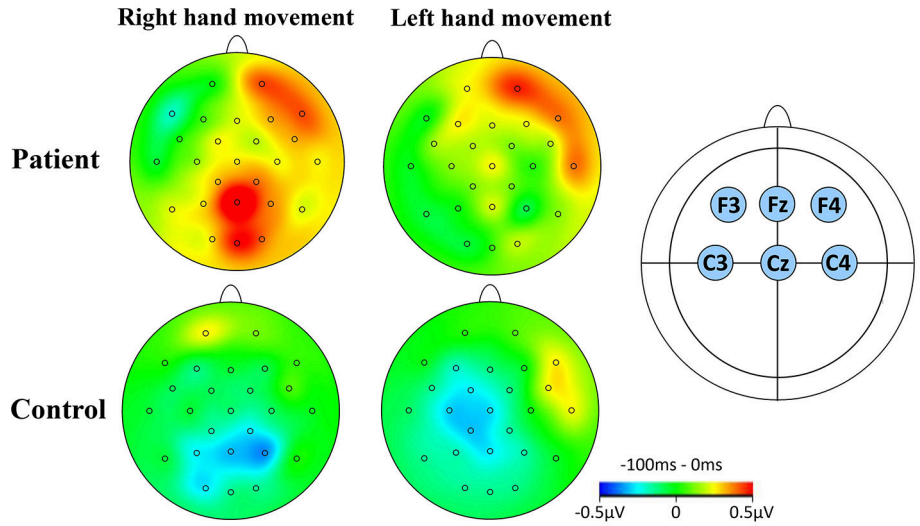

FIGURE 2 | CNV topographical distributions. **(A)** The window for the mapping was −100 to 0 ms relative to S1. Red contour lines indicate positive activity, blue contour lines indicate negative activity. The greyscale fill between the contour lines indicates amount of activation (positive or negative). The small circles on the topographies indicate the electrodes sites. The rows indicate the two groups studied during RHM and LHM. **(B)** The location of the six electrodes of interest.

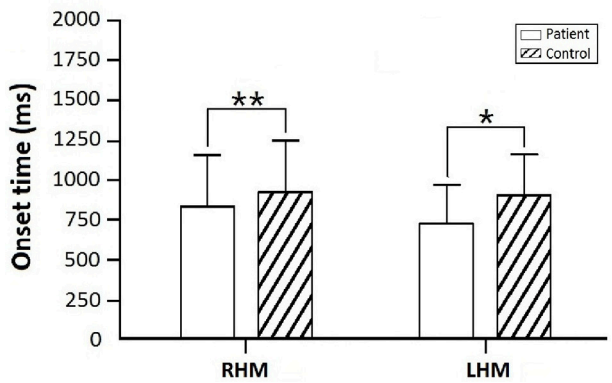

FIGURE 3 | Onset time for the subacute stroke group in comparison to control group. Asterisks indicate significant differences within RHM and LHM (**$p < 0.01$; *$p < 0.05$).

Peak Amplitude

Analysis Between Subacute Stroke Group and Control Group

The mixed model ANOVA analysis on the CNV peak amplitude between the subacute stroke group and control group during RHM and LHM revealed a significant TASK × GROUP × LATERALITY interaction [$F_{(5, 240)} = 5.635$, $p < 0.001$]. Furthermore, comparisons between the subacute stroke group and their match control group indicated a significant main effect of TASK for CNV peak amplitude [$F_{(2.619, 125.713)} = 3.390$, $p = 0.025$]. Thus, separate ANOVAs were calculated for each level of TASK.

Comparison between subacute stroke group and control group within RHM condition

Analysis between the two groups during RHM indicated no significant LATERALITY × GROUP interaction [$F_{(2.980, 71.520)} = 1.605$, $p = 0.196$]. Therefore, LATERALITY and GROUP were tested for individual effects. Significant GROUP effect [$F_{(1, 24)} = 9.379$, $p = 0.002$] and LATERALITY effect [$F_{(2.738, 262.837)} = 4.364$, $p = 0.001$] were observed. Then, subsequent independent sample *t*-tests revealed significantly larger CNV amplitudes in the subacute stroke group at midline (Fz, Cz), ipsilateral (F4, C4), and contralateral (C3, F3) electrodes than the control group when conducting right hand movement. **Figure 4** gives the graphical representations of the CNV amplitudes during RHM. **Table 2** illustrates the comparison of CNV peak amplitude between the two groups within RHM condition.

Comparison between subacute stroke group and control group within LHM condition

No significant LATERALITY × GROUP interaction [$F_{(2.078, 49.883)} = 0.905$, $p = 0.415$] was observed in CNV amplitude between the subacute stroke group and the control group. Therefore, LATERALITY and GROUP were tested for individual effects. Analysis showed significant GROUP effect [$F_{(1, 24)} = 14.47$, $p = 0.001$] and LATERALITY effect [$F_{(2.920, 70.073)} = 7.185$, $p < 0.001$]. Further investigation of these effects revealed that there was a significantly larger CNV amplitude in the subacute stroke group at midline (Fz, Cz), contralateral (F4, C4), and ipsilateral (F3, C3) regions than the control group when conducting right hand movement. **Figure 5** gives the graphical representations of CNV amplitudes for the patient and control groups during LHM. **Table 3** shows the comparison of CNV peak amplitudes between subacute stroke group and control group within LHM condition.

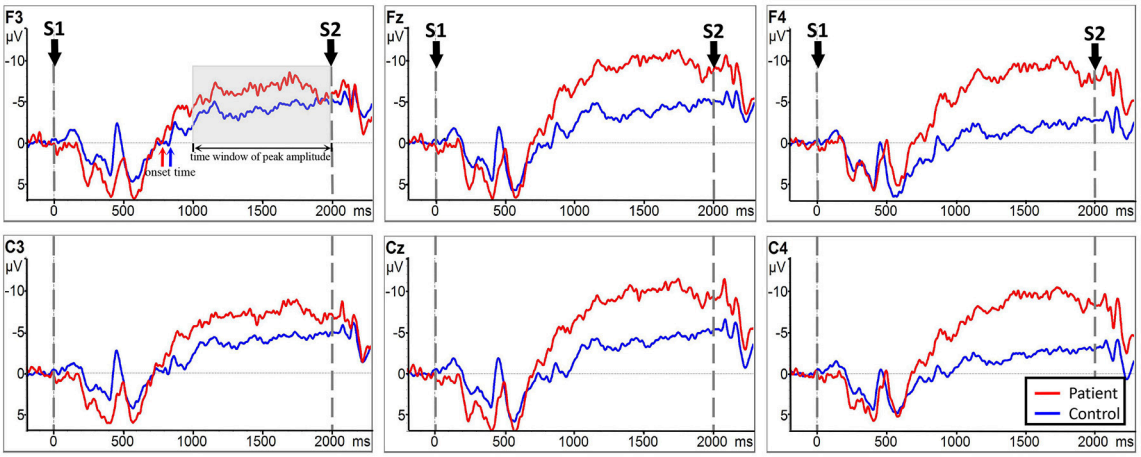

FIGURE 4 | CNV amplitudes for the subacute stroke group (red line) and control group (blue line) during RHM. The Y-axis represents CNV waveform (μV) and the X-axis represents time (ms). Negative is plotted upwards. Baseline is the first 200 ms of the epoch, i.e., 200 ms before S1 onset. The 0 ms point is S1 onset. Red/blue arrows represent the onset of the late CNV in patient group/control group. The gray time window indicated the time window to detect the peak amplitude.

TABLE 2 | Comparison of CNV peak amplitude between subacute stroke group and control group within RHM condition.

Electrodes	Stroke group	Control group	*p*-value
C3	−14.057 (16.037)	−7.830 (8.010)	0.005**
Cz	−14.112 (17.994)	−7.055 (9.056)	0.001**
C4	−11.713 (15.935)	−7.173 (6.047)	0.005**
F3	−11.942 (16.422)	−8.616 (6.943)	0.009**
Fz	−12.387 (15.454)	−7.010 (9.533)	0.001**
F4	−11.063 (15.973)	−6.450 (7.190)	0.006**

*Asterisks indicate significant differences (**p < 0.01).*

Comparison Between RHM and LHM Within the Subacute Stroke Group

Analysis indicated no significant LATERALITY × GROUP interaction [$F_{(2.153,\ 51.669)} = 0.856$, $p = 0.438$]. Further analysis showed no statistically significant main effect of GROUP [$F_{(1,\ 24)} = 0.100$, $p = 0.755$] or LATERALITY [$F_{(2.372,\ 56.938)} = 1.209$, $p = 0.051$] on CNV amplitude between RHM and LHM within the subacute stroke group. Thus, there was no statistically significant difference in CNV amplitude between RHM and LHM in the subacute stroke group. **Figure 6** shows the EEG traces recorded at each electrode during LHM and RHM in the subacute stroke group.

When comparing laterality factors (contralateral, midline, ipsilateral) within the TASK movement condition (RHM and LHM), there was no statistically significant hemisphere LATERALITY effect on CNV amplitude during RHM [$F_{(5,\ 65.715)} = 2.015$, $p = 0.126$].

During LHM, a significantly main effect of LATERALITY on CNV amplitude was observed [$F_{(1.944,\ 46.663)} = 3.820$, $p = 0.030$]. Further investigation of the hemisphere LATERALITY effect revealed that midline electrodes (Cz) had a higher CNV amplitude than contralateral (C4) electrodes ($p = 0.007$).

Correlations Between CNV Peak Amplitude With ARAT in the Subacute Stroke Group

Figure 7 shows the results of Spearman's rank correlation coefficient analysis between the CNV peak amplitude observed at different regions and the ARAT within the subacute stroke group. During RHM, significant correlations were observed in the front-ipsilateral side ($r = 0.510$, $p = 0.009$), midline ($r = 0.428$, $p = 0.033$), and ipsilateral side ($r = 0.442$, $p = 0.027$). During the LHM condition, a significant correlation was observed in the front-contralesional side ($r = 0.496$, $p = 0.012$), midline ($r = 0.446$, $p = 0.026$), and contralesional side ($r = 0.496$, $p = 0.012$).

DISCUSSION

The primary aim of this study was to investigate the difference in the cognitive anticipation process between the lesioned and non-lesioned hemisphere in subacute stroke survivors and to compared those with healthy individuals. The association between the electrophysiological process and the functional level as measured by the ARAT in the stroke group was also investigated.

Onset of CNV

Results of this present study are consistent with existing literature reporting extended anticipation time. We found that this occurred in the subacute stroke population when compared with the control group, as evidenced by the statistically significant early CNV onset time during left hand and right hand movement. This finding is consistent with a previous investigation that reported a significantly earlier onset time in the paretic hand movement than in the non-paretic hand movement in people with chronic stroke using movement-related slow cortical

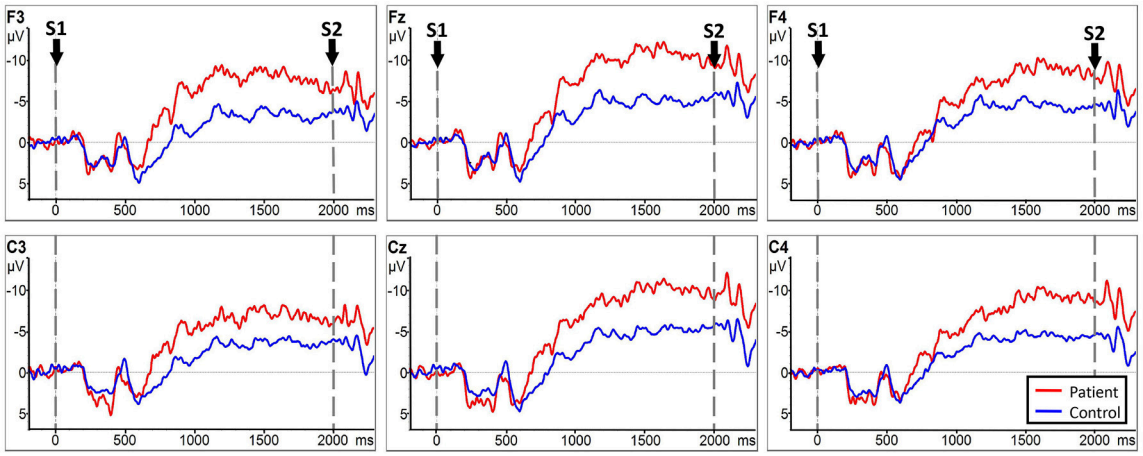

FIGURE 5 | CNV amplitudes for the subject stroke group (red line) and control group (blue line) during LHM. The Y-axis represents CNV waveform (μV) and the X-axis represents time (ms). Negative is plotted upwards. Baseline is the first 200 ms of the epoch, i.e., 200 ms before S1 onset. The 0 ms point is S1 onset.

TABLE 3 | Comparison of CNV peak amplitude between subacute stroke and control group within LHM condition.

Electrodes	Stroke group	Control group	*p*-value
C3	−12.250 (14.180)	−7.826 (3.529)	0.005**
Cz	−15.453 (11.262)	−7.727 (6.187)	0.001**
C4	−14.165 (14.923)	−8.566 (5.644)	0.001**
F3	−12.932 (11.318)	−6.869 (5.986)	0.007**
Fz	−15.800 (11.153)	−8.587 (6.364)	0.001**
F4	−12.017 (11.461)	−7.973 (5.029)	0.001**

*Asterisks indicate significant differences (**$p < 0.01$).*

potentials (SCP) (33). This supports the theory that extended planning time is needed for the brain to start exciting the motor network that leads to movement execution of the paretic arm. The results of this present study are consistent with existing literature suggesting that extended anticipation (planning) time is present within the subacute stroke population when compared with a control group. This study however did not observe any difference in CNV onset time between the lesioned and non-lesioned side during LHM and RHM. This is contrary to previous studies that reported a significant difference in CNV onset time between paretic and non-paretic hand movement (5, 33). The different findings between the two studies are likely related to the difference in experimental design. In the study by Deecke et al. (40), slow cortical potential measurement incorporated both anticipation of an upcoming movement as well as the motor potential occurring at the time of movement execution. Thus, SCP did not only reflect the cognitive processing behavior but also the additional time required for motor network excitation. The study by Dean et al. (5), recorded CNV onset from S2 (response cue) until feedback (task execution), whereas this study measured from S1 (pre-cue) until S2 without task execution. Thus, the potentials reported by Dean et al., did not only reflect the anticipation but also the potentials during movement. The findings in this study demonstrated for the first time that the motion anticipation phase alone is earlier in subacute stroke participants than healthy participants. Furthermore, advanced motor anticipation occurred not only in the paretic hand but also in the non-paretic hand, as evidenced by the lack of difference in CNV between the lesioned and non-lesioned hemisphere.

CNV Amplitude Related to Motor Expectancy

This study evaluated motor anticipation with CNV elicited by a stimulus-locked open/close hand movement paradigm. People with motor impairment are expected to have a larger peak amplitude that reflects the increase in the brain's computational demand to execute a movement (41). The study observed a significantly larger peak amplitude of CNV during RHM (affected hand) in the stroke group over the contralateral (C3), midline (Fz and Cz), and ipsilateral (C4) regions than that in the matched control group. This finding is consistent with published literature and supports the notion of an increase in psychological anticipation during the affected hand movement. This study also observed an increase in the activity pattern at contralateral (C4), midline (Fz and Cz), and ipsilateral (C3) locations during the LHM (unaffected hand) in the stroke group when compared with the control group. This suggests that increased psychological anticipation activity also occurs during unaffected hand movement. This higher activity level may be related to the compensatory over activation in the non-lesioned hemisphere and the lack of cross hemispheric inhibition from the lesioned to non-lesioned hemisphere.

Within the stroke group, extensive anticipation activation was observed at the frontal, contralateral, midline, and ipsilateral regions during the affected hand movement. No difference was found between the contralateral (C3) and ipsilateral (C4) side, with a significantly larger peak amplitude observed at the midline (Cz) than ipsilateral (C4) side. This suggests that there is no

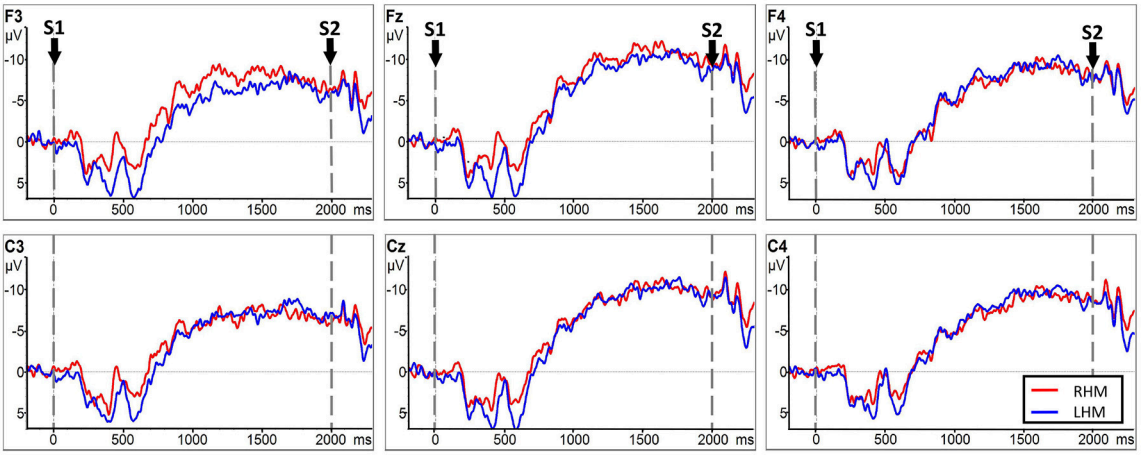

FIGURE 6 | CNV amplitudes for the subacute stroke group group during RHM (red line) and LHM (blue line). The Y-axis represents CNV waveform (μV) and the X-axis represents time (ms). Negative is plotted upwards. Baseline is the first 200 ms of the epoch, i.e., 200 ms before S1 onset. The 0 ms point is S1 onset.

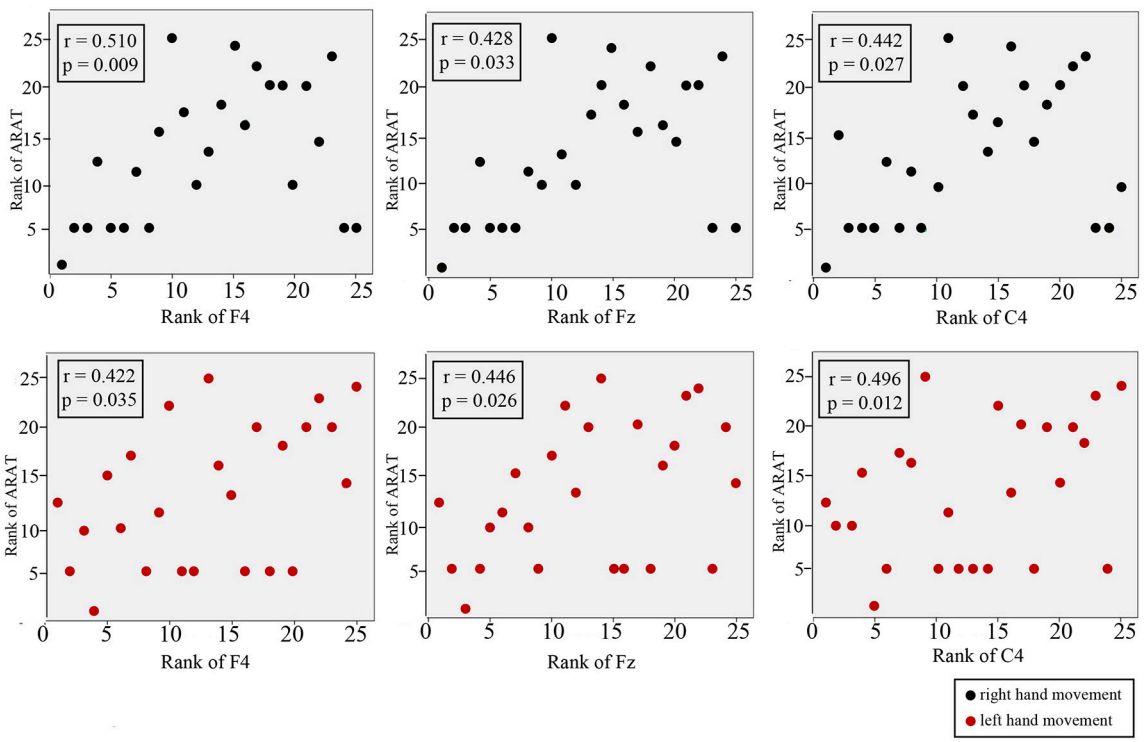

FIGURE 7 | Correlation between CNV amplitude with ARAT in stroke participants. The Y-axis represents the rank of ARAT and the X-axis represents the rank of CNV. CNV recorded at midline, front-contralesional/front-ipsilateral side, and contralesional/ipsilateral side shown for RHM (black circles) and LHM (red circles).

definitive hemisphere laterality and that most of the anticipation activity originates from the midline region during affected palmar movement. This is consistent with studies that reported increased effort in response to the inability to control the process in the hemisphere (42–44). These results did not demonstrate the effect a pattern of larger CNV amplitude over the contralateral region, as reported in previous research in the chronic stroke population (5, 19, 45, 46). The difference in findings may be related to the chronicity of the sample population. Cortical map expansion has been repeatedly reported in animal (47) and human experiments (48) after cortical damage. The expansion happens during the early stages of a stroke due to neuroplasticity and up to 8 weeks after training had stopped (49). Once the sequence of the motor task is learned, the size of the mapping representation returns to its original size (50). The lack of a significant difference in CNV amplitude between the left and right hemisphere may

suggest that the subacute stroke patients are still going through the learning process to regain the palmar grasp movement. Thus, cortical expansion is occurring during this stage due to the neuroplasticity process, and a significantly larger CNV amplitude is generated along with bilateral changes in the adaptive compensation function of the brain (41). This theory is given further support from early literature that has repeatedly shown that movement of the affected hand is associated with increased bilateral activation of sensorimotor cortex (51–54).The lack of difference in the peak CNV amplitude may also be related to the incongruous over activation that occurs in the unaffected hemisphere or to an imbalance in inter hemispheric inhibition (55–59).

Correlation Between Electrophysiological Measures and Clinical Scale

A higher ARAT score is indicative of higher motor function of the paretic hand (60). Though it appeared that a better ARAT performance correlated with a smaller CNV peak amplitude, it is not possible to draw a firm conclusion because there is insufficient data available from the high and low CNV amplitude comparison. This study observed the strongest significant positive correlation at the front-ipsilateral side, which suggests that motor function may be represented by neural pathway modulation that is responsible for motor function. The significant moderate correlations suggested that hand function may be associated with cortical excitability. The correlation level observed in this study may be affected by the spread of the data. A known limitation of the correlation coefficient is that it is affected by the spread of the data, i.e., the bigger the data range, the higher the chance of a high correlation (61).

Limitations

There are some important points regarding the limitations of this study. One limitation was that we recruited a relatively small sample size of subacute stroke participants and matched healthy controls (both groups $n = 25$). Future research will be needed both to enroll chronic upper limb hemiparesis stroke subjects and enlarge the sample size to explore the effects of neurophysiologic mechanisms identified in the present study. Second, this study focused on participants with moderate to severe motor deficits of the affected upper limbs. Further research is suggested to investigate whether stroke patients with mild motor deficits of the affected upper limbs can also elicit electrophysiological changes of motor anticipation. Third, the ERP has the characteristic of temporal resolution of the millisecond, which can accurately capture extremely weak signals from the brain and observe the cortical excitability of motor anticipation in real time (62). To explore further insight into the strict frequency locked cortical excitability of motor anticipation, event related synchronization technology is recommended for further research. The flipping of scalp sites may be considered a limitation. However, it is not uncommon in published literature that involves ERP or fMRI to flip the scalp site in an attempt to increase statistical power. In addition, the preliminary analysis of the present results indicated there was no statistically significant difference in CNV onset time or amplitude between patients with a left and right hemispheric lesion. Thus, the inverted electrodes in right-hemisphere lesioned patients were unlikely to alter the current findings.

CONCLUSIONS

This study investigated the electrophysiological changes of motor anticipation during a palmar grasp task in subacute stroke survivors. The earlier CNV onset time and the higher peak amplitude are indicative of increased brain computational demand during palmar grasp task post-stroke. These are indicative of an increase in brain computational demand during the palmar grasp task. The lack of difference in CNV amplitude between the lesioned and non-lesioned hemisphere in the subacute stroke group may suggest that the non-lesioned hemisphere may play a role in the anticipatory process. Further investigation is required to understand the role of the non-lesioned side in movement recovery and the impact of intervention on electrophysiological changes.

AUTHOR CONTRIBUTIONS

All authors have read and approved the final manuscript. All authors meet the four primary ICMJE criteria for authorship. In addition, all authors have been actively involved in the study in different capacities: LC designed the study and conducted all stages of the study including data collection, analysis, interpretation, and drafting of the manuscript. YM participated in the design of research protocol and interpreted the results. YL participated in the participants recruitment. MD participated in the recruitment and data analysis. LL revised the manuscript interpreted the data. JZ and ZX assessed the motor deficit of the affected upper limbs with Research Arm Test (ARAT). DH and WL managed the trial. WL analyzed and interpreted the data and revised the manuscript.

FUNDING

This study was supported by four research grants from Sun Yat-sen University Clinical Research 5010 Program (2014001), Provincial Science and technology project of Guangdong Province (2015B020233006, 2016A020220009), and Guangzhou science and technology project (201604020108).

REFERENCES

1. GBD 2015 DALYs and HALE Collaborators. Global, regional, and national disability-adjusted life-years (DALYs) for 315 diseases and injuries and healthy life expectancy (HALE). 1990-2015: a systematic analysis for the Global Burden of Disease Study 2015. *Lancet* (2016) 388:1603–58. doi: 10.1016/S0140-6736(16)31460-X
2. Vorkas PA, Shalhoub J, Lewis MR, Spagou K, Want EJ, Nicholson JK, et al. Metabolic phenotypes of carotid atherosclerotic plaques relate to

stroke risk: an exploratory study. *Eur J Vasc Endovasc Surg.* (2016) 52:5–10. doi: 10.1016/j.ejvs.2016.01.022
3. Lawrence ES, Coshall C, Dundas R, Stewart J, Rudd AG, Howard R, et al. Estimates of the prevalence of acute stroke impairments and disability in a multiethnic population. *Stroke* (2001) 32:1279–84. doi: 10.1161/01.STR.32.6.1279
4. Varghese JP, Merino DM, Beyer KB, McIlroy WE. Cortical control of anticipatory postural adjustments prior to stepping. *Neuroscience* (2016) 313:99–109. doi: 10.1016/j.neuroscience.2015.11.032
5. Dean PJA, Seiss E, Sterr A. Motor planning in chronic upper-limb hemiparesis: evidence from movement-related potentials. *PLoS ONE* (2012) 7:e44558. doi: 10.1371/journal.pone.0044558
6. Hakkennes S, Keating JL. Constraint-induced movement therapy following stroke: a systematic review of randomised controlled trials. *Aust J Physiother.* (2005) 51:221–31. doi: 10.1016/S0004-9514(05)70003-9
7. Go AS, Mozaffarian D, Roger VL, Benjamin EJ, Berry JD, Blaha MJ, et al. Heart disease and stroke statistics—2014 Update: a report from the american heart association. *Circulation* (2014) 129:e28–292. doi: 10.1161/01.cir.0000441139.02102.80
8. Schaefer SY, Haaland KY, Sainburg RL. Hemispheric specialization and functional impact of ipsilesional deficits in movement coordination and accuracy. *Neuropsychologia* (2009) 47:2953–66. doi: 10.1016/j.neuropsychologia.2009.06.025
9. Wetter S, Poole JL, Haaland KY. Functional implications of ipsilesional motor deficits after unilateral stroke. *Arch Phys Med Rehabil.* (2005) 86:776–81. doi: 10.1016/j.apmr.2004.08.009
10. Kalaska JF. From intention to action: motor cortex and the control of reaching movements. *Adv Exp Med Biol.* (2009) 629:139–78. doi: 10.1007/978-0-387-77064-2_8
11. Takahashi CD, Reinkensmeyer DJ. Hemiparetic stroke impairs anticipatory control of arm movement. *Exp Brain Res.* (2003) 149:131–40. doi: 10.1007/s00221-002-1340-1
12. Hermsdörfer J, Hagl E, Nowak DA. Deficits of anticipatory grip force control after damage to peripheral and central sensorimotor systems. *Hum Mov Sci.* (2004) 23:643–62. doi: 10.1016/j.humov.2004.10.005
13. Tan C, Tretriluxana J, Pitsch E, Runnarong N, Winstein CJ. Anticipatory planning of functional reach-to-grasp: a pilot study. *Neurorehabil Neural Repair* (2012) 26:957–67. doi: 10.1177/1545968312437938
14. Nowak DA, Hermsd Rfer J, Topka H. Deficits of predictive grip force control during object manipulation in acute stroke. *J Neurol.* (2003) 250:850–60. doi: 10.1007/s00415-003-1095-z
15. Mehrholz J, Pohl M, Platz T, Kugler J, Elsner B. Electromechanical and robot-assisted arm training for improving activities of daily living, arm function, and arm muscle strength after stroke. *Cochrane Database Syst Rev.* (2015) CD006876. doi: 10.1002/14651858.CD006876.pub4
16. Walter WG, Cooper R, Aldridge VJ, Mccallum WC, Winter AL. Contingent negative veriation: an electric sign of sensorimotor association and expectancy in the human brain. *Nature* (1964) 203:380–4. doi: 10.1038/203380a0
17. Golob EJ, Ovasapyan V, Starr A. Event-related potentials accompanying motor preparation and stimulus expectancy in the young, young-old and oldest-old. *Neurobiol Aging* (2005) 26:531–42. doi: 10.1016/j.neurobiolaging.2004.04.002
18. van Boxtel GJ, Brunia CH. Motor and non-motor aspects of slow brain potentials. *Biol Psychol.* (1994) 38:37–51. doi: 10.1016/0301-0511(94)90048-5
19. Leuthold H, Jentzsch I. Neural correlates of advance movement preparation: a dipole source analysis approach. *Brain Res Cogn Brain Res.* (2001) 12:207–24. doi: 10.1016/S0926-6410(01)00052-0
20. Sterr A, Dean P. Neural correlates of movement preparation in healthy ageing. *Eur J Neurosci.* (2008) 27:254–60. doi: 10.1111/j.1460-9568.2007.05975.x
21. Leuthold H, Sommer W, Ulrich R. Preparing for action: inferences from CNV and LRP. *J Psychophysiol.* (2004) 18:77–88. doi: 10.1027/0269-8803.18.23.77
22. Vanhoutte S, Van Borsel J, Cosyns M, Batens K, van Mierlo P, Hemelsoet D, et al. CNV amplitude as a neural correlate for stuttering frequency: a case report of acquired stuttering. *Neuropsychologia* (2014) 64:349–59. doi: 10.1016/j.neuropsychologia.2014.09.036
23. Smith AL, Staines WR. Externally cued inphase bimanual training enhances preparatory premotor activity. *Clin Neurophysiol.* (2012) 123:1846–57. doi: 10.1016/j.clinph.2012.02.060
24. Falkenstein M, Hoormann J, Hohnsbein J, Kleinsorge T. Short-term mobilization of processing resources is revealed in the event-related potential. *Psychophysiology* (2003) 40:914–23. doi: 10.1111/1469-8986.00109
25. Gomez CM, Marco J, Grau C. Preparatory visuo-motor cortical network of the contingent negative variation estimated by current density. *Neuroimage* (2003) 20:216–24. doi: 10.1016/S1053-8119(03)00295-7
26. Praamstra P, Stegeman DF, Horstink MW, Cools AR. Dipole source analysis suggests selective modulation of the supplementary motor area contribution to the readiness potential. *Electroencephalogr Clin Neurophysiol.* (1996) 98:468–77. doi: 10.1016/0013-4694(96)95643-6
27. Brunia CHM, Boxtel GJMV, Böcker KBE. Negative slow waves as indices of anticipation: the Bereitschaftspotential, the contingent negative variation, and the stimulus-preceding negativity. In: *The Oxford Handbook of Event-Related Potential Components*. Oxford: Oxford University Press (2011). p. 189–207.
28. Bares M, Nestrasil I, Rektor I. The effect of response type (motor output versus mental counting) on the intracerebral distribution of the slow cortical potentials in an externally cued (CNV) paradigm. *Brain Res Bull.* (2007) 71:428–35. doi: 10.1016/j.brainresbull.2006.10.012
29. Bender S, Resch F, Weisbrod M, Oelkers-Ax R. Specific task anticipation versus unspecific orienting reaction during early contingent negative variation. *Clin Neurophysiol.* (2004) 115:1836–45. doi: 10.1016/j.clinph.2004.03.023
30. Brunia CH, van Boxtel GJ. Wait and see. *Int J Psychophysiol.* (2001) 43:59–75. doi: 10.1016/S0167-8760(01)00179-9
31. Lang W, Beisteiner R, Lindinger G, Deecke L. Changes of cortical activity when executing learned motor sequences. *Exp Brain Res.* (1992) 89:435–40. doi: 10.1007/BF00228259
32. Lang W, Obrig H, Lindinger G, Cheyne D, Deecke L. Supplementary motor area activation while tapping bimanually different rhythms in musicians. *Exp Brain Res.* (1990) 79:504–14. doi: 10.1007/BF00229320
33. Yilmaz O, Birbaumer N, Ramos-Murguialday A. Movement related slow cortical potentials in severely paralyzed chronic stroke patients. *Front Hum Neurosci.* (2015) 8:1033. doi: 10.3389/fnhum.2014.01033
34. Carroll, D. A quantitative test of upper extremity function. *J Chronic Dis.* (1965) 18:479–91. doi: 10.1016/0021-9681(65)90030-5
35. Lyle RC. A performance test for assessment of upper limb function in physical rehabilitation treatment and research. *Int J Rehabil Res.* (1981) 4:483–92. doi: 10.1097/00004356-198112000-00001
36. Oldfield RC. The assessment and analysis of handedness: the Edinburgh inventory. *Neuropsychologia* (1971) 9:97–113. doi: 10.1016/0028-3932(71)90067-4
37. Folstein MF, Folstein SE, McHugh PR. "Mini-mental state". a practical method for grading the cognitive state of patients for the clinician. *J Psychiatr Res.* (1975) 12:189–98. doi: 10.1016/0022-3956(75)90026-6
38. Jung TP, Makeig S, Humphries C, Lee TW, McKeown MJ, Iragui V, et al. Removing electroencephalographic artifacts by blind source separation. *Psychophysiology* (2000) 37:163–78. doi: 10.1111/1469-8986.3720163
39. Krishef C. *Fundamental Statistics for Human Services and Social Work*. Boston, MA: PWS Publishers (1987).
40. Deecke L, Scheid P, Kornhuber HH. Distribution of readiness potential, pre-motion positivity, and motor potential of the human cerebral cortex preceding voluntary finger movements. *Exp Brain Res.* (1969) 7:158–68. doi: 10.1007/BF00235441
41. Jankelowitz SK, Colebatch JG. Movement related potentials in acutely induced weakness and stroke. *Exp Brain Res.* (2005) 161:104–13. doi: 10.1007/s00221-004-2051-6
42. Verleger R, Binkofski F, Friedrich M, Sedlmeier P, Kompf D, Anarchic-hand syndrome: ERP reflections of lost control over the right hemisphere. *Brain Cogn.* (2011) 77:138–50. doi: 10.1016/j.bandc.2011.05.004
43. Riecker A, Groschel K, Ackermann H, Schnaudigel S, Kassubek J, Kastrup A. The role of the unaffected hemisphere in motor recovery after stroke. *Hum Brain Mapp.* (2010) 31:1017–29. doi: 10.1002/hbm.20914
44. Slobounov S, Hallett M, Newell KM. Perceived effort in force production as reflected in motor-related cortical potentials. *Clin Neurophysiol.* (2004) 115:2391–402. doi: 10.1016/j.clinph.2004.05.021
45. Mathews S, Ainsley DP, Sterr A. EEG dipole analysis of motor-priming foreperiod activity reveals separate sources for motor and

spatial attention components. *Clin Neurophysiol.* (2006) 117:2675–83. doi: 10.1016/j.clinph.2006.08.001
46. Leuthold H, Jentzsch I. Planning of rapid aiming movements and the contingent negative variation: are movement duration and extent specified independently? *Psychophysiology* (2009) 46:539–50. doi: 10.1111/j.1469-8986.2009.00799.x
47. Sanes JN, Suner S, Lando JF, Donoghue JP. Rapid reorganization of adult rat motor cortex somatic representation patterns after motor nerve injury. *Proc Natl Acad Sci USA.* (1988) 85:2003–7. doi: 10.1073/pnas.85.6.2003
48. Pascual-Leone A, Grafman J, Hallett M. Modulation of cortical motor output maps during development of implicit and explicit knowledge. *Science* (1994) 263:1287–9. doi: 10.1126/science.8122113
49. Karni A, Meyer G, Rey-Hipolito C, Jezzard P, Adams MM, Turner R, et al. The acquisition of skilled motor performance: fast and slow experience-driven changes in primary motor cortex. *Proc Natl Acad Sci USA.* (1998) 95:861–8. doi: 10.1073/pnas.95.3.861
50. Nudo RJ, Plautz EJ, Frost SB. Role of adaptive plasticity in recovery of function after damage to motor cortex. *Muscle Nerve* (2001) 24:1000–19. doi: 10.1002/mus.1104
51. Nelles G, Spiekermann G, Jueptner M, Leonhardt G, Muller S, Gerhard H, et al. Reorganization of sensory and motor systems in hemiplegic stroke patients. A positron emission tomography study. *Stroke* (1999) 30:1510–6. doi: 10.1161/01.STR.30.8.1510
52. Weiller C, Chollet F, Friston KJ, Wise RJ, Frackowiak RS. Functional reorganization of the brain in recovery from striatocapsular infarction in man. *Ann Neurol.* (1992) 31:463–72. doi: 10.1002/ana.410310502
53. Weiller C, Ramsay SC, Wise RJ, Friston KJ, Frackowiak RS. Individual patterns of functional reorganization in the human cerebral cortex after capsular infarction. *Ann Neurol.* (1993) 33:181–9. doi: 10.1002/ana.410330208
54. Verleger R, Adam S, Rose M, Vollmer C, Wauschkuhn B, Kompf D. Control of hand movements after striatocapsular stroke: high-resolution temporal analysis of the function of ipsilateral activation. *Clin Neurophysiol.* (2003) 114:1468–76. doi: 10.1016/S1388-2457(03)00125-1
55. Battaglia F, Quartarone A, Ghilardi MF, Dattola R, Bagnato S, Rizzo V, et al. Unilateral cerebellar stroke disrupts movement preparation and motor imagery. *Clin Neurophysiol.* (2006) 117:1009–16. doi: 10.1016/j.clinph.2006.01.008
56. Duque J, Hummel F, Celnik P, Murase N, Mazzocchio R, Cohen LG. Transcallosal inhibition in chronic subcortical stroke. *Neuroimage* (2005) 28:940–6. doi: 10.1016/j.neuroimage.2005.06.033
57. Hummel FC, Steven B, Hoppe J, Heise K, Thomalla G, Cohen LG, et al. Deficient intracortical inhibition (SICI) during movement preparation after chronic stroke. *Neurology* (2009) 72:1766–72. doi: 10.1212/WNL.0b013e3181a609c5
58. Nowak DA, Grefkes C, Ameli M, Fink GR. Interhemispheric competition after stroke: brain stimulation to enhance recovery of function of the affected hand. *Neurorehabil Neural Repair* (2009) 23:64–56. doi: 10.1177/1545968309336661
59. Xu GQ, Lan Y, Zhang Q, Liu DX, He XF, Lin T. 1-Hz repetitive transcranial magnetic stimulation over the posterior parietal cortex modulates spatial attention. *Front Hum Neurosci.* (2016) 10:38. doi: 10.3389/fnhum.2016.00038
60. Sun R, Wong WW, Wang J, Tong RK. Changes in electroencephalography complexity using a brain computer interface-motor observation training in chronic stroke patients: a fuzzy approximate entropy analysis. *Front Hum Neurosci.* (2017) 11:444. doi: 10.3389/fnhum.2017.00444
61. Lee J, Koh D, Ong CN. Statistical evaluation of agreement between two methods for measuring a quantitative variable. *Comput Biol Med.* (1989) 19:61–70. doi: 10.1016/0010-4825(89)90036-X
62. Shibasaki H, Hallett M. What is the Bereitschaftspotential? *Clin Neurophysiol.* (2006) 117:2341–56. doi: 10.1016/j.clinph.2006.04.025

Conflict of Interest Statement: The authors declare that the research was conducted in the absence of any commercial or financial relationships that could be construed as a potential conflict of interest.

Advantages of publishing in Frontiers

OPEN ACCESS
Articles are free to read for greatest visibility and readership

FAST PUBLICATION
Around 90 days from submission to decision

HIGH QUALITY PEER-REVIEW
Rigorous, collaborative, and constructive peer-review

TRANSPARENT PEER-REVIEW
Editors and reviewers acknowledged by name on published articles

Frontiers
Avenue du Tribunal-Fédéral 34
1005 Lausanne | Switzerland

Visit us: www.frontiersin.org
Contact us: info@frontiersin.org | +41 21 510 17 00

REPRODUCIBILITY OF RESEARCH
Support open data and methods to enhance research reproducibility

DIGITAL PUBLISHING
Articles designed for optimal readership across devices

FOLLOW US
@frontiersin

IMPACT METRICS
Advanced article metrics track visibility across digital media

EXTENSIVE PROMOTION
Marketing and promotion of impactful research

LOOP RESEARCH NETWORK
Our network increases your article's readership